SEISMIC IMAGING METHODS APPLIED TO DEVONIAN CARBONATE REEF ENVIRONMENTS OF WESTERN CANADA

ANDREW JOSEPH BURTON

INFORMATION TO USERS

This manuscript has been reproduced from the microfilm master. UMI films the text directly from the original or copy submitted. Thus, some thesis and dissertation copies are in typewriter face, while others may be from any type of computer printer.

The quality of this reproduction is dependent upon the quality of the copy submitted. Broken or indistinct print, colored or poor quality illustrations and photographs, print bleedthrough, substandard margins, and improper alignment can adversely affect reproduction.

In the unlikely event that the author did not send UMI a complete manuscript and there are missing pages, these will be noted. Also, if unauthorized copyright material had to be removed, a note will indicate the deletion.

Oversize materials (e.g., maps, drawings, charts) are reproduced by sectioning the original, beginning at the upper left-hand corner and continuing from left to right in equal sections with small overlaps.

Photographs included in the original manuscript have been reproduced xerographically in this copy. Higher quality 6" x 9" black and white photographic prints are available for any photographs or illustrations appearing in this copy for an additional charge. Contact UMI directly to order.

Bell & Howell Information and Learning
300 North Zeeb Road, Ann Arbor, MI 48106-1346 USA

UMI®
800-521-0600

SEISMIC IMAGING METHODS APPLIED TO DEVONIAN CARBONATE REEF ENVIRONMENTS OF WESTERN CANADA

by

ANDREW JOSEPH BURTON B.Sc.

A thesis submitted to the

School of Graduate Studies

in partial fulfillment of the

requirements for the degree of

Master of Science

Department of Earth Sciences

Memorial University of Newfoundland

September 1998

St. John's Newfoundland

ABSTRACT

A surface seismic profiling (SSP) reflection survey from south-central Alberta in Western Canada is reprocessed with the intent of differentiating between on-reef reservoir and off-reef non-reservoir rocks of the Devonian Nisku Formation. The associated seismic resolution is fundamentally low due to large seismic wavelength, thin reservoir formation, and large target depth. The reservoir response is also weak relative to strong impedance contrasts associated with the overlying clastic-carbonate-evaporitic stratigraphy. Hence, the reservoir identification component of seismic interpretation is based largely on subtle changes in data character and event timing. For such an exploration play, where geology is conformable to the method, conventional common midpoint (CMP) processing objectives include obtaining the maximum frequency bandwidth and true relative amplitude (TRA) in a surface consistent manner. However, since the primary indicators can be distorted by near-coincident multiple reflections generated by mechanisms that may vary laterally in timing and magnitude, it is necessary to distinguish between primary and multiple arrivals based on a combination of indicators including differential moveout, predictability, comparison with well log synthetics, and evaluation of vertical seismic profiles (VSP). The nature of the multiple determines whether conventional SSP methods can be adapted to multiple suppression, but existing techniques have been less than successful in the identification and/or suppression of significant multiples without compromising Nisku target response. The basis of this thesis research is to review CMP methods as applied to a particular Nisku SSP response, and to determine whether a practical solution to the multiple problem can be reached by integrating log and VSP wellbore data with SSP data. Because constraints on

multiple energy are realisable when VSP data are incorporated, and since the available well control coincides closely with the SSP data, VSP analysis and multiple reflectivity inversion are considered as design criteria for an adaptive approach to multiple identification and suppression.

The methodology employed in this analysis of Nisku reflectivity involves application of basic time-sequence analysis tools and standard seismic processing tools as related to seismic wave propagation within a layered earth. It will be shown that multiple energy can be identified in SSP data using hyperbolic semblance velocity analysis, range-limited stacks, and trace autocorrelations. Further, it will be shown that VSP data can be used to identify the same multiple energy and also to identify the mechanism responsible for the multiple reflection. For this particular Nisku study, the conventional methods of multiple suppression by prediction and moveout discrimination are evaluated along with an adaptation of a least squares inversion method. All methods face limited success due to the nature of the multiple contamination, but the overall analysis complements Nisku interpretation and thereby improves likelihood of drilling success.

ACKNOWLEDGEMENTS

I am grateful to everyone involved in initiating and supporting the institutions of science at Memorial University of Newfoundland. In hindsight, I am very appreciative of the opportunities and insights added to my life experience through my undergraduate and graduate studies at Memorial. In particular, I acknowledge those who provided resources to motivate my graduate research:

To my thesis and research supervisor, Dr. Larry Lines, for his ingenuity and practical knowledge in the implementation of theoretical geophysics, especially least squares inversion techniques. To my thesis and research supervisor Dr. James Wright, and to Dr. Chuck Hurich for direction, suggestions and advice. Thanks to these people for their roles in the establishment of the Memorial University Seismic Imaging Consortium (MUSIC).

To our computing resources manager, Tony Kocurko, for his quick response to computing dilemas and for keen upkeeping of the plethora of hardware and software.

Thanks to Dave Cooper of Pancanadian Petroleum Ltd. for providing surface and vertical seismic profiling data and wellbore constraints. Special thanks to Bill Goodway for suggesting the corridor stacking method, to Lee Hunt for AVO insight, and to Bill Nickerson for comments on the draft of this thesis.

Special thanks to Frank VanHumbeck, Larry Matthews, and Mike Corrigan of Canadian Hunter Exploration Ltd. for providing other Devonian reef seismic data.

To Statcom Ltd. of Calgary, Alberta for placing confidence in me as a novice geophysicist. Three years of industry processing was a crucial supplement to my ability to complete this thesis. Also thanks for tape copy and reformatting services.

To all the industry sponsors of MUSIC for providing financial support, software, resources, seismic data, and research direction.

To Landmark Graphics Corporation for providing INSIGHT [TM] software (originally owned by Inverse Theory and Applications Ltd.), to the Colorado School of Mines for their free Seismic Unix (SU [TM]) software library, and to Dan Hampson and Brian Russell for providing STRATA [TM], GLI [TM], and AVO [TM] software. These software packages are used for standard SSP VSP seismic processing presented in this thesis.

To Brian Hoffe, Paul Barnes, Jinming Zhu, George Langdon, Simon O'Brien, Bingwen Du, Irene Kelly, Cindy Grant, Jeremy Peng, Hanxing Lu, Wenjing Wu, Ayon Dey, Richard Wright and others past and present in our department for creating a friendly and co-operative working environment in MUSIC. Special thanks to Jinming Zhu and Simon O'Brien for modelling software and many useful suggestions.

To the Government of Newfoundland and Labrador for a Career Development Award to financially supplement my graduate studies.

To the Natural Sciences and Engineering Research Council (NSERC) and Petro Canada Inc. for financially supporting the Industrial Chair for Applied Seismology at Memorial.

To my entire loving family for encouragement and sacrifice. For them I dedicate this thesis to my daughter, Maggie Muriel, and son, Clay Andrew.

TABLE OF CONTENTS

LIST OF FIGURES

LIST OF ABBREVIATIONS USED

AGC: Seismic automatic gain control

AVO [TM]: Hampson and Russell amplitude versus offset analysis software

COF: SSP common offset gather

CMP: SSP common mid point gather

CDP: SSP common depth point gather, equivalent to CMP for horizontal layers

CSP: SSP common source point gather

CGP: SSP common geophone point gather

CSPG: Canadian Society of Petroleum Geologists

f-k: temporal frequency vs spatial wavenumber domain

FRT: VSP field record time

GLI [TM]: Hampson and Russell generalised linear inverse SSP refraction statics software

GMA: Geo-Microcomputer Applications Ltd. industry standard well log format

HSVA: hyperbolic semblance velocity analysis

INVEST: inverse velocity stacking, a PRT method

ITA: Inverse Theory and Applications Ltd. SSP/VSP processing software called INSIGHT [TM], (now owned by Landmark Graphics Corporation)

MUSIC: Memorial University Seismic Imaging Consortium

NMO: SSP normal moveout dynamic correction for reflection from horizontal layers

PD: Seismic prediction distance for predictive deconvolution operator design

PRT: Seismic parabolic Radon transform

SEG: Society of Exploration Geophysicists

SEG-D: Standard binary SSP seismic data, type 'D'

SEG-P1: Standard ASCII SSP survey data, type 'P1'

SSP: Surface seismic profile

STRATA ^{TM}: Hampson and Russell stratigraphic seismic impedance inversion software

S/N: Seismic signal to noise level

tau-p: seismic time vs ray parameter domain

TRA: Seismic true relative amplitude

TVD: Wellbore true vertical depth

TWT: SSP two-way reflection time

TT: VSP first break time in FRT

-TT: VSP FRT advanced by TT

+TT: VSP FRT delayed by TT

VSP: vertical seismic profile

x-t: lateral offset vs seismic time domain

CHAPTER 1. INTRODUCTION

Nisku reef plays within the Devonian carbonate environment in Western Canada have proven to be challenging targets for conventional seismic applications. The associated hydrocarbon indicators are unpredictable since only subtle variations in seismic response exist between on-reef and off-reef situations. This interpretative difficulty exists in part because of the relatively low reservoir reflectivity compared to the dominant reflectors. Also, the temporal resolution required to distinguish reef build-up from open marine or tight carbonate settings is often not available with surface seismic profiles (SSP) due to limited frequency content. These inherent difficulties are compounded by the superposition of spatially variant interbed and surface-related multiple generating mechanisms. Given that Nisku reefs are host to significant hydrocarbon reserves, it is essential to improve the interpretability of conventional SSP data under these adverse conditions. Hence, the application of conventional imaging methods to a particular Nisku seismic experiment forms the framework for this thesis. Since the goal of seismic imaging is to recover a true earth reflectivity sequence from which to extract direct hydrocarbon indicators, data characteristics must be utilised appropriately during processing to identify limitations in the methodology arising from validity of assumptions. Given that many processes assume that multiple reflections are absent from the signal, the goal of this thesis is to adopt a processing strategy that seeks to provide reliable Nisku hydrocarbon indicators in such cases.

The Lower Nisku formation and adjacent geologic members are too thin to be well resolved by realisable seismic wavelets propagating at high velocity with low temporal frequencies at large depth of burial. This requires that subtle changes in seismic response (waveform character, timing, and amplitude) must form the basis for reservoir facies and

porosity distinction. Preserving these hydrocarbon indicators using the common midpoint (CMP) method relies on retention of optimum bandwidth during processing for surface consistency in true relative amplitude (TRA), refraction statics, and wavelet deconvolution. INSIGHT [TM] and SU [TM] software is used for seismic processing. GLI [TM] software is used to invert SSP first break picks for a refraction static solution and for a meaningful near surface model. Events picked during velocity analysis must be validated as primaries to ensure that stacking will improve resolution and signal-to-noise (S/N) level by multiple attenuation. Adaptation of other multiple suppression techniques based on identified multiple characteristics during CMP and vertical seismic profile (VSP) processing will further reduce interpretation pitfalls.

In general, multiple attenuation methods are adapted to the differential normal moveout (NMO) behaviour between primaries and multiples. Multiples generally have greater NMO than primary reflections. The CMP stack process in x-t space acts as a moveout filter by preferentially enhancing near-zero wavenumbers. When primary NMO correction is applied, multiples are usually over-corrected for NMO and attenuated as coherent noise. If correct NMO is assigned to multiple events, local primaries are attenuated instead. Depending on the relative signal levels and differential NMO between both events, stacking may not provide sufficient attenuation and two-dimensional (2D) filtering or predictive deconvolution is applied adaptively. Surface related and longer period multiples spend more time in shallow lower velocity media hence may exhibit significant moveout relative to NMO corrected primary energy. Such cases can be treated by frequency-wavenumber (f-k) or Radon transform (tau-p) separation.

For shorter period multiples that travel in faster media or without significant angular components, differential NMO becomes smaller and prediction can be implemented on a post-stack basis under normal incidence assumptions. Multiple energy and lateral variation in periodicity are identified locally by use of trace autocorrelation. The success of the method requires that significant primary energy components be excluded from operator design lags. Pre-stack prediction may require offset dependent operator design or offset limitation to adapt to differential NMO, but is advantageous since stacking may enhance S/N to a higher level than post-stack prediction. For offsets conforming to normal incidence (constant multiple period with offset), prediction should be applicable to both pre-stack and post-stack SSP data.

An industry data set from Alberta is analysed for Nisku Devonian reef seismic response. The wellbore data associated with this case study represent a 1:3 success ratio based on the timing and amplitude response of a 2D SSP profile. Nisku well control for three distinct reservoir environments exists in the form of sonic and density logs, and VSP. Synthetic seismograms for non-porous shelf, porous reef build-up, and shaled-out embayment facies suggest that interbed multiples are significant in the CMP stack. Processed CMP gathers at these locations indicate small differential multiple NMO relative to the co-incident primary, a trait typical of a short period interbed mechanism. However, VSPs at well locations directly indicate the presence of a near-surface peg-leg multiple generator. If this mechanism involves reverberation between topography and the base of the weathering layer, then a peg-leg multiple could display moveout similar to its primary counterpart as depicted by Snell's Laws of reflection and refraction for the low velocity layer. When weathering thickness changes laterally, the near-surface TWT delay varies

significantly relative to subsurface interbed delay associated with faster media. Lateral analysis of multiple generation indicators becomes more difficult as system complexity increases. Significant multiple moveout identified at an off-well CMP location may be due to lateral variation in the ray-path geometry of the surface mechanism, or to subsurface interbeds dominating multiple response locally. Impedance contrasts within this Nisku system can result in a seismic response that is non-linear in reflectivity as illustrated by Robinson (1967), and thereby multiples can occur with significant energy relative to primary reflections. The system may appear non-linear due to the superimposing of different multiple generating mechanisms. The relative strength of contributing mechanisms under both circumstances can be expected to change as lateral changes in the generating geology occur. Multiple suppression should be based on an understanding of the complexity of the combined transmission and backscattering effects on such a response.

Multiple identification and application of conventional methods suffer from a combination of methodological failures in this Nisku study. First, multiple periodicity as deduced from the autocorrelations of synthetic seismograms based on well logs appears somewhat chaotic, partly because the frequency spectrum of the primary reflectivity $R_p(t)$ is non-white within the seismic bandwidth and possibly due to lateral changes in mechanisms and/or mechanism timing. This makes prediction distance criteria difficult to define and brings into question the validity of prediction for multiple attenuation. Secondly, differential NMO between the multiple and adjacent primaries is small due to the geophysical nature of the mechanism. This makes velocity filtering difficult to implement, and makes CMP stacking insufficient for multiple suppression. To deal with this multiple problem, two alternate methods are used in an attempt to define the mechanism and thereby determine the

most appropriate multiple attenuation technique. The VSP corridor stacking technique (Hardage, 1983) indicates prediction distance for deconvolution operator design at well locations. The inversion for multiples method (Lines, 1996) attempts construction of a reflectivity spike sequence to complement multiple identification and suppression, and the method does not rely on the assumption of system linearity.

Reflectivity inversion is applied under iterative least squares formalism. This is attempted using a modified algorithm implementation as developed by Lines (1996). This analysis requires the earth model $R_p(t)$ sequence derived from logs and SSP weathering model, a wavelet w(t), and the best band-limited SSP estimate of the earth's normal incidence full impulse response $R_f(t)$. STRATA ^{TM} software is used for SSP wavelet extraction. VSP data provide constraints for depth-to-time log conversions, a validation process for log blocking, and direct multiple identification. If successful at the well location, criteria for multiple attenuation techniques could be derived from lateral extrapolation of inverted well reflectivity controlled temporally by seismic horizons and by modelled near surface layers. The resulting global reflectivity inversion would be interpreted for lateral variations in multiple generating mechanisms and timing characteristics. If the events creating a multiple mechanism could be mapped, prediction distance could be monitored laterally and used to attenuate multiples on SSP data. Alternatively, spectral division deconvolution can be used to shape the inverted impulse response $R_f(t)$ to the inverted $R_p(t)$. Unlike the predictive method, this technique attempts to remove multiple energy from the same autocorrelation lags as occupied by colour in $R_p(t)$ while preserving the colour at relative amplitude. These techniques are considered and tested for robustness in the improvement of seismic resolution where applicable.

1.1 Western Canadian Devonian Petroleum Reservoirs

The Upper Devonian geology of the Western Canadian Sedimentary Basin (WCSB) in Alberta is spread over four units, each hosting carbonate reservoir zones. The first unit in the stratigraphy (Figure 1.1.1) is the Wabamun Group and the second unit is the Nisku Formation of the Winterburn Group. The third unit, forming the Southern Alberta Shelf, is the Leduc Formation of the Woodbend Group. This formation is replaced by the Ireton shale basinward. The fourth unit is the Swan Hills Formation of the Beaverhill Lake Group. The reservoir zone associated with the present study is in the Lower Nisku in south-central Alberta.

The Nisku Formation consists of laterally continuous regressive dolomitised shelf carbonates of Late Frasnian age (~370 Ma) deposited around the Winterburn Basin during arid climatic conditions. This unit extends across Alberta and Saskatchewan in Canada, and across Montana and North Dakota in the United States. Oil and gas occur in the Nisku under a variety of trap conditions. An exaggerated geologic cross section (Figure 1.1.2) exemplifies Nisku pinnacle-island reefs which are famous for containing oil in dolomitised bank edges. Pinnacle reef formation is controlled by basin slope location, but other factors contribute to reservoir formation. These are described geologically in the AAPG Memoir series (Vail et al, 1977). A general overview of WCSB hydrocarbon production from the Nisku can be found in the CSEG/CSPG Geophysical Atlas (Rennie et al, 1989). Kuhme (1987) discusses the economic importance of Devonian reefs, the present state of play, and offers an outline of reef distinction criteria. While publications on the seismic detection of limestone reefs are common, studies on distinction of porosity are rarely published (eg. Fraser and Jain, 1988). This may be for good reason, since the seismic method offers little

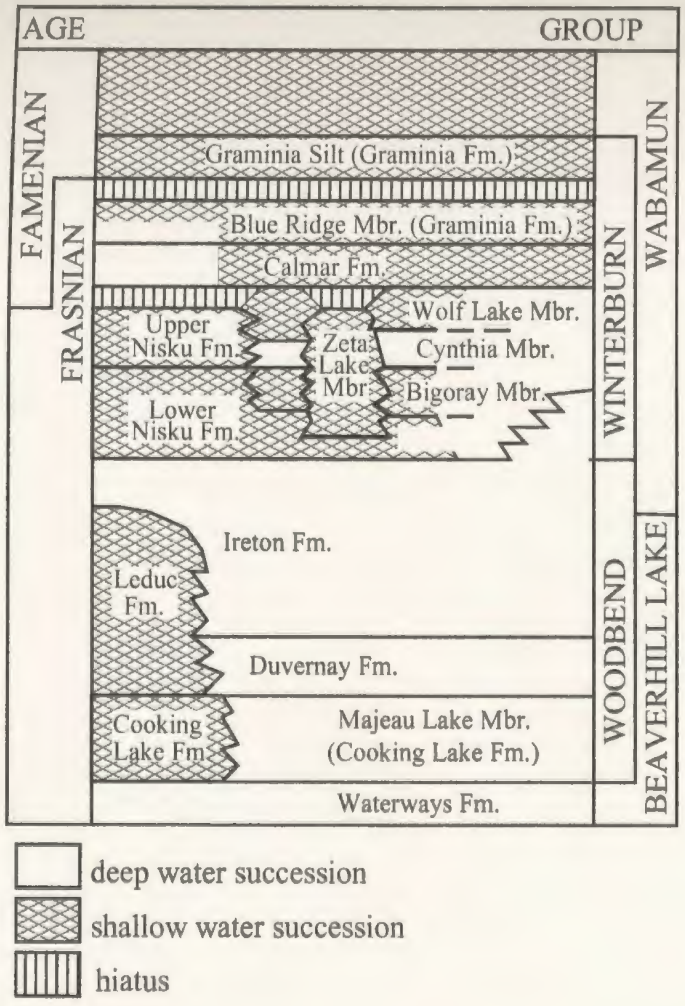

Figure 1.1.1. Regional stratigraphy of Upper Devonian Geology (left) from the WCSB in Central Alberta. The Nisku SSP/VSP multiple case study presented in the text is from southeast of Calgary (right).

Nisku regional geology

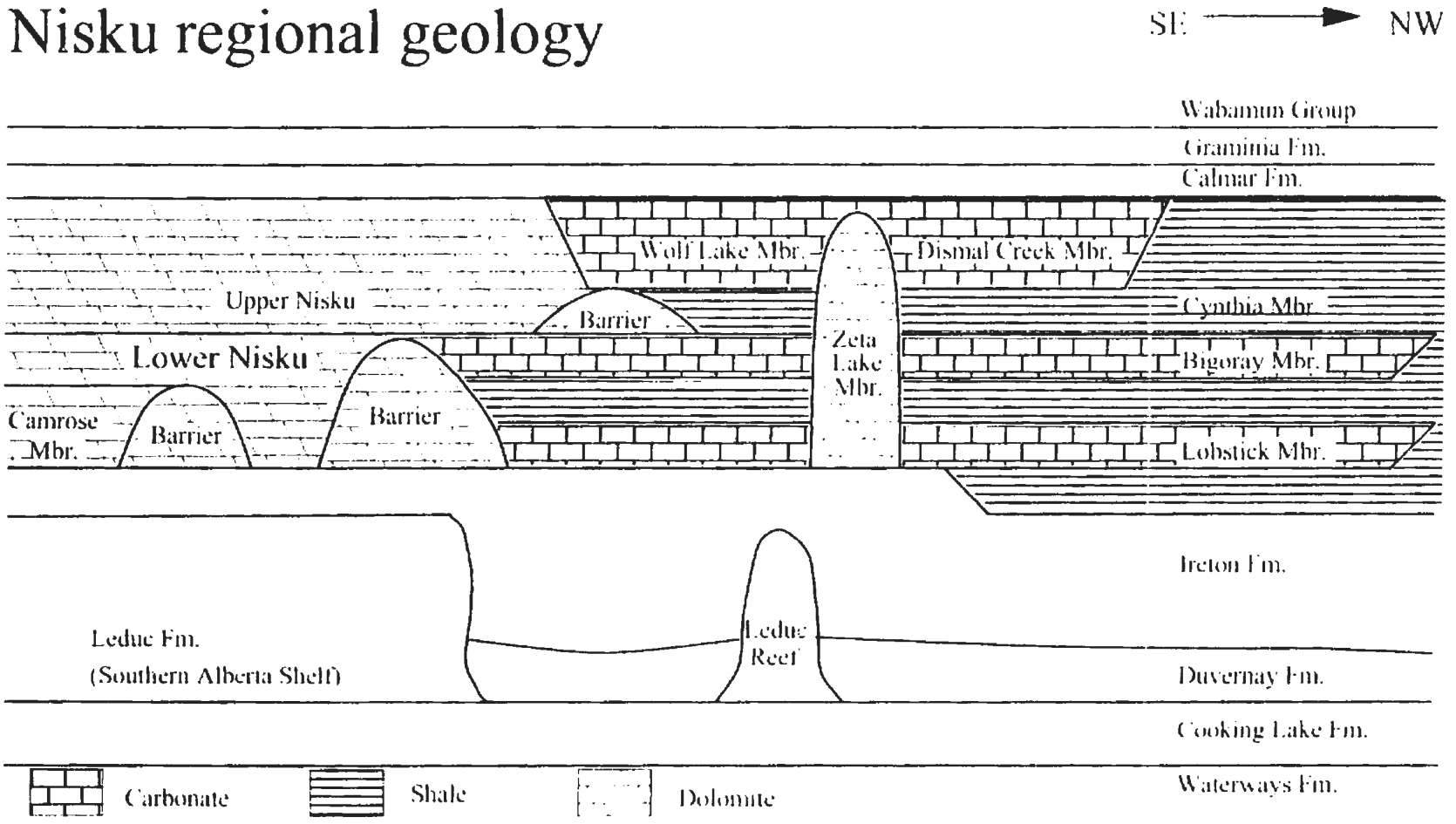

Figure 1.1.2. Simplified Upper Devonian geological cross section showing the Nisku Formation distribution for the shelf to slope region. The reservoir zone under investigation is in the Lower Nisku on the shelf inside the barrier reef. Porosity needs to be distinguished from an anhydritized facies (tight shelf) and from a shaled out facies (embayment). Also, the spatial relationship between the Cynthia shale source rock and the extent of the host rock is poorly defined by seismic (shelf/slope transition).

detection criteria in many cases as proven by poor success ratios experienced in industry drilling programs.

The seismic objectives in this Nisku study are two-fold. The first objective is to identify the lateral transition from carbonate shelf to embayment, while the second objective is to identify porosity. On the shelf, a stratigraphic trap is created by a tight Upper Nisku overlying the Lower Nisku which contains zones of porous dolomitised carbonate within non-porous unaltered carbonate or altered carbonate having anhydritic fill. At the shelf slope transition, Nisku carbonates are replaced at the same stratigraphic level by Nisku shales of the East Winterburn Shale Basin. The lateral facies distinction between tight shelf, porous reservoir, and embayment may be identifiable from stacked seismic data on the usual basis of amplitude and/or frequency change, or by acoustic impedance inversion. Pre-stack SSP data may also be used to identify lithology on an AVO basis. However, frequency content of conventional seismic profiles may be insufficient to resolve the key seismic reflectors and/or the shelf slope transition geometry. Also, multiple reflection interference is a potential problem in non-elastic seismic stratigraphy since subtle amplitude discrimination criteria may be masked. Methods of multiple suppression and increased bandwidth may help to derive better reef porosity discrimination criteria.

1.2 Data Processing Objectives

The solution to the Nisku interpretational problem in this case study relies on CMP processing of SSP data to provide porosity criteria. The most conventional of these criteria is the amplitude and character associated with a CMP stack for which TRA has been preserved with high S N ratio and maximised bandwidth. The fundamentally low resolution is enhanced by extension of high-end bandwidth, while character information is enhanced by overall bandwidth. However, care is required to maximise the number of octaves within the seismic bandwidth since other events are recorded along with primary reflections, making it difficult to maintain sufficient S N. Hence, the effectiveness of CMP methods in the treatment of seismic noise will determine the quality of porosity and or facies distinction criteria in this geologic setting.

The key to increasing Nisku resolution rests with restoring and maintaining high frequency spectral content. Deconvolution operators, if applicable, must be designed from x-t areas of low seismic noise in a surface consistent manner. Optional spectral enhancement techniques are less constrained by local geology but some phase adjustment criteria must be defined. Maintaining high-end bandwidth in the stack relies on optimised static corrections and moveout estimation, which are inherently related processes that determine the validity of the CMP stacking assumption.

Extension of the low frequency information is difficult when surface modes interfere with reflection events. For this Nisku study, shot holes have been drilled consistently to a depth of 24m to reduce air blast from hole blow-out, and geophone arrays provide surface wave attenuation. This is important since stacking may not attenuate low frequency band-limited coherent noise. Anti-alias spread design attempts sufficient sampling of refraction

energy which can be reverberative, and aliased noise trains are difficult to remove without compromising primary amplitudes. However, deep shot holes that do not penetrate the sub-weathering layer may introduce spatially variant wavelet ghosting given sufficiently low and variable weathering velocity at the shot location. For this reason, whitening deconvolution design should attempt to remove any ghosting effect by extending the operator length to include wavelet ghosting based on uphole information. Refraction analysis must assume that the shot has not penetrated the weathering layer so that first breaks represent refraction within a layered earth. The main SSP data processing objective is to generate conventional gathers processed surface consistently for statics, TRA, and wavelet deconvolution before application of fine-tuned stacking velocity analysis. Each of these basic processes is important in the preservation of subtle variations in the seismic response.

While realisable bandwidth may remain insufficient to detect the lateral change from embayment to shelf facies on the basis of character, amplitude anomalies may exist due to changes in lithology with or without porosity changes. Also, pre-stack gathers may be analysed for AVO response as a hydrocarbon indicator. However, interbed and surface peg-leg multiple energy modes are suspect at the same stratigraphic level as the primary reef response, making amplitudes unreliable (Lu and Lines, 1995). The common processing sequence is to detect and suppress the multiple energy using conventional surface reflection methods, but these approaches may not be appropriate for specific Devonian reef targets.

For this case study, a thick surface weathered layer requires that shot holes be drilled to a depth on the order of four times the standard industry depth. Given typical velocities encountered in the near-surface, this suggests that this layer has the potential to act as a

surface peg-leg multiple generator. Assuming that deconvolution corrects for wavelet variation due to shot burial, weathering traveltime at the receiver location should indicate prediction distance for peg-leg attenuation. At the same time, well bore log and VSP data will be processed to evaluate multiple problems which are interdependently related to SSP processing. The applicability of various multiple attenuation methods to identified multiple problems will be assessed for methodological problems. The best approach will be applied in the most appropriate data domain in conjunction with standard SSP processing methods.

1.3 Modelling and Inversion Objectives

The processing and interpretation of the seismic response from any structural or stratigraphic exploration play may be complemented by physically meaningful constraints from a variety of sources. The applicability of each type of constraint to the problem at hand rests predominantly with availability. Typically, a subsurface geologic model of some reliability and detail will exist, and possibly some form of well bore log survey could be extrapolated laterally into the model. To improve the interpretative nature of the CMP response, these sources of data are used to perform forward modelling. These results may be further complemented by other geotechnical evaluations, and generally the success of the method depends on the sensitivity of the seismic response to model parameterisation. Once a model has been created, least squares optimisation techniques provide adjustments to the model parameters based on the real data. Recent improvements in computing power have allowed realistic application to the seismic method. Subtle variations in the CMP seismic response, when complemented by inverse modelling techniques that incorporate well and VSP data, may form a basis of discrimination between on-reef and off-reef settings.

Forward modelling has been applied for Devonian amplitude versus offset (AVO) response. Lu and Lines (1995) have illustrated that AVO analysis may offer a basis for distinguishing lateral facies changes in the Nisku. Forward AVO modelling under full reflectivity (including multiples) may enhance the usefulness of AVO attribute stacks as generated from the multiple contaminated data. However, since full reflectivity modelling under AVO [SI] software is limited to one layer with overburden, the results are not readily applicable to Nisku exploration. Alternatively, a radial trace model that includes Zoeppritz calculations and first order multiples could be generated and examined for AVO effects, possibly constituting a more valid criteria for AVO analysis. Because offset is involved in the forward modelling of AVO effects, more parameters are involved and sensitivity increases, making inverse modelling less reliable and not a standard component of AVO analysis. Instead, instantaneous attributes (or raw amplitudes) from near-offset stack data following predictive multiple attenuation designed under reflectivity inversion and or VSP criteria may be a more robust tool for reservoir distinction than AVO analysis in this Nisku case.

Least squares parametric reflectivity inversion for multiples has been applied successfully to synthetic data (Lines, 1996). The method first generates a synthetic impulse response using a known wavelet w(t) and a primary reflectivity sequence $R_p(t)$ defined by fixed reflector positions. Then, $R_p(t)$ magnitudes were altered and inversion converged to the correct solution under conditions of non-linear reflectivity. However, when applied to real data, the parameterisation process is critical due to uncertainty in reflectivity timing, number of layers, and surface contribution to multiple generation. The impedance sequence I(t) derived from well log impedance temporally constrained by VSP checkshots provides the

best model blocking information for generation of $R_p(t)$. The blocking process is validated by dominant upgoing reflections as identified on VSP data, and STRATA [TM] is used for optimal estimation of w(t) for inversion. If successful, w(t) can also be used for filter design to shape stack spectra to that of the inverted primary synthetic. This matching filter would attempt to remove all multiple effects at once and should work well for windows containing one multiple waveform. Prediction may benefit from the analysis if prediction distance and multiple mechanism can be identified for operator design. However, when coloured primary reflectivity occupies the same autocorrelation lags as the multiple, most hope is placed in a matching filter operation to preserve underlying primary energy at relative amplitude.

Normal incidence modelling by data integration will be analysed for multiple generating mechanisms that distort the targeted petroleum reservoir facies. Success of parametric reflectivity inversion for $R_p(t)$ at well locations qualifies multiple mechanisms inferred during VSP and CMP processing. Nisku interpretation should be improved away from wells using primary response improved in amplitude and character by logical application of multiple attenuation methods. Resolution may remain insufficient for accurate lateral extension of the inverted $R_p(t)$ model timing by mapping dominant near-offset seismic horizons, but acoustic information from well logs can be intuitively incorporated into the model to provide sufficient layering. This approach may compensate for low resolution in a 2D inversion. The most significant reason for inversion failure may be lack of intrabed delay associated with blocky models. In this Nisku case study, success of this method was limited to an appreciation for the multiple-generating role of dominant reflectors in the CMP response.

In summary, the research goal of this thesis is two-fold. The primary goal is to obtain reliable hydrocarbon indicators from SSP data. The secondary goal is to integrate wellbore information into this process. The methodology used in accomplishing these goals involves deriving a unique strategy for the application of available signal processing techniques in the imaging of a particular Nisku SSP experiment. The goals of this thesis do not necessarily demand the development of exciting new theory or technology, but instead the topic of multiple attenuation must be thoroughly analysed in unison with the physics of seismic imaging and the implementation of procedures available to improve signal-to-noise ratio in seismic data. Considerable effort is directed at attacking the difficult problem of identifying and removing multiple reflections in seismic data. This requires the creation of good graphics to support the scientifically sound discussion and documentation of multiple suppression and improved image quality as related to a particular Nisku SSP experiment. Thorough exploration of the problem will require that many small nuances be investigated for importance.

CHAPTER 2. PROCESSING METHODS FOR SURFACE SEISMIC PROFILES

Surface seismic profiling has become a standard method in the geophysical detection of oil and gas reservoirs. The objective of the processing strategy applied to field data is to provide a response from which hydrocarbons can be detected. This will generally depend on data quality, target depth, and target characteristics. For land SSP acquisition, processing is applied to remove signal distortion caused by wavelet propagation (deconvolution), to removing the differential time delay associated with lateral variation in the surface low-velocity layer (static correction), and to remove the differential time delay associated with increased travel path due to offset (normal moveout). Following the application of these processes, signal level is increased by summation (stacking). The deconvolution process attempts to maximise signal bandwidth, while static and dynamic corrections are essential to preserving this bandwidth in the stacking process. The objective of this chapter is to seek an appropriate processing strategy that incorporates these fundamental processes into an assessment of data quality and multiple interference. Conventional multiple suppression techniques are presented, and amplitude versus offset (AVO) analysis is discussed in relation to porosity distinction under conditions of multiple contamination. The goal is to produce a seismic response from which hydrocarbon discrimination criteria can be derived while maintaining the integrity of the seismic signature of the Nisku.

The SSP processing strategy adopted in this study serves to investigate multiple contamination and conventional multiple suppression over the extent of a Nisku survey. Data gathers are prepared using a trace binning strategy to simplify lateral performance analysis. Windowed SSP trace autocorrelations (both before and after stack) and velocity spectra are utilised in multiple identification. The characteristics of the data will indicate the

usefulness of conventional suppression techniques. The success of the suppression will determine if CMP gathers can be used in conventional AVO analysis.

SSP data for a Devonian Nisku reef prospect are assumed to be contaminated by multiple interference at the target zone. VSP analysis (Chapter 3) will be used to confirm whether multiple generation occurs in the near surface. Since shot holes are drilled to a depth of 24m to reduce surface wave contamination, the thick weathering layer is suspect. Smoothed uphole information limits surface velocity to the range 600-900m s. Under this constraint, first break inversion indicates a weathering thickness of 24 to 40m, or a two-way weathering delay of 70 to 120ms. A sub-weathering velocity of 2700m s suggests a reflection coefficient of 0.6, making the weathering layer a very efficient peg-leg multiple generator. Given the large velocity contrast at the base of weathering, Snell's Law predicts that the only energy transmitted beyond the weathering zone originates from small angles of incidence. The large velocity contrast produces a lot of refraction and most of the energy is taken up in the higher angles of incidence. Refraction from a horizontal base of weathering is the main assumption behind refraction static corrections applied to SSP data, often valid under conditions of layered geology in the WCSB. When the weathering layer is bounded by horizontal topography, raypaths for reflections and their reverberations will represent propagation at near-normal incidence. Under these conditions, the periodicity of a peg-leg multiple is expected to remain consistent for near offsets. Hence, SSP near-offset data can be processed for multiple removal by predictive deconvolution. The procedure may offer a viable approach to the multiple problem in such cases. Secondary interbed multiple mechanisms may require suppression methods based on differential moveout relative to near-coincident primaries, or based on other criteria.

2.1 SSP Geometry, Scaling, Statics, and Deconvolution

The SSP method involves propagating acoustic energy from a surface seismic source into a geologic halfspace and recording reflected energy by means of surface mounted geophones. These signals are recorded as a function of time (t) and lateral offset (x) from the source and can provide insight into distributions of various earth properties, the most fundamental of which is the relative magnitude of contrasts in acoustic impedance at reflecting boundaries. To quantify the relative partitioning of energy at an acoustic interface, the earth primary reflectivity function $R_p(\theta,\alpha,\beta,\rho,\sigma)$ is defined (Zoeppritz, 1919) in terms of angle of incidence (θ) and layer properties of compressional velocity (α), shear velocity (β), density (ρ), and Poisson ratio (σ). In the case where reflected P-wave amplitudes represent normal incidence propagation (Figure 2.1.1), the equation for R_p simplifies to $R_p=(I_2-I_1)/(I_2+I_1)$ where layer impedance (I) is defined by the product $\rho\cdot\alpha$. For a complete discussion, refer to Robinson and Treitel (1980). When the real earth can be reasonably represented by a horizontally stratified homogeneous layer acoustic model, the traces can be processed as gathers sharing common midpoint (CMP) between shot and receiver (Telford et al. 1977). This method yields enhanced estimates of the earth R_p function from which other properties such as porosity and structure may be inferred. For reliable interpretation of this response, CMP methods applied to SSP data must accommodate limitations due to data quality and validity of assumptions regarding the nature of the earth model and the propagating wavelet w(t).

Processing methods for SSP data follow from the idea of data multiplicity associated with CMP acquisition (Figure 2.1.2). In the CMP method, the receiver spread typically moves relative to a central source location. At some point in the processing stream, traces

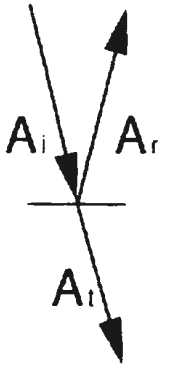

A_i =incident p-wave amplitude
A_r =reflected p-wave amplitude
A_t =transmitted p-wave amplitude
I_i =incidence layer impedence
I_t =transmission layer impedence
R=reflection coefficient= A_r / A_i
T=transmission coefficient= A_t / A_i

Energy is proportional to $I A^2$

$E_r / E_i = (A_r / A_i)^2 = R^2$ $\qquad$ $E_t / E_i = (I_t / I_i)(A_t / A_i)^2 = (I_t / I_i) T^2$

For conservation of energy $\quad 1 = E_r + E_t = (I_t / I_i) T^2 + R^2$

$$T^2 = (I_i / I_t)(1 - R^2)$$

Since the quantity $(1 - R^2)$ does not change with direction, transmission efficiency is determined by impedence ratio.

Figure 2.1.1 Normal incidence partitioning of plane wave energy at an acoustic interface within horizontally layered media.

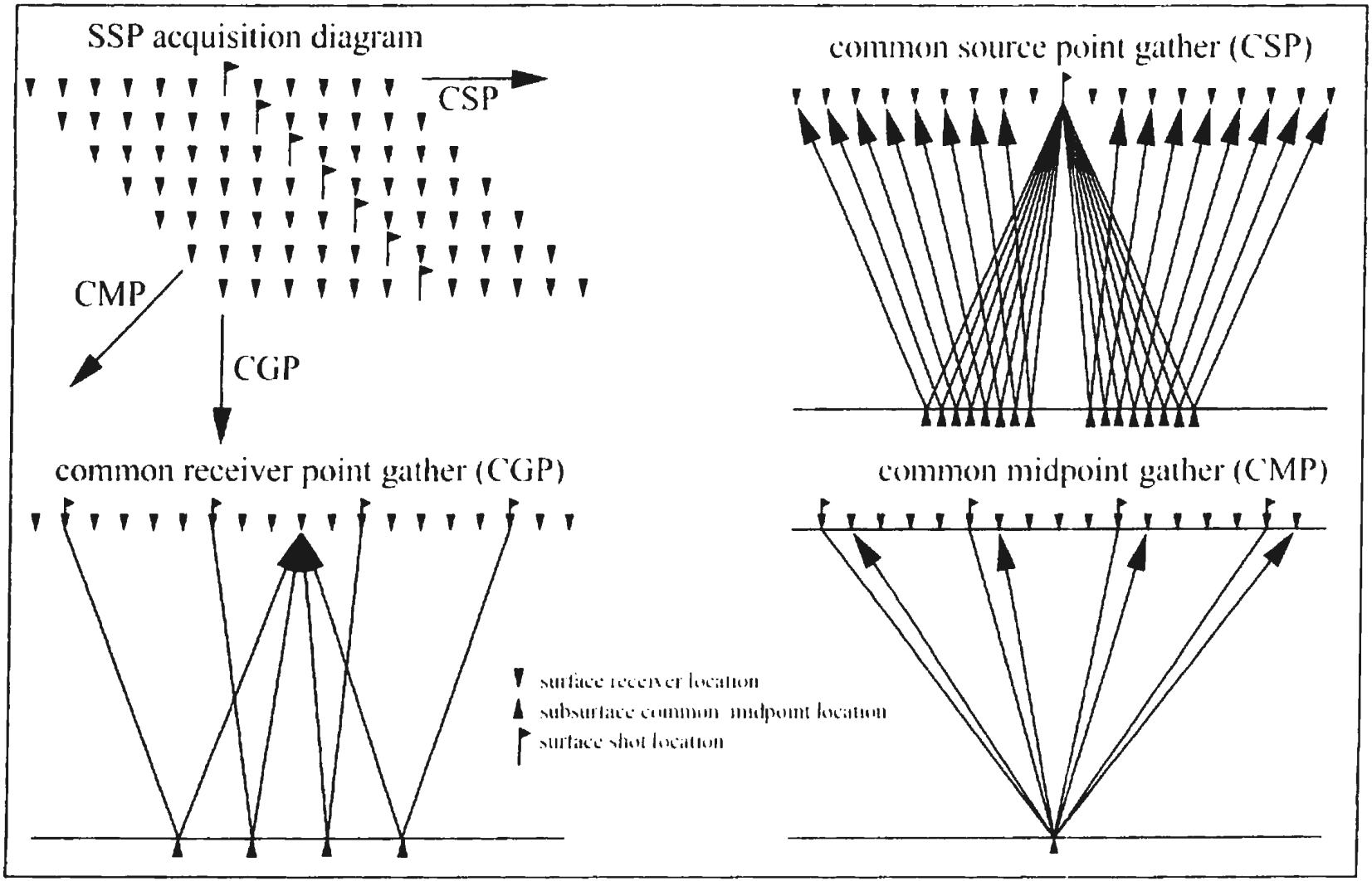

Figure 2.1.2 Conventional SSP land acquisition design and related data domains of common shot point gathers (CSP), common receiver point gathers (CGP), and common midpoint gathers (CMP). Less subsurface area is sampled in the CMP domain, minimizing differences in traveltime with offset direction.

are sorted from common shot (CSP) gathers to CMP gathers to facilitate processing and stacking, the main advantage being that the subsurface volume sampled by reflection raypaths is minimised in the CMP domain. Since this helps obviate differences in traveltime with offset direction, typical pre-stack velocity analysis and multiple suppression methods are applied to CMP gathers as opposed to CSP. However, since conventional land SSP acquisition employs a shot point for every N geophone stations, CMP fold is reduced relative to CSP fold and aliasing becomes a concern, both at far offsets where reflection moveout is greatest, and at offsets where surface modes are present. This may require the use of groups of CMP's sorted to common absolute offset (COF) gathers, a routine pre-stack analysis domain for land acquired SSP data. The misleading term 'COF stack' is used in industry to represent supergathers created by binning a sufficient number of adjacent CMP gathers to represent all offsets and then sorting on offset before summing within single absolute-offset bins. The number of CMP's included in a COF gather depends on the binning strategy (Figure 2.1.3). To achieve receiver spacing in CMP gathers when a shot occurs at every Nth receiver requires that N adjacent CMP's be gathered, but 2N CMP's are usually binned to obviate gaps in shooting geometry. (In this case study, receiver spacing is 17m and shot spacing is 85m prompting for 10 CMP binning). Single offset binning minimises structural, static, and dynamic smearing effects but if S.N is insufficient, then NMO can be applied and subsequently removed after more offsets are stacked in each bin. This creates an Ostrander gather as commonly implemented in AVO analysis (Ostrander, 1984), and such a gather can be used to enhance evaluation of CMP oriented processing techniques in CMP space.

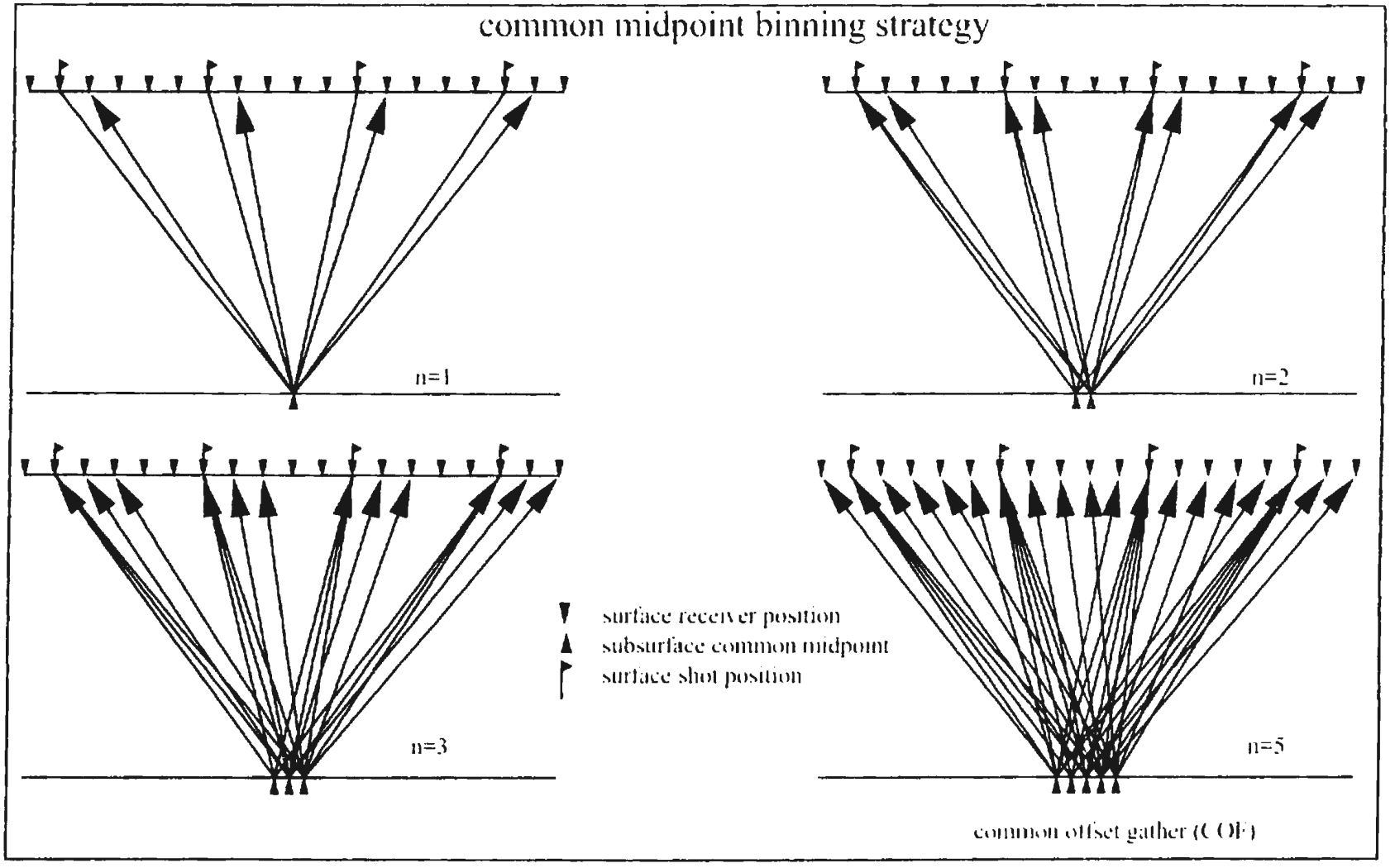

Figure 2.1.3 Common midpoint binning strategy for conventional SSP land acquisition. For a shotpoint at every fifth station, 5 CMP's are required to represent all offsets in a common offset gather (COF). As more CMP's are binned, offset representation becomes redundant, thereby increasing S/N following stacking within each offset bin.

The PanCanadian Nisku SSP data set was supplied as digital SEG-D shot records with observers and line-chaining reports, and a digital SEG-P1 survey for the straight line shooting geometry. Following conversion of data format, CMP pre-processing generally involves application of geometry, trace edits, and gain compensation (Yilmaz, 1987). The combined effects of spherical divergence and absorption suggest the use of a t^2 gain recovery but this is typically reduced to $t^{1.5}$ for adequate compensation in the WCSB. Trace editing is performed interactively with editing criteria and data conditioning determined by data quality and noise characteristics. CSP gathers are edited under full-band automatic gain control (AGC) conditions to remove low S/N traces in the zone of interest, while common receiver groups (CGP) were corrected for polarity reversal in that domain. During editing, first breaks were picked for refraction static analysis, and variation of seismic noise was assessed to select appropriate regions of data space for reflection analysis. As illustrated by a simplified x-t distribution of events in a compressional SSP land experiment (Figure 2.1.4), this region should exclude times for first break energy (events 1 and 3) and other non-reflective events such as ground roll.

Design windows used in surface consistent scaling and deconvolution should exclude contaminated regions of x-t space. If this is impossible, or if intermediate processing would benefit from the removal of this noise, then some rejection criteria are required. Shot records for this survey indicate coherent noise in the form of surface trapped Rayleigh waves (ground roll), reverberating refraction energy (head waves), and other source generated noise which is largely incoherent. Ground roll and head waves propagate as plane waves having linear moveout defined by apparent velocity $V_{app}=x/t$. Usual rejection criteria follows from examination of data in f-k space where such events with linear moveout

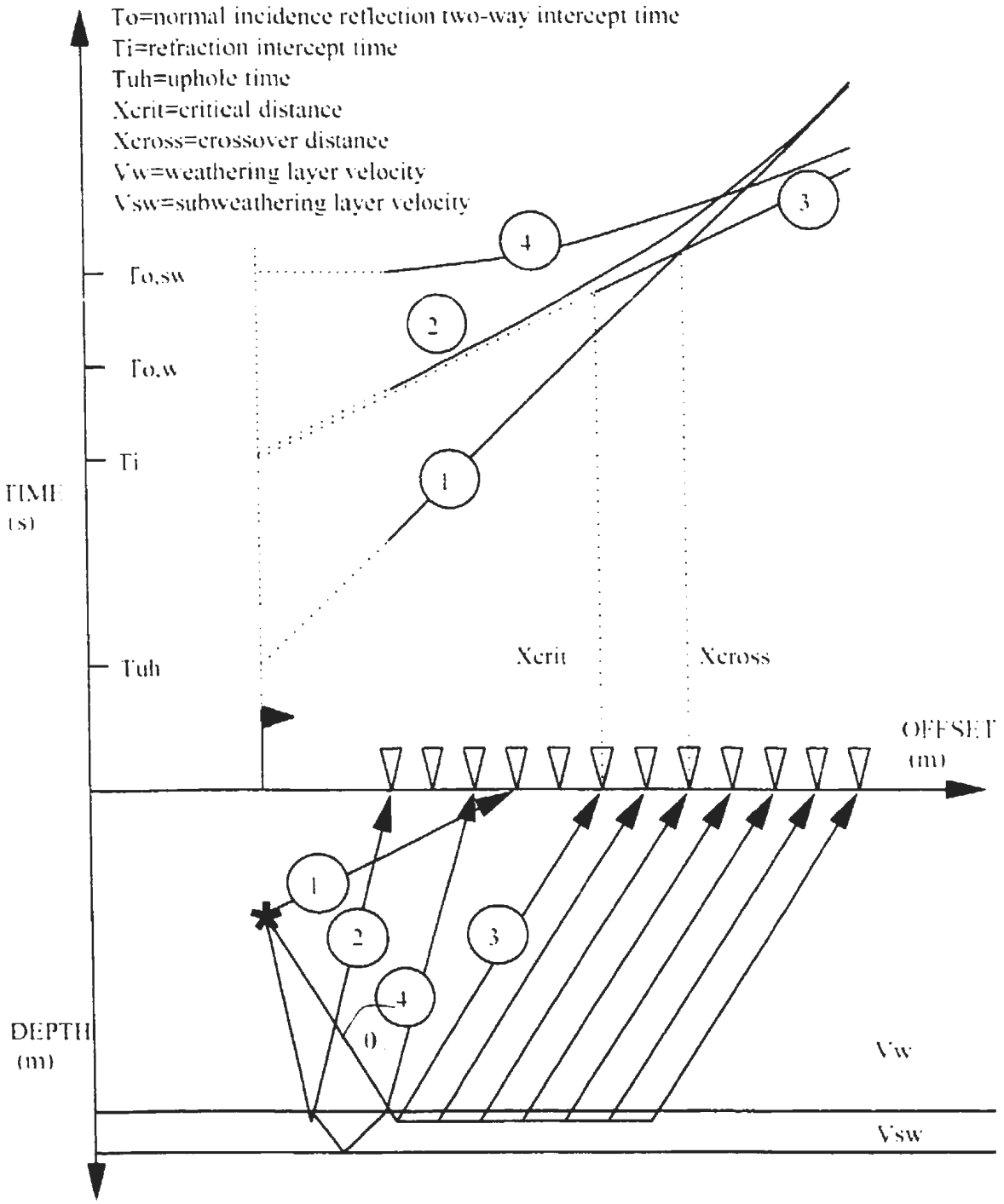

Figure 2.1.4 The expected time-offset distribution of events in a p-wave SSP land experiment. The direct arrival (event 1) intersects with the refracted arrival (head wave, event 3) at the crossover distance, and is asymptotic to the reflected arrival (hyperbolic, event 2) at sufficient offset. Total internal reflection occurs at the critical distance where event 2 intersects with event 3. Later reflections (event 4) are distributed in x-t space as a function of velocity distribution with depth.

transform to points along velocity trajectories defined by f-k. In this domain the nature of event aliasing and dispersion can be assessed.

At the embayment location, a CSP gather (Figure 2.1.5a) illustrates typical SSP data quality for this survey. Apparent velocity defined by refracted first breaks indicates a three layer near surface structure. At this location, head waves are non-reverberative and propagate at about 2700m/s to 300m, then at 2900m/s to the far offset of 2057m. In the zone of interest, data are characterised by strong reflections (hyperbolic events) with interference at near and mid offsets by seismic noise. Reflection amplitudes compare with surface wave amplitude (reasonable S/N) because arrays are designed to attenuate horizontal propagation. Residual direct arrival (V_{app}=860m/s) propagates slower than uphole velocity at the shot (970m/s) but correlates with uphole velocity laterally (see Figure 2.1.7). High-amplitude noise dominating near offsets consists of coherent air blast (hole blowout) in conjunction with incoherent anelastic deformation effects (shot generated noise), as well as residual ground roll contamination. The lack of well developed air blast (with apparent velocity near 330m/s) is also not surprising since holes are drilled to a depth of 24m. Overall, a lack of coherency is exhibited by this near offset noise for this TRA display, but the corresponding f-k spectrum indicates coherency associated with this energy. This noise dominates the low frequency band 0-20Hz, and this energy could be spatially aliased (wrap around in f-k space). The low frequency reflection response would benefit from the removal of this noise. The refraction mode is identified in f-k space based on apparent velocity and is well sampled spatially within the frequency band 0-85Hz by anti-alias spread design. Because deeper reflections tend to have progressively less moveout than the refraction from sub-weathering due to $V_{RMS}(z)$ increasing , reflection energy can be enhanced by f-k polygon rejection of all

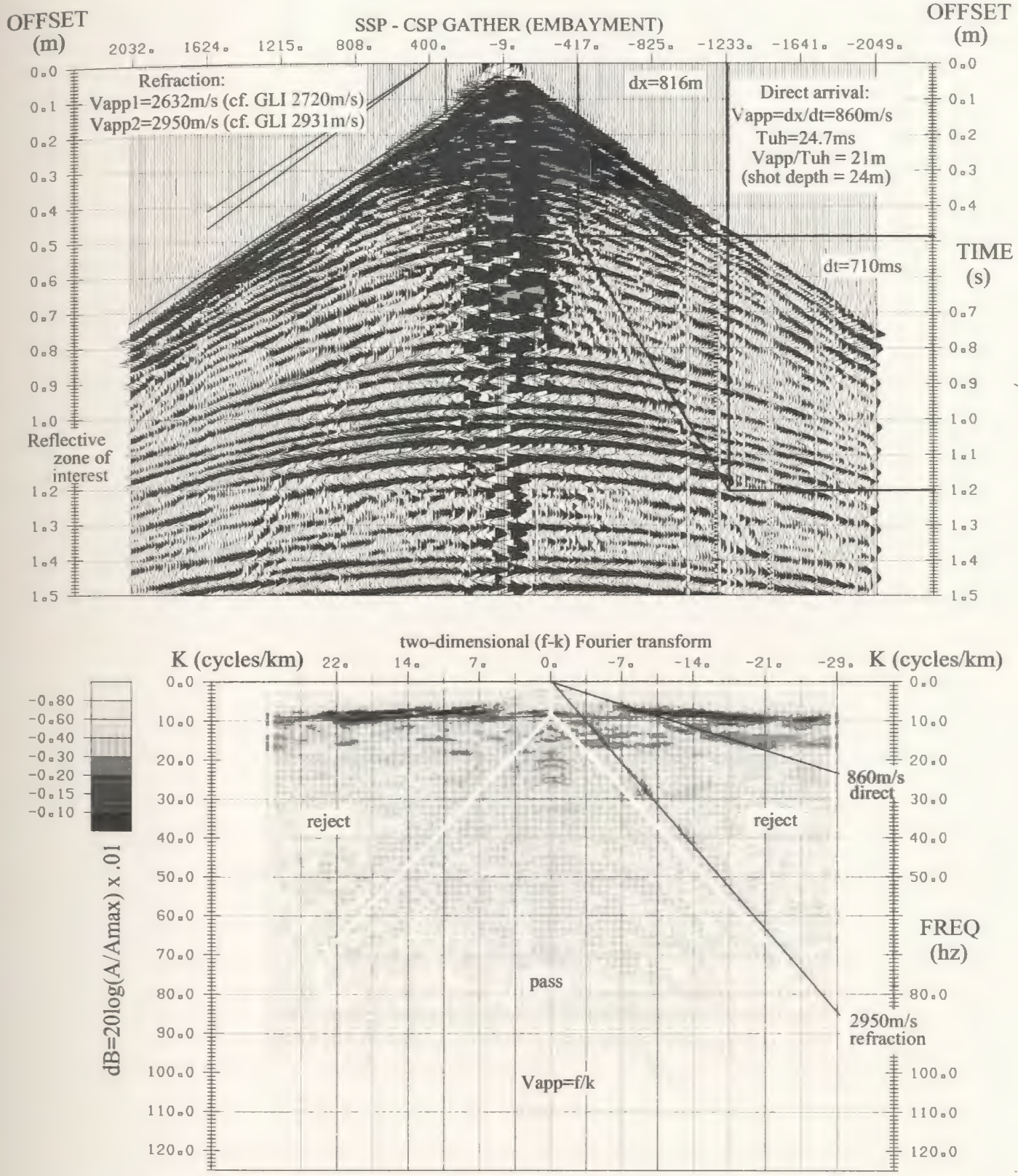

Figure 2.1.5a Shot record (top) from the embayment location (stn. 5210). Gain compensation and total static (fixed datum above topography) is applied to bandlimited (12/15-80/95Hz) TRA data. The f-k spectra (bottom) shows coherent noise (refraction mode at 2950m/s) and less-coherent source generated noise, airblast, and residual grondroll (dispersive near-offset low-frequency high-amplitude noise) which can be removed by f-k filtering to improve shallow analysis.

energy with $V_{app}<V_{sw}$. The f-k spectrum (Figure 2.1.5b) shows improved S/N but residual blast noise occupies near-zero wavenumbers (as does reflection energy) and becomes smeared on the inverse transform.

A shot profile from the shelf location indicates how coherent noise varies over the survey (Figure 2.1.6). Here, the refracted mode is highly reverberative, and shot generated noise is strong at near offsets. Both of these coherent noise modes appear dispersive in f-k space, as is expected for wave propagation within low velocity media. Ground roll appears to be directional in nature, suggesting a lateral change in surface conditions and possibly variation in array attenuation.

Although the seismic noise appears strong relative to reflection energy, the problems are not severe enough to warrant the usage of f-k enhancement for a final conventional stack since surface consistent design windows can exclude the noise. Intermediate processing for an improved near offset response will benefit from f-k rejection applied to COF gathers where events with negative wavenumbers can also be rejected. However, since head waves propagate faster than critical reflections from the same reflecting refracting interface, this shallow reflection and possibly others will be attenuated at sufficient offset. Since critical reflections are usually muted before stack, the normal incidence response should be improved by f-k enhancement following deconvolution.

Following noise evaluation, surface consistent scalars were calculated for TRA shot receiver normalisation. Near offset traces out to 357m were excluded, and far offset was limited to 1800m to minimise offset effects while including the best data and maintaining reasonable receiver fold for statics. Bandwidth was maximised at 12/16-80/100 Hz due to lack of coherent noise within the design window. Finally, shot and receiver

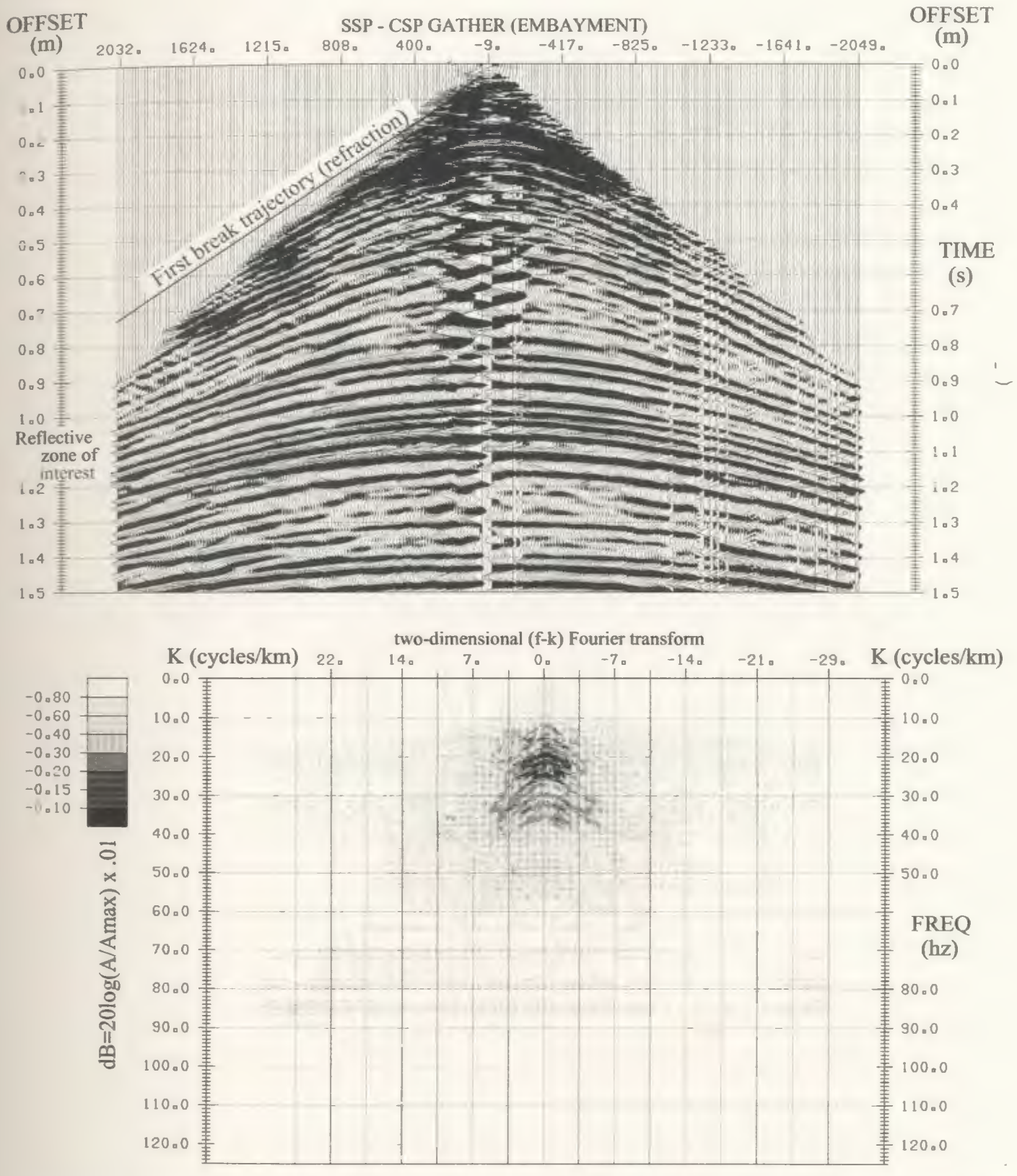

Figure 2.1.5b Post f-k shot record (top) from the embayment location. Filter design attempts to remove velocities less than or equal to the refraction mode. Note that near-offset amplitudes are compromised by residual shot generated noise (non-coherent), but reflection energy is now the dominant energy in the record.

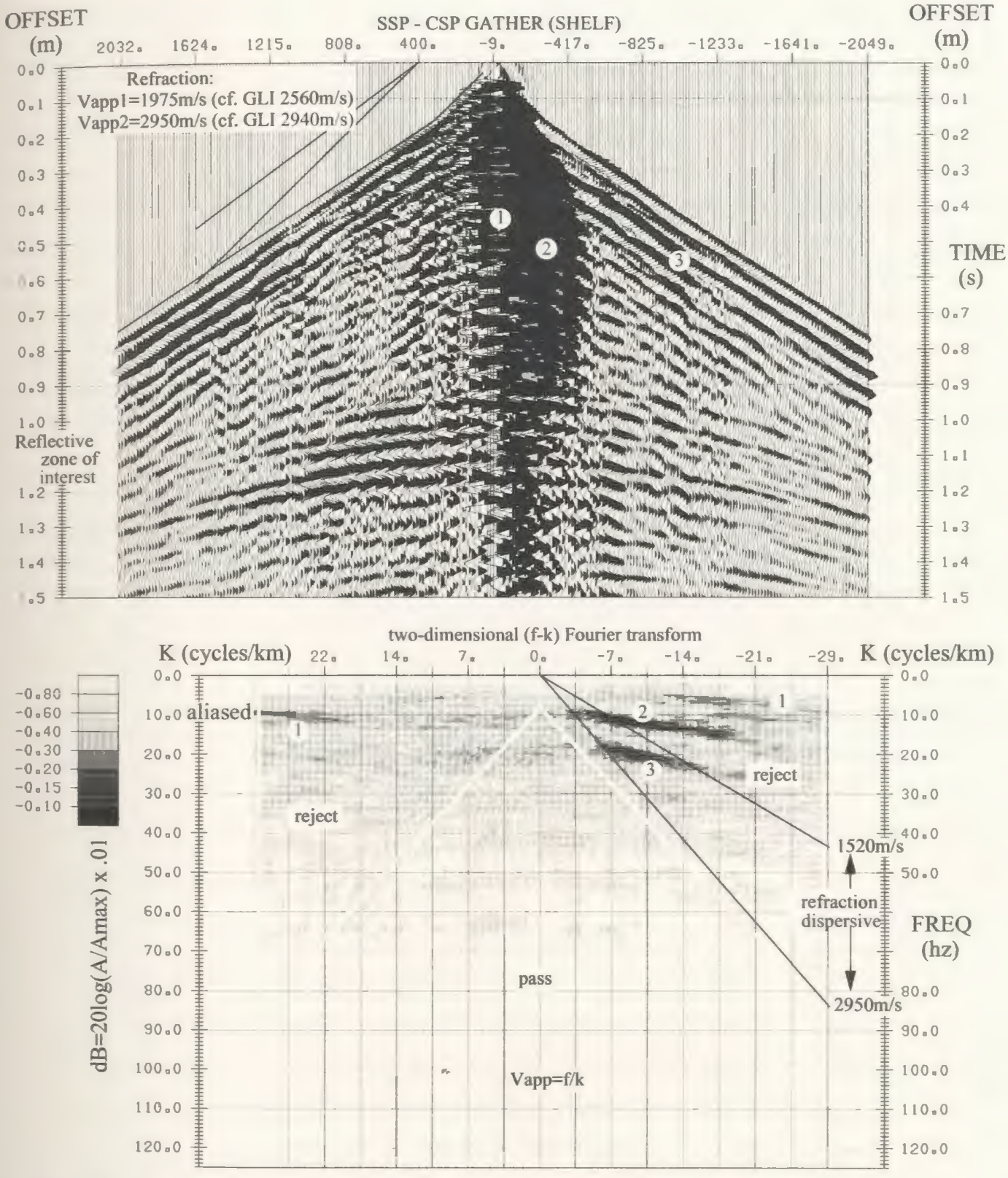

Figure 2.1.6 Shot record (top) near the shelf location (stn 6960). The f-k spectra (bottom) shows three coherent noise components: 1) aliased airblast and/or shot generated noise, 2) dispersive residual surface mode (ground roll), and 3) dispersive refraction mode and reverberations. (Refraction energy may appear dispersive in part due to more than one refracting layer).

scalars were computed by iterative least squares. These scalars attempt to balance reflection signal before computation of surface consistent deconvolution operators, the next sequential step in SSP processing.

First break refraction analysis is typically performed before any phase effects of deconvolution are introduced. The data are generally scaled using a short AGC window to help define the first breaks, and a down-kick typically represents the refraction break given industry normal polarity. Once completed, the picks are analysed for lateral variation in timing delay at the shot and receiver due to changes in near-surface thickness and velocity. Typically, the largest occurrence of this variation is in the surface weathered layer. However, since the crossover distance X_{cross} is generally at least double the weathering thickness, the direct wave is usually not well sampled as the first break. This is typical since conventional station spacing ranges over 10-30m with one to five stations in the shot gap, while weathering thickness may average 1-40m over a line. Instead, uphole times and shot depths determine weathering layer velocity, or velocity on the order of 600-800m/s is assumed in the WCSB.

GLI [TM] was used to analyse first break SSP times, create and update a near surface model, and generate static corrections to remove distortions caused by near surface anomalies (Hampson and Russell, 1984). During first break analysis, the layering and velocity properties of the initial model are defined based on manual linear fit to refracted first breaks. Lateral variation in layer thickness and velocity is obtained by associated changes in slope and intercept of successive subweathering layers. (Vertical velocity gradients require curved refraction trajectories hence are not incorporated). In general, the offset range of the acquisition geometry sets the limit on maximum refractor depth for a

given velocity distribution, and within this depth range the number of resolvable layers is allowed to vary by specifying layer pinch-out to zero thickness. In the WCSB, the typical static model consists of 1 to 3 layers above a hardrock surface. The picked first breaks represent refraction from the base of weathering (at layer 2 velocity), and base of subweathering (at layer 3 velocity, or hardrock velocity). The inverted GLI [TM] weathering model and associated delay characteristics of the present Nisku survey are presented in Figure 2.1.7.

The forward modelling scheme in GLI [TM] uses a ray-tracing approach so that the geologic model requires smoothing to prevent instability, but consequently sacrificing resolution. The fundamental ambiguity between layer velocity and thickness suggests a longer smoother for velocity than thickness in order to attribute rapid changes to thickness. The recommended depth smoother length is on the order of 1/15th of the typical maximum offset picked. Smoothing may be applied to layer thickness or elevation for equally reliable statics. Smoothing layer thickness may cause short-wavelength topography to be mirrored in layer boundaries, although thickness is sampled directly by first breaks. Smoothing elevation causes absolute boundaries to be smoothed thereby creating a more geologically meaningful model since topography is not expected to be controlled directly by subweathering relief. In comparison, a velocity smoother on the order of double the maximum offset picked is recommended.

The GLI [TM] static calculation method involves downward continuation from topography through the model to the base of the deepest layer, then upward continuation to a seismic reference datum (SRD). This effectively replaces the derived model with equivalent thickness at a replacement velocity (V_{REPL}). The static solution after complete inversion

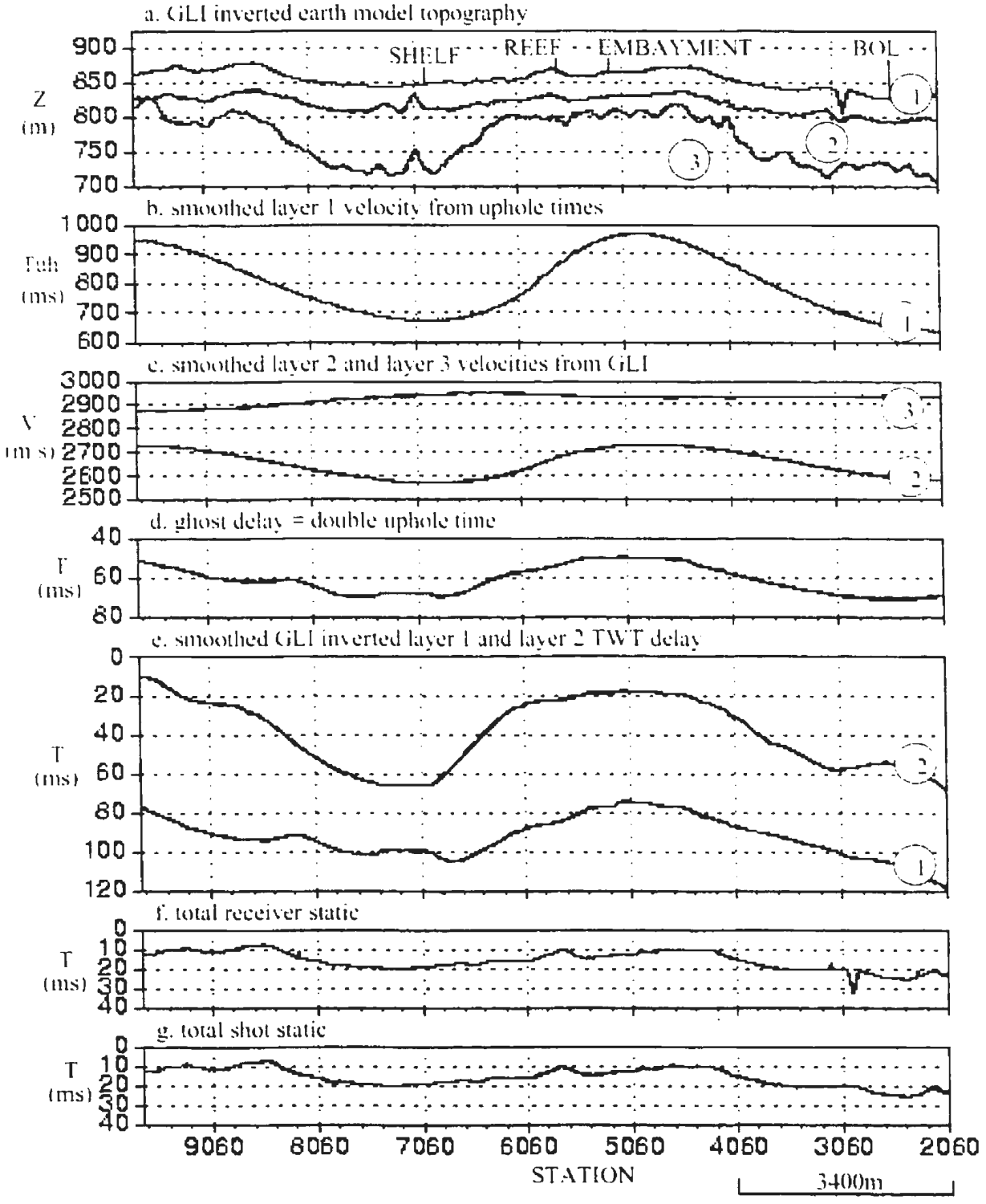

Figure 2.1.7 GLI surface model topography (a) inverted from SSP first breaks. Smoothed layer 1 velocity (b) is derived from uphole times and constant shot depth of 24m. Smoothed layer 2 and 3 velocity (c) is inverted from GLI. Ghosting delay (d) is compared to smoothed weathering layer delays (e) as derived from GLI. Total receiver static (f) and total shot static (g) are also presented.

consists of long-wavelength effects from the smoothed derived earth model, including long- and short-wavelength elevation statics from topography to processing datum. Hence, the depth smoother length is also used to distribute statics between short- and long-wavelength components, but a separate short-wavelength static calculation follows the model based correction. High frequency statics still exist since a relatively small number of layers are used, and also due to smoothing of model layer thickness and velocity so that the model misses detail.

Short wavelength surface consistent residual statics roll through the spread (unlike structural components or residual NMO which may be mistaken for static), so that shot and receiver components must be solved to correct representative traces within CMP bins. These statics are computed from static corrected refraction picks as simple surface consistent time delays in the final residual error, then incorporated into the solution (Wiggins et al, 1976; Chun and Jacewitz, 1981). This requires good quality picks and sufficient fold and offset representation for all shots and receivers, but may eliminate the need for residual statics based on correlation of reflection events.

Following the refraction static analysis, a surface consistent residual static analysis attempts to remove statics based on correlation of reflection events relative to the CMP stack. This requires CMP gathers with equalised and deconvolved amplitudes corrected for model statics and NMO. Hence, the success of the method depends on signal to noise (S/N) ratio, structural effects, and problems associated with independent application of static and dynamic corrections that are inherently related by the time variable in the NMO equation. Since the quality of the refraction statics solution will effect coherency in velocity analysis,

it is beneficial to solve high frequency statics using refraction information so as to avoid iterative reflection statics and velocity analysis.

In contrast to static correction using a fixed SRD and V_{R1-P1}, the floating datum idea seeks to minimise the total static applied within a CMP bin by choice of these parameters. Following velocity analysis and NMO application, each CMP is referenced to a fixed datum before or after mute and stack. In this sense a floating datum will introduce false regional structure from a velocity analysis timing viewpoint, but local stacking velocity (V_{RMS}) estimates should be more correct since normal incidence two-way-time (t_0) will be more correct in the NMO equation. Hence, a floating datum is suggested for large variations in total static, a condition generally associated with large changes in topography. Such cases may also warrant spatial variance in temporal design of deconvolution operators to maintain consistent reflection content.

The deconvolution operator design objective is to include the same coherent reflectors within the design window while excluding surface modes and other zones of anomalous signal. For near offsets, low frequencies are dominated by surface waves. Reflections undergo frequency dependent absorbtion that increases with frequency, time, and offset. Tuning of closely spaced reflections also varies with offset due to NMO. For these reasons, high frequency components at maximum offset and low frequency components at near offsets may bias spectral estimates used in surface consistent deconvolution operator design. The conventional approach is to include an offset component in a least squares inversion but generally this component represents an average over the entire line. Instead, wavelet spectra may be better represented in the near offset signal by avoiding data space suspected of being anomalous. Refraction and their reverberations

typically exist for all offsets, but pre-deconvolution filtering to remove this undesirable signal will influence operator design. Wavelet spectra should not be modified by any filter response before operator design. Prior to and after deconvolution, bandwidth should only be restricted by a low-cut filter which serves to remove bias, and frequencies should be allowed to extend to a level corresponding to the anti-alias field filter. Also, provided that design windows are at least ten times the operator length, spectral estimates are less sensitive to variations in temporal content caused by static effects. This robustness allows deconvolution to provide reasonable results in many cases without lateral variation in operator design.

To assess the appropriateness of operator design, stacking of spectra in various domains before and after deconvolution may be required to determine lateral and temporal variance in frequency content and hence operator design. Operator length is typically chosen based on short lag values of trace autocorrelation (Sheriff, 1981), the zero-phase time response equivalent of trace power spectra. Since stacking is a linear process, autocorrelations after stack should give the same operator criteria as stacked autocorrelations. At increased autocorrelation lags, offset effects of NMO become obvious and the stack will attenuate these components while enhancing the short lags due to lack of NMO in the basic wavelet. NMO application will cause wavelet stretch increasing with offset, thus distorting the basic wavelet at short lags while longer lags will become more consistent with offset and hence stack better. To preserve offset effects under boosted S/N conditions, it is convenient to assess autocorrelations of COF gathers across the survey. Once an operator length is chosen, pre-whitening is required to avoid operator instability.

Appropriate levels can be determined by relative level of high frequency signal after deconvolution. This is best determined by amplitude spectra as opposed to autocorrelations.

Pre-processed SSP COF gathers (Figure 2.1.8) represent slightly boosted CMP S/N conditions for this Nisku study. At the beginning of line (BOL) and shelf locations, refractions and their reverberations are a problem at mid and far offsets while at the reef, near offsets show residual ground-roll. Shallow times and small offsets are considered too contaminated by noise to be included in design, and a low S/N shallow image is expected. Although wavelet spectra require restoration, tuning effects in the short autocorrelation lags appear strong for far offsets at the reef location suggesting offset limitation in operator design. Otherwise, autocorrelations show a somewhat consistent short-lag character over the survey and indicate that a standard 80ms operator length should be appropriate for spiking deconvolution.

When data quality is poor and standard deconvolution design criteria leads to unstable operators, trace-wise spectral balancing is an option. The RHO filter (Claerbout, 1985) application involves scaling spectral amplitudes by their powered frequency value (f^{ψ}) such that power values (ψ) exceeding unity increase amplitude more for higher frequencies. Averaged post-whitening spectra would indicate the required powering. A problem in this method is the inability to balance high amplitude spectral components caused by mono-frequency noise sources or by event tuning. A more adaptive approach involves division of the bandwidth into several components, each gained by AGC in time before recompositing by addition. Relative amplitude can be maintained in time by subsequently removing AGC effects. Frequency bands and tapered overlap zones are selected by averaged pre-whitened spectra, and supported by post-whitened spectra based on recovery of major spectral roll-

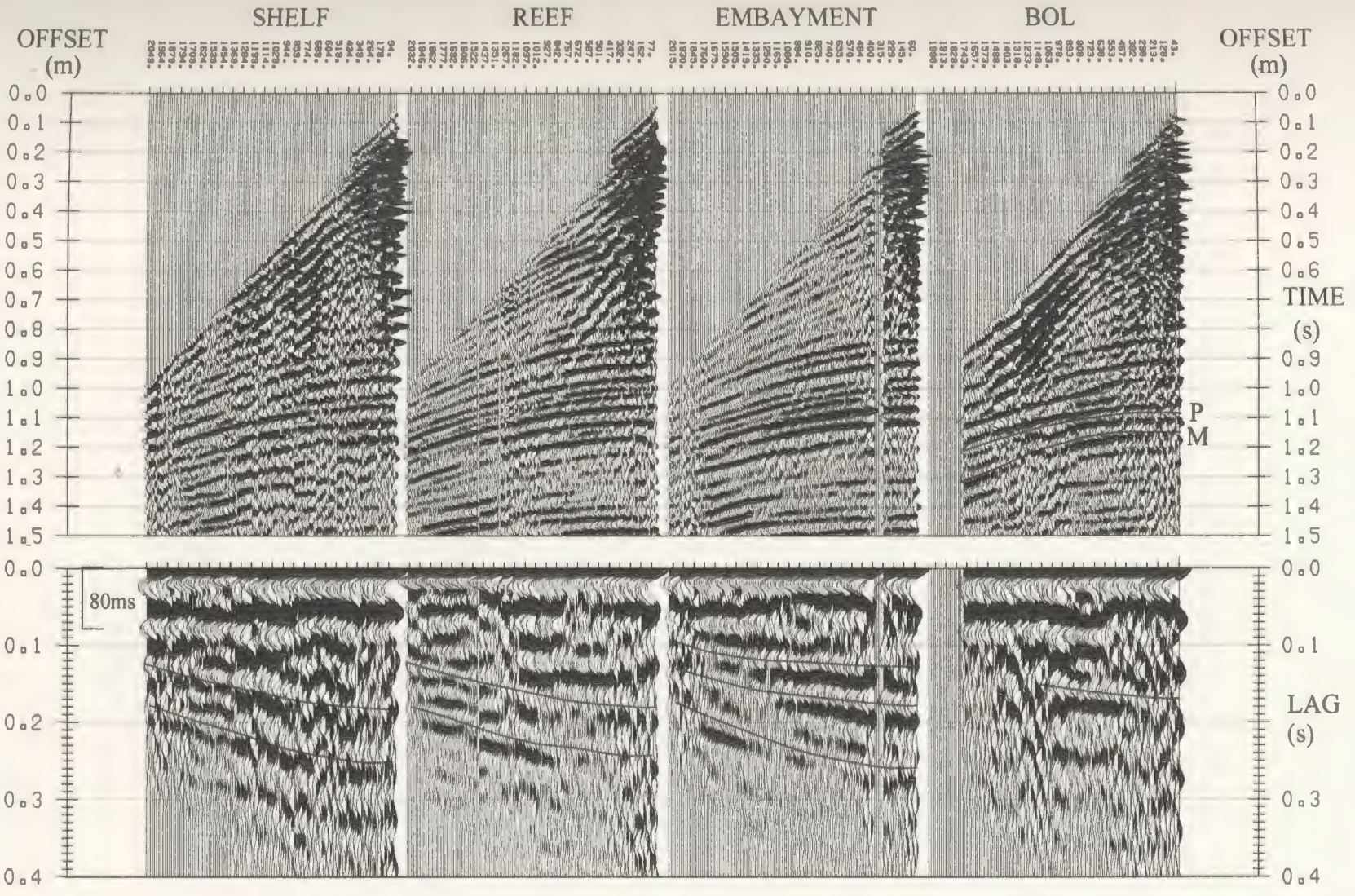

Figure 2.1.8 Preprocessed SSP common offset (COF) gathers (top) gathered using station spacing (17m) as absolute surface offset bin size within 10 adjacent CMP's. Processing stream is gain, statics, bandpass (12/15-80/95Hz), mean scaling (1.0-2.0s) and front end mute. Autocorrelation design window (bottom) is 700-1300ms at 34m and 1000-1300ms at 2057m. Basic spiking deconvolution operator design criteria suggests that a standard 80ms operator length should be sufficient.

offs. Wavelet phase is not affected, and phase compensation typically requires the aid of a synthetic, making this method less attractive for minimum phase sources than for zero-phase sources.

Phase adjustment following spectral balancing could be determined from analysis of Q filtering effects using a model based approach aided by VSP processing. Inverse Q phase compensation could be applied, and any residual phase could be determined by synthetic matching. This approach could be attempted without any Q analysis for comparison, since constant phase adjustment plus static shift is equivalent to phase spectra that increases linearly with frequency (in analogy to Q). Fortunately, spiking deconvolution provides a stable well-behaved residual wavelet in this Nisku study, obviating the need for frequency domain methods.

Some aspects of conventional SSP pre-processing have been introduced in this section in a general context. The SSP data from a specific experiment have been presented in the form of CSP gathers to illustrate the basic events recorded in SSP reflection experiments, to illustrate data conditions, and to illustrate details of parameter selection as appropriate. Further details relating to pre-processing are presented in Chapter 5. The results from first break analysis were presented in this section to illustrate the potential for peg-leg multiple generation in the weathered layer. The concept of COF gathers is introduced to facilitate the assessment of data quality in the CMP domain, and this processing viewpoint will be carried through the text for the purpose of evaluating multiples and multiple suppression.

2.2 SSP Velocity Analysis, CMP Stacking, and Multiple Identify

Multiple reflections in SSP data can be identified in a variety of ways. Hyperbolic semblance stacking velocity analysis can indicate multiples on the basis of moveout. Pre-stack autocorrelations of x-t (or tau-p) gathers can be used to identify obvious differential NMO that results in changing periodicity of events with offset (or ray parameter). Range limited stacks can also be used to identify multiple events on a moveout basis, and stack autocorrelations can be used to identify lateral changes in mechanisms. Windowed and band-limited autocorrelations from the shallow section are useful in investigating near-surface related multiples (surface related noise is wide-band in the shallow section). Multiples may be identified, but suppression must overcome problems that exist due to wavelet nonstationarity, low S/N, more than one multiple mechanism, coloured primary reflectivity, and small differential NMO.

In CMP processing, the basic principle is that CMP gather reflection arrivals are closely approximated by the hyperbolic t-x relation $t^2 = t_0^2 + x^2 / V_{rms}^2$ where t is the event two-way arrival time, t_0 is the zero-offset reflection intercept time, x is the lateral offset and V_{rms} is the root mean square velocity (Dix, 1955). Velocity analysis involves choice of the optimum velocity that maximises some chosen measure of hyperbolic coherency. For poor S/N conditions or where geology deviates from plane-parallel layering, advantages exist for using post-stack imaging criteria such as constant or function velocity stacking methods (Yilmaz, 1987). Lateral variation in velocity is chosen based on stack response to a suite of hyperbolic moveouts. For Plains data with good S/N conditions, the velocity spectrum is a measure of pre-stack hyperbolic coherency derived from CMP gathers processed for statics, deconvolution, binning, and signal enhancement. The coherency measure is contoured to

indicate optimal stacking velocity value that gives maximum coherency for each zero-offset time at a particular subsurface CMP location. This method is favourable since it allows choice of more realistic interval velocity distribution by providing discrimination against multiples on the basis of differential NMO.

Different measures of coherency are available for computation of the velocity spectrum. The procedure for the hyperbolic semblance velocity analysis (HVSA) measure at each vertical incidence time is to sum along a series of hyperbolic curves corresponding to an expected range of RMS velocities. The resolution of the method is controlled by summation within a properly aligned time gate at each offset, and is limited by the amount of constant-velocity NMO stretch (for a given bandwidth, window length must increase as velocity decreases). This method offers fine resolution of closely spaced events and discriminates against waveform amplitude variation. In contrast, the energy-normalised cross-correlation measure involves application of the suite of expected NMO curves before correlation over a window centred on each vertical incidence time. Unlike the semblance method, this method is negatively biased by wave amplitude variations (although it is common practice to apply AGC before velocity analysis) and is limited in resolution by length of correlation window. With properly prepared SSP data, hyperbolic semblance velocity analysis (HSVA) should optimise data input to residual statics, AVO, stacking processes, and multiple identification.

Characteristics of semblance velocity spectra allow multiple discrimination. In the marine case of surface layer related multiples, travel paths bounce at least once in the water column. The simple multiple is the water bottom primary reflection bounced between the air-water and water-bottom interfaces, and may be present with significant amplitude for

several orders of ringing with moveout increasing for each successive order. Peg-leg multiples are sub-bottom primary reflections trapped in the water column, and include redundant raypaths since the water bottom reflection is also bounced once from the deeper reflector. The V_{rms} trend for such a multi-ordered peg-leg ringing is to 'spin off' from the primary reflection toward lower RMS velocities than the primary velocity, becoming asymptotic to water velocity for large order ringing. As the multiple period increases relative to record length, multiples become more difficult to interpret as compared to shorter period reverberation. Interpreting the multiple as a primary results in a flat spot or an inversion in V_{rms}, which translates into an inversion in interval velocity. In such cases this seismic pitfall is controlled by knowledge that small scale velocity inversions over large depths are likely to be unreal.

The largest problem typically encountered when performing HSVA on Plains SSP is low S/N ratio. HVSA assumes that the signal under analysis is primary reflection events from near-horizontal reflectors, hence all non-hyperbolic events are considered as noise. If a good S/N level exists, then the next significant problem is the quality of the static solution. This quality rests on the assumption that the data conform to CMP assumptions, namely that reflections from the near-horizontal subsurface follow near-vertical raypaths through the near-surface low-velocity weathered zone. This criterion is usually well obeyed when large differences in velocity exist across the base of this layer (according to Snell's law), but the base of the weathering layer may not be near-horizontal. If the refraction statics solution is of poor quality as a result, then the residual statics must be determined by correlation methods applied to reflection energy. The success of this method is limited by the nature and

quality of the defined velocity distribution, as velocity analysis and reflection statics complement each other.

GLI [TM] statics are applied before HSVA analysis is performed. Typically, analysis would progress along with the overall statics solution. Initially, a single brute stack velocity function might be picked and applied to data with only datum-based refraction model statics applied. After a brute CMP stack and surface consistent residual reflection statics, a typical spatial velocity analysis increment of 1000m could be employed and checked again following successive passes of residual statics. The spatial density of the analysis will allow discrimination against local non-dynamic effects, meaning that analysis positions should be chosen to allow dynamic corrections to be extrapolated through zones of obvious structure as identified on the CMP stack. Factors that control quality and efficiency of velocity analysis include record length, offset window, front-end mute, gather and offset binning, bandwidth, residual statics, scaling, and semblance sampling parameters.

Semblance sampling parameters should be set initially to cover the expected velocity range so as to identify multiples and to identify the range of velocity variation within zones of interest. If desired, temporal variation in velocity range can be accommodated by linear extrapolation, but a consistently wide initial range allows identification of narrower velocity ranges associated with primaries and multiples. A constant velocity range also removes the possibility of NMO stretch due to velocity increase (NMO decrease) with time, so the only source of stretch in the analysis is attributed to changing normal incidence time. Given typical Plains acquisition parameters and velocities encountered, NMO stretch effects are usually absent in velocity analysis but must be considered when the blocky V_{RMS} function is applied to the data. Once the velocity range has been selected, the inclusive number of

hyperbolic trajectories are defined for each normal incidence time by equal division of the velocity range. In general, this should be set to allow the maximum trajectory-moveout accuracy of one sample at the far offset. However, this accuracy is easily lost in the presence of structural and static components, and the process of NMO stretch reduces signal enhancement realisable by optimised velocity analysis.

Following stacking velocity analysis, NMO is computed and the dynamic corrections are applied to CMP gathers. Because velocity generally increases with depth (or time), the NMO for primary energy has the natural tendency to decrease with increasing zero offset time. By analogy, the effect of NMO application is to cause temporal stretching of non-zero offset traces since an event (wavelet or wavelet superposition) is of finite duration and not a series of spikes defining a hyperbolic trajectory in t-x space. This NMO stretch causes a shift to lower frequencies that becomes more pronounced as offset increases. For a given offset, times at the beginning of the event are shifted upward in time more than times at the end of an event. The event spans more than one normal incidence time sample hence the end of the event has less NMO than its beginning for the same velocity. This effect would become more pronounced as the velocity gradient increased with depth, and the event lost more frequency band with offset due to absorption and phase delay. Although control of NMO stretch is provided by specification of tolerance, this definition is not based on usable seismic bandwidth. Instead, this refers to the amount by which the Nyquist frequency (F_N) can be stretched before further offset samples at that vertical incidence time are muted. Once dynamic corrections have been applied, the data can be stacked.

Processed COF gathers are used to illustrate the application of HSVA and related multiple identification in this Nisku study. The gathers (Figure 2.2.1a) show boosted

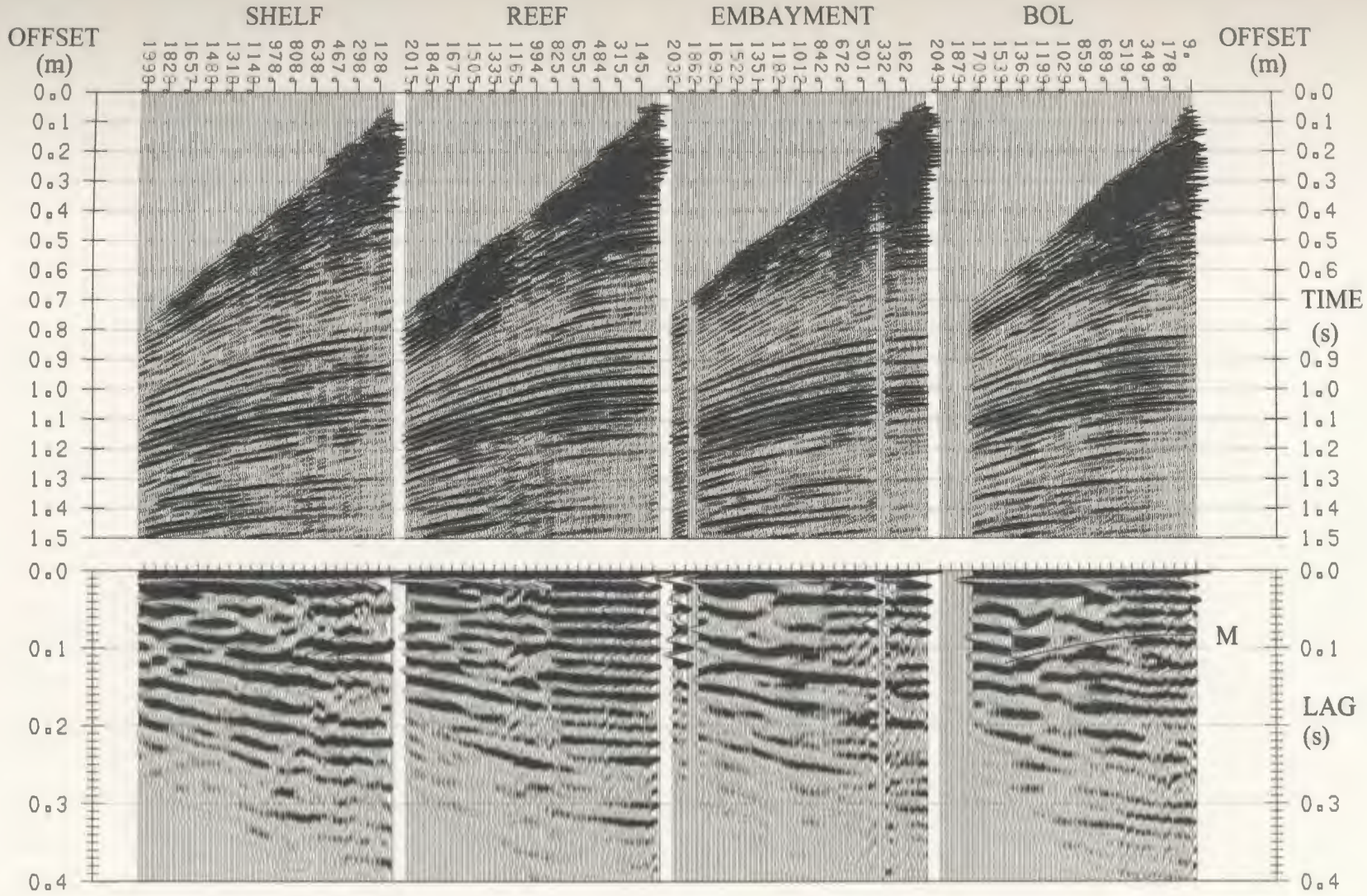

Figure 2.2.1a Processed SSP COF gathers (top) and autocorrelations (bottom). Processing stream is gain, statics, spiking deconvolution, f-k reject, normal moveout, bandpass, mean scaling, front end mute, trim statics and NMO removal. Spiking deconvolution is surface consistent with simultaneous shot and receiver components using 1% PW and 80ms operator. F-k rejection attenuates refraction mode and reverberations, surface modes, and negative wavenumbers. Autocorrelation design window is 700-1300ms at 34m and 1000-1300ms at 2057m.

frequency content after deconvolution, but since operators have been derived from the deeper portion of the data to avoid noise, the shallow amplitudes have been overcompensated partly due to wavelet non-stationarity. Deep window autocorrelations show more tuning effects with offset at short lags than raw data due to bandwidth, show at least one multiple at the BOL location on a moveout basis, and show dominant short period reverberation at near-offsets, especially at the reef location. Velocity spectra (Figure 2.2.1b) indicates multiple energy near 1.2s, and this indicator is strongest at BOL where differential NMO is greatest and agrees with results obtained by using velocity picks in the NMO equation. After primary NMO application (Figure 2.2.1c), autocorrelations indicate the expected influences of NMO stretch with offset, but also show changing multiple periodicity with offset at BOL. These aspects of pre-stack multiple indication can be further analysed in an efficient manner by processing the whole line using the preceding strategy, and stacking.

CMP stacking is generally performed using the n'th root principle (McFadden et al, 1986). This method involves division of stack amplitude at any given time sample by the number of non-zero (non-muted) elements raised to the n'th power. The S/N ratio is increased statistically by the square root of the number of samples, invoking a typical powering of 50%. However, land SSP data usually suffer from variable fold requiring a stack power of unity to avoid post-stack temporal banding of amplitudes by reducing the stack to a simple averaging process in time. Variable fold conditions are common due to laterally varying front-end mute caused by NMO stretch or spatially variant mute functions, or from gaps in the shooting program. Although random noise can be discriminated against by this method, fold must be temporally consistent throughout the survey to allow the n'th root principle to be utilised in improved S/N. Instead, post-stack S/N amplitude

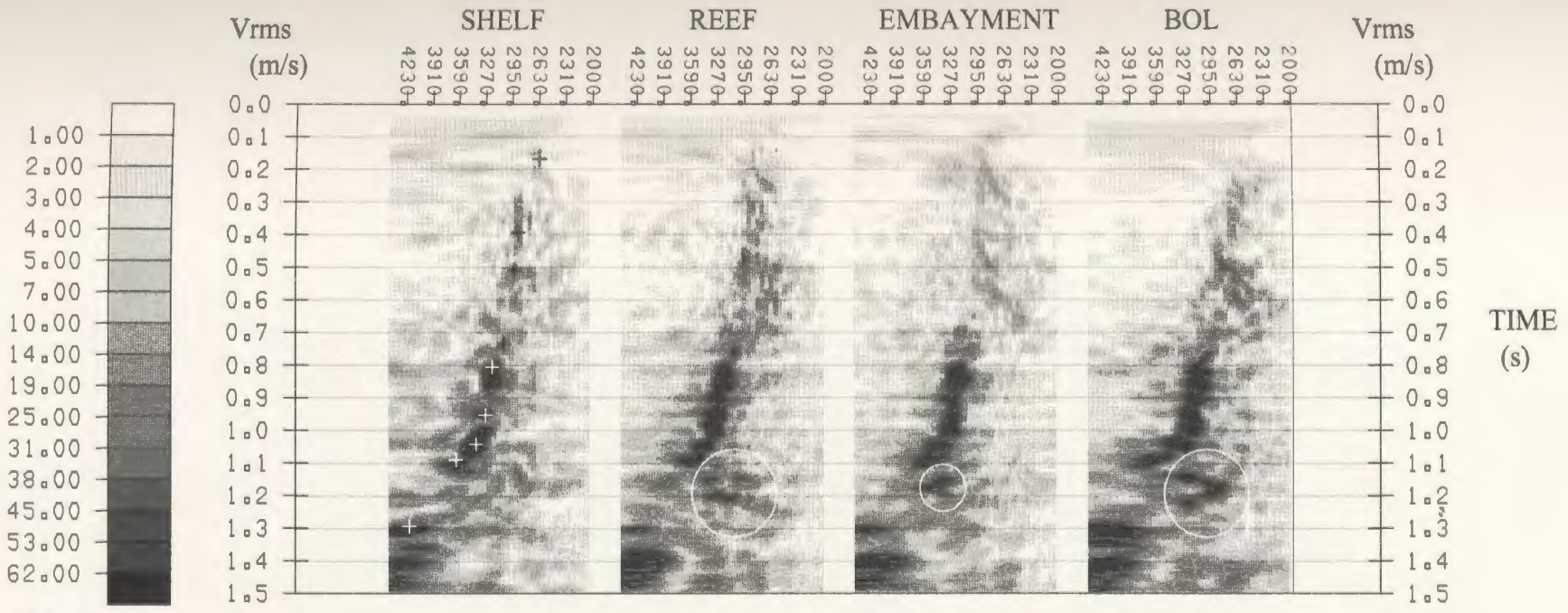

CDP 6970

TIME	V-RMS	V-INT
180	2650	2650
399	2775	2874
512	2875	3203
742	3025	3335
817	3175	4391
946	3275	3848
1049	3400	4384
1092	3550	6167
1293	4025	5979

CDP 5700

TIME	V-RMS	V-INT
194	2925	2925
412	2900	2878
503	2925	3036
717	3050	3325
823	3200	4072
948	3275	3731
1049	3425	4600
1086	3525	5668
1315	4375	7140

CDP 5175

TIME	V-RMS	V-INT
196	2900	2900
417	2875	2853
493	2925	3185
735	3100	3429
818	3200	3977
953	3275	3697
1051	3375	4226
1091	3500	5902
1300	4175	6669

CDP 2550

TIME	V-RMS	V-INT
190	2700	2700
404	2750	2794
502	2775	2876
721	3075	3671
816	3100	3284
946	3200	3768
1043	3275	3932
1081	3475	7009
1288	4200	6834

Figure 2.2.1b Hyperbolic semblance velocity spectra from processed SSP COF gathers (top). Significant multiple energy is identified by apparent inversions in stacking velocity (circled) immediately below the Nisku level. Based on velocity contrasts between the salt reflection and the underlying multiple energy, differential moveout at far offset should be on the order of 30-45ms at BOL. Spectra are overlain with approximate Vrms picks at the shelf location where the least indication of multiples exists. RMS stacking velocities and Dix interval velocities are listed (bottom).

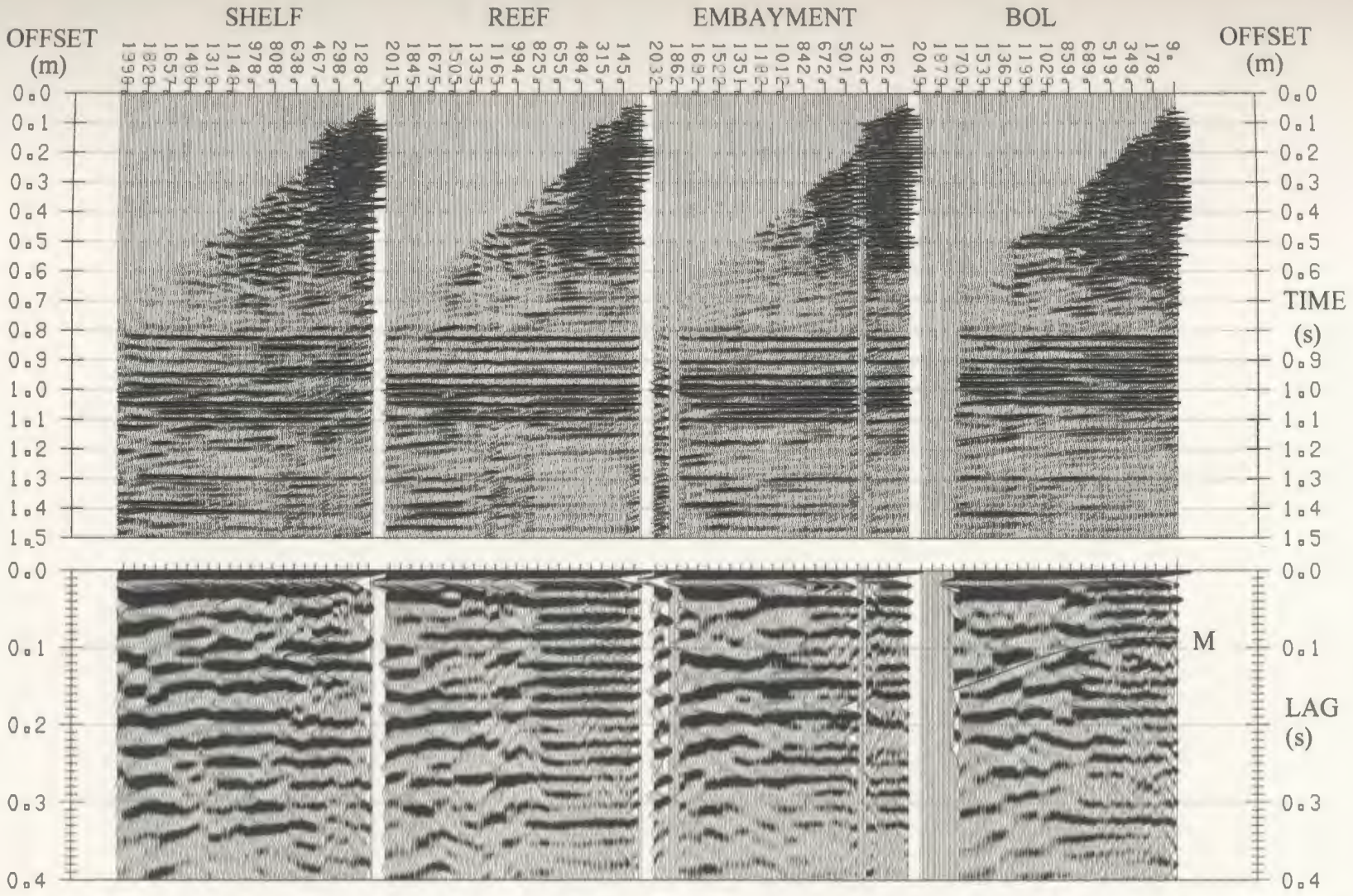

Figure 2.2.1c Processed SSP COF gathers with dynamic corrections (top), and autocorrelations (bottom) from design window 700-1300ms. The multiple at BOL (near 1100ms) can be identified on the basis of increasing differential moveout with offset. Events that correlate without change in period with offset may be primaries, or due to a mechanism that propagates multiples with near-normal incidence. Effects of NMO stretch and residual NMO must also be considered.

problems are handled by a version of time-variant scaling in conjunction with appropriate noise rejection processes.

The initial common midpoint stack produced for a project line is referred to as the brute stack. It is generally brute because of robust static solutions, crude velocity estimates, and tight mute functions. However, this stage is very diagnostic of problems associated with statics and/or geometry, and also allows a preview of the overall data quality. Any coherent noise that does not stack out due to differential moveout may require additional pre-stack processing, or suggest later post-stack attenuation. Zones of reflectivity and structure can be identified for velocity analysis, and the brute stack also forms a model for surface consistent correlation statics. This model may require massaging to make it an effective tool for residual statics, but the single largest effect will be band-limitation since low- and high-frequency high-amplitude noise in the wide-band pre-stack data will not contribute to the correlation. Generally, iterative statics-velocity analysis takes the brute structural stack to TRA preliminary stack, leaving behind undesirable effects of intermediate processing. Although the brute stack is diagnostic of static problems, the surface location of these problems may be masked by the subsurface consistency of CMP gathers. Instead, the data can be stacked on both a shot and receiver basis, but statics in either domain will deteriorate the stack in the other domain depending on static wavelength relative to spread length. Typical problem areas for statics are where gaps exist in shot spacing due obstacles, but geophones are usually continuous. For this reason, shot statics should first be investigated across shooting gaps if static bust(s) occur.

Following application of the best surface consistent static solution, dynamic correction, front-end mute and relevant pre-stack noise attenuation, the data are stacked at a

preliminary stage. The remaining processing steps typically required include subsurface consistent trim statics within CMP gathers. This technique is applied under tight control as these statics are generally dependent on data quality relative to any dominant reflector(s). Following this process, the data are stacked to the final product and post-stack processing methods are applied to improve the CMP image. These techniques include coherency and bandpass filtering, amplitude equalisation, and migration.

To illustrate the CMP stack for this Nisku study, COF gathers are processed to final stack (Figure 2.2.2a). The largest variation in coherent reflectors across the line exists in the continuity of the Mississippian-Banff response. It is not known if this variation is geologic, but well logs would suggest that the change may be due to multiples. To utilise the stack in multiple identification, near and far stacks are compared to the full stack (Figure 2.2.2b). The multiple identified at BOL during HSVA is well attenuated in the full stack whereas less attenuation is achieved in the partial stacks but significant moveout can be observed from near to far for event M4 between the two (event M4). Due to the high S/N ratio of this multiple, autocorrelations (Figure 2.2.2c) should show differences in lags corresponding to the multiple period. However, higher frequency content in the near stack makes the correlation difficult. A version of the stack autocorrelations limited to far stack bandwidth (Figure 2.2.2d) does show significant change in period for energy at lags near 100ms at BOL. Also, the shallow autocorrelations now show a ringing response that can be correlated with the modelled weathering TWT delay, but S/N is low. The multiple in the deeper far stack window is not expected to show this correlation since shots and receivers are not coincident. The deeper near stack window also does not show this lateral change in periodicity as expected for a normal incidence section, but offsets are less than 900m in the

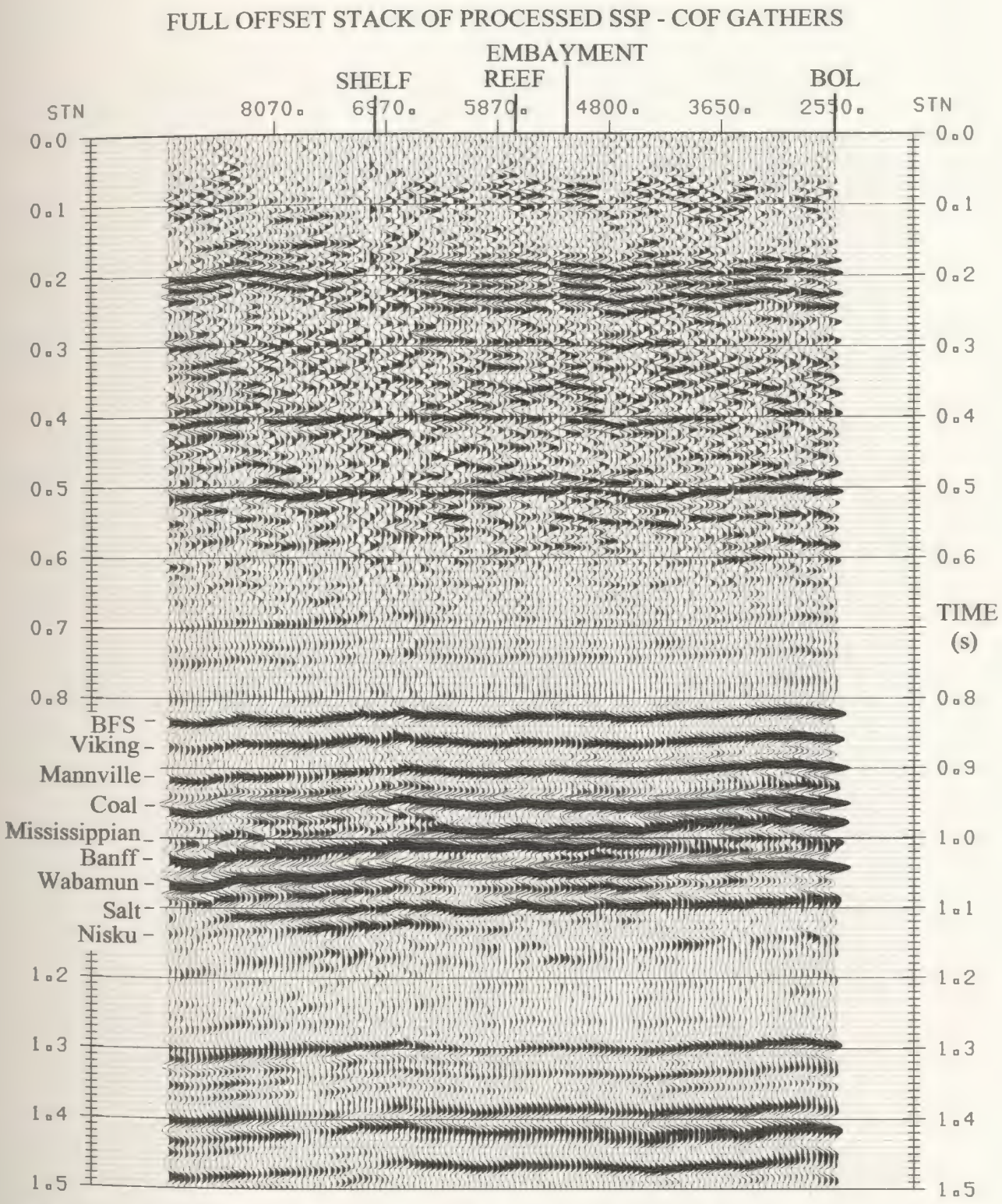

Figure 2.2.2a Full offset stack of processed SSP COF gathers. The shallow section (0-600ms) was processed post-stack with AGC scaling, then the S/N of the whole section was enhanced by f-x noise reduction. The Nisku response is considered to be the trough immediately following the trough-to-peak salt event. At the shelf location, Nisku response (1115ms) is strong compared to response at the reef and embayment.

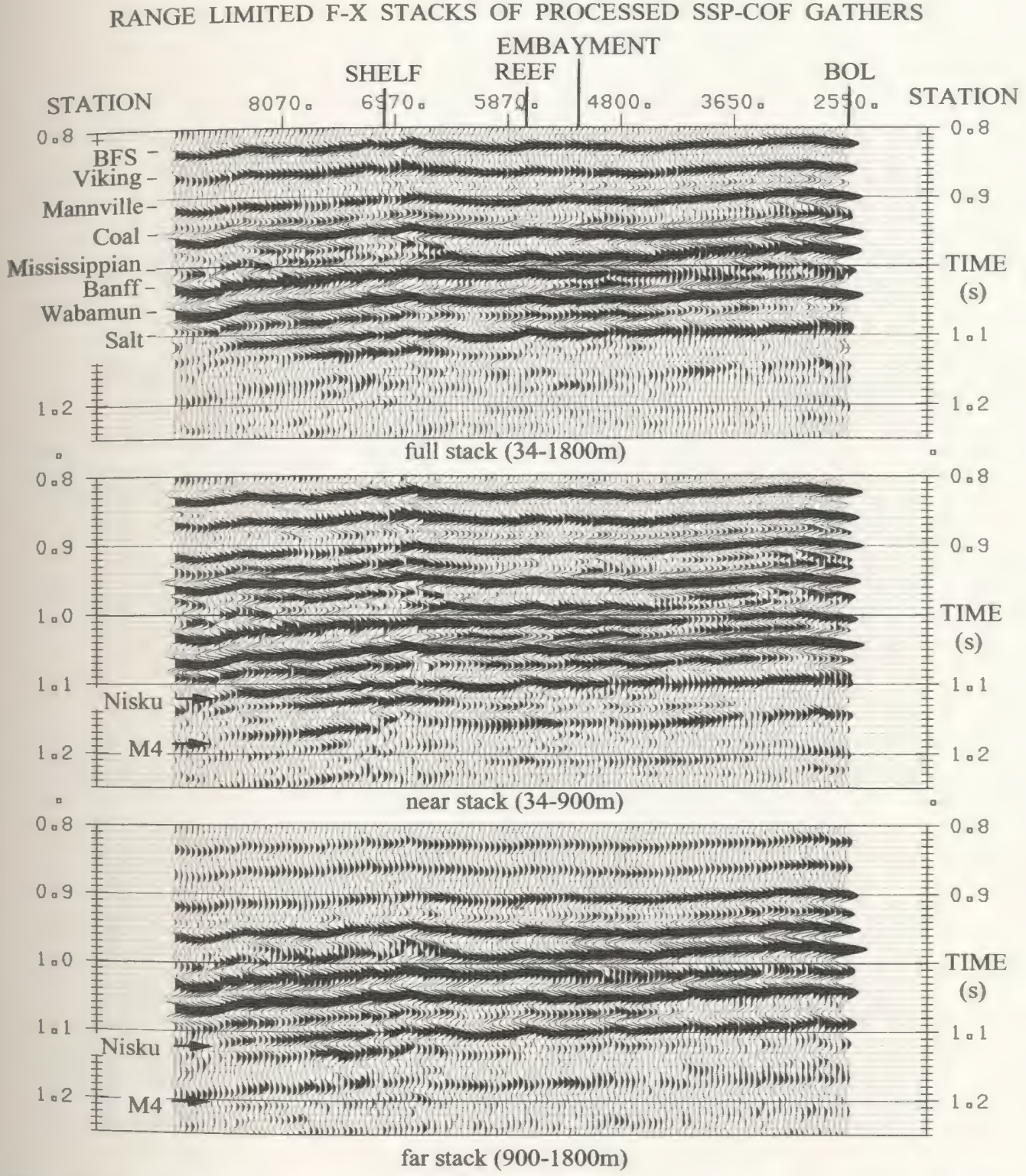

Figure 2.2.2b Range limited f-x stacks of processed SSP-COF gathers. The full stack (34-1800m, top) is the addition of the near stack (34-900m, middle) and far stack (900-1800m, bottom). Near the reservoir zone (where multiple energy is suspect from velocity analysis), differences exist between the near and far stacks due to differential moveout between multiples and primaries.

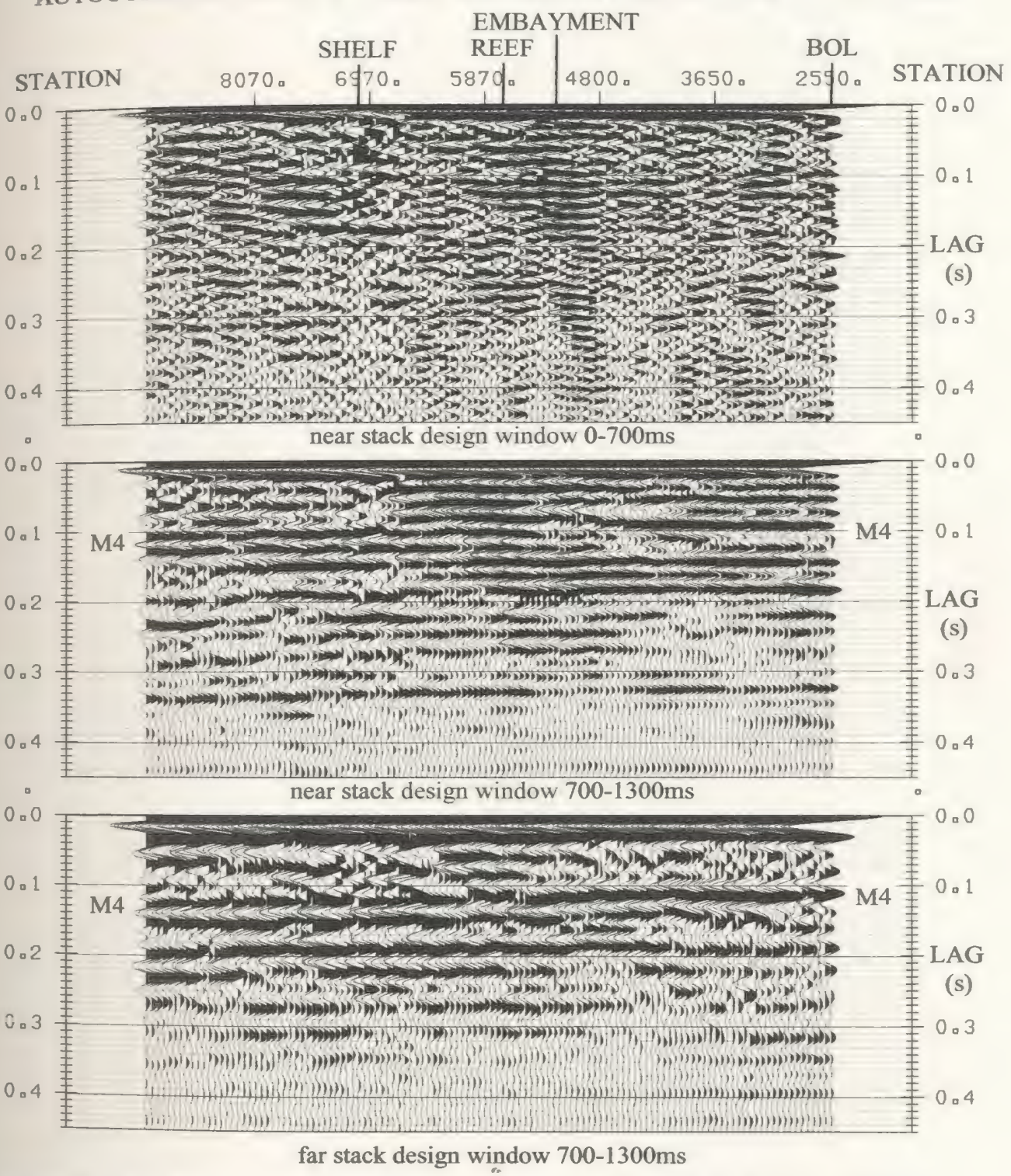

Figure 2.2.2c Windowed autocorrelations of near and far offset stacks. Shallow design window (top) suggests lateral changes in dominant reflectors, but suffers from lateral change in surface wave condition, has variable but low fold, and is biased by missing reflection from base of weathering. Increased periodicity with offset for multiple M4 (near 100ms at BOL) is not clearly indicated by the deeper design window.

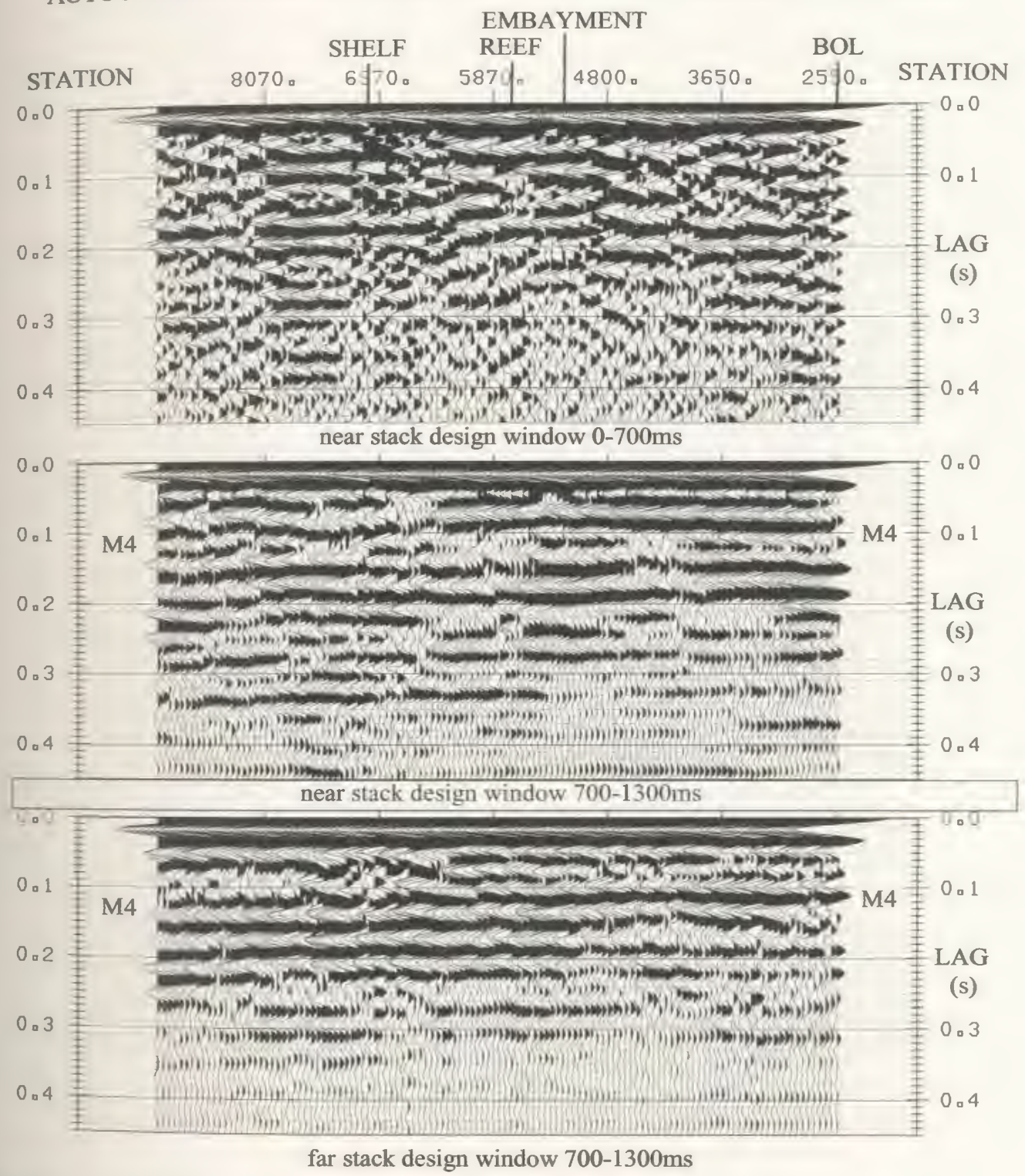

Figure 2.2.2d Bandlimited autocorrelations (12/15-35/45Hz) of of near and far offset stacks showing effects from 700-1300ms.

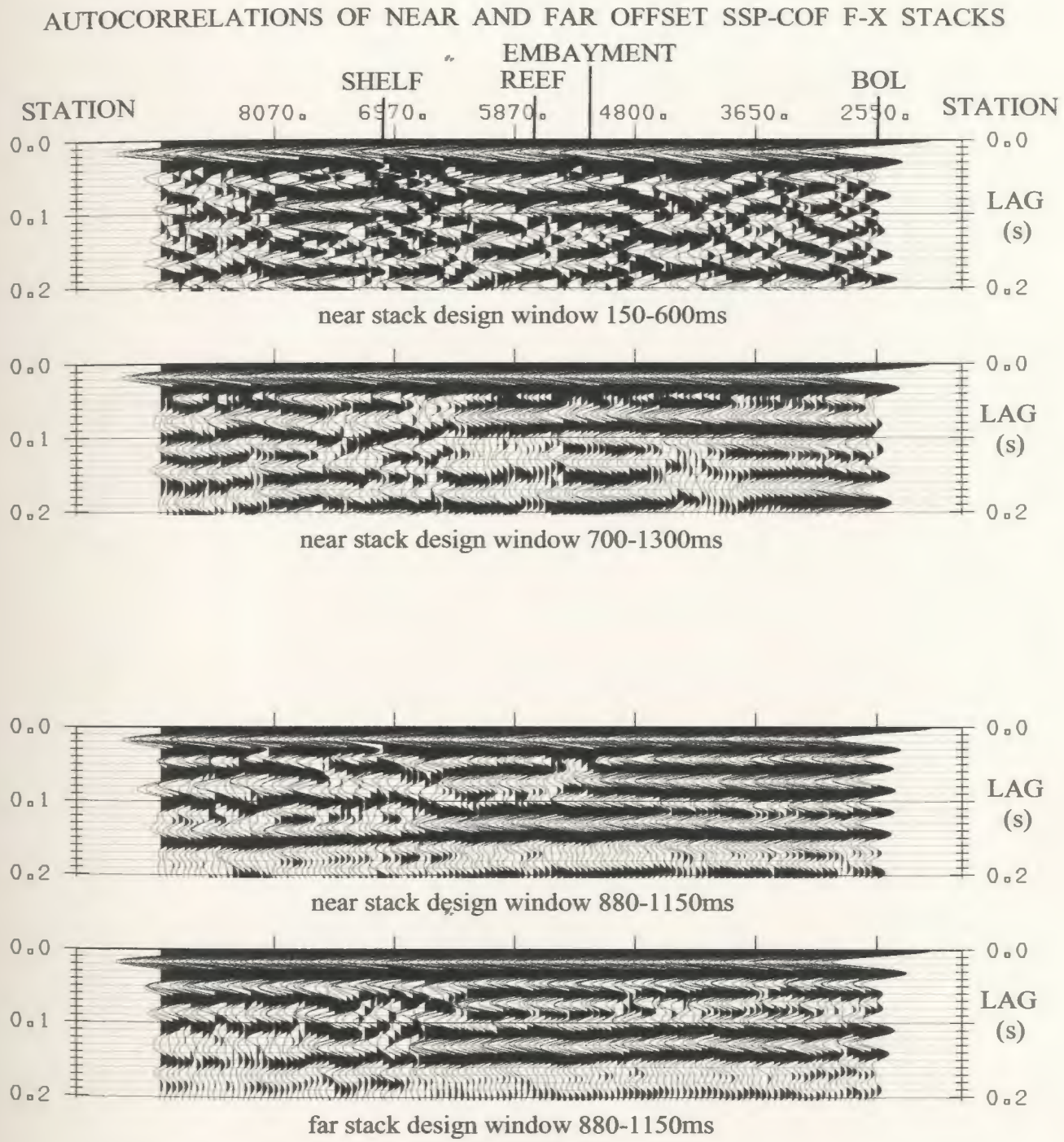

Figure 2.2.2e Bandlimited autocorrelations (12/15-35/45Hz) of near and far offset stacks showing effects from 880-1150ms (Mannville to Nisku). Moveout effects are not noticeable when multiple M4 is excluded from design. Changes may be attributed to lateral reflectivity changes, and to multiple interference related to shallower events (eg. surface pegleg).

shallow section. Also, primary amplitudes in the deeper section will dominate amplitudes of surface peg-legs. In addition, primaries may be correlating at the same lags. A short autocorrelation window (Figure 2.2.2e) excluding the multiple but including Mannville to Nisku illustrates that primaries correlate at lags comparable to the two-way weathering delay, and first order interbed multiples between the primaries will also correlate at the same lags. The shallow correlations display ringing near 100ms similar to deeper events (Figure 2.2.2e, top). Windowed correlations (Figure 2.2.2e, bottom) show that events correlate at similar lags without moveout between near and far stacks, suggesting dominant primaries. To improve Nisku resolution, multiple suppression should address the possibility of surface related and interbed multiples.

2.3 SSP Multiple Suppression

In the present study, two sources of multiple contamination are expected. First, the thick low-velocity surface layer is a potential generator of first-order peg-leg multiples. Second, strong impedance contrasts above the Nisku level are a potential source of interbed multiples. Available multiple suppression methods will be applied in Chapter 5 dependent on identified multiple characteristics.

One of the most widely used methods of multiple suppression is predictive deconvolution (Robinson, 1967, Peacock and Treitel, 1969). This method has met with most success when applied to marine data with water bottom multiples, but is equally applicable to land data under proper implementation. However, because pre-stack application to land data is difficult due to changing multiple period with offset, predictive deconvolution is usually applied to post-stack data. To improve the process, moveout effects may be

minimised by offset limitation in the stack so that the multiple becomes less distorted. If the vertical variation in geology is random then the autocorrelation is used to estimate the multiple period. When well log data are available, it is typical to support operator design based on differences in the autocorrelation of primary-only and primary-plus-multiple synthetics. However, predictive deconvolution is generally not applicable in the Nisku case because of similarity between primary and full reflectivity autocorrelations. Given this lack of basis for design due to coloured $R_p(t)$, pre-stack multiple attenuation is typically left to the CMP stacking process based on residual moveout (Mayne, 1962), or optimally by weighted stacking (Schoenberger, 1996). When stacking is insufficient at multiple suppression, prediction applied to near-offset data may still be useful in some areas, provided that a prediction design criterion can be derived from VSP's or $R_p(t)$ inversion. In particular, VSP detection of interbed multiples of variable periodicity is possible using "inside" and "outside" corridor stacking (Hardage, 1983). Another method uses a prediction filter derived from the downgoing VSP wavefield to deconvolve multiples from SSP data (Hampson and Mewhort, 1983). However, redundancy in SSP raypaths produce different amplitude relationships between primaries and multiples as compared to VSP (discussed in Chapter 3). Multiple mechanism and source wavelet determine the commonality of the basic operator shape but predictive operator weighting should be derived from the SSP data. For application away from the well, predictive operators should be based on lateral SSP mapping of the multiple mechanism events. Provided that the sampled VSP depth interval extends above and below these events, VSP data can be used for unambiguous identification of this mechanism so as to validate these prediction design criteria.

An alternative multiple suppression method commonly applied to pre-stack CMP gathers involves the Radon transform from t-x to tau-p space (Treitel et al. 1982). In transform space the tau (τ) variable is chosen to define a functional relationship for Snell's ray parameter (p) in terms of two-way time, offset, and velocity. This relationship is chosen to best suit data conditioning and transform performance can be improved by optimisation criteria. Noise component energy computed as the sum of squared amplitude differences between the inverse transform and the original record can be minimised by selection of transform sampling variables. Spectral characteristics of the signal and noise also form constraints. The success of Radon filtering generally depends on the significance of AVO effects, since far offsets are required to represent differential NMO. Also, structural and residual static components do not conform to this transform method.

In the context of SSP multiple suppression, many τ-p multiple suppression techniques implement either a parabolic (PRT) or hyperbolic (HRT) Radon transform. Primaries and multiples that overlap in x-t space may transform to isolated events in τ-p space where separation criteria may be formed on the basis of muting or autocorrelation before the inverse transform. Autocorrelations may indicate that multiple periodicity is constant in p so that pre-stack prediction can be applied in τ-p space without offset dependent operator design. Automatic muting can be achieved in t-x space by passing amplitudes that correspond to a select range of p values that varies with τ as defined by primary velocities or moveout. Inverse velocity stacking (INVEST, Hampson, 1986) involves computing the forward PRT using corrected CDP gathers by summation at each normal incidence time along parabolic trajectories defined by moveout sampling at far offset. The primary energy is inverse transformed based on tolerable residual NMO and the

noise can be added back. When fast multiples coincide with deeper primary reflections, small differential NMO reduces the success of the method by influencing NMO correction. This problem may require frequency limitation or extra whitening to better resolve the target events for enhanced velocity analysis. This prompted the incorporation of a whitening technique into the optimised forward HRT (Sacchi and Ulrych, 1995). The tuned velocity profile should optimise τ-p filtering applied to full-band data on which interpretation may rest. A similar approach has provided the best industry estimate of Nisku $R_p(t)$ response for this SSP case study (Hunt et al, 1996).

One other pre-stack multiple suppression technique involves f-k separation (Ryu, 1982). In this method, a NMO correction may be applied that over-corrects primary energy while leaving multiple energy under-corrected. This allows f-k suppression of multiples by muting the negative f-k quadrant. This method is ineffective for near offsets where both events share zero k values, but works well on far offsets and provides enhanced data for velocity analysis. The method is applicable to CSP gathers since it is less sensitive to structural effects, but application in the CMP domain may require binning of groups of gathers to avoid aliasing. With sufficient offset (deep windows), a far stack with f-k attenuation may be compared to a near stack. Full-offset stacks before and after f-k multiple rejection are usually comparable since the improved S/N achieved by the filter is lost in the stack due to amplitude reduction of components with moveout, while in the stack itself the moveout components provide the suppression. This method is similar to tau-p methods in its reliance on far offsets and differential moveout for multiple discrimination. Neither method is capable of preserving AVO effects. Unlike predictive deconvolution, both methods are also automatic in that the multiple period is largely irrelevant. These methods are viable

intermediate processing aids, and in many cases provide substantial improvement in results when applied carefully. Even if unsuccessful, these methods may provide recognition criteria for the effects of multiple interference.

2.4 SSP Amplitude Versus Offset

In the WCSB, AVO analysis has proven to be a reliable tool in the detection of shallow gas. Historically, conventional CMP reflection has been successful in gas exploration due to 'bright spot' response associated with gas accumulation. However, large reflection amplitudes can also be associated with non-gaseous layers making reservoir differentiation difficult. To compensate, Ostrander (1984) illustrates that discrimination can be made based on the effect that large change in Poisson's ratio (σ) has on the P-wave reflection coefficient as a function of offset, or angle of incidence (θ). For a non-gaseous interface, little change in σ occurs and $R_p(\theta)$ varies little with θ. For gaseous interfaces, a large change in σ is expected and $R_p(\theta)$ varies significantly, even within the offset limits of pre-critical reflection. Based on this observation, pre-stack seismic data for any hydrocarbon play can be analysed for AVO effects as predicted by model studies. In estimating σ for layers in the model, results from various authors suggest values for shale of 0.2-0.3 and porous sandstone (gas saturated of 0.1 and brine saturated sandstone of 0.4). Ostrander (1984) also suggests that for a given porous matrix, a weaker framework (lower elastic moduli) implies a larger increase in σ from gas to liquid. This implies that a relatively strong carbonate framework may be less detectable than sandstone of similar porosity.

AVO effects in carbonate environments may allow discrimination between shale embayment facies and porous dolomite/limestone (Lower Nisku) overlain by seismically

faster low porosity carbonate (Upper Nisku). Although normal incidence reflectivity offers little amplitude distinction due to low impedance contrasts, the Poisson's ratio contrast ($\delta\sigma$) is larger for the porous reef case so AVO analysis is possible. For AVO modelling on the embayment well, assignment of a σ value to the Lower Nisku will be influenced by shale content. This open marine member is predominantly massively bedded dolomitised mudstone, not fissile like a shale (personal communication, Lee Hunt, 1995). It is reasonable to assume behaviour to be more like porous dolomite with regards to σ. Poisson's ratio is about 0.27 for dolomitised anhydritic carbonate, and for the porous case is about 0.28. A predominantly shale open marine member would have a much higher σ (an estimate for local shale is 0.4), whereas an unaltered carbonate member would be about 0.28-0.30. In the reservoir zone, blocked shear and sonic logs give σ values that compare to these predictions. These contrasts in σ model to suggest an AVO decrease for porous reef build-up below upper Nisku carbonate, with an AVO increase expected for the shale off-reef case.

The Knott-Zoeppritz equations describe plane-wave amplitudes for reflected and refracted energy assuming no interbed multiples and only geometric wave effects in reflectivity computation. For reflected waves, Shuey (1985) simplified these equations to include a small, intermediate and large angle term. Hilterman (1989) further simplified this to a small angle term and a large angle term valid for $\theta < 30$ degrees, $\delta\sigma = 0.33$ (or $V_p/V_s = 2.0$), and $R_p(0,t)$ less than 0.33. Based on straight ray reflection, θ_i values at the Nisku are not expected to exceed 30 degrees nor are contrasts in σ expected to exceed 0.25. Reflectivities of adjacent strata may approach or exceed 0.33 but modelled conditions will be within the limits of Hilterman's approximation.

AVO is crucially dependent on data preparation, even under discrete reflectivity conditions such as the well resolved Colony gas sand plays which occur in the WCSB at a shallower stratigraphic level than the Nisku. Current AVO techniques for deriving porosity distinction criteria should be applied to multiple-free SSP data or after successful multiple suppression. Attempts at Nisku AVO analysis following pre-stack multiple suppression will be biased if amplitudes are not preserved. Since the stacking process associated with the Ostrander gather generation can suppress residual multiple energy, predictive suppression may be more applicable for AVO purposes as compared to 2D transforms.

The success of AVO at the Nisku level may require a more vigorous approach including volumetric analysis and forward modelling under assumptions of full reflectivity. The complexity of reflector distribution requires more than two horizons are parameterised to predict AVO response. Forward modelling can be performed using radial Radon transforms (RRT) which incorporate a Zoeppritz AVO definition. Parameterisation for this modelling can be derived initially from logs and complemented by $R_p(t)$ inversion of SSP data away from the well (see Chapter 3). The inverted reflectivity can be used to derive impedance estimates from which blocked rock properties can be extracted. The full reflectivity AVO response from the blocky model could be compared to SSP data, but the net AVO response at Nisku level may be too complex to allow robust modelling.

In Chapter 2, I have reviewed SSP processing techniques with emphasis on application to a Nisku experiment. Preliminary analysis of the SSP data illustrates the method and concepts, and multiple discrimination criteria indicate that suppression will be difficult. The processing techniques presented in this chapter are not new, but the approach of using COF gathers to facilitate multiple identification in the SSP experiment is non-

conventional. I have shown that the multiples can be recognised on the basis of differential NMO from stack data, during HSVA, and from autocorrelations. More importantly I have shown that each of these approaches have specific limitations imposed by the data. Three things are evident in the target zone. First, differential NMO is minimal. Second, primary reflections share similar autocorrelation lags with multiples. Third, the multiple condition varies laterally. The lack of clear multiple discrimination criteria poses a problem for multiple suppression. In an effort to overcome these difficulties, wellbore data will be introduced in Chapter 3 for the purpose of providing a course of action for multiple suppression. Because wellbore data provides criteria for derivation of a blocky impedance model that can be used in multiple suppression, the wellbore data discussion will be followed by an introduction to seismic modelling and inversion in Chapter 4. The overall data analysis and integration will seek to provide avenues of approach for satisfying data processing objectives. If the multiple mechanism(s) can be identified on the basis of wellbore data and confirmed in SSP data at well locations, then the application of existing suppression techniques can be assessed for improvements to Nisku SSP resolution.

Based on SSP indicators, multiple suppression by predictive deconvolution may be the best approach. I have attempted to enhance the signal in the shallow SSP section for the purpose of providing criteria for operator design to suppress multiples common to both the shallow and deeper (target) portions of the SSP data. The application and further support of this approach is presented in Chapter 5. The application of conventional AVO modelling will be determined by the success of full-offset pre-stack SSP multiple suppression. The near-offset stack processed for prediction may represent the best porosity dictinction criteria available, formed on the basis of character and timing (stack response) or acoustic inversion.

CHAPTER 3. PROCESSING METHODS FOR WELLBORE DATA

When non-reservoir facies are encountered during Nisku SSP explorational drilling, wellbore analysis may clarify pitfalls in the SSP interpretation. In this Nisku study, wells from three distinct facies are projected onto the CMP stack for this purpose (see Figure 2.2.2a). At each well, available information includes impedance in depth and VSP data. In this chapter, fundamentals relating to the acquisition and processing of this wellbore data are reviewed in relation to its integration with processed SSP data. The goal of this chapter is to use wellbore data as a tool in SSP multiple identification and suppression.

VSP data will contribute to two areas of this research. First, well log processing attempts to produce a synthetic seismic trace in time from impedance information in depth using the convolutional model. VSP first breaks are used to control sonic adjustments during the depth to time impedance conversion component of this process. Second, multiple suppression may benefit from mechanism identification. Later arrivals of a VSP experiment are used to distinguish up-going and down-going energy, thereby identifying multiple activity. Acquisition and source differences between VSP and SSP are discussed as this relates directly to data integration and multiple suppression. Further use of Impedance information for modelling and inversion is presented in Chapter 4, and the methods are implemented in overall integration with SSP data in Chapter 5.

3.1 Wellbore Log Survey and VSP Checkshot Processing

After delineation of structural or stratigraphic traps using SSP surveys, wells are drilled and logs can be used along with down-hole seismic methods to improve the fundamentally low resolution SSP results. Operational problems arise due to cased versus uncased wellbores. Poor hole conditions and highly deviated wells may require cemented casing, producing anomalous VSP noise at depths of poor cementing conditions where compressional waves produce casing reverberation. Also, VSP tube wave resonance may become more severe in a cased hole. Cased holes are beneficial by allowing the use of multi-sensor down-hole seismic array (DSA) tools to be used for VSP. Casing and cement has little effect on VSP check shot signal (first breaks) used for editing and calibration of the sonic and density logs. Sonic velocity is logged at a fine increment (typically at 0.3048m) by measuring refracted waves from the wall of the hole which must be done before the high velocity steel casing is put in place. In good hole conditions, formations can be altered by mudcake from the drilling process which produces a decrease in the apparent velocity measured by this logging process. VSP arrivals provide reliable compensation for sonic drift induced by borehole effects and also by fundamental frequency dependent dispersion. Dispersion dictates that a 20 KHz sonic signal will propagate faster than a 50 Hz seismic signal by up to 6% (Schlumberger, 1989). The shortest travel path of seismic ($\lambda = V/f$, typically on the order of 100m) suggests that VSP check shot depths should be spaced at 150m maximum (Hardage, 1983) while including depths (knees) of changes in lithology (formation tops), borehole conditions, sonic character, drift data, and the sonic log top. VSP recording should also include a seismic datum checkshot (if below topography) and also be used to identify the base of weathering and possible surface multiple mechanisms. Since

detailed VSP checkshot acquisition increases well shutdown time, raw drift as provided by conventional cased hole VSP should be validated before drift compensation.

Computation of raw drift and validated selection of drift curve parameterisation provides adjustment in sonic logs. For check shot VSP usage, geophone depth is referenced to the processing datum and the profile is shifted in time accordingly using an appropriate replacement velocity. First break transit time is then measured and corrected to true vertical time using deviated hole and offset source co-ordinates. Raw drift is then the integrated (summed) sonic time subtracted from the corrected shot time at each shooting level. The drift curve is derived from the raw drift values. The check shot correction is then distributed to the sonic times over each knee interval, and validated by checking integrated sonic time against corrected shot time at each shooting level (within accuracy of shot time). This becomes more accurate with more shots, making VSP a viable tool in relating seismic features to geological structure and extending resolution of impedance anomalies identified by SSP reflections. Following adjustment, the integrated sonic interval transit times are then used at the well location to convert SSP time to depth, and in synthetic seismogram generation for reflection event verification.

The main objective of well log processing is to produce a synthetic seismic trace at the well location from the sonic transit time using the convolutional model. In this model, the earth is represented by a series of equal transit time layers parameterised by acoustic impedance. In-situ density measurements are typically acquired using a neutron source, but if not available an empirical relationship between velocity and density may be used provided the geology is dominantly clastic. The normal incidence primaries-only reflectivity sequence is then derived from the time impedance, and from this the reverberatory impulse response is

computed (Wuenschel, 1960). In general, multiples may occur either when the wave is travelling upward or downward, with multiple order defined by the number of bounces in a given layer. The process of including extra path traverse effects may be viewed as the addition of many delayed and scaled versions of the primary reflectivity. The delay for each successive multiple component depends on the two-way travel-path within the layer while scaling is governed by energy partitioning. (In reality, multiple amplitudes are also reduced due to extra spherical divergence and anelastic absorption associated with the longer travel-path.). Following this computation, a wavelet estimate is generated and convolved with the reflectivity to yield the synthetic trace at the well location. The synthetic seismogram is then matched to seismic data to identify amplitude and phase misties, multiple problems, and tie points for horizons.

Once a synthetic seismogram has been produced, a standard processing practice is to determine residual phase in the SSP data. Stacked traces from the well vicinity are rotated typically at thirty-degree increments and compared to the zero phase synthetic. The comparison may be made using inverted impedance traces, but generally the time response is employed as impedance inversion may not be applicable. When several wells are available, lateral variation in phase adjustment suggest that averaging be applied for a result closer to zero phase for improved interpretation.

The wellbore dataset under analysis includes compressional wave transit time (sonic velocity α), density (ρ), and shear wave (β) well logs at three cased well locations, and also VSP data. These three locations tie the SSP data with reasonable closeness, and these locations are referred to as reef, shelf, and embayment on the SSP data presented in the text. The logs may be used for AVO modelling in a blocky sense, although β is usually extracted

only in the vicinity of the reservoir. The sonic and density logs are usually extracted over a more complete depth interval (Figures 3.1.1, 3.1.2,and 3.1.3), and will be used for synthetic seismogram generation after conditioned depth to time conversion based on VSP check shots. Shallow recordings were employed in the VSP surveys, but only to the degree of providing the minimum in drift correction. Given the reef, shelf, and embayment wells, the reef well has the least deviation from vertical (less than 5 degrees) and depths are given as recorded. Both the shelf and embayment wells are deviated by about ten degrees. The well deviation survey is used to adjust measured log depth and DSA tool depth to true vertical depth (TVD) relative to SRD. Lateral VSP source offset is incorporated for static adjustment of first break time for use in check-shot analysis, based on a straight ray approximation referenced to SRD using an appropriate replacement velocity.

When multiple checkshots are available from a VSP survey, the edited checkshot velocity profile serves as the best depth to time (TVD to TWT) log conversion curve. Transit times between checkshots are not integrated and scaled in this process but instead the velocity profile is used to map depth points to time so that impedance may be converted without the sonic values. Depending on the desired output sample rate and the velocity between checkshots, this may involve mapping one depth point to several samples or skipping depth points at even increments within checkshots. In this way the depth log is not assumed to represent sonic transit times that require scaling to fit the checkshots. The VSP checkshots and the resulting time logs are presented in section 5.2. Since the SSP is corrected to SRD based on a smoothed model, bulk shifting is applied to the time logs to compensate for residual datum corrections and thus make synthetics tie with SSP.

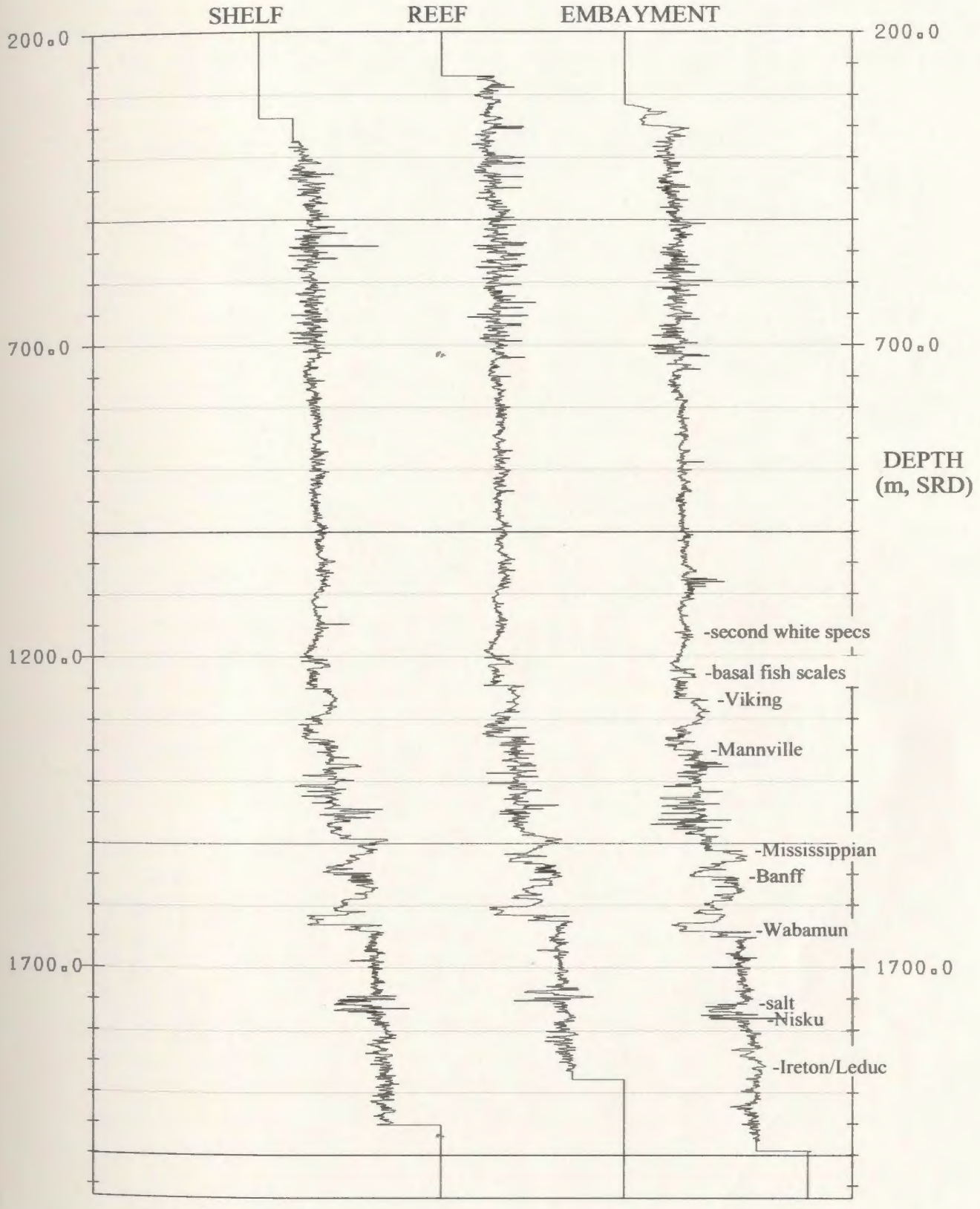

Figure 3.1.1. Velocity depth logs for the Nisku field. Depths are TVD (kb) adjusted to SRD (900m). Logs are padded by velocity extrema of 1000m/s (1000us/m) at top and 8500m/s (118us/m) at bottom for display purposes, but initial and final log values are extrapolated to log extents for synthetic generation. Geologic tops are given.

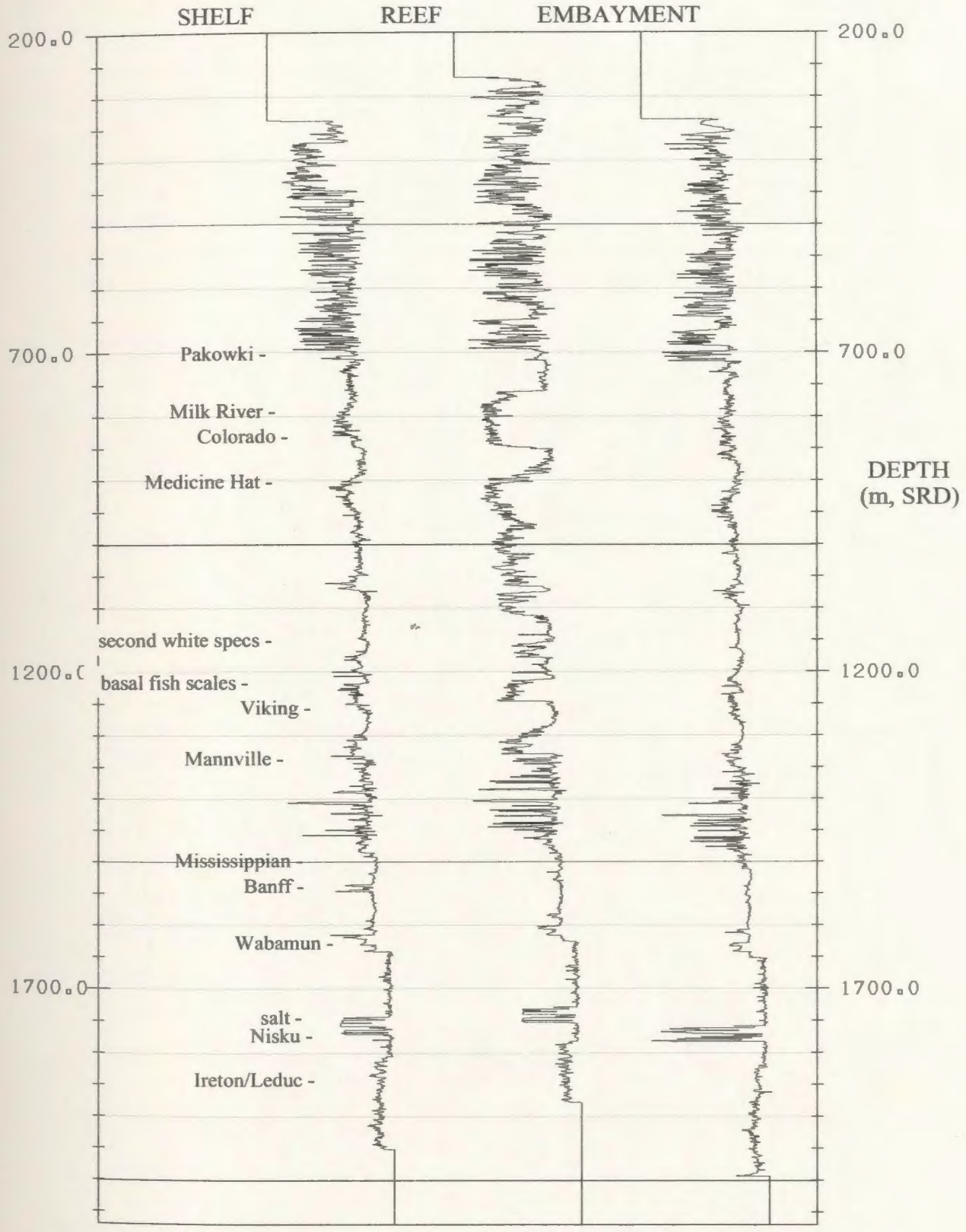

Figure 3.1.2. Density depth logs for the Nisku field. Depths are TVD (kb) adjusted to SRD (900m). Logs are padded by density extrema of 1000g/cc at top and 3000g/cc at bottom for display purposes, but initial and final log values are extrapolated to log extents for synthetic generation. Geologic tops are given.

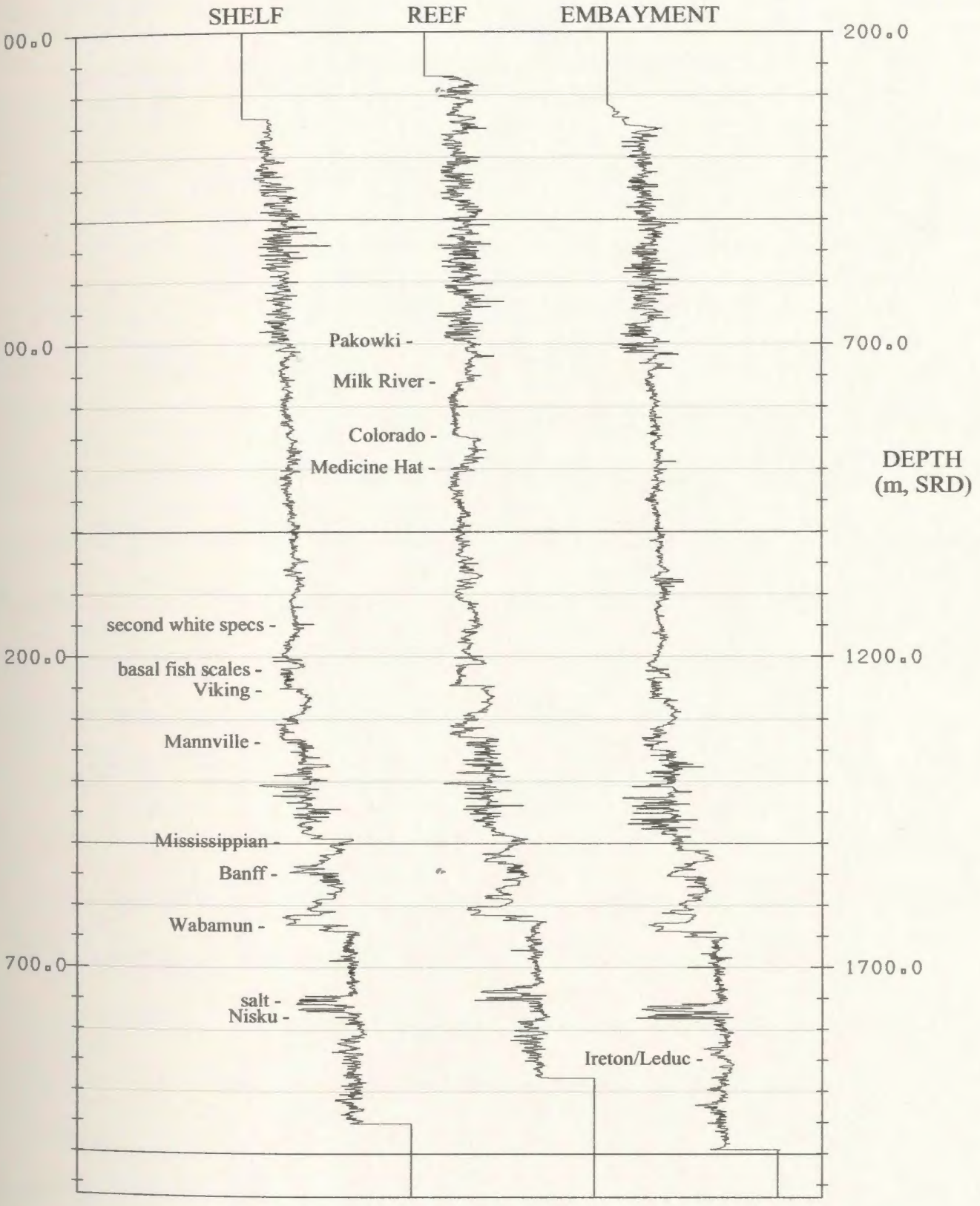

Figure 3.1.3. Impedence depth logs for the Nisku field. Depths are TVD (kb) adjusted to SRD (900m). Log values derived from sonic and density logs. Geologic tops are given approximatly.

3.2 VSP Wavefield Separation and Deconvolution

VSP acquisition involves a fixed near-surface seismic source and downhole geophones secured at various depths (Figure 3.2.1). Thorough descriptions of VSP methods and their advantages are outlined by Hardage (1983). Unlike surface-recorded data, VSP geophones respond to both down-going and up-going energy, allowing insight into fundamental properties of propagating wavelets and reflective transmissive earth processes. Multiples, mode conversions, and wavelet modifications can be identified to improve the structural, stratigraphic and lithologic interpretation of SSP data. Resolution is improved in a static sense by involving only a one-way near-normal path through the weathered layer. Frequency content does not suffer from the attenuation effects of a full two-way travel-path. In analogy to the SSP method, reflectors may be identified below the well bottom. Vertical (corridor) stacking may be used to improve the S/N ratio and discriminate against multiples. Basic VSP processing attempts to separate the up- and down-going compressional wavefields, discriminate against noise, and whiten the spectra of the result. Following processing, the VSP seismic response should be superior to CMP data at well locations. However, the VSP vibrator frequency sweep may not compare to CMP high-end frequency content realisable from minimum phase surface consistent deconvolution.

For land VSP acquisition, vibrator sources provide sufficient penetration power without damage to cased wellbores. The zero phase nature allows precise time break determination (provided propagational effects on wavelet phase are small), and waveshaping is less constrained than for an impulsive source. However, source differences may reduce the usefulness of VSP in comparison to dynamite SSP data. If a string of receivers was employed then the damage caused by one offset charge of dynamite might be justifiable

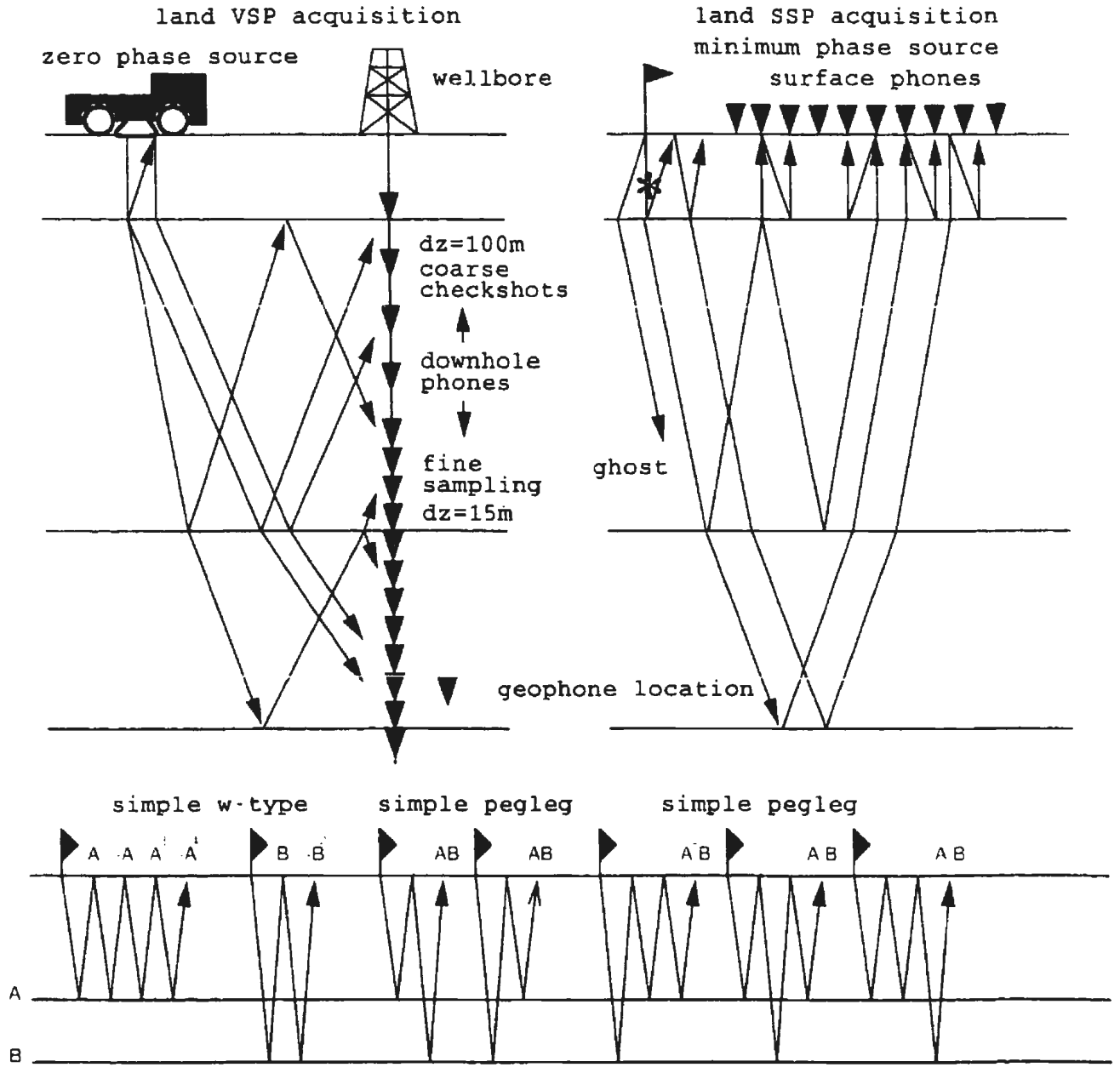

Figure 3.2.1 In VSP acquisition both upgoing and downgoing waves are recorded while SSP records only upgoing energy. Note the fundamental differences in source signature and surface placement. Also, surface recorded multiples hold different amplitude relationships than VSP recorded multiples due to redundancy (bottom).

compared to multiple vibrator sweeps, but DSA tools are not yet this technically advanced. Fortunately, the source signature derived from a vibrator source at a fixed surface location is relatively consistent from one tool depth to the next. In comparison, the SSP response that is used to compare to the VSP response is derived from various surface locations and shot conditions.

For a VSP, analysis of the vertical compressional wavefield involves trace editing and polarity corrections before any first break picking. The pre-processed records may require suppression of refracted energy that can mask the down-going wave, but generally first arrivals represent direct paths for a horizontally layered model and small source-to-receiver lateral offset. These picks can be used during processing to facilitate separation of down-going compressional events from up-going energy. The evaluation of the separation process may be improved by first attenuating any coherent noise energy.

VSP processing creates wavefields that are expressed in terms of different time co-ordinates, or time frames. Figure 3.2.2 (left) shows that the arrival times for the down-going wavefield will increase as the depth of receiver increases. On the other hand, up-going reflection times from a subsurface horizon will decrease with increasing receiver depth since the receiver is moving closer to the reflector. In field record time (FRT), down-going compression arrivals have opposite time-dip from up-going events suggesting the use of f-k filtering for separation. Consider TT to be the first arrival traveltime for down-going arrivals. As shown in Figure 3.2.3 (right), a time frame (-TT) formed by advancing FRT by first arrival time, by subtracting time TT, would flatten the down-going wave while increasing wavenumbers of up-going events, possibly causing aliasing. Similarly, a time frame delayed by first arrival time (+TT) would flatten up-going events for zero source-to-

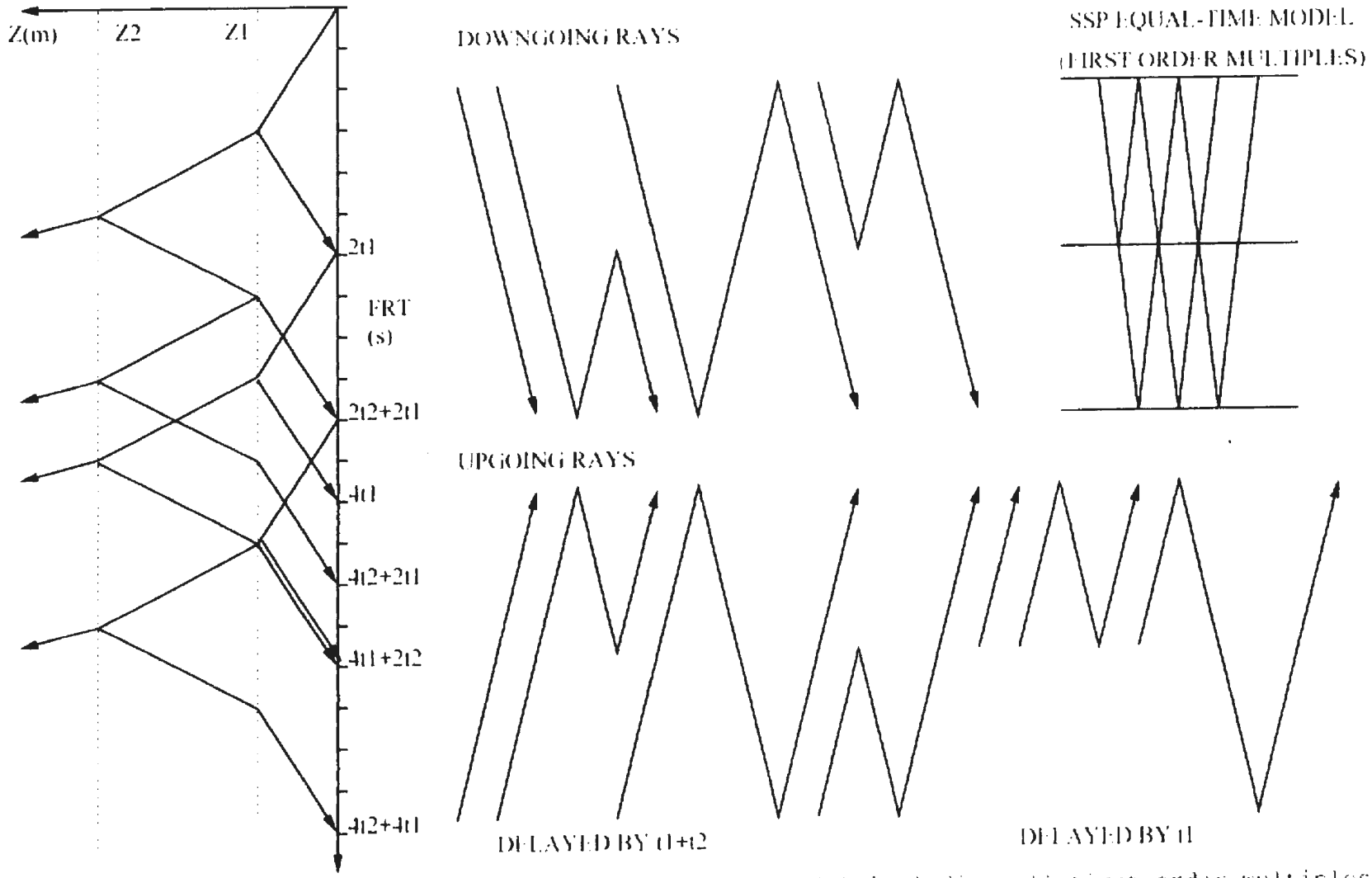

Figure 3.2.2 As illustrated in this simple three layer model including all first order multiples, the separated VSP wavefields can unambiguously define the depth of the multiple generating interface if event discontinuities can be preserved. If the timing of both multiple generators is similar, then the layer 2 primary upgoing event will be obscured by a simple interbed multiple for depths above layer 1 (similar to surface recordings). Even when timing is dissimilar, autocorrelations of surface recordings will contain redundant amplitude information as compared to downgoing VSP wavefields since more raypaths are sampled.

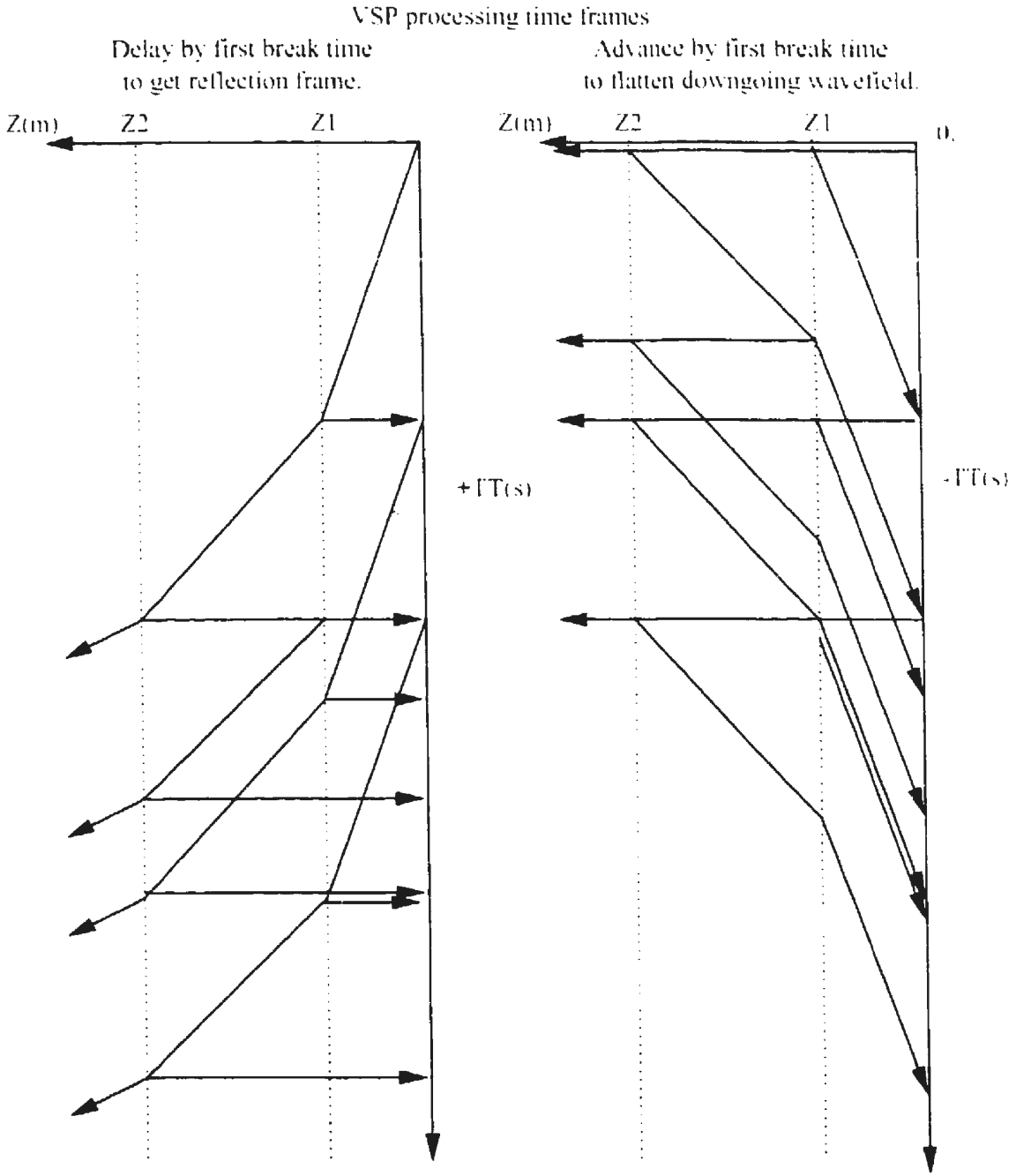

Figure 3.2.3 Using VSP first breaks as a reference frame facilitates wavefield separation and interpretation of downgoing versus upgoing energy. In +TT time, upgoing events are positioned to the TWT at which they are recorded at surface, and upgoing multiples are recorded only at depths shallower than the up-generating surface. In -TT time, downgoing events are delayed relative to the initial compression by the TWT of the generating mechanism, and downgoing multiples are only recorded at depths deeper than the down-generating surface.

receiver lateral offset and horizontal reflectors, as shown in Figure 3.2.3 (left). This time shift effectively places up-going compression events in a TWT time frame comparable with CMP data. It is in +TT time where corridor stacking is carried out. In this domain, corridor stacking involves summation of the up-going reflection energy along depth-limited lines of constant time.

In the VSP method, the main coherent noise modes are tube waves generated in the wellbore by conversion of surface generated Rayleigh waves. Tube waves may be controllable by a synchronised source array, but generally a single vibrator unit is preferred for consistent source signature and processing is adapted to attenuate tube waves. In cased holes, the tube mode typically propagates down the wellbore as a high amplitude reverberatory noise train with propagation velocity considerably less that than compressional velocity. The tube mode is also reflected at the bottom of the hole so that it exists also as an upgoing noise source. Hardage (1983) discusses tube wave phenomena relative to VSP acquisition.

Tube waves pose a problem for VSP interpretations in two ways. These problems become more serious when shallow reflectors are included. First, tube amplitudes are often spurious due to casing conditions, making them hard to attenuate under TRA conditions without compromising underlying compressional events. Second, due to partitioning, down-going energy has inherently higher S/N than up-going making it better to interpret down-going multiples in –TT time. However, since common propagation direction implies wavenumber similarity, tube suppression introduces more severe smearing effects on compressional amplitudes. For this reason it is usually better to remove down-going tube waves and compressional events and interpret the up-going wavefield, since the up-going

tube wave interferes only with reflections at arrival times well beyond the zone of interest. With this in mind, the down-going wavefield can still be interpreted for multiples following f-k zero wavenumber rejection of the down-going tube wave and up-going compressions. Also, the delay between first break and tube arrival increases with depth, making tube waves less of a problem in short period multiple evaluation when shallow reflectors are excluded.

Wavefield separation is an important VSP processing objective where the down-going compression is separated from the up-going compression. The processing strategy may include a combination of f-k energy mode separation, static adjustment based on event arrivals times, coherency filtering, and subtraction. An effective f-k method of removing spatially aliased energy modes is through application of a moveout trajectory that flattens the event, transforming to f-k space, rejecting near-zero wavenumbers, inverse transforming and removing the moveout. Down-going compressional energy may be isolated by flattening on the first break trajectory (-TT time with additional time delay) before the f-k transform, and down-going tube waves are isolated in a similar fashion. However, a drawback of the f-k rejection method is that muting in the f-k domain is equivalent to mixing of a limited aperture in the x-t domain which results in extrapolation of events outside of the zone of real data. In some cases poor f-k performance may require an alternate approach to wavefield separation.

Another separation method involves median filtering (Stewart, 1985) of the flattened energy mode before subtraction of that mode in z-t space. In simplest form, a three-point median filter can be applied along the time axis for spike rejection. In a VSP separation application, the filter length is designed to attenuate specific out-of-phase energy while the in-phase energy is enhanced. Optimal median rejection of up-going events across depth

traces in –TT time should be realised by a filter length corresponding to 1.5 wavelengths. However, there is no constant wavenumber associated with up-going energy in –TT time unless zones of constant velocity are processed. This strategy may call for operators on the order of 11 points in length, becoming less effective when short period multiples are under investigation. Dynamic corrections and structural effects are also an issue in median rejection of up-going waves. Hence, if edge effects of an efficient f-k filter can be tolerated by muting or tapering of the shallowest and deepest traces, then less overall wavefield distortion may be achievable. The success of the separation method will still depend on how well tube waves behave, since residual tube energy will distort the separation process, leaving spurious remnants and distorted up-going compressions. This noise can be attacked based on some noise criteria, such as spike rejection in time and space.

After the down-going modes are attenuated from the original gather, the remaining energy in the delay zone between the first break and the up-going tube wave arrival should be dominantly up-going compressional waves. The coherency and S/N of this wavefield can be further enhanced to evaluate multiple generating mechanisms. In VSP, all primary up-going energy will intersect with the down-going compression at the depth of the reflector. This up-going energy gets reflected back down at the multiple generating interface, and back up again at the depth of the reflecting interbed. The up-going interbed multiple is first detected at interbed depth where multiple delay relative to first break is the two-way-time between the deeper interbed reflector and the multiple generator. If the generator depth and interbed delay of the multiple can be measured, then a constraint can be placed on the reflecting surfaces involved. The characteristic of preserving discontinuities is best found in a short median filter. However, if moveout or structural components are present, this filter

will not behave optimally so trim statics or dynamic corrections should be applied after f-k separation and before short median S/N enhancement.

Standard processing of VSP data acquired with a vibrator source includes a waveshaping operation which involves shaping the trace spectra to that of a desired residual wavelet. This process takes place in the frequency domain by spectral-division within the sweep bandwidth on a trace-wise basis. The desired wavelet is a whitened zero-phase version of the input Klauder wavelet that has been modified by propagation effects. The down-going compressional wavefield travels a shorter path than the up-going wavefield at any given depth so that it suffers the least from Q-attenuation. The initial down-going pulse makes the best wavelet estimate for VSP deconvolution of up-going energy instead of methods that make assumptions about reflectivity and wavelet spectra. Initially, a three-point median filter is applied in –TT time to boost the S/N ratio. The resulting wavelets contained within a specified time window centred on the first break are used to derive the frequency domain operators to apply to the separated up-going wavefield. Since the down-going wavefield has a displacement polarity opposite to the up-going wavefield, the up-going deconvolved result requires polarity change. If signal to noise is low, these wavelets could be stacked to create an average, but trace-wise application better compensates for propagation effects.

The pre-processed VSP data for each well illustrates the various time frames applied in VSP processing (Figures 3.2.4a,b,c). These data are described in more detail in chapter 5. Compared to surface peg-leg effects between SSP and VSP data, the down-going VSP surface source wavelet will be followed by a multiple of opposite polarity with lag equal to the TWT delay of the weathered layer. The down-going wavelet from the reef well displays

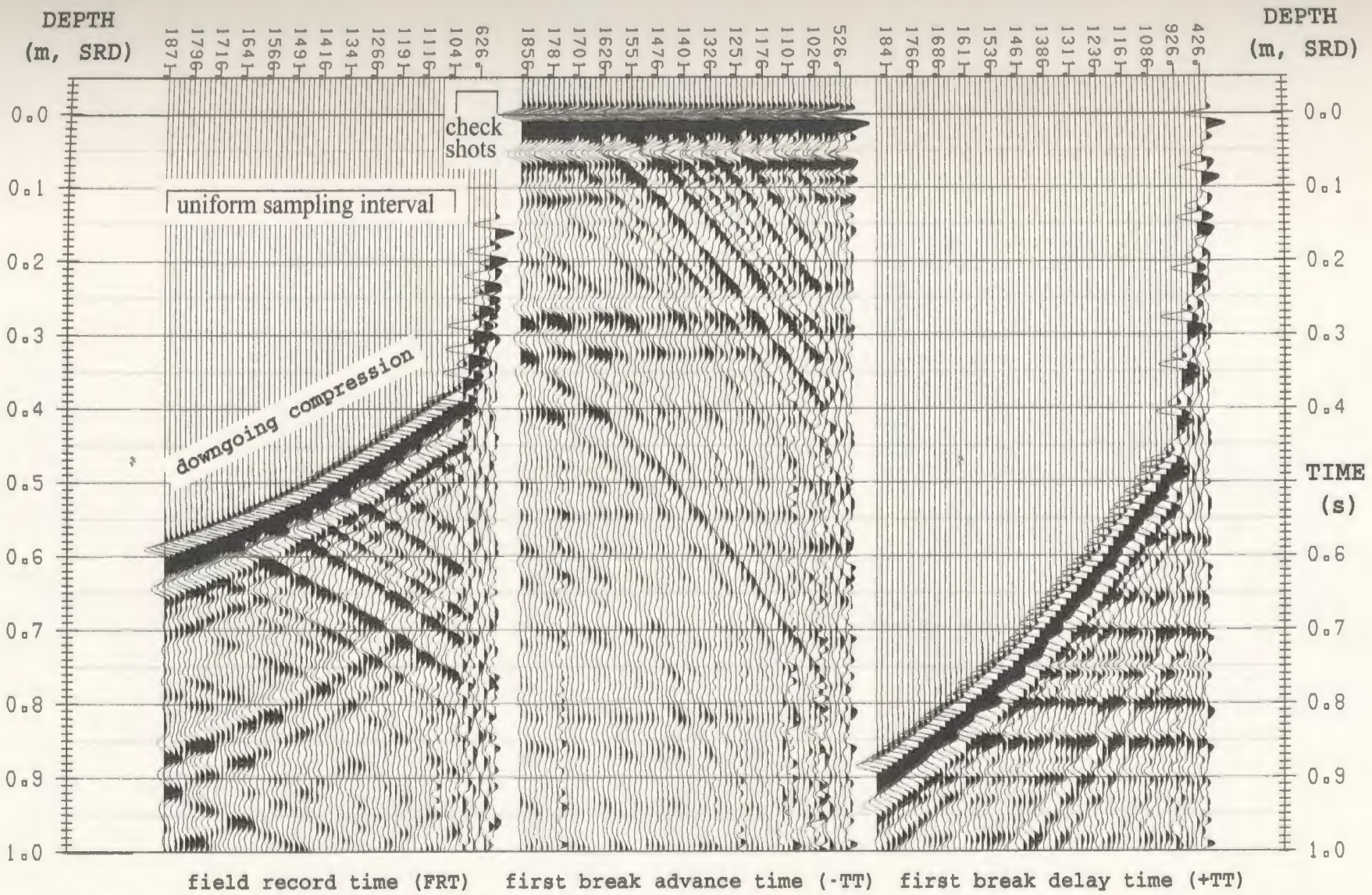

Figure 3.2.4a Various VSP processing time frames (REEF). In FRT time, downgoing events dip to the left while upgoing events dip to the right. In -TT time, each downgoing event is aligned in phase, delayed relative to the initial downgoing compression by the TWT between the multiple generator and the deeper reflector, and recorded only at depths below the multiple generator. In +TT time (bulk shifted for display), each upgoing event is conditionally aligned in phase, positioned to the TWT at which they are recorded by SSP, and recorded only at depths above the multiple generator.

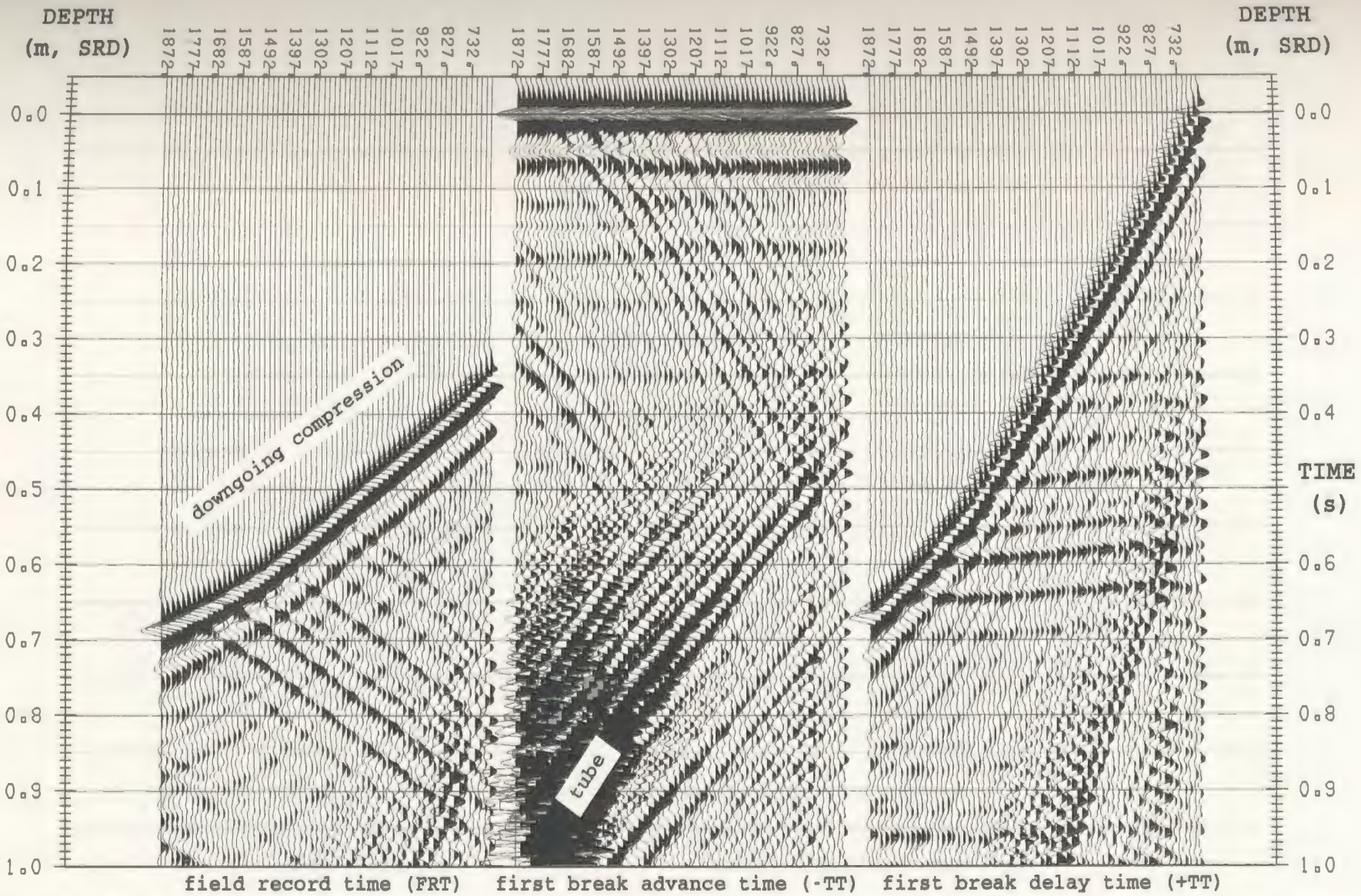

Figure 3.2.4b Various VSP processing time frames (SHELF). Downgoing tube wave energy is aliased in FRT and +TT time, but is unaliased in -TT time. Since only minor structure (deviation from horizontal stratification) exists at this location, residual moveout exibited by upgoing events in +TT time can be attributed to source offset and hole deviation. First breaks were optimized by correlation statics along the first trough (time zero in -TT), and +TT time has been bulk shifted for display.

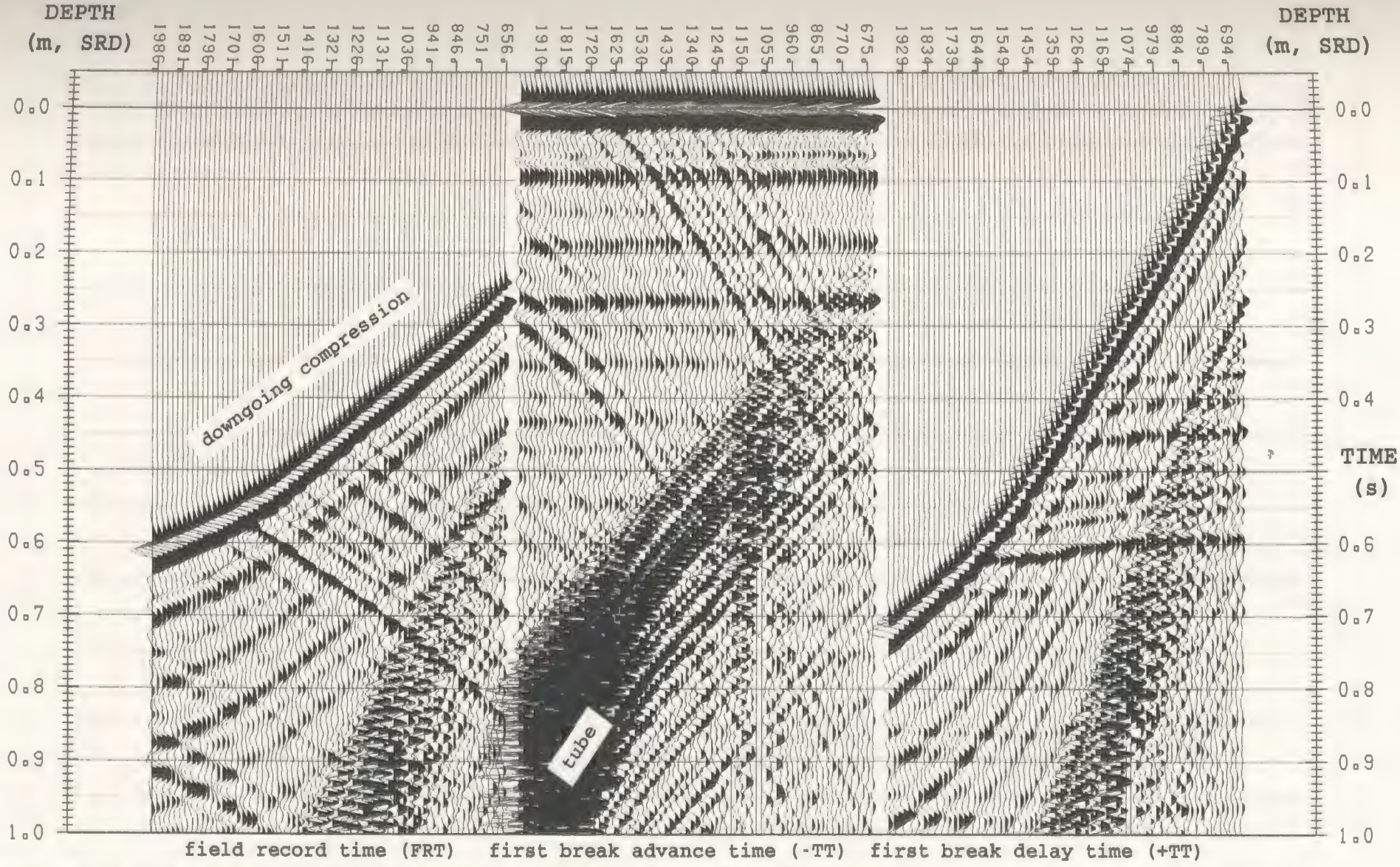

Figure 3.2.4c Various VSP processing time frames (EMBAYMENT). Downgoing tube wave energy is aliased in FRT and +TT time, but is unaliased in -TT time. Since only minor structure (deviation from horizontal stratification) exists at this location, residual moveout exibited by upgoing events in +TT time can be attributed to source offset and hole deviation. First breaks were optimized by correlation statics along the first trough (time zero in -TT), and +TT time has been bulk shifted for display.

a mixed phase nature, indicative of a short period multiple from above the VSP start depth. Based on the GLI [TM] static model, the weathering delay should be comparable for the reef and embayment locations while at the shelf this delay is greater. However, both off-reef VSPs do not appear to be modified in short lags to the same degree as at the reef. As no source parameters were provided with the reef VSP, an vibrator sweep equivalent to the shelf and embayment VSPs (10-96 Hz linear sweep) is assumed. The wells are offset from the SSP to an amount on the order of 100m, and this may limit the usefulness in surface multiple identification.

3.3 VSP Corridor Stacking and Multiple Identity

The VSP method allows investigation of multiple reflections present in conventional SSP profiles. The object is to distinguish multiple events from primaries at the zone of interest and to identify the multiple generating mechanisms. The major multiple problem can be identified following wavefield separation. This is demonstrated for reef exploration by Burton and Lines (1997). Any evaluation of multiple suppression methods on SSP data should be improved as a result of VSP multiple identification.

Both the up-going and down-going wavefields hold information regarding the multiple wavefield. Preferably, TRA can be preserved to identify energy partitioning associated with propagation. In the case of medium to long period multiples, events should terminate sharply at the depth of the multiple generator and exist only at deeper depths. In the case of short period multiples, this wavefield variation may be temporally visible due to phase distortion, but more subtle multiple effects may require the higher dynamic range available by decibel representation of amplitude spectra. Since the VSP source is consistent for all shots, variation in spectral character should be present within a strong interbed zone. Amplitude variation within the initial down-going compression may also indicate an interbed multiple generator, but spectral indicators are less sensitive to TRA preservation.

In the down-going wavefield, the uppermost trace represents the total energy entering the sampled zone. This energy consists of the initial down-going event modified by the near surface response. This trace can be used to remove shallow multiples from deeper traces in various ways. Predictive deconvolution can be used to successively remove each multiple on a basis of dominant energy or increasing period as designed from the autocorrelation, and this is more applicable to longer period multiples. The timing relation is

simply the delay of the generating layer, so that short period multiples that cause wavelet distortion may not be a weathering effect but may come from anywhere in the shallow section. Instead, the whole trace could be used as a wavelet to be de-phased from the deeper traces (waveshape the whole trace to a band-limited spike), or the trace could be simply subtracted from the deeper traces. The result would be to preserve interbed multiple effects generated within the sampled VSP interval.

In the up-going wavefield, multiples share a similar timing relation to the down-going multiples but amplitude relationships are different since the transmission coefficient is directional. However, the same periodicity as derived from multiples in the down-going wavefield should be applicable to predictive suppression of up-going multiples, but amplitude variations may hinder the correlation and the application.

Corridor stacking of VSP gathers is applied to the up-going wavefield. For a zero-offset source, horizontal layers without structure, and a non-deviated borehole, up-going events are aligned in the +TT time frame. As in CMP stacking, the addition of traces with coherent energy in phase causes the signal level of that energy to be increased over random noise by the square root of the number of traces input. The objective is the same in stacking up-going VSP energy, but the primary objective is to enable discrimination between primary and multiple events. There are essentially two regions of the VSP over which corridor stacking can take place - termed "outside" and "inside" by Hardage (1983). Because multiples are delayed in time relative to the interbed interface primary reflection, stacking within a time window delayed slightly from the first break trajectory will represent all primaries as well as any interbed multiples with period less than or equal to the time window length. This is called the "short", "front", or "outside" corridor stack and should be

dominantly primary energy. The stacking of arrivals that appear later in time will be called the "long", "back", or "inside" corridor stack. This should include effects from multiples with period in excess of the delay window. In comparison, the term "full" VSP corridor stack is coined in this text to obviate the need of excluding a short delay window in the stacking process. This stack contains all up-going energy so that multiple effects with period longer than the delay window used in the outside stack may be identified. The regional division between the inside stack and the full stack is a viable tool in multiple discrimination.

The process of autoconvolution (Sheriff, 1981) has been applied to identify interbed multiple components of the down-going VSP wavefield at the reef well in this Nisku study (Molyneux et al, 1996). Interbed multiples produced within layers were analysed by analogy to the retro-convolution method as applied to reflection SSP (Anstey and Newman, 1967). In the case of the down-going wavefield, autoconvolution amplitudes exclude up-going transmission and raypath redundancy effects recorded by SSP. This latter effect was illustrated previously in Figure 3.2.1 and Figure 3.2.2 for the case of an isolated layer in a homogeneous halfspace bounded by horizontal layers characterised by one-way transit time. Considering all possible raypaths up to and including first order multiples, the up-going wavefield contains all down-going raypaths plus extra raypaths due to two-way transit, constituting redundance in SSP recordings. One of these extra raypaths will be classified as a peg-leg multiple, recorded by SSP as two events that share the same raypath and delay. Since the trend for impedance is to increase with depth, it follows that transmission should be more efficient upwards (due to the directional nature of R_p). Although severest transmission losses are included in the down-going autoconvolution, the applicability to SSP

prediction operator design based on autocorrelations of autoconvolutions rests with including up-going transmission and identifying the order of the multiple to be attenuated so as to adjust the primary-to-multiple amplitude relation.

The method applied by Molyneux et al (1996) focuses on separation of interbed multiple components generated within the finely sampled portion of the VSP (see Figure 3.2.1). To do this, the down-going wavefield is separated and surface related multiples generated above the sampled zone are removed by shallow trace subtraction to boost interbed multiples. The autoconvolution is generated at each depth level and waveshaped to restore the spectra, then each trace is convolved with a series of reflectivities derived from the well log between trace depths (upwards) to modulate the primary amplitudes to relative surface amplitudes. Since autoconvolution effectively creates a time frame equivalent to ·TT time, the data can be stacked for comparison to SSP. This analysis concluded that multiple interference at the reef location was caused by a near surface effect with a period of 60ms.

CHAPTER 4. FORWARD MODELLING AND REFLECTIVITY INVERSION

The objective of this chapter is to present a review and discussion on the available methods pertaining to impulse response modelling. To help achieve the overall research goal, it would be beneficial to use models for multiple analysis. In particular, the normal incidence seismic resolution could be extended at the well by model based reflectivity inversion. Success of this inversion in satisfying normal incidence criteria would lead to alternative multiple suppression techniques and thereby improve Nisku exploration.

4.1 Normal Incidence Synthetic Seismograms

To fully understand the character associated with a complex reverberating reflectivity sequence, a depth model must be derived from which a seismic response may be generated. From depths to lithologic tops picked during the logging process, and from interpreted acoustic boundaries, the depth parameter members that require perturbation may be identified so as to generate synthetic seismograms which mimic the observed suite of responses observed in proximity to the response of the reservoir facies. The character response of potential reservoir facies may be sufficiently different from that of laterally equivalent non-reservoir facies so as to allow distinction based on normal incidence synthetics.

Rock layers that bound thin beds may differ significantly in impedance. The reflectivity at the top will be opposite in sign to reflectivity at the bottom since the thin bed is anomalously high or low in impedance. This pair of closely spaced reflectors is referred to as a dipole pair. In the case of sufficiently small primary reflectivity (R_p), the primary response of such a dipole is the dipole effect on the wavelet plus the effect of the net difference in R_p between both interfaces. The impulse response sequence (R_I) of an isolated

layer is linear in R_p for $R_p < 0.3$ (Robinson, 1967), meaning that for $R_p > 0.3$, the unbalanced dipole can play a significant role in multiple generation. In this case the short lag interbed multiple reverberation represents the intrabed effect (Schoenberger and Levin, 1974). However, another R_p sequence that adequately describes the primary response locally in time may not account for future anomalous amplitudes in the true R_t sequence due to the misrepresented role of energy partitioning in the impulse response. Hence, in order to model R_t for non-clastic reservoir facies and overburden associated with Devonian reef hydrocarbon plays, thin beds of anomalous impedance with sufficient lateral extent and continuity may constitute a significant portion of R_p. Since any contributor to R_s also forms a potential mechanism for multiple generation, these units should be well represented in the forward modelling scheme. However, since thin beds can impose difficulties upon the averaging mechanisms associated with well surveys, detailed model parameterisation must be limited to exclude thin bed aliasing caused by the physical size of the logging tool (Walden and Hosken, 1988). Thin bed definition is still derived from constrained time conversions of α and ρ well logs, but local geology and/or several logs can confirm the lateral existence of a thin bed so that logging problems are not mistaken for impedance anomalies. It is important to validate log resolution. Also, reflector continuity must satisfy Fresnel zone requirements (Sheriff, 1977) in order to create a reflector for SSP. In the context of this research, a reflector as identified on the logs will be required to show a primary response on the synthetics and be represented as a continuous event across the SSP extents.

As soon as thin beds reach the impedance level to be a multiple generator, the timing of the impulse response becomes important. For WCSB sonic logging, α is expected to

reach 6km s at Nisku reservoir depth of 1800m. This suggests that a sample rate (δt) for conversion to TWT without losing R_p information should be about δz α=0.1ms. However, since the logging tool is physically longer than δz, a minimum δt must be determined to avoid aliasing. The averaging of slowness (1 α_{sonic}) imposed by the logging tool is effectively a high-cut filter with response dependent on receiver separation, δt, and α_{sonic}. T The δt sampling used in depth to time log conversion should be chosen to minimise any aliasing from the logging process. When sampling doubles from 1ms to 2ms, there is increased likelihood of destructive interference from multiples coincident in TWT with each other and or with primaries. The most accurate R_t sequence available from logs will avoid alaised thin beds while preserving maximun resolution in event timing. Once w(t) has been convolved with the R_p or R_t sequence, the high frequency content is lost and the data may be resampled to match the sampling of the SSP VSP data.

Routine computation of broadband synthetics should be carried out using a block-averaging interval dependent on the nature of the log (Schoenberger and Levin, 1979, Walden and Hosken, 1988). In an equal TWT model, blocking should be at least 1ms TWT since larger values will generally underestimate both delay due to intrabed multiples and attenuation due to transmission losses (Schoenberger and Levin, 1974). Sonic logging tools have typical F_N on the order of 600-900Hz (Walden and Hosken, 1985) implying that dt<1ms (F_N=1 2δt=500Hz) may lead to high frequency aliasing of log data. Within Nyquist limits, the highest resolution estimate of what is actually sampled by SSP (δt=1ms) should enhance synthetic character over that of higher δt values.

The dipole reflectivity effect associated with thin beds forms a loose resolution criteria (Widess, 1973) that any bed thinner than one eighth of the dominant wavelength

($\lambda_0/8$) cannot be resolved (zero net response). This criterion is based on an impedance anomaly within uniform halfspace and neglects energy partitioning by assuming sufficiently small R_p values so that R_I is a linear function of R_p (hence no significant multiples). This and other resolution criteria as devised by Rayleigh and Ricker have been summarised by Kallweit and Wood (1982). Although these criteria are measures that assess the resolving power of wavelet deconvolved SSP VSP, they are meaningful only when applied to peak amplitude and corresponding TWT extracted from isolated traces. Hence, the task of implementing these criteria in the interpretation of non-elastic sequences is non-trivial.

Adequate parameterisation of the R_p sequence must also consider the significance of a free surface in multiple generation. As illustrated by Wuenschel (1960), a poor match between the computed and recorded signal may indicate significant free surface contributions to multiple energy. In general for land seismic, when compared to deeper subsurface reflectors the weathering medium is expected to exhibit a high level of attenuation (large Q) thus reducing and distorting contributions from ghosting and peg-leg mechanisms. In addition, the weathering interfaces may be very irregular due to sub-weathering topography and its effect on overburden under local depositional factors, thus decreasing the contribution to multiples by energy scattering. Hence, the effects of an anomalously low impedance surface layer may be very difficult to predict by normal incidence modelling. This suggests that seismic modelling from topography should be adapted to surface multiples. The simpler normal incidence approach is to include a free surface and weathering reflectivity. Ghosting due to shot burial in the weathering layer can be included by a shift and scale process. Notches in SSP data due to actual ghosting (at frequencies $n/\delta t_{ghost}=n/2T_{uh}$) will be somewhat compensated for by wavelet deconvolution

so ghosting is omitted from the synthetic. (Ghosted sources may call for alternative spectral whitening procedures). For these and other reasons, the object of synthetic analysis is to determine a match between seismograms and the seismic data. In this Nisku study, a 35Hz Ricker synthetic from R_I excluding surface multiples matches deconvolved SSP character to a satisfactory degree except in the region of the reservoir.

4.2 Offset Modelling

More complex responses such as focusing due to geometric horizon distribution may form a recognition criterion and modelling might demand methods implementing the wave equation. Similarly, effects associated with the interference of multiples and primaries will require careful reconstruction and manipulation of synthetic gathers so as to re-create the effect of stacking on the data. Errors in V_{rms} influenced by multiples will produce variable character in stacked amplitudes due to variations in lateral moveout correction. This effect is compounded by amplitude variation with offset, which is more difficult to model laterally due to parameter uncertainty.

To forward model pre-stack shot gathers, a frequency-offset (f-x) wave equation method was considered. This method is adequate for complex structure and gives better representation of correct amplitudes than kinematic ray tracing which produces constant amplitude for all dips. The approach is similar to the f-x migration algorithm but waves propagate in opposite directions under user defined maximum dip. In this method, a band-limited impulse source is downward continued to the bottom of the subsurface model, then both source and receivers are upward continued to the surface. Reflectivity is introduced at each upward step calculated as the magnitude of the gradient of the velocity field with the sign of the vertical derivative of the velocity field. Shot geometry is defined and variable surface topography is introduced with surface co-ordinates. The velocity field is defined by depth horizons. Density cannot be included for AVO effects, and the one-way wave propagation excludes multiples. The comparable normal incidence f-x approach that includes diffractions is an alternate approach to modelling primary Devonian reef response.

but a practical approach that includes multiples is preferred. One such method involves the use of autoconvolution and the radial trace transform.

The mathematical concept of linear moveout is being developed as a direct indicator of V_{INT} and as a multiple analysis tool (personal communication, Simon O'Brien, 1997). A radial trace gather is defined as a deformation of a dynamically uncorrected x-t gather to a V_{RMO}-t gather, where radial velocity is given by lines of constant x/t. When offset data comply with CMP assumptions, Snell's ray parameter (p) expresses the slowness of horizontal translation of the wavefront as $p=dt/dx=\sin\theta/V_{INT}$. For media where $V_{INT}=c$ constant, the tip of a ray moves laterally as $x=ct\sin\theta$ so that a radial v-t trace contains all energy that propagates at angle θ. This renders shot and receiver directionality constant in TWT, making this domain useful for compensation of wide-angle reflections, an important component of post-critical water-bottom multiples. The inverse transform can be useful in x-t shot modelling. The radial trace for normal incidence propagation ($\theta=0$) is defined by the R_I sequence generated by auto-convolution of the R_p sequence. The inverse process could be used to derive R_p that convolves with itself to match the pre-stack CMP radial traces for all θ. However, the amplitude relationship between primaries and multiples is misrepresented in the autoconvolution of R_p due to neglected transmission effects and wavelet shaping by the convolution process (squared amplitude spectra). To partially compensate for these effects, attenuation due to energy partitioning should first be incorporated based on impedance estimates. Then, following the autoconvolution, wavelet shaping should attempt to restore the amplitude spectra. In any case, the primary usage of this method is to investigate the timing characteristic of multiples for identification purposes.

Simple shot synthetics are computed in the radial trace domain using heterogeneous media parameterised in time by α and ρ, and optionally by β for variable σ. Radial trace domain velocities (x t) are incremented within extrema of α, while the time parameter remains unchanged on the forward transform. On the inverse transform, moveout is calculated using simple hyperbolic NMO equations, while amplitudes are determined using the Zoeppritz equations to include AVO effects. The main reason for using the transform is to compute multiples using autoconvolution and to incorporate simple AVO.

Hyperbolic reflection events that result from forward shot modelling in the radial trace domain are distorted for a combination of two reasons. First, ringy sync functions are incorporated for radial amplitudes instead of spikes. Second, an amplitude interpolation scheme is employed on the inverse transform to t-x space. To minimise these effects, it is best to convolve the source wavelet in the radial trace domain before interpolation. Primaries can be generated with or without all interbed multiples, or primaries with only surface multiples. To see the separate or combined effects these energy modes, the various outputs are manipulated algebraically.

Q-filtering effects on both phase and amplitude can be modelled using a migration-like approach (Hargreaves, 1987). These effects can be applied to a synthetic shot derived from the geologic model. The Q time function is supplied for zero offset, and extrapolation to far offset is based on V_{rms}. This analysis can complement model discrepancy analysis when Q effects are not included, and may also enlighten phase adjustment for spectral flattening analysis. Attenuation effects are expected to be less of an influence on model discrepancy than AVO effects.

AVO [M] incorporates AVO effects into pre-stack shot gather modelling of the primary and first order interbed multiple reflections generated from a single layer model. The requirement is to know the overburden and layer parameters, which implies that the multiple mechanism horizons are identified as layer boundaries. Since assignment of Zoeppritz parameters must relate to local boundary conditions, the AVO horizon must form the bottom of the acoustic layer whose top generates the multiple. To facilitate modelling the AVO effects at a horizon whose response coincides with a medium period multiple generated from above such a layer, successive models could be scaled and superimposed on one another. This should alleviate the need for the net layer response to be discrete relative to the response of adjacent layers. Amplitude and timing considerations that come into play will determine the usefulness of this exercise. Clearly this modelling procedure requires careful interpretation of multiple generating mechanisms.

4.3 Parametric Reflectivity Inversion for Multiples

To complement the interpretation of SSP data, optimised R_p models can be generated based on subsurface f(t) information. The source of initial model parameterisation and the nature of the interpretation problems will determine the robustness of the method. The exercise should illuminate aspects of any stratigraphic seismic play. In particular, the objective for this study is to identify multiple mechanisms occurring within a complicated reflectivity distribution and to evaluate multiple suppression techniques.

The inversion method implemented in this section was modified from an approach applied to multiple contaminated synthetic seismograms (Lines, 1996). The object is to modify estimated R_p values so that the resulting R_t synthetic adequately matches normal incidence seismic data. The convolutional model is non-linear in R_p, and the time positions are fixed. This method is somewhat similar to an earlier approach of parameter estimation (van Riel and Berkhout, 1985) where the convolutional model was assumed linear in R_p, but the number of reflectors and the time positions were allowed to vary as non-linear parameters. Berkhout has since developed inverse scattering methods for removal of surface related multiples. Lines' (1996) method should be more applicable to interbed multiples, but the incorporation of a priori information on the number of reflectors and positioning will determine this potential.

4.3.1 Least Squares Methods

Least squares optimisation methods serve to identify a best fit model response given inaccurate, insufficient, and inconsistent data. The biggest underlying assumption concerns the nature of the experimental data error. The formulation requires Gaussian error distribution about the mean, statistical error independence, zero mean error, and error of unit variance. If these conditions hold, then the likelihood that the residual error is due to random measurement error is related to the sum of squares of residual errors. This quantity may be expressed as a quadratic form in the parameter update vector, and then the least squares approach attempts to minimise the sum of squared errors with respect to parameter change coefficients. In other words, the computation of parameter updates is automated so that the difference between the data and the model response is minimised subject to constraints and under an absolute or fractional error convergence criterion.

If the model trace is linear in parameters, then a perturbation of the model trace about the initial guess is approximated by the first two terms of a Taylor series expansion. The inverse problem is then formulated to iteratively solve a linear system of equations $Adg=b$ (Lines and Treitel, 1984). This inverse problem is posed in terms of the error vector:

$e=x-y=b-Adg$	residual error vector
$b=x-y_0$	model discrepancy vector
x	data vector
$y=y_0+Adg$	model response vector
dg	parameter update vector (solution)
$g=g_0+dg$	updated parameter vector
A	rectangular Jacobian matrix

The solution vector contains updates to the parameters, and the discrepancy vector contains differences between the data and the model response. The Jacobian matrix of members $A_{ij}=dy_i/dg_j$ is composed of n rows and m columns, where a row exists for each data point and a column exists for each parameter. Since each column represents the derivative of the data vector with respect to each parameter, and since each column would require recomputation after each iteration, a considerable effort is associated with computing derivatives using differencing operator calculations. If a large number of pararmeters are required, then an approximation may be required or an analytic solution may be the best approach. Once Jacobian and model discrepancy elements are computed, the parameters are adjusted in a least squares sense until the convergence criterion is met. The convergence criterion generally require that the quantity e^Te be small enough.

The results are generally non-unique since the system is underdetermined. To combat the associated tendency for the Jacobian matrix to be deficient in rank and have singularities, the Marquardt-Levenburg method of damped least squares is adopted. The level of damping generally depends on the quality of the initial guess (Draper and Smith 1981), and may be viewed as a prewhitening procedure. In addition to damping, singular value decomposition (SVD) is employed to constrain eigenvectors that contribute to the solution. This process is referred to as 'winnowing'. The assignment of damping and minimum singular value parameters is part of the interpretative implementation of least squares inversion.

4.3.2 Inversion Formalism

To use the inversion process to invert for multiples, the method is to obtain a R_p model that adequately describes seismic data. The comparison is made by forward modelling using the one-dimensional convolutional earth model parameterised by $R_p(t)$. In this model, the primaries-plus-multiples seismic trace is represented as $y(t)=w(t)*R_I(t)$ where * denotes convolution of the defined wavelet $w(t)$ with the earth's impulse response function $R_I(t)$.

To perform the least squares optimization, the normal equations $Ag=b$ must be solved. In this formulation, the difference vector is composed of differences between the SSP data and the R_I synthetic. The parameter change vector contains updates to $R_p(t)$, and the Jacobian elements are derivatives of the data vector with respect to each parameter. If $R_p(t)$ is not highly reverberatory in nature, then the data are dominated by primaries and the distinction between $w(t)*R_I(t)$ and $w(t)*R_p(t)$ may not be significant. The model will then be almost linear in parameters and the approximation $R_p(t)=R_I(t)$ allows derivatives to be assigned simply as wavelet coefficients $dx_i\ dR_i=w_i$. The rectangular Jacobian matrix is composed of n rows and m columns, where a row exists for each data point and a column exists for each parameter (reflector). The Jacobian columns can then be visualised as single wavelets delayed by the reflector position within data space.

In the case where multiples contribute significantly to SSP data, the approximation $R_p(t)=R_I(t)$ does not hold. The model is then non-linear in $R_p(t)$ coefficients and requires iterative application of least squares. In this case, Jacobian elements are derivatives of the data vector with respect to each parameter. This derivative can be approximated by the differencing method which involves perturbing each model parameter individually by a

physically subjective amount and computing the resulting difference vector. This can become computationally intensive depending on the number of parameters and the size of the data window.

Sources of unknowns in a convolutional model scheme that lead to the ill-posed nature of the procedure include wavelet phase and band-limitation. The missing low-band information is replaced by a blocky version of the log data in the initial guess, but since the minimisation is applied to band-limited temporal amplitudes the trend contained in the inverted $R_p(t)$ is easily altered. This information could form a loose constraint on the quality of the initial guess and the solution. Although log generated R_p sequences typically display a net positive integration because velocity generally increases with depth, the trend for windowed and blocked R_p models may not agree.

The missing high frequency information represents unresolved thin layer effects, and this is part of the interpretation problem at hand. Although the best expected resolution could be set according to a wavelength criterion, a character identification criterion is still required to achieve feasible reflectivity definition. In essence, this inversion technique forms such a criterion, but the detail of the initial guess defines this potential. Thin bed dipole reflectors that affect energy partitioning may prove crucial to the scaling of successive inverted R_p sequences. Hence, modelling a sufficient number of layers reduces the overdetermined nature of this technique but increases the underdetermined nature and hence solution ambiguity.

In the context of the present problem, this suggests a limit for allowable reflection coefficient size. However, if the layer (bounded by multiple generating surfaces) had sufficient delay then the non-linear effects may not be significant in the zone of interest and

a linear system would hold. When a multiple dominates primary reflection energy at the same record time, the inversion process could adjust the secondary primary to obtain a best-fit amplitude agreement instead of modifying the shallower primaries responsible for the multiple. The degree to which amplitude has been preserved and to which multiples dominate the record will determine this tendency for failure. In any case, the linear inversion approach must be applied iteratively to combat the non-linear nature of the model. The final parameterisation will be exact (but still ambiguous) only if the model is truly linear.

The input data required for inversion for multiples take three forms. First, a w(t) is needed to convolve with $R_i(t)$ before least squares minimisation between the model response and the CMP data. Initially a 35Hz Ricker wavelet 100ms in length was used to produce an acceptable match to the data. The match was improved using an appropriate constant phase wavelet estimate as extracted from the seismic data and constrained well log impedance using STRATA [TM]. Since this extraction method assumes primaries only, the extraction window was chosen to exclude the multiple contaminated zone near well TD. As expected, the extracted wavelet provided less absolute error overall than the Ricker wavelet largely due to amplitude spectra.

The next required inversion information is the CMP data. The best realisable estimate of the true normal incidence impulse response for this horizontally stratified earth comes from the near offset stack. Offsets were subjectively limited to within 34-1000m during this partial stack, and the stack is enhanced by mild f-x random noise suppression. Since little structure exists for this target, migration is not necessarily required and any added noise due to the lower stack fold need not be removed by editing as usually required before migration. Instead, the f-x operator designed from 3 lateral traces provides sufficient

smoothing without the damage associated with trace mixing. However, if the focusing ability of migration is deemed crucial to amplitude preservation then f-x should only be considered following migration. Following this preparation, the stack amplitudes were windowed over 0.8-1.2s.

The final required input is the primary reflectivity sequence in time. As in any least squares optimisation procedure, this parameter vector requires an initial guess. Sources of initial reflectivity parameterisation will be determined by the resolution required by the interpretation problem. Any combination of stacking velocities, well logs, or other information may be incorporated to define or constrain an initial guess. Even checkshot scaled sonic values should even be forced to meet this criteria since first break picks may be in error due to transmission delay, giving velocities slower than actual. In carbonate sequences where Q-filtering is usually mild, wavelet amplitude spectra should not show significant change over limited depth extents unless intrabed multiples are severe.

In any case, the highest resolution reflectivity estimate available comes from well log impedance constrained in time by VSP check shots corrected for source offset and hole deviation at each well location. Once this model at logging resolution has been constructed, the number of reflectors must be reduced to a reasonable number in a blocky sense using appropriate criteria. Initially, code was developed to select from a reflectivity sequence in time values and indices of significant reflection coefficients above a certain threshold. The results are generally dependent on the depth-to-time conversion block-averaging interval, and hence lack geologic credibility and expected acoustic character.

Instead, blocky reflectivity should be parameterised using interpretation criteria. Due to the non-unique nature of this inversion, the number of layers and reliability of reflectivity

timing should be tested against the depth equivalent of the separated upgoing VSP wavefield to improve reliability. The VSP information was used to validate time-impedance blocking and unbalanced dipoles were designed to mimic data character (in terms of dipole differentiating effect). As mentioned, thin bed effects could render the inversion unstable and should be interpreted with caution.

Optionally, one could use a match between data horizon times and primaries-only synthetic times to derive pseudo-checkshots using a wavelet estimate. This character matching operation could be employed by adjusting the depth-time curve in a layer stripping approach until synthetic time character closely matches data character at that time level. This method assumes that there is little delay due to multiples, the wavelet is sufficient, and primaries are being matched. This process was initiated at the Viking peak and proceeded to the top of salt trough. These checkshot pairs can be validated against transit time integration, with the required scale factors optionally applied to transit times between checkshots. Using this method, all scale factors were within ten percent deviation. This method could be implemented and improved for the case where VSP checkshots are not available. Alternatively, stacked sections could be inverted for acoustic impedance (and hence reflectivity) based on the conditioned well data using STRATA ^{TM}, but in general this inversion is not applicable to data contaminated by multiples. VSP checkshots are available for this study so the preferred method is to map sonic depths to VSP time and thereby avoid drift correction between checkshot depths. If VSP checkshots were distributed as recommended, then more reliable drift could be computed to optimise sonic integration.

When sonic logs are blocked in depth, slowness is averaged instead of velocity so as to preserve timing of the logs, but in this case the time-impedance version is blocked and

timing is controlled by the checkshots. Following the manual blocking at well positions, these data may be interpolated using horizons tracked from the amplitude envelope of the seismic data. With real data, the algorithm can restore errors in amplitude to some degree but convergence under non-linear conditions is enhanced given a quality initial guess. Once defined, the positions of the parameterised reflectivity will remain fixed but amplitudes undergo iterative least squares adjustment to minimise the difference between the data and the model.

CHAPTER 5. APPLICATION OF METHODOLOGY, RESULTS, AND DATA INTEGRATION

In this chapter I examine the application of the methodologies following from the Nisku exploration data introduced in previous chapters. The integration and comparison of results is a non-trivial exercise influenced by differences between each method, and compounded by conditions of data and geology. In light of the SSP multiple condition, the strategies adopted will facilitate both the interpretation of and evaluation of multiple identification and suppression. The first goal of this chapter is to produce a wide band primaries-only CMP stack from SSP data by removing the effects of multiple reflections. The second goal is to provide multiple distinction criteria so as to avoid misinterpretation. The third goal is to derive a blocky primary reflectivity sequence that best describes the SSP nearoffset stack at well locations. To accomplish these goals, the first objective is to maintain data integrity over a wide frequency bandwidth while dealing with or overcoming any limitations imposed. The second objective is to further assess, verify, and suppress the multiple condition in the SSP data using available criteria. The degree to which these goals are fulfilled for this SSP experiment will determine the degree to which the thesis goal of improved (and reliable) Nisku resolution for enhanced hydrocarbon indicators is met.

In the first section of Chapter 5, SSP COF gathers are processed and presented in accordance to pre-processed data in Chapter 2 to evaluate the application and performance of conventional multiple suppression techniques. The aspects of conventional processing as applied to this SSP experiment are first described. The resulting pre-stack gathers are processed for predictive deconvolution to remove surface peg-leg multiples. This is attempted using lateral and temporal variation in SSP design criteria to provide appropriate

criteria for predictive deconvolution design. A Radon transform technique is also assessed for applicability. The stack data before multiple suppression is used in data integration for comparative identification of multiple interference.

In the second section of Chapter 5, log data and VSP data are processed in relation to Chapter 3 to evaluate multiple generation and the use of wellbore data in SSP multiple suppression for this experiment. Surface related multiples are suspect based on the SSP static model and from raw VSP's, and interbed multiples are expected based on the wellbore impedance distribution. Aspects of synthetic seismogram generation are considered in relation to suspected multiples and event timing. The subjectivity of the derived blocky acoustic models at each well is discussed along with time conversion influence on synthetic character. To complement the analyses, pre-stack VSP wavefields are processed and interpreted in light of the suspect SSP multiple mechanisms. The log data are correlated with the VSP's to support the blocky models, but extra detail is included in these models for reflectivity inversion.

The third section of Chapter 5 integrates SSP, VSP and synthetic data to allow robust identification of SSP multiple interference in post-stack SSP data at well locations. This incorporates the best multiple indicators: SSP offset limited stacks for differential moveout, VSP corridor stacks for multiple period, and impulse response for theoretical multiples. In the fourth section, normal incidence reflectivity inversion is implemented using the blocky model with and without near surface reflectors. The subjectivity of the blocking process becomes important in light of the complex response. More importantly, inversion from surface to target depth and below may be more appropriate than windowed inversion unless surface effects can first be removed by conventional methods.

5.1 Surface Seismic Data Analysis

The processing strategy adopted for this Nisku SSP analysis is outlined in Figure 5.1.1. Following geometry application, SSP processing was initiated by interactive picking of first break times. All shots and all offsets (34-2057m) were picked for improved statistics (excluding near offset picks interpreted as direct arrivals). These data along with survey geometry are required for GLI [TM] refraction analysis. Visual inspection of refracted arrivals supported a three layer earth model. With topography varying over 805-878m, a SRD elevation of 900m and replacement velocity comparable to subweathering velocity (2900m/s) ensures that the total datum static is a positive delay. This ensures data time zero is positive thus avoiding zeroed amplitudes by static application. Given that the maximum two-way refraction correction to datum is about 40ms delay for this survey, the effect of misrepresenting t_0 in the NMO equation is small and a floating datum is not required. The first breaks were processed to the typical maximum offset of 2057m, suggesting a depth smoother length of 137m and velocity smoother length of 4114m as recommended under software documentation. This is because the objective of GLI [TM] statics analysis is to compute the weathering time delay at the expense of true definition of thickness and velocity.

In this study case, shot holes were drilled to a depth of 24m in an effort to reduce surface wave modes. With near offset of 34m and group spacing of 17m, if the shot is assumed to be located at the base of weathering or shallower, then the direct wave will be sampled by one or two traces at best. Since this is not sufficient statistically, weathering velocity determination must rely on uphole times (700 to 950m/s). This information is utilised in the model along with inverted weathering thickness and subweathering velocity to

2400% STRUCTURAL STACK (N)

Client: Pancanadian Petroleum Ltd.
Area: Nisku
Line: confidential SP's: 106-871

SSP ACQUISITION PARAMETERS

contractor: confidential
date acquired: 1991 instrument: I O System 1
tape format: 2.5 byte SEGD tape density: 6250 bpi
lowcut filter, slope: 3hz @ __dB/oct anti-alias freq: 120 hz
record length: 3000ms sample rate: 2ms
number channels: 240 data + 4 aux nominal fold: 24
geophone type: Sensor SCM-4 geophone frequency: 14hz
geophones/group: 9 over 1/m group interval: 1/m
source array: 1x4kg at 18-24m shot interval: 85m

2057m . . .. 34m . S . 34m 2057m
240 121 120 1

PROCESSING HISTORY

1.geometry application: variable fold SEGD records
2.shot resort: sequential
3.trace edits:
4.polarity reversals: receivers
5.gain application: s'(t)=s(t)*t**1.85
6.surface consistent scaling: shot + receiver I.L.S. (iter=5)
conditioning filter: 12/16-80/100hz
offset window: 357-1800m
time window at near offset: 500-2200ms
time window trajectory: 2900m/s
7.first break picks: interactive, all shots
8.refraction static analysis: Hampson and Russell GLI(2d)
datum elevation/replacement velocity: 900m - 2900m/s
two refracting layers, surface velocity from upholes
9a.shot consistent deconvolution: I.L.S.(iter=3) Lev. M.P.
operator length/prewhitening: 100 ms 3%
9b.receiver consistent deconvolution: I.L.S.(iter=3) Lev. M.P.
operator length/prewhitening: 80 ms 1%
deconvolution design window: 500-2200ms at 357m
900-2200ms at 1800m
10.refraction static application:
11.semblance velocity analysis: bin 3 cmp 1 offset
spatial density: 212.5m (25cmp's)
12.cmp sort: nominal 24 fold
13.surface consistent residual statics: shift: +/- 16ms
window: 750-1400ms
14.nmo application: mute at 50 percent stretch
15.front end mute: offset(m): 300 650 2057
time(ms): 300 650 750
16.trim statics: shift: 10ms window: 750-1400ms
model: 3 cmp mix band: 20/30-70/85hz
17.stack: nth root (n=1)
18.bandpass: 12/15-100/120hz
19.mean energy equalization: window: 750-2000ms

Figure 5.1.1. Conventional Nisku SSP stack label. The actual processing stream adopted in this research is described in the text.

derive static adjustments. The static contributions from the surface weathered layer indicate significant potential for peg-leg multiple generation (see Figure 2.1.7).

With the GLI [TM] solution applied, there were no statics busts or high frequency statics evident on shot, receiver, or CMP stacks. Surface consistent residual reflection statics using stack power optimisation (Ronen and Claerbout, 1985) involves conventional linear inversion and correlation of squared amplitudes within a CMP gather. This method generated sparse single sample static adjustments implying that short wavelength statics are solved precisely by GLI [TM] given quality and consistent first break picks. Typical failure of refraction algorithms inferior to GLI [TM] increases processing effort by demanding iterative velocity and residual static analyses. Since structural and residual NMO are misrepresented in the CMP stack model, correlative reflection statics can fail independent of S/N level. Although an improved stack can be produced by CMP trim statics, a loss occurs in surface consistency of statics and hence control of dynamic corrections. The more reliable Nisku structural section is obtained with the GLI [TM] solution based on quality first breaks from weathering layer(s) that conform to the CMP static assumptions.

Following static application, data scaling and wavelet deconvolution were performed in a surface consistent manner. The design window for these analyses ranged from 500-2200ms at 357m to 900-2200ms at 1800m. This design window attempts to exclude near offset noise as well as far offset effects of increased Q-filtering and event tuning. Including an offset component in deconvolution design compensates for average offset dependence over the survey in an average sense. The far stack suggests that this process is needed. However, shot and receiver components alone may provide better compensation for lateral variation in spectra and hence w(t) recovery for Nisku character. Offset zones of significant

tuning are identified on raw autocorrelations and excluded in favour of a near offset response. Also, 1800m is considered sufficient offset for HSVA, AVO and multiple identification.

In the deconvolution process, a single operator design from the shot and receiver domains simultaneously was tested against an approach where the design was cascaded from the shot domain to the receiver domain. The single operator design used a standard length of 80ms and unity PW. The cascaded operator was applied with 100ms operator and 3% PW followed by a 80ms operator and unity PW. Nisku character changed from a singlet to a doublet suggesting higher resolution due to improved de-ghosting. For a 60ms wavelet, an average ghost delay of 60ms (T_{gh} 2) supports a 120ms shot domain operator while an average weathering peg-leg delay of 90ms supports a 150ms receiver domain operator. However, since R_p is coloured by dominant primaries correlating within these lags, assumptions require that standard deconvolution be applied without including ghosted and surface peg-leg extensions to the wavelet. For this reason the processing stream adopted in this study employs the standard 80ms spiking operator. Unity PW provides sufficient pre-stack noise, but lower values may provide slightly higher resolution with noise tolerated by stack S N. Within the bandwidth 12/15-80/95 Hz, this operator provides a well-behaved residual wavelet and preserves primary colour. Nisku character will still be influenced by ghosting, surface peg-legs, and interbed multiples.

Following deconvolution, SSP data are prepared for velocity analysis. Logistically, HSVA is designed based on data acquisition, S/N ratio, and velocity characteristics. Due to the subtle nature of this play and due to unknown multiple generation mechanisms, lateral velocity control was maintained using a tight spatial increment of 212.5m (25 CMP's). The

first 100 CMP's were skipped so as to start with full fold coverage (2400%), then at each location 10 CMP's were binned on absolute offset using station spacing to ensure that all offsets are represented in the analysis. In accordance with the binning process, further enhancement to S/N ratio is gained by band-limitation (15/20-70/80 Hz), f-k noise rejection (non-hyperbolic events), front-end mute (first breaks and earlier amplitudes), and short AGC scaling (200ms). This processing improves the semblance calculation as influenced by the reflection signal. Next, parameter values are required to define the appropriate suite of hyperbolic trajectories.

Initially, the hyperbolic t-x semblance was calculated for global velocity estimates and diagnostic purposes. The stacking velocity function ranged from 1800-5300m/s incrementing at 100m/s to produce semblance from 36 hyperbolic trajectories at each zero offset time (a moveout increment near 8ms for the Nisku). Processed COF gathers and velocity spectra (see Figure 2.2.1) indicates primary energy from 800-1100ms and significant related low-order multiple energy of variable nature occurring at later times (1100-1250ms) and lower velocity. Lack of direct indication of shorter period multiples in the shallow section suggests that the deeper multiples are interbeds. However, the shallow primaries have less offset and less attenuation so that the semblance of a near-normal incident weathering peg-leg may not be separated from primaries to the degree of peg-legs from deeper reflectors. Still, the shallow stacking velocity semblance structure should represent the same peg-leg mechanism as embedded in the deeper zone.

Subsequent detailed velocity analysis was designed to optimise NMO correction at the Nisku level. With local stacking velocity near 3500m/s at a normal incidence TWT of 1100ms, the semblance was parameterised by a velocity range from 2000-4500m/s with 101

velocity steps of 25m/s to give the maximum accuracy of one sample (2ms) between trajectories at the far offset (2057m). Depending on bandwidth, the fine increment does not necessarily improve semblance resolution but removes round-off picking error associated with larger increments. For a frequency component of 100Hz at the Nisku level, significant cancellation will occur over a linear trajectory when absolute velocity error exceeds 50m/s. This ensures a picking precision of 2ms at the far offset, while accuracy is determined by visual fitting of hyperbolae to events (optimised by data preparation) during interactive interpretation of supergather-semblance pairs.

The quality of the velocity analysis panels in the shallow section was low, largely due to reverberating refraction modes, source generated noise, and groundroll. The low S/N ratio was improved by implementing a f-k approach in absolute offset CMP domain. First, NMO was applied using initial stacking velocities then CMP trim statics were applied and the NMO was removed. Since NMO will distort wavenumbers of linear energy modes, pre-NMO rejection is the best way to deal with reverberating refraction energy. (However, aliased groundroll may become unaliased following NMO). The apparent velocity trajectory for low-cut rejection can then be defined near the refraction velocity. All data with lower apparent velocity (including surface waves) are rejected. Also rejected are negative wavenumbers associated with aliased groundroll, as well as aliased near offset shot generated noise. These sources of aliased noise support usage of directional f-k rejection. Semblance can then provide more reliable estimates of shallow reflector position and velocity distribution and can also be used as a direct measure of testing effectiveness of multiple suppression.

The near offset stack (see Figure 2.2.2b) used for wavelet extraction (STRATA [TM]) at each well site produced wavelets with near-zero residual phase at the reef, –50 degrees at shelf, and 50 degrees at embayment. This variation could be influenced by various factors. Minor influence is attributed to the deviation of the off-reef wells and the surface offset from the SSP. Also, the synthetics used by STRATA to extract the wavelets were generated under a 2ms depth-to-time conversion, while a 1ms block size was considered more appropriate. Major influence can be attributed to the different weathering delay and ghosting period at each SSP location (again see Figure 2.1.7).

Based on evidence supporting a surface peg-leg multiple condition, the processed COF gathers are deconvolved with operator lag set as the GLI [TM] model delay. This application has been attempted in three different designs. First, since deeper primaries are known to correlate at lags similar to weathering delay, shallow window operator design is preferred. Since the mechanism has an expected normal incidence nature, only near offsets with sufficient correlation gates are used in the design. Compared to multiple contaminated SSP data (see Figure 2.2.1c), post-prediction pre-stack auto-correlations (Figure 5.1.2a) show significant reduction in the level of near offset ringing at the reef, but little change occurs in correlation over the target window. The desired effect is to remove only the peg-leg component of the correlation over the effective lag window (near 100ms) where primaries are known to correlate. The reef auto-correlations are now more comparable to the shelf and embayment locations but the process has little effect overall.

The post-prediction near stack (Figure 5.1.2b) shows little change in data character as compared to before (Figure 2.2.2b, middle). The multiple (M4) that arrives just after the Nisku reflection should be suppressed, but only subtle changes can be observed. At the reef

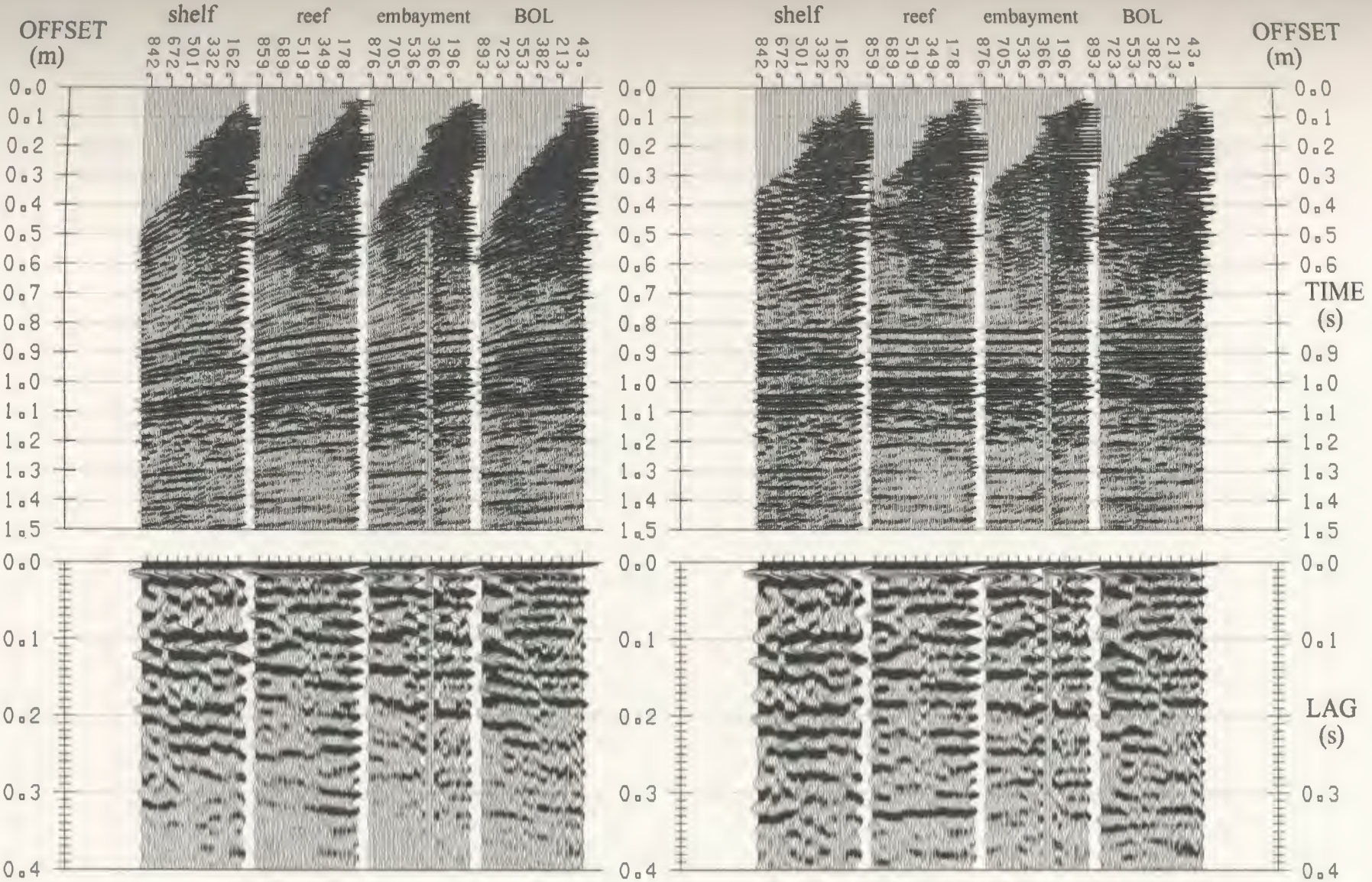

Figure 5.1.2a Multiple attenuated SSP-COF gathers (top). Processing stream is gain, statics, spiking deconvolution, f-k reject, normal moveout, bandpass, mean scaling, trim statics, predictive deconvolution (right), and NMO removal (left). Prediction distance is set based on the modelled two-way delay in the surface weathering layer, but adjusted based on interpretation of bandlimited autocorrelations of stack data. Operator length is 80ms designed over the shallow portion of the response (150-800ms at 34m and 400-800ms at 900m). Autocorrelation (bottom) design window is 700-1300ms after NMO (right), and varies from 700-1300ms at 34m to 850-1300ms at 900m before NMO (left).

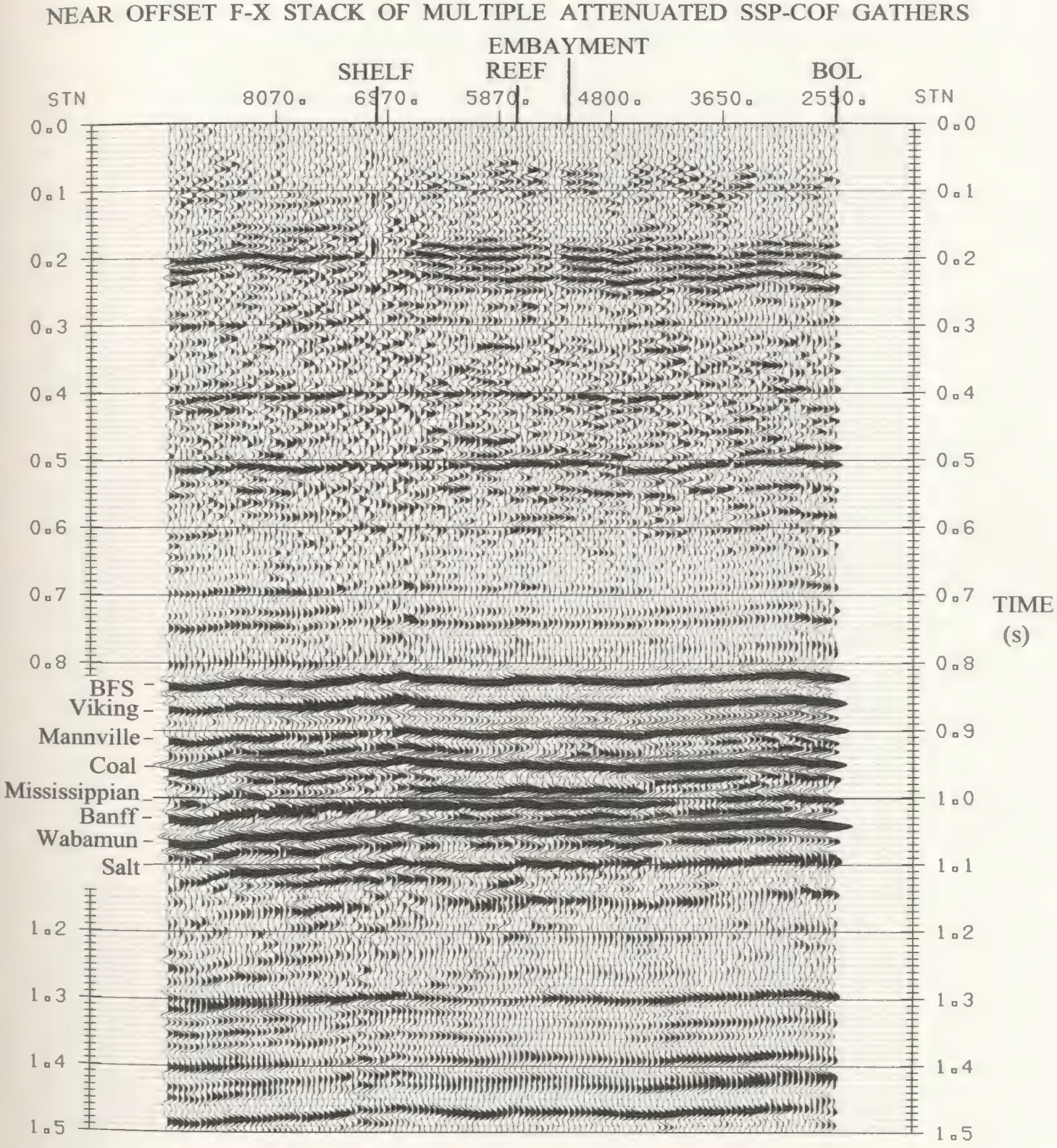

Figure 5.1.2b Near offset f-x stack of SSP-COF gathers with multiple attenuation by predictive deconvolution. The multiple under attack is surface pegleg generated within the weathering layer. Energy near 1150ms has been boosted by the prediction process either by energy introduction due to inappropriate design, or by allowing another multiple of differen period to stack with less interference.

location, a subtle change occurs at the Nisku. This appears to be a local effect related to shorter peg-leg periods in this area. Stack auto-correlations (Figure 5.1.2c) show minor improvement in shallow signal as compared to before (see Figure 2.2.2c) while signal in the target zone appears unchanged. Band-limited versions of these data (Figure 5.1.2d) shows that there is very little change in signal as compared to before (Figure 2.2.2d) over the low frequencies where multiples are strongest. Poor suppression performance can be explained by poor S/N in the shallow section such that pre-stack prediction to remove peg-legs is not reliable.

The second approach to prediciton was to include all offsets in a pre-stack design window over the target zone. This suppressed autocorrelation energy at operator lags where primary energy is included (Figure 5.1.3; see also Figure 2.2.2e). Although inappropriate, this suppression allows multiple energy to correlate stronger at the BOL location near 220ms delay corresponding to a second order surface peg-leg multiple. Primaries still dominate the correlation at the well locations, where the surface peg-leg could propagate as a plane wave or with less energy.

The third attempt at prediction design uses a post-stack approach to remove near surface effects. Because of poor S/N in the shallow stack, f-x noise attenuation was applied for enhancement. Autocorrelations before prediction (Figure 5.1.4a) show significant ringing in the shallow window. Operator design was applied so as to remove shallow reverberation, and post-prediction correlations (Figure 5.1.4b) indicate that energy in the deeper window has become more balanced. Figure 5.1.4c compares the pre-processed near offset stack (top) to after prediction (middle), and indicates significant change at the Nisku with little change elsewhere. The Nisku anomaly is easily identified near 1120ms at the reef

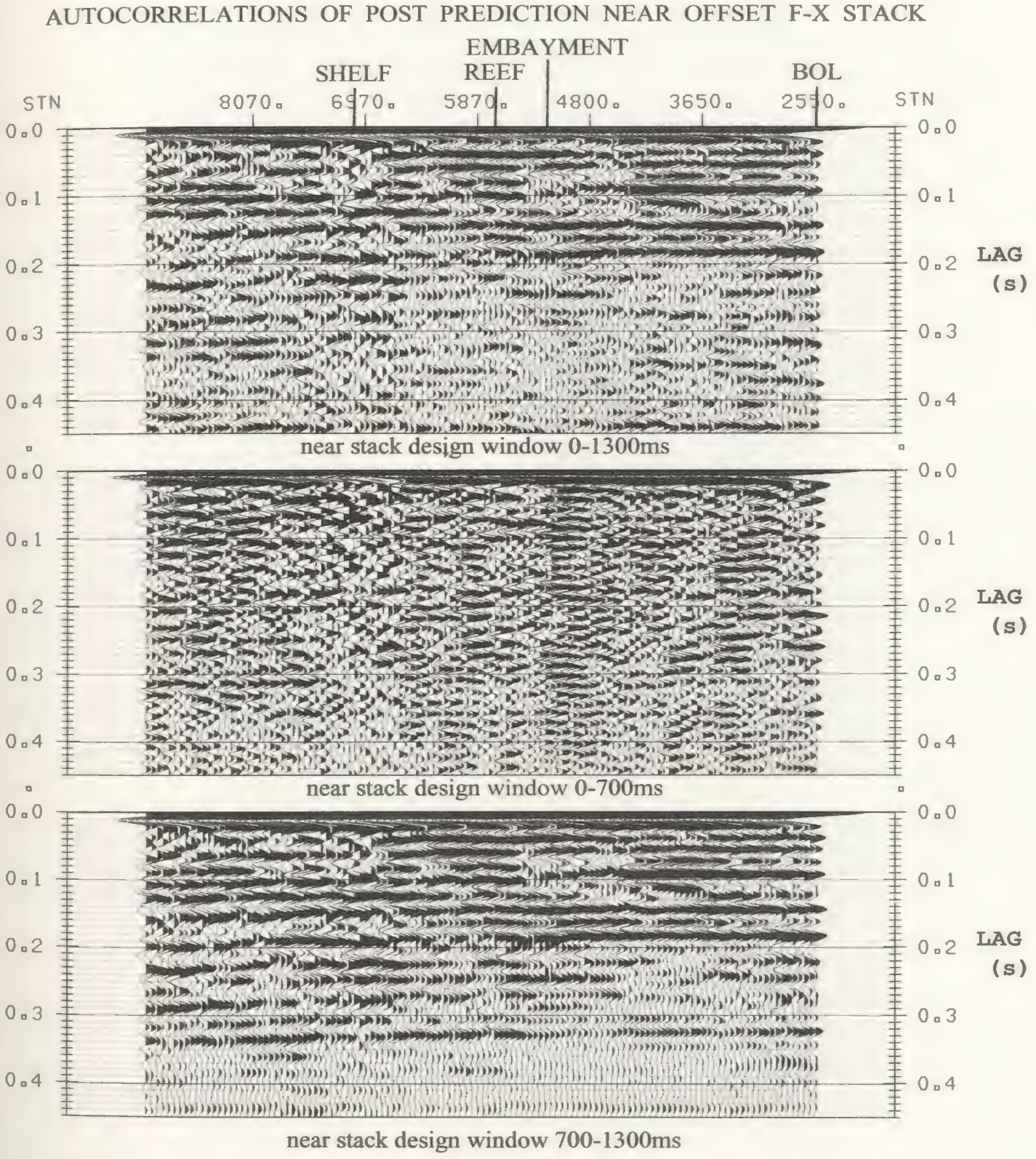

Figure 5.1.2c Windowed autocorrelations of near offset f-x stacks of SSP-COF gathers with multiple attenuation by predictive deconvolution Design window varies from 0-1300ms (top), 0-700 (middle), and 700-1300ms (bottom). Since the pre-stack prediction operator design is based on the shallow data, this is where the most change is expected to occur. Also, the character is now more consistent for the deeper window.

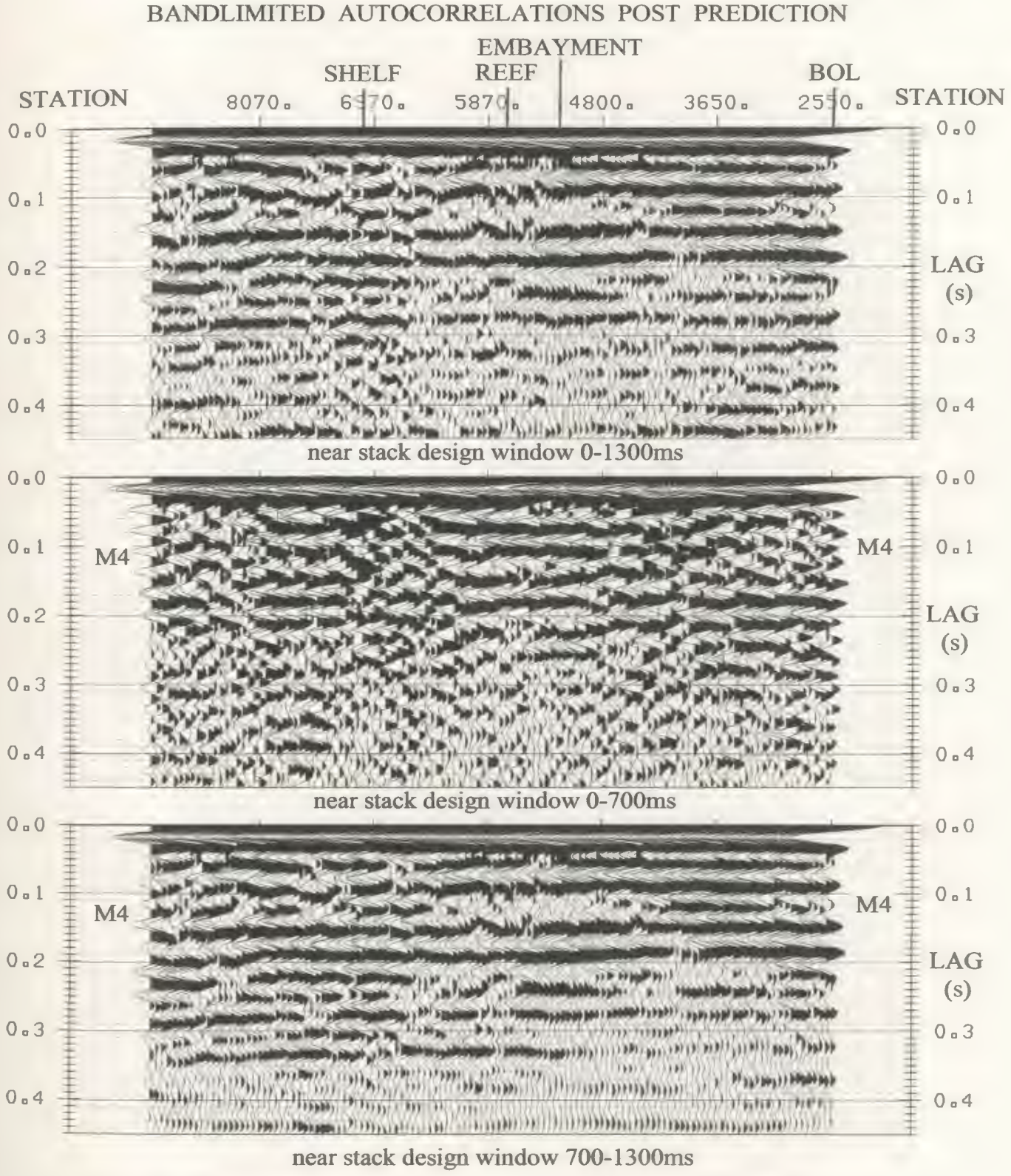

Figure 5.1.2d Bandlimited autocorrelations (12/15-35/45Hz) of of post prediction near offset f-x stack.

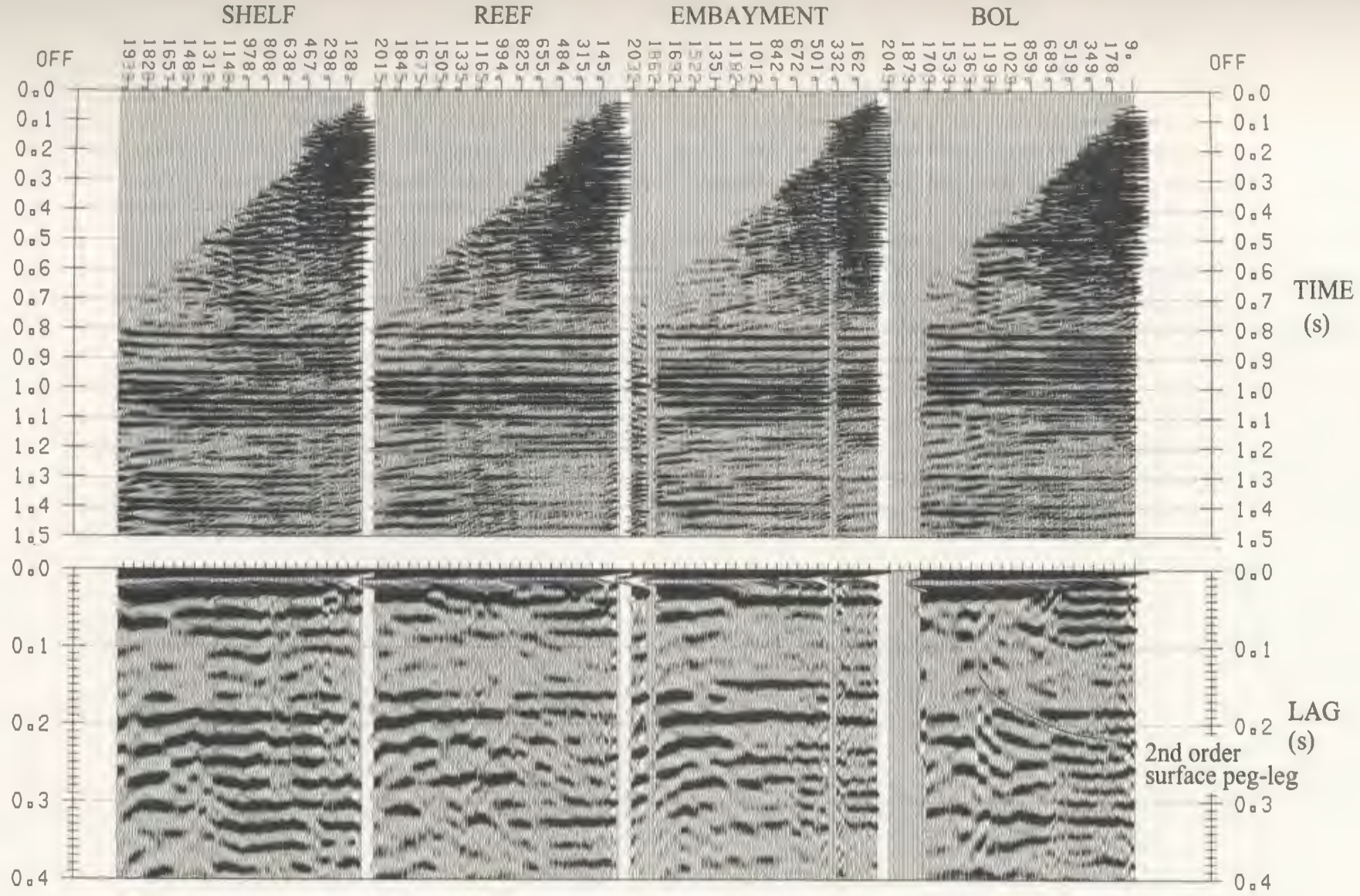

Figure 5.1.3 SSP COF gathers with dynamic corrections (top) following prediction design over a deep window (700-1500ms at 34m and 750-1500ms at 2057m) using weathering delay as prediction distance. Autocorrelations (bottom) are computed over design window 700-1300ms. Primaries are known to correlate at the lags suppressed by the prediction. The second order surface peg-leg is now evident at the BOL location (near offset time about 220ms).

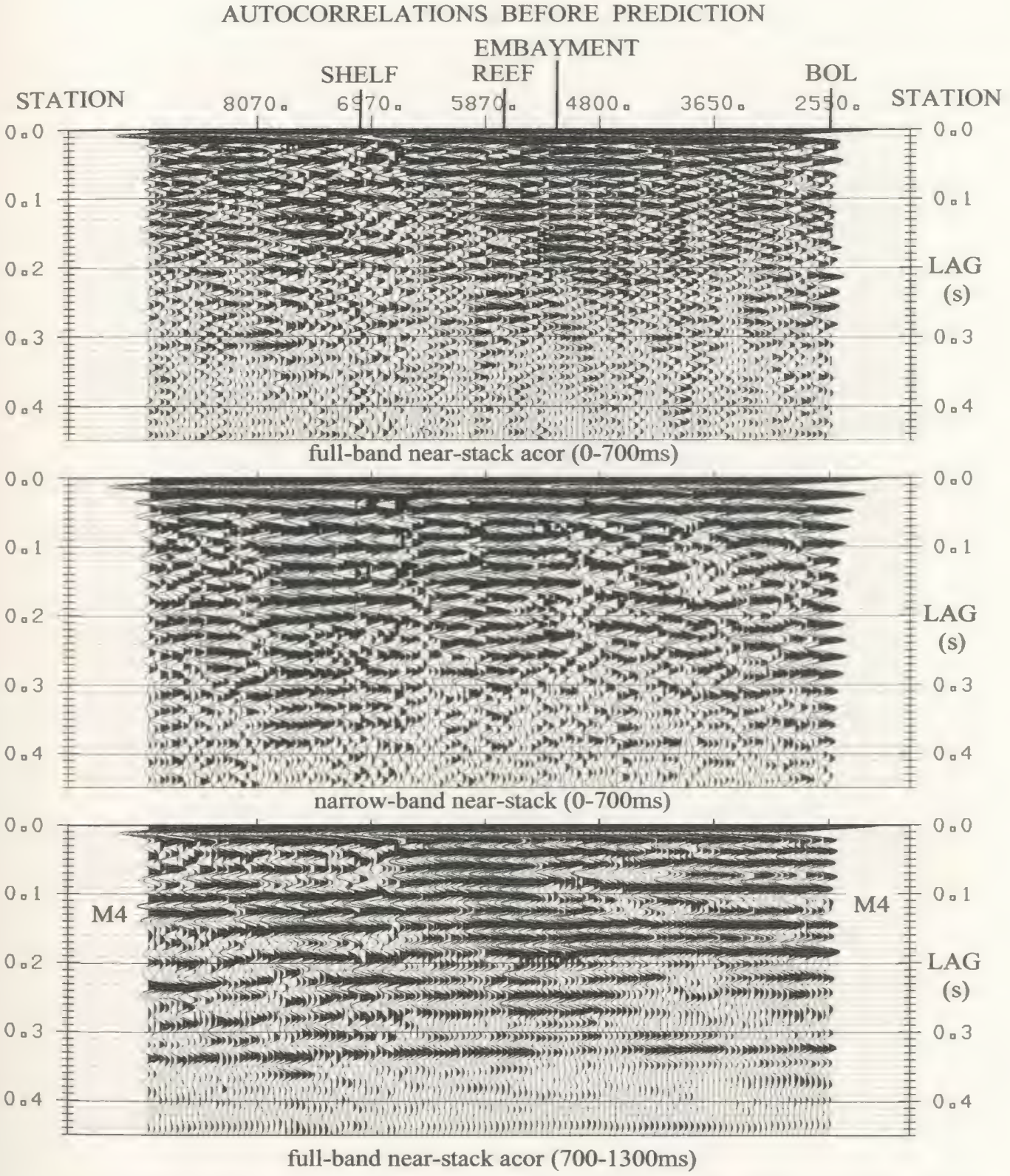

Figure 5.1.4a. Near-stack autocorrelations before predictive deconvolution. Inconsistency in amplitudes of the primaries correlating near lags of 100ms and 200ms are likely to be caused by surface related multiples. Shallow design assumes that shallow reflectivity is white within the seismic bandwidth. Deep-window contamination by shallow multiples could be causing inconsistent amplitudes across the line (M4).

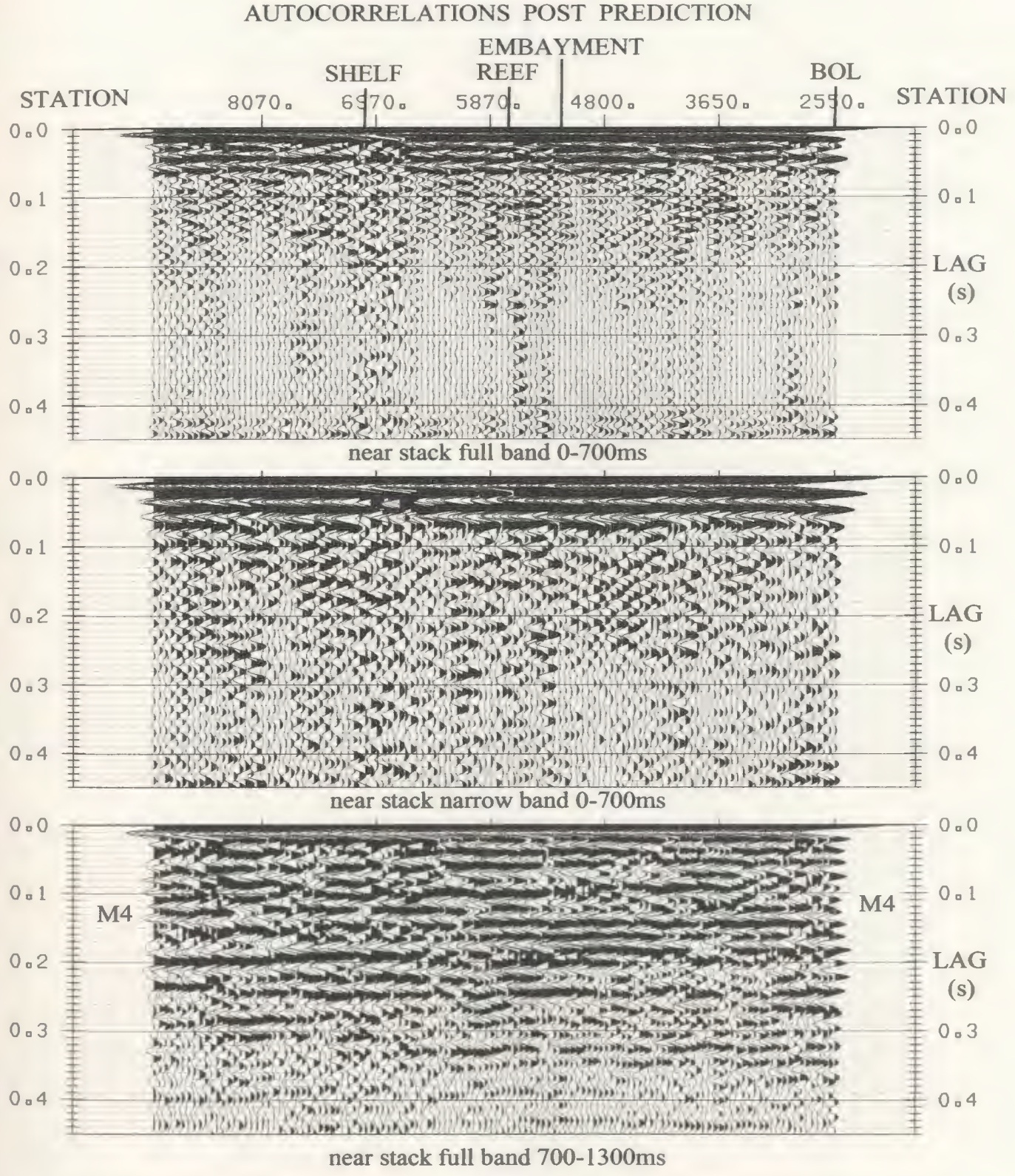

Figure 5.1.4b. Near-stack autocorrelations following predictive deconvolution based on shallow window design. The primary events correlate more consistency in amplitude across the line near 100ms (M4) and 200ms. Interbed multiples may still interfere. Cascaded prediction operator design (3 passes, 120ms operator).

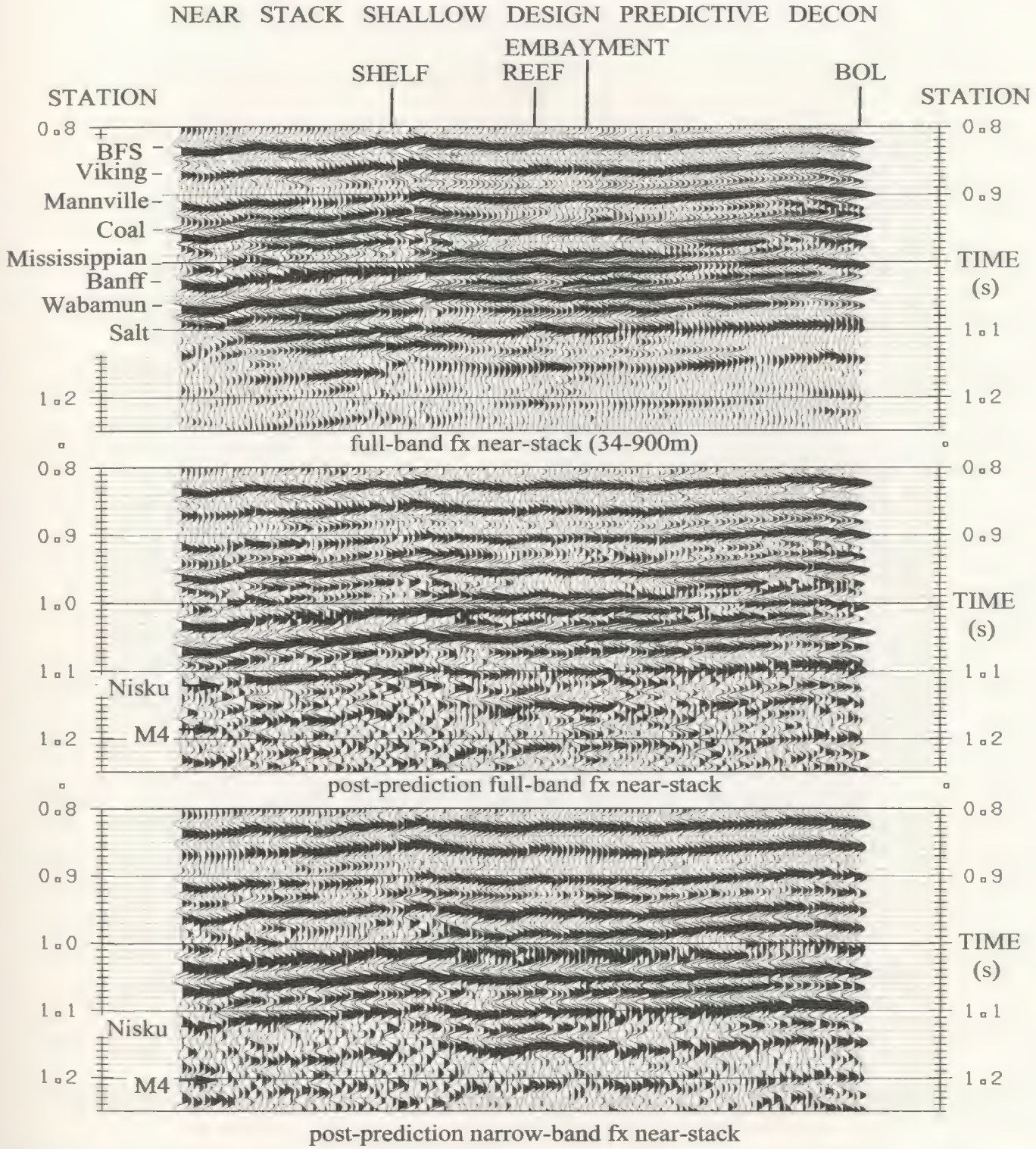

Figure 5.1.4c. Pre-processed near-offset f-x stacks. Contributions to the sub-Nisku multiple (M4) from near-surface multiples should be suppressed by post-stack prediction using shallow design criteria. Cascaded prediction (3 passes, 120ms operator) for lags outside 80ms.

on the narrow band stack (Figure 5.1.4c, bottom), and appears to terminate laterally before reaching each off-reef well location. Removal of surface reverberation appears to have provided a criterion for reef identification given the apriori knowledge of well results.

An alternative approach to multiple suppression involves the Radon transform. The slant stack transform of the COF gathers (Figure 5.1.5a) involves transforming points in x-t space to lines in tau-p space. Hyperbolae transform to ellipses but when multiples and primaries are coincident with little moveout difference, the corresponding energy is not well separated in tau-p space. The hyperbolic velocity filter (HVF, Mitchell and Kelamis, 1990) transforms points to lines restricted in p based on primary stacking velocity (Figure 5.1.5b) essentially performing tau-p muting for multiple suppression. The inverse transform autocorrelations (Figure 5.1.5c) indicate less multiple contamination near 100ms lag at the BOL location where moveout was the greatest, but the reverberation is still strong at the reef. HSVA (Figure 5.1.5d) indicates reduced multiple semblance, but only a far offset stack can benefit from this S:N improvement and only where moveout is significant. The parabolic Radon transform (INVEST [TM]) was tested and found to be comparable but somewhat less effective than the HVF approach, largely due hyperbolic distortion caused by NMO stretch.

In this section, some results have been presented from the testing of conventional multiple suppression techniques applied to pre-processed SSP COF gathers. In summary, conventional prediction and moveout discrimination methods have been illustrated to be less than successful in providing consistent treatment of peg-leg multiples laterally. In some cases, a far stack with Radon multiple suppression may be of use if frequency content can be sacrificed (loss with offset). However, prediction can be useful in suppressing dominant

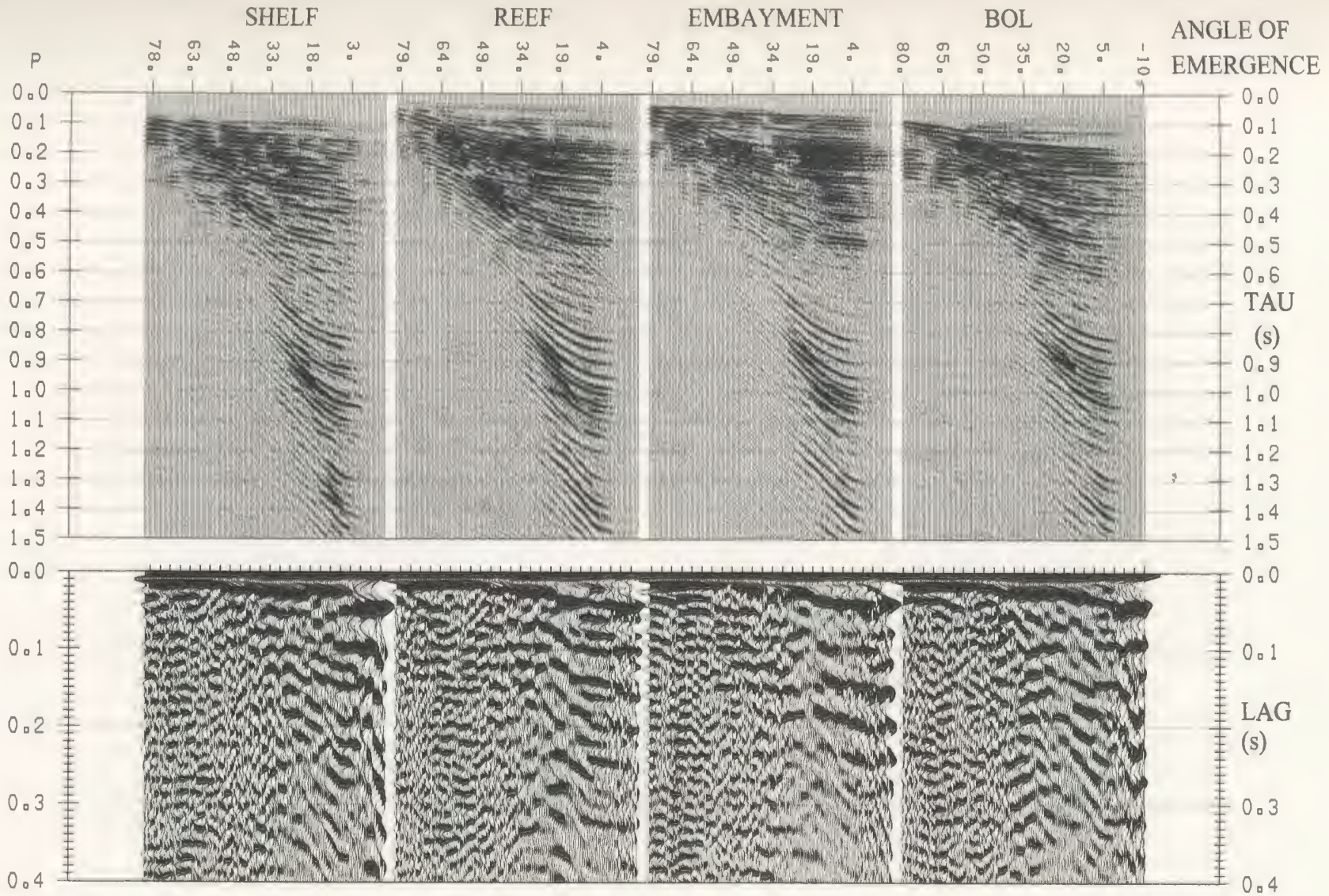

Figure 5.1.5a Slant stack transform of processed SSP COF gathers (top) and autocorrelations (bottom). Decomposition variable is angle of emergence as defined by a near surface velocity of 2900m/s, and ranges from -10 degrees to 80 degrees by an increment of 0.75 degrees (121 traces). Autocorrelation design window is 700-1300ms at -10 degrees and 300-1300ms at 80 degrees. There is no obvious benefit to prediction design in tau-p space.

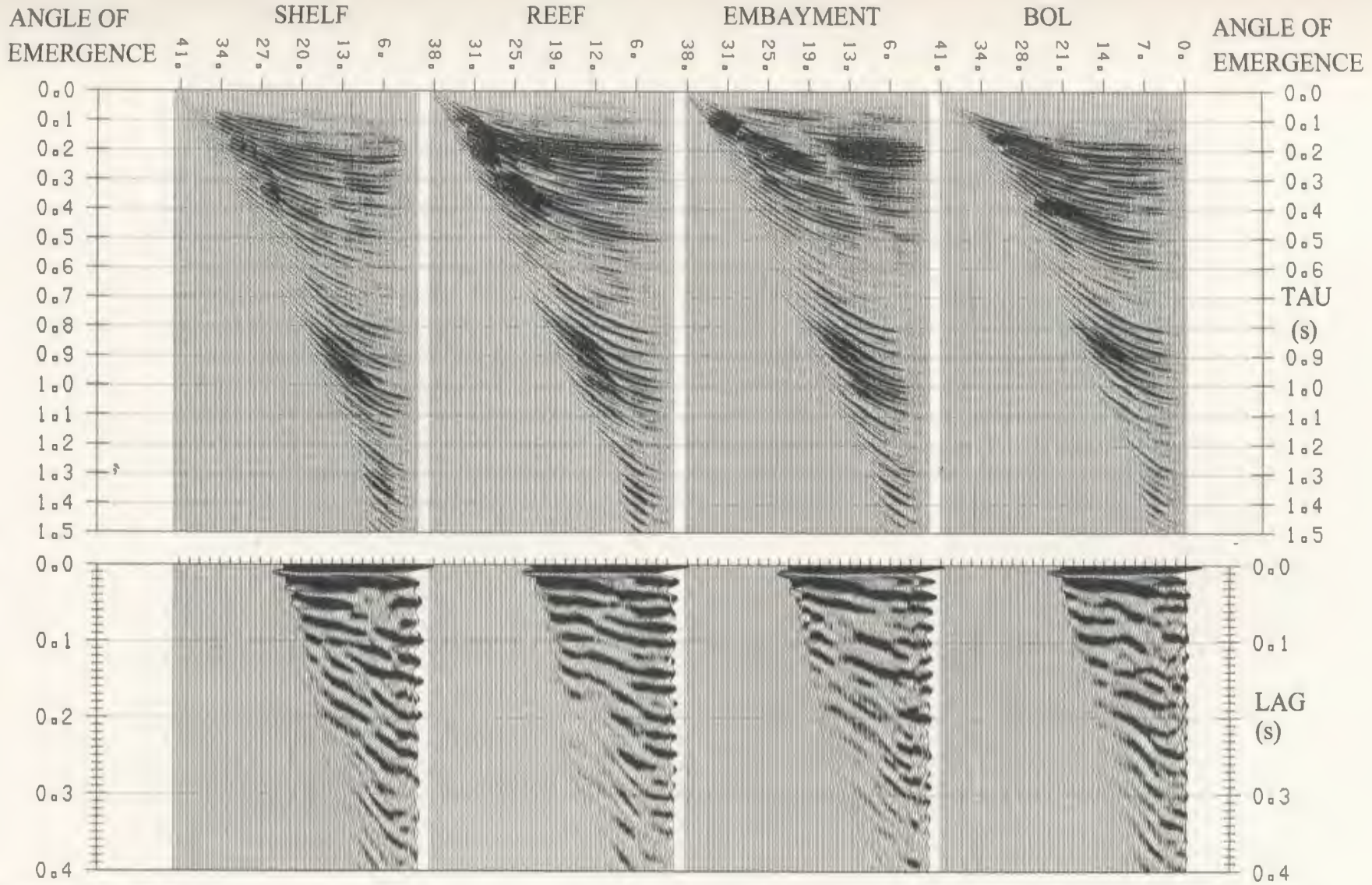

Figure 5.1.5b Hyperbolic velocity filter (HVF) applied to processed SSP COF gathers (top). Decomposition variable is angle of emergence as defined by stacking velocity, and muting occurs for all tau-p points existing outside the range defined by the limits of 90 to 110 percent of stacking velocity. Autocorrelation (bottom) design window is 700-1300ms at 0 degrees and 300-1300ms at 41 degrees. The signal is cleanerr than before by virtue of the hyperbolic nature of the transform, but energy has been smeared significantly.

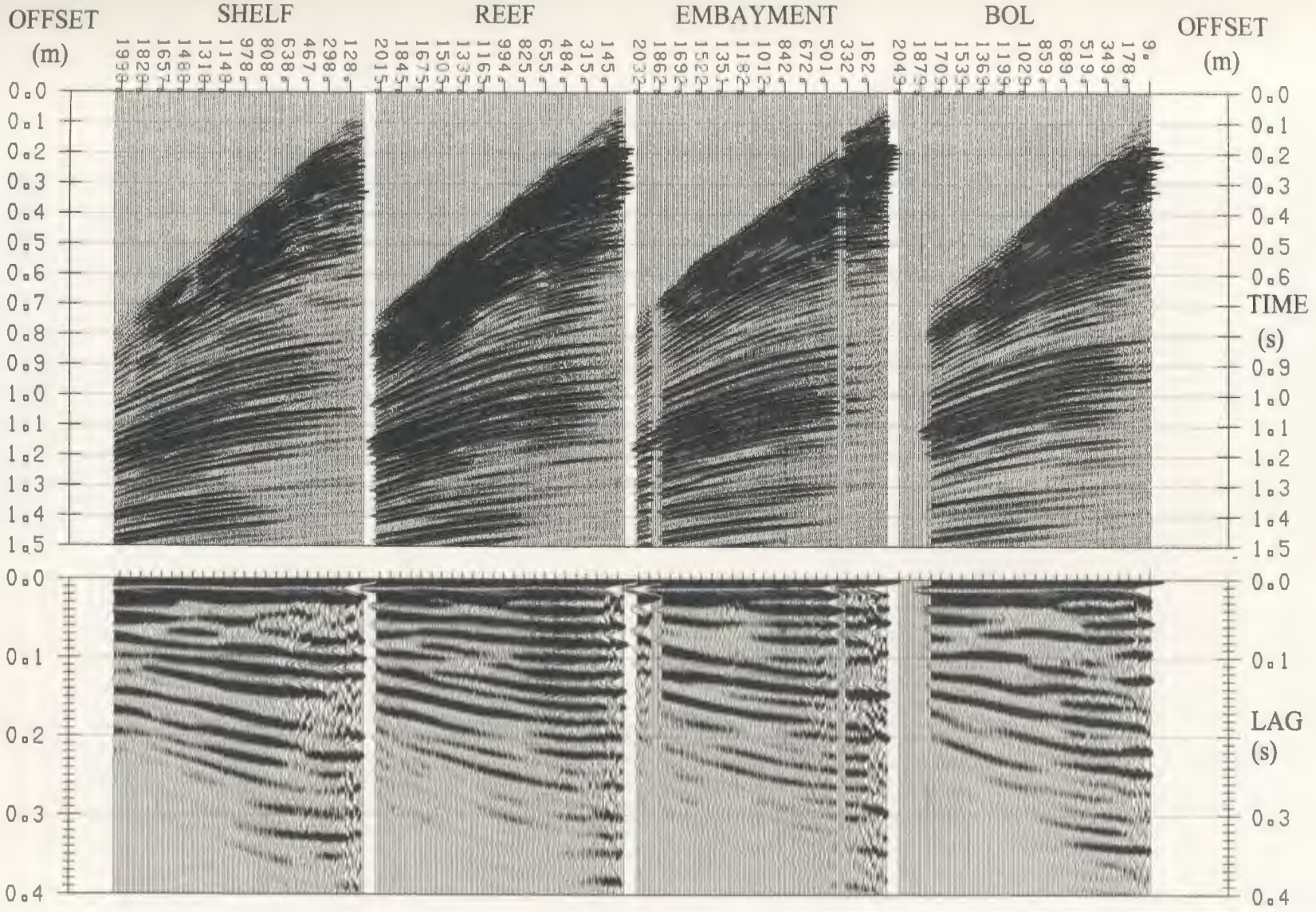

Figure 5.1.5c Inverse transform tau-p SSP COF gathers (top) following hyperbolic velocity filtering to exclude slant stack components with emergence angles outside limits defined by 90 to 110 percent of stacking velocity. Autocorrelation (bottom) design window is 700-1300ms at 34m and 1000-1300ms at 2057m. In comparison to before HVF, the multiple at BOL location has been suppressed but the reef location still indicates a ringing problem associated with near surface reflectors.

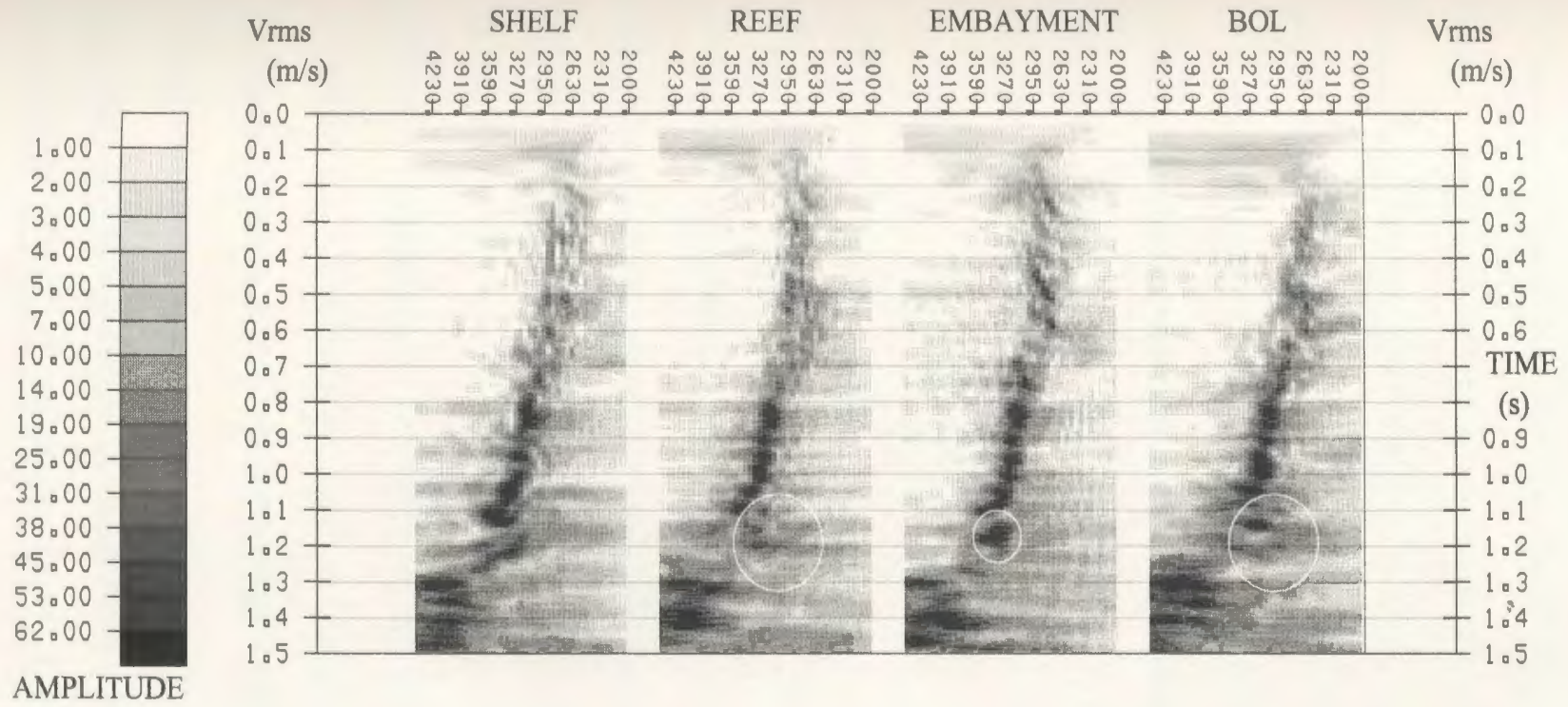

Figure 5.1.5d Hyperbolic semblance velocity spectra from SSP COF gathers with multiple suppression by HVF. The multiple interference at reef level is still apparent because moveout is insufficient to allow discrimination on this basis. There is less multiple energy at the BOL location where moveout is greatest (compare to Figure 2.2.1b), but HVF performance appears low overall.

primaries for the purpose of identifying weaker multiples at different lags, and this suggested multiple interference in agreement with surface peg-leg delay. More importantly, a robust prediction design based on the assumption of random reflectivity distribution in the near surface does provide an Nisku response with anomalous behaviour at the reef location and a more balanced autocorrelation over the deeper window. The synthetic seismograms presented in the next section suggest that this Nisku response is in agreement with the primary synthetic from both off-reef locations where the Ireton and Leduc formations are penetrated. The embayment penetrates the furthest, and supports significant primary energy at that level. This supports the use of shallow data for the predictive suppression of peg-legs embedded in the deeper window.

5.2 Wellbore Data Analysis

The corrected VSP checkshot velocity is used to map depth logs to time. This was done using a 1ms block-size, and the resulting logs were blocked more coarsely (Figure 5.2.1a,b,c) to define reflectivity models for inversion. The appropriate blocksize for conversion was tested using synthetics with samplings of 0.2, 0.5, 1.0 and 2.0ms (Figure 5.2.2a,b,c). In this analysis the time impedance trace is input into normal incidence reflectivity generation for primaries-only (right) and for primaries plus all multiples (left) followed by convolution with a 35Hz Ricker wavelet before resampling to 2ms. Surface reflectors are excluded in the model by padding sufficient zeroes before the start of the log. Autocorrelations (attached to each trace) show similarity between primaries-only and impulse response synthetics, explaining difficulty in prediction design. Significant differences exist between the 1ms and 2ms block size, suggesting that this test should be

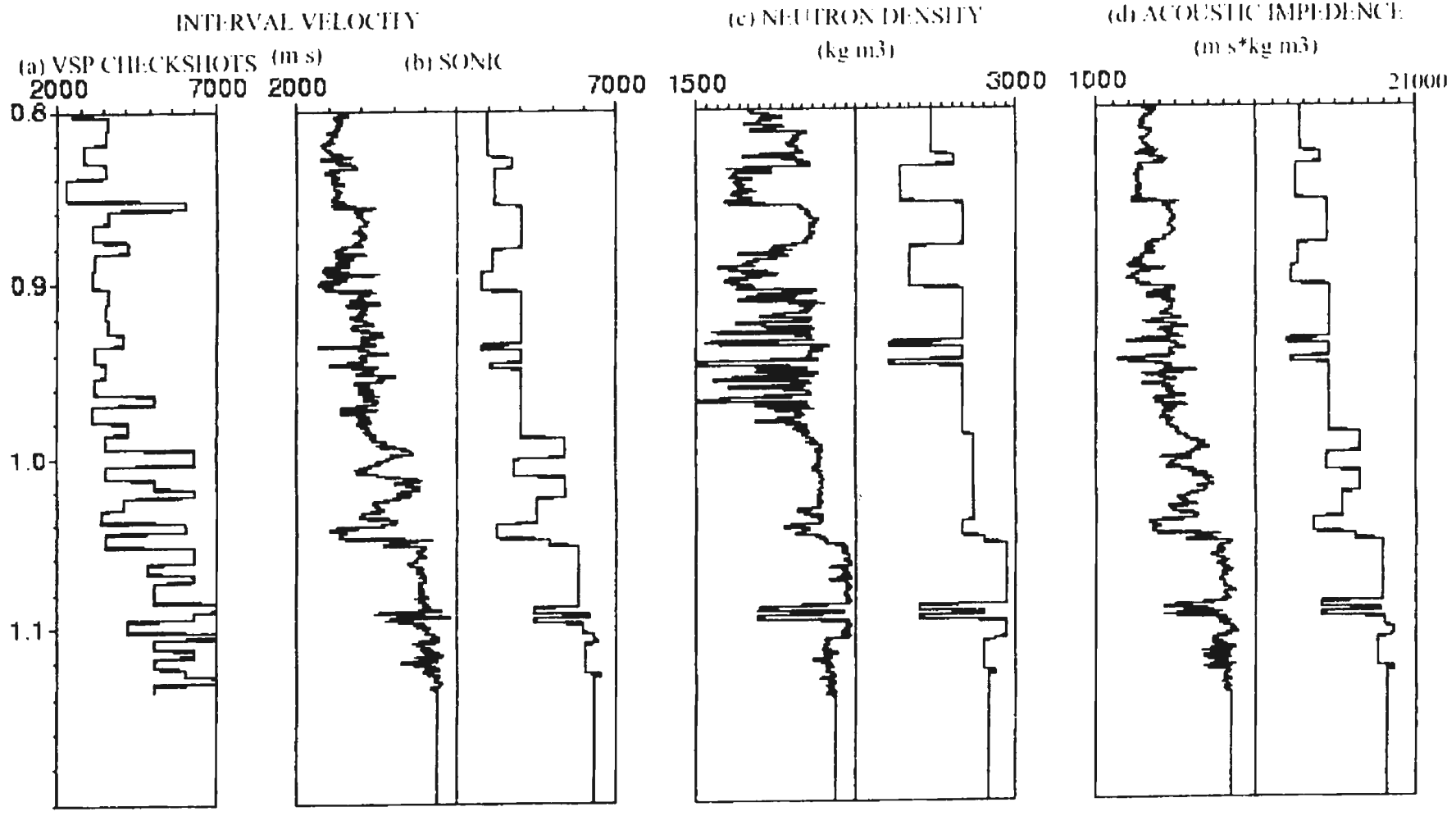

Figure 5.2.1a Wellbore log blocking at reef location. VSP interval velocity function (a) as derived from corrected checkshots provides constraints for mapping wellbore log samples to time. The resulting product of sonic velocity (b) and neutron density (c) provides acoustic impedence (d) from which to derive the reflectivity model at well locations.

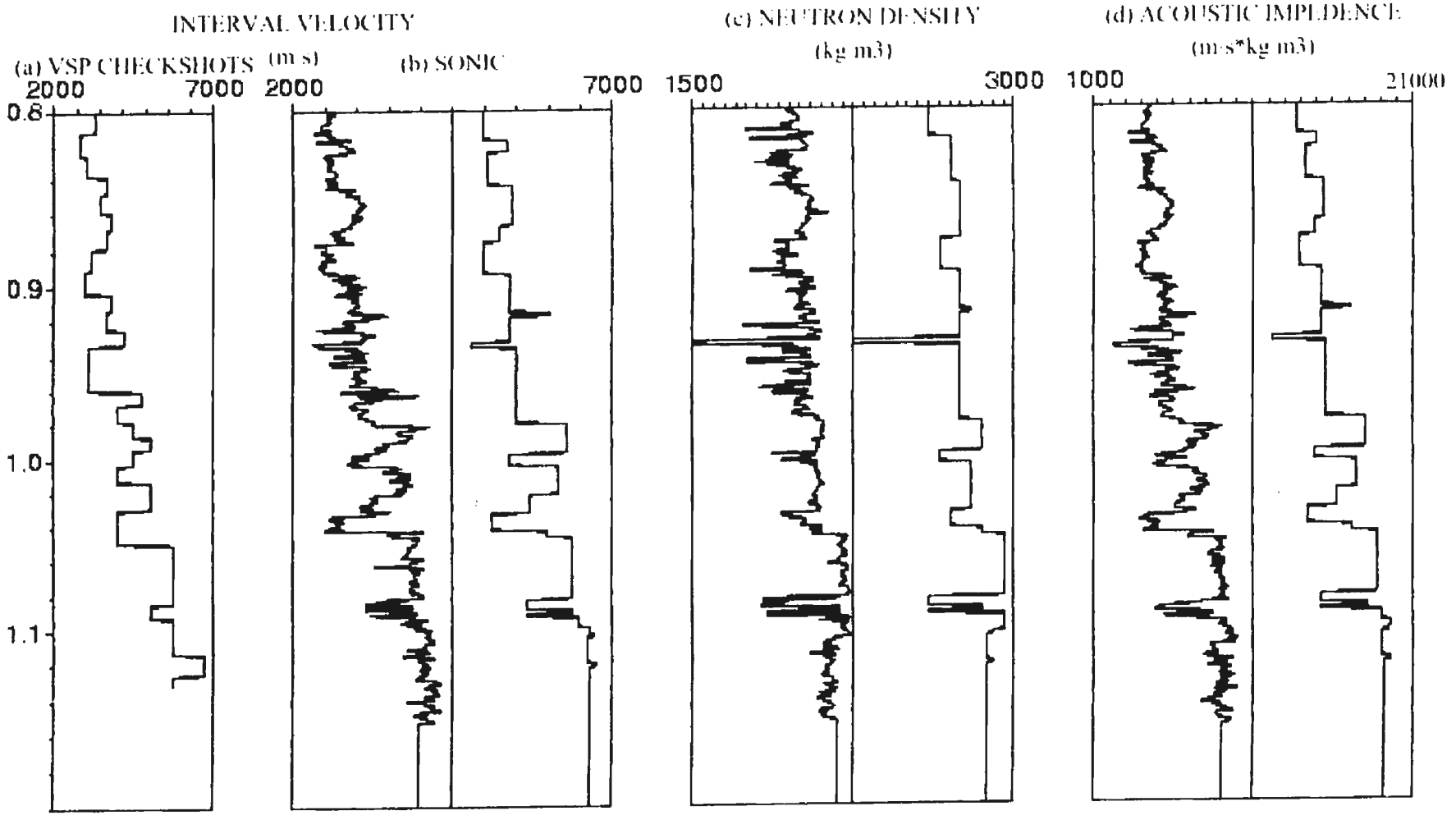

Figure 5.2.1b Wellbore log blocking at shelf location. VSP interval velocity function (a) as derived from corrected checkshots provides constraints for mapping wellbore log samples to time. The resulting product of sonic velocity (b) and neutron density (c) provides acoustic impedence (d) from which to derive the reflectivity model at well locations.

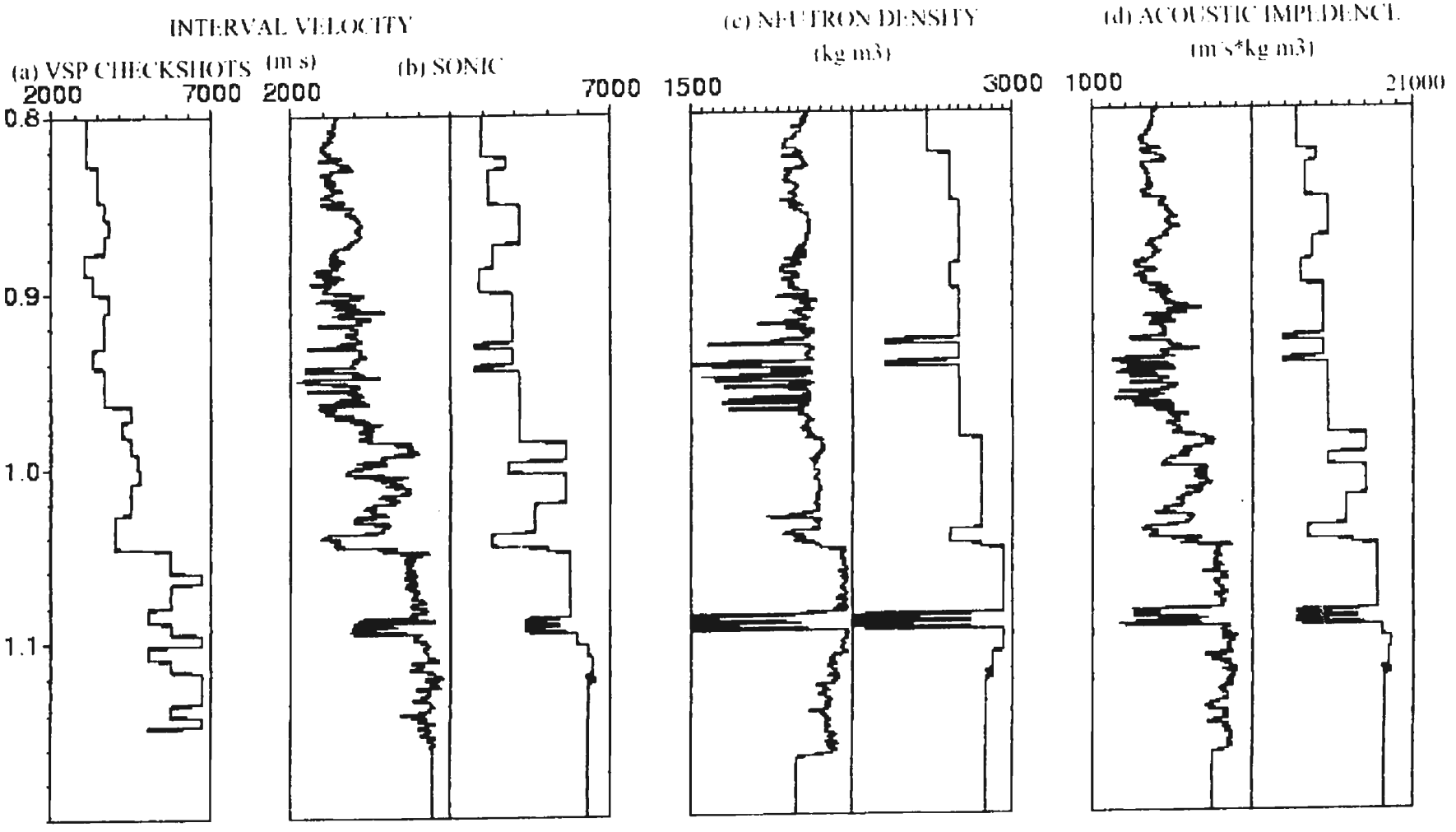

Figure 5.2.1c Wellbore log blocking at embayment location. VSP interval velocity function (a) as derived from corrected checkshots provides constraints for mapping wellbore log samples to time. The resulting product of sonic velocity (b) and neutron density (c) provides acoustic impedence (d) from which to derive the reflectivity model at well locations.

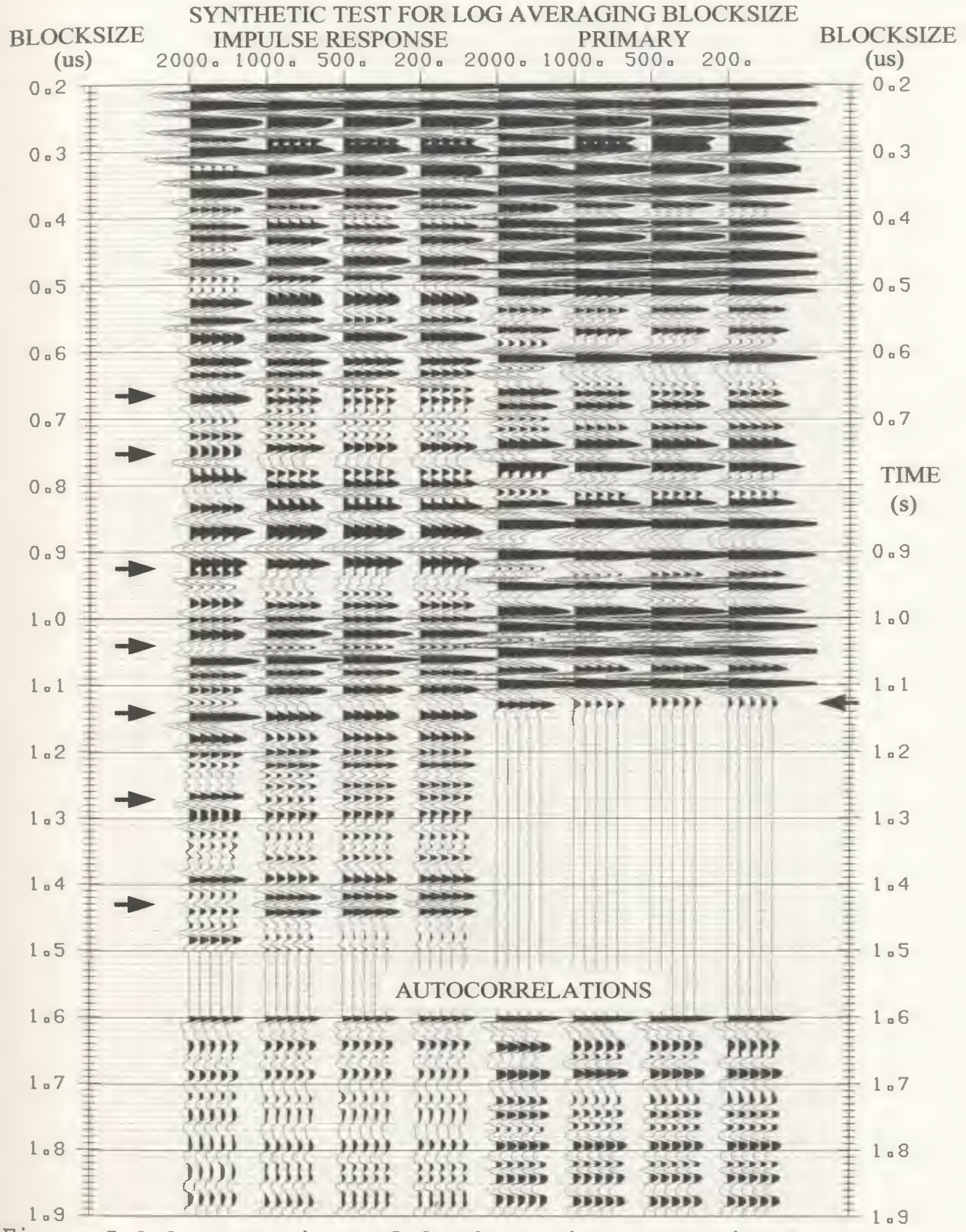

Figure 5.2.2a Comparison of depth-to-time conversion rates on synthetic response for the REEF well. The impedence blocksize before convolution with a 35Hz Ricker is annotated in microseconds at the top. All traces are resampled to 2ms following bandlimitation by the convolution process, and the autocorrelations appended to the bottom are computed over the window 0.7-1.5s.

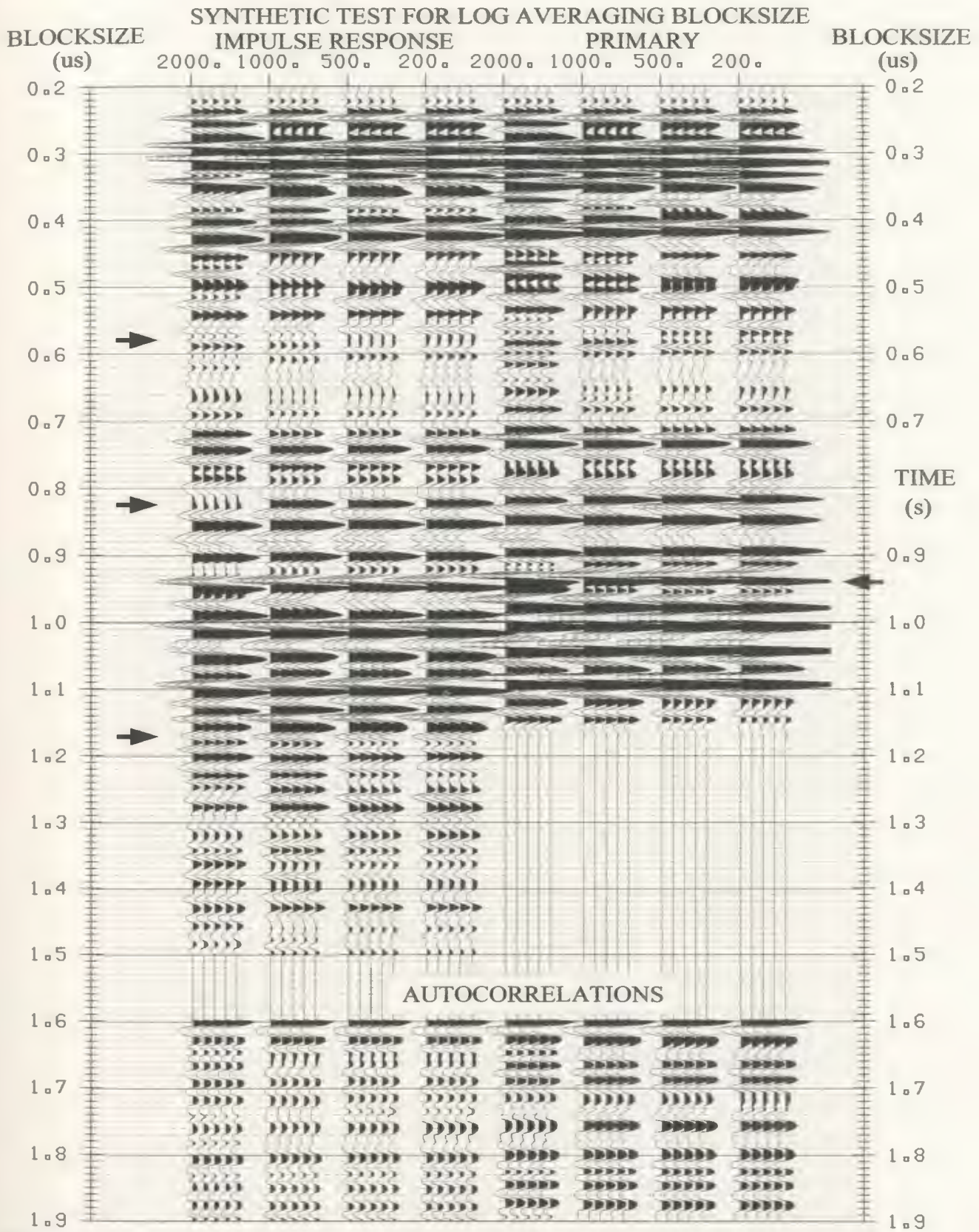

Figure 5.2.2b. Comparison of depth-to-time conversion rates on synthetic response for the SHELF well. The impedence blocksize before convolution with a 35Hz Ricker is annotated in microseconds at the top. All traces are resampled to 2ms following bandlimitation by the convolution process, and the autocorrelations appended to the bottom are computed over the window 0.7-1.5s.

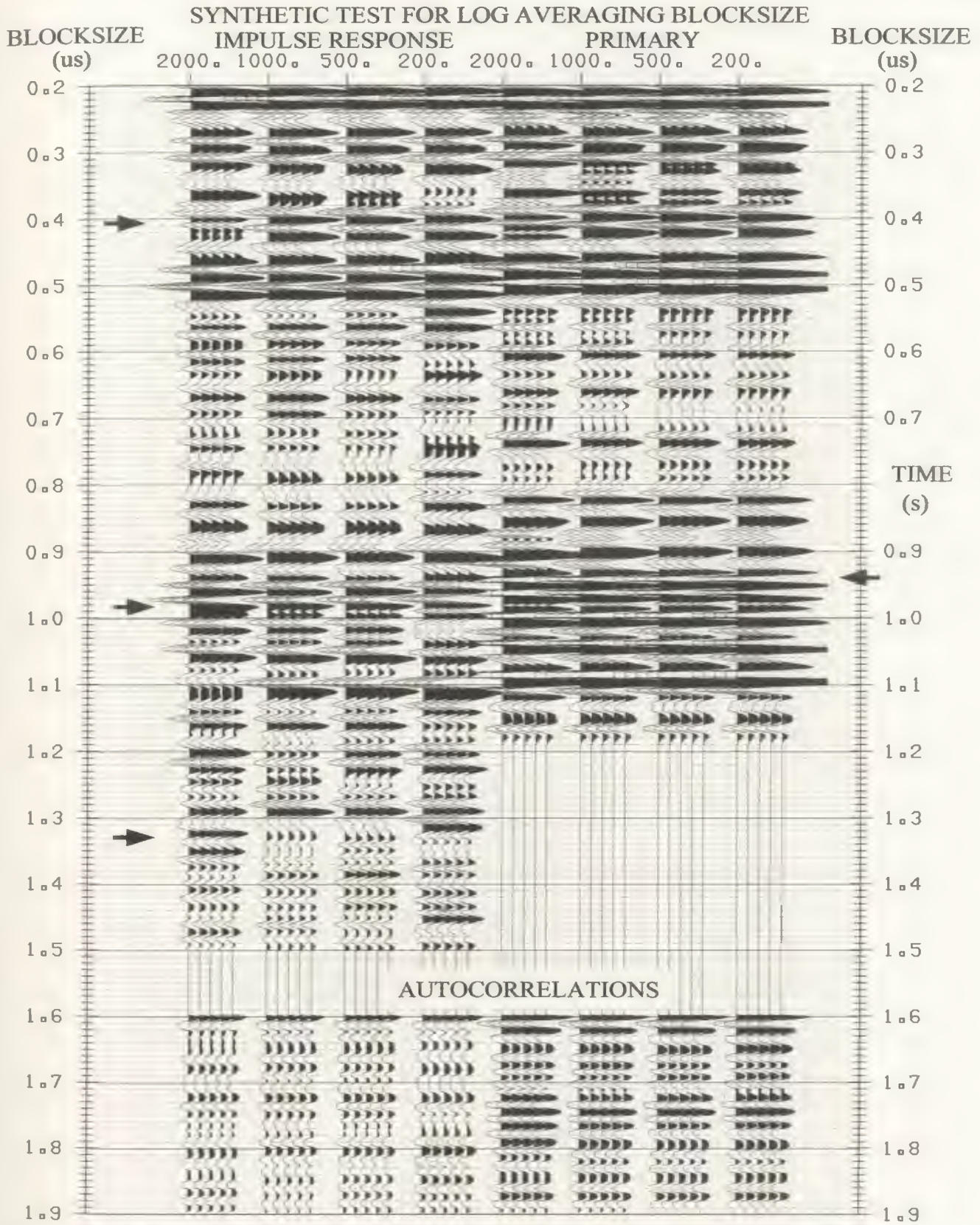

Figure 5.2.2c Comparison of depth-to-time conversion rates on synthetic response for the EMBAYMENT well. The impedence blocksize before convolution with a 35Hz Ricker is annotated in microseconds at the top. All traces are resampled to 2ms following bandlimitation by the convolution process, and the autocorrelations appended to the bottom are computed over the window 0.7-1.5s.

performed for all non-clastic environments (minimum 2ms is typical of industry software). The 1ms blocking was chosen to satisfy anti-aliasing requirements for the logging tool (note lack of change within the zone of interest for finer sampling), and implies a depth blocking of about 10 samples at the zone of interest. The depth-to-time conversions for α_{sonic} and ρ, and the resulting I(t) sequence, are shown in Figures 5.2.3, 5.2.4, and 5.2.5 respectively.

In this Nisku SSP study, response at reef level is partially masked by a highly reverberatory R_I sequence. Multiple mechanisms are expected to involve the Wabamun carbonate and the underlying salt. At Wabamun depth of about 1600m (1050ms), interval velocities increase to about 6000m/s from 3200m/s. Within 100m shallower in the section (near 1000ms), the Mississippian and Banff units both represent velocity change to 5500m/s from 4200m/s. At about 1350m (near 900ms), the Mannville Group velocity increases to 4200m/s from 3200m/s, and a cyclic distribution exists within this group (in particular, a low density coal unit near 950ms). The salt layer 150m below the Wabamun (near 1100ms) has a velocity of about 5000m/s as compared to the 6000m/s background. In addition to significant changes in α, the ρ distribution in the section is clearly not related to α by Gardner's equation, and this source of impedance contrast must be considered. Meanwhile, the surface velocity from uphole times is estimated to range from 700 to 950m/s within a 40m thick layer that sits above a refracting layer with velocity of 2700m/s. In addition to at least first order interbed multiples involving the Wabamun, significant intrabed delay and strong surface related peg-leg multiples can be expected to occur.

Based on well log impedance, the complexity of overall multiple interference is apparently caused by unrelated timing delays of various interbed mechanisms. These mechanisms become related by producing first order multiples at an incidence time adjacent

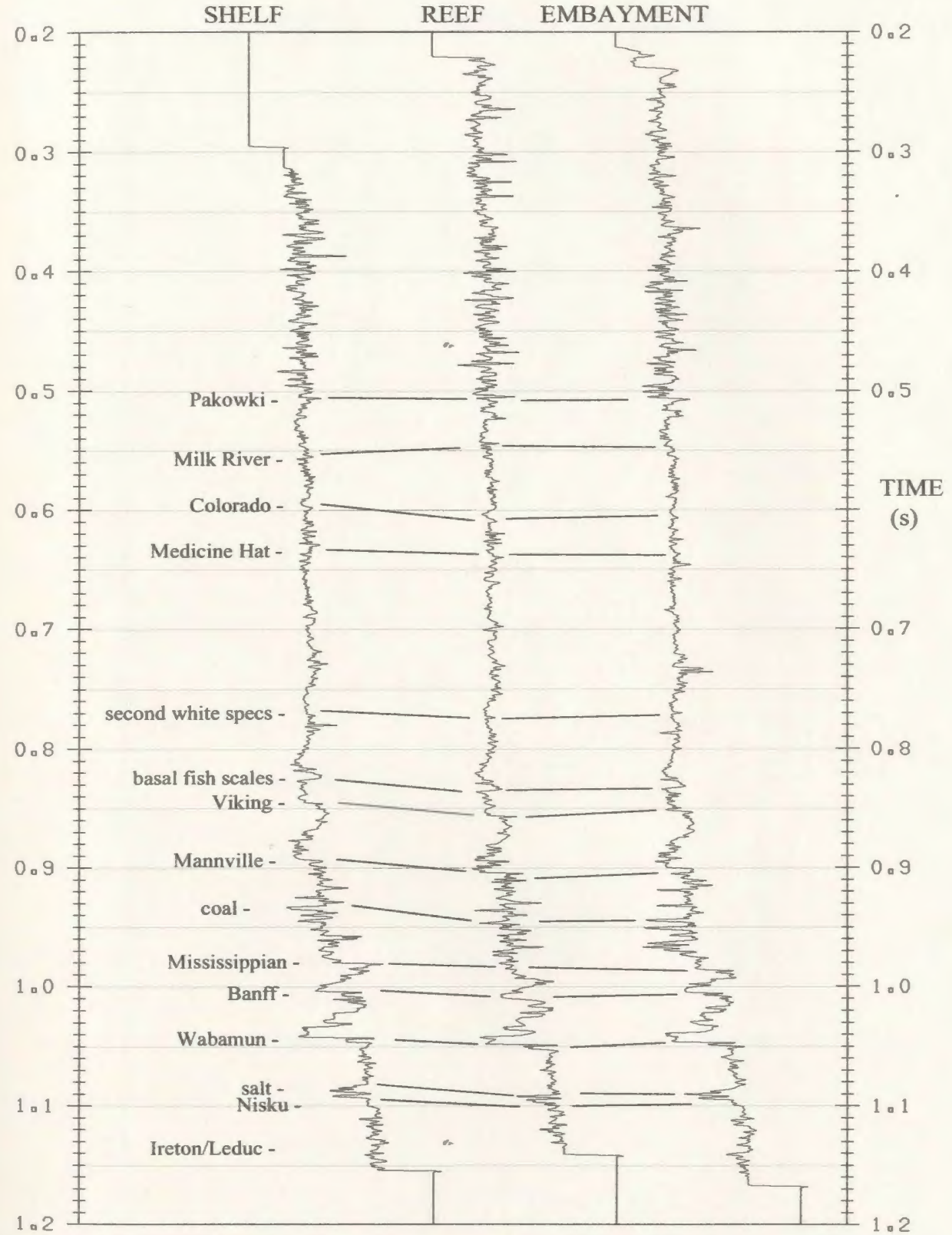

Figure 5.2.3. Velocity time logs at 1ms sampling for the Nisku field. Times are adjusted to SRD (900m) during constrained depth to time conversion using VSP checkshots. Logs are padded by velocity extrema of 1000m/s (1000us/m) at top and 8500m/s (118us/m) at bottom for display purposes. Geologic tops are given.

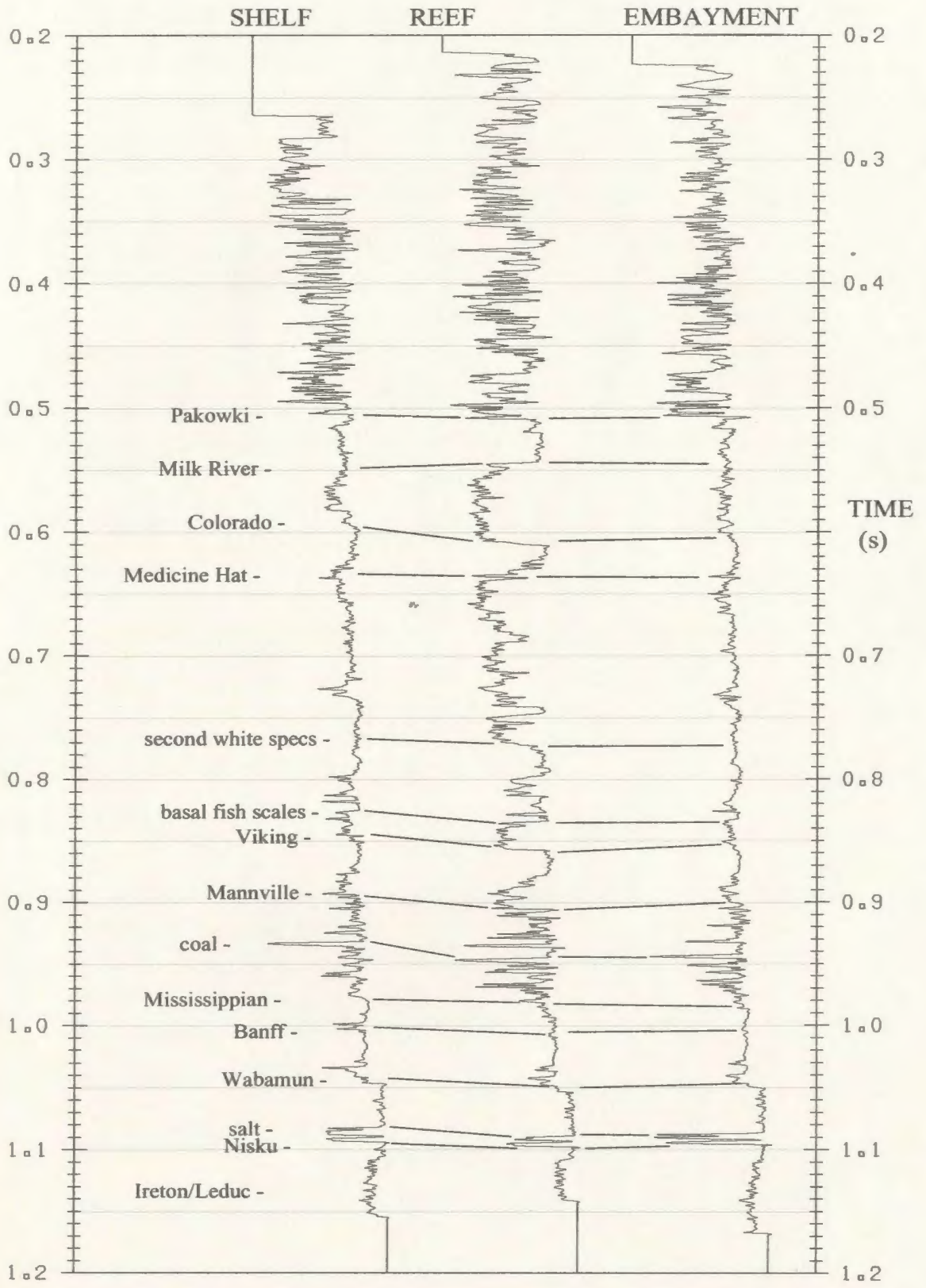

Figure 5.2.4. Density time logs at 1ms sampling for the Nisku field. Times are adjusted to SRD (900m) during constrained depth to time conversion using VSP checkshots. Logs are padded by density extrema of 1.0g/cc at top and 3.0gm/cc at bottom for display purposes. Geologic tops are given.

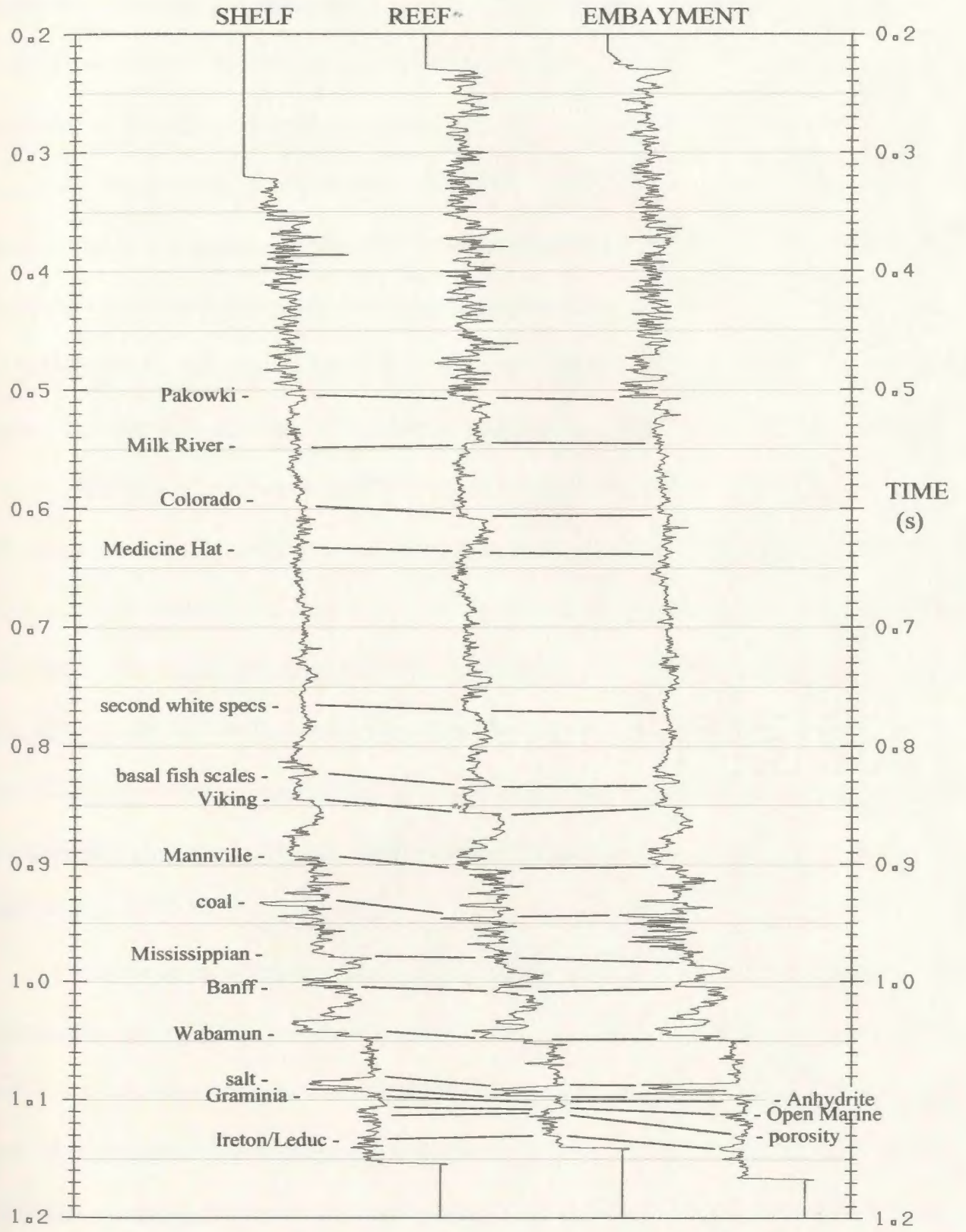

Figure 5.2.5. Impedence time logs at 1ms sampling for the Nisku field. Times are adjusted to SRD (900m) during constrained depth to time conversion using VSP checkshots. Log values derived from sonic and density logs. Geologic tops are given.

to Nisku response. For this reason, well log synthetic seismograms are prone to misrepresentation of multiples because the timing of the events is crucial to the net impulse response at Nisku level. VSP's recorded in these wells should validate the existence and temporal distribution of reflectors. Also, VSP's should illuminate the depths at which multiples are generated and thereby identify interbed mechanisms. The focus will now be shifted to VSP analysis to provide a correlation between seismic and wellbore impedance contrasts for the purpose of identifying key reflectors in the impulse response. Blocked impedance models derived from this analysis will be used for reflectivity inversion.

The embayment and shelf VSP's are of the same vintage and shooting parameters. The depth increment used in acquisition was 20m, resulting in an effective vertical sampling closer to 19m due to hole deviation on the order of 10 degrees. The reef well VSP was acquired under different circumstances than the two other wells. The sampling was 15m and the well deviation was less than 5 degrees. In industry, depth correction due to hole deviation is not usually performed unless deviation exceeds 10 degrees, but will generally depend on target depth. Hence, results from the off-reef VSP's may not be as reliable as the reef VSP.

The basic principles described in Chapter 3 were tested on the vertical compressional component of the VSP data from the three wells (see Figure 3.2.4a,b,c). Both off-reef surveys suffered from tube wave contamination, and this energy was suppressed using f-k zero wavenumber reject following tube mode flattening. The down-going tube wave was a problem for the embayment well (possibly due to casing), resulting in spurious residual energy whereas the f-k filter effectively removed the tube mode from the shelf well. An improvement to the embayment well up-going energy was achieved in +TT time following

f-k tube wave rejection by using a three point temporal median filter (spike rejection) followed by trim statics before a final three point lateral median filter. This operation reduced residual tube mode that would otherwise deteriorate subsequent processing. No tube wave mode was present within the uniformly sampled depth range for the reef well. otherwise processing was consistent for all VSP's.

To initiate analysis, the amplitude spectra of the down-going wavefield were analysed for stationarity before waveshaping (Figure 5.2.6). The initial compression was isolated and the resulting spectra showed that some frequency attenuation occurs gradually as expected due to Q-attenuation, but there is no significant change at the Wabamun (where the velocity increases sharply) or at any other depth. Since frequency content does not decrease significantly over the recorded depth interval, an average wavelet might be considered sufficient for the de-phasing procedure compared to the less stable tracewise application. However, high S/N allows tracewise application so that subtle wavefield changes are accounted for in the de-phasing operation especially since up-going energy shows marked change in character below the Wabamun. It is expected that this is due to interbed multiple interference.

The down-going compressional wavefield for each well is separated by f-k zero wavenumber rejection of the flattened up-going compressional mode and the down-going tube mode (Figure 5.2.7a,b,c, top left). S/N is improved by a 3 point median filter following trim statics (top middle), then de-phasing is applied using an 80ms wavelet starting at the interpreted absolute first break (top right). This wavelet length was chosen to preserve multiple effects as recorded in the SSP data.

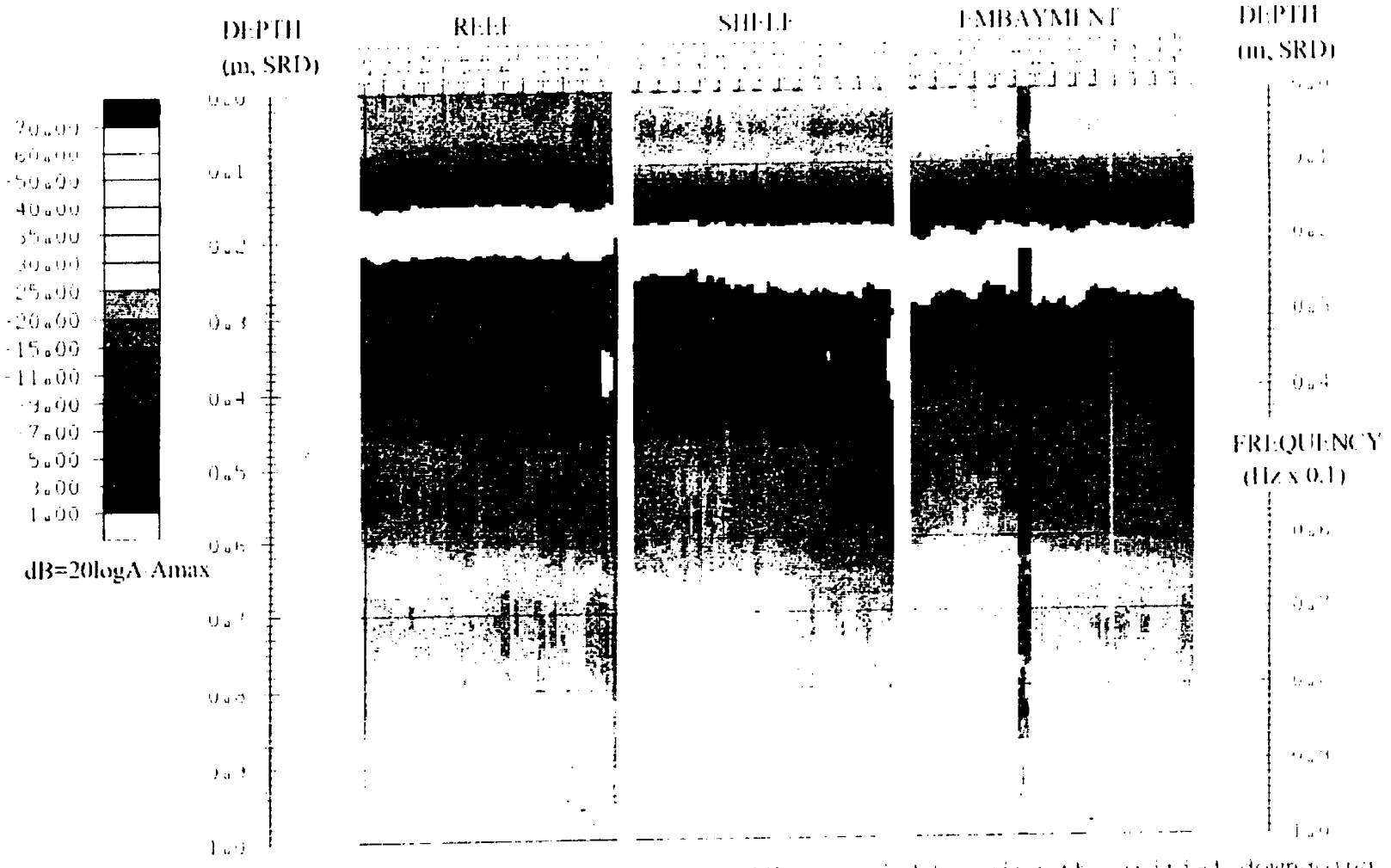

Figure 5.2.6 Amplitude spectra for the downgoing VSP wavefields using the initial downgoing compression contained in the window -40ms to 60ms. There does not appear to be any sharp change in spectra at Wabamun depth or any other depth. Changes are gradual, as would be expected from increasing intrabed multiple effect and increasing frequency attenuation.

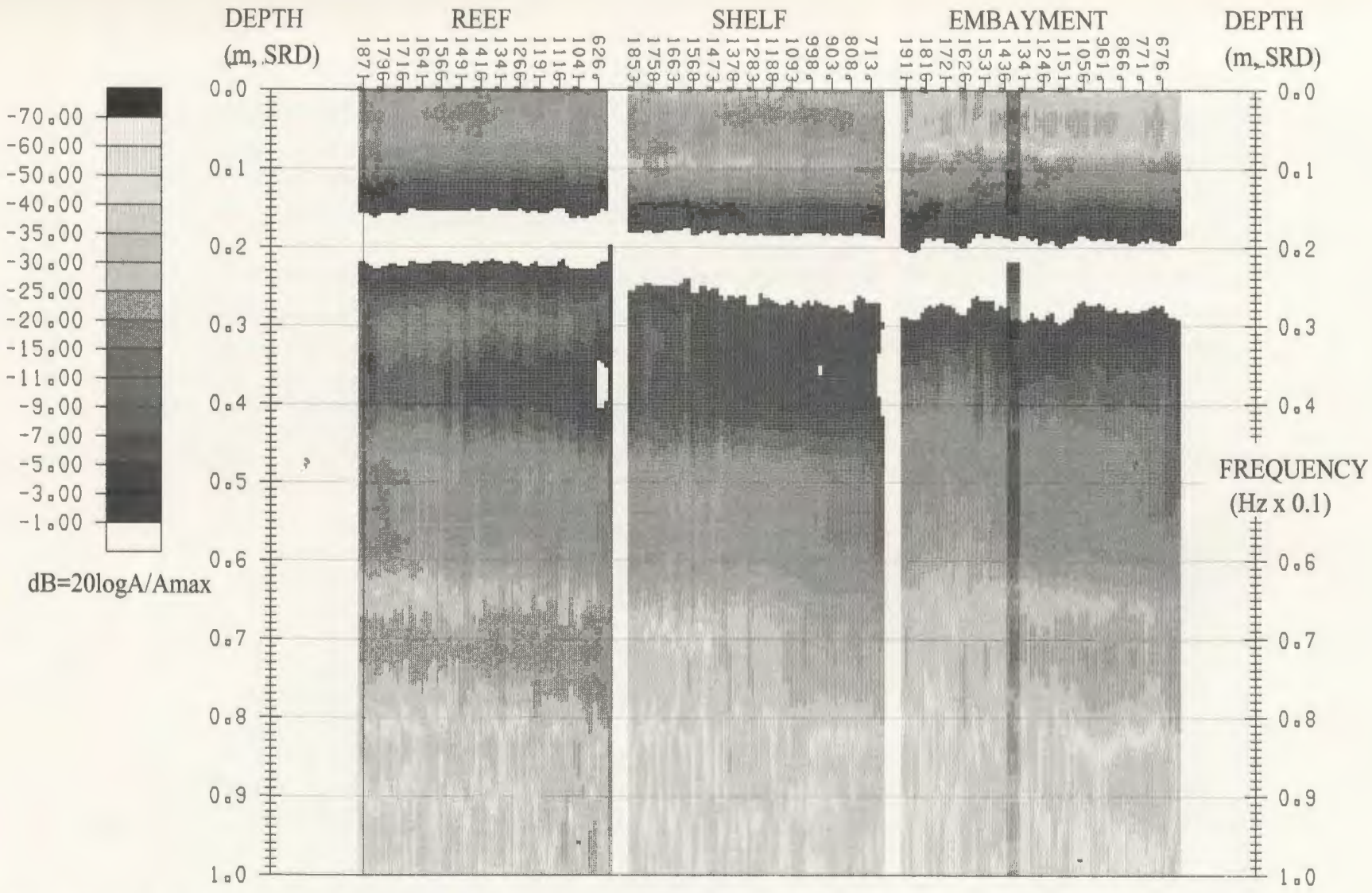

Figure 5.2.6 Amplitude spectra for the downgoing VSP wavefields using the initial downgoing compression contained in the window -40ms to 60ms. There does not appear to be any sharp change in spectra at Wabamun depth or any other depth. Changes are gradual, as would be expected from increasing intrabed multiple effect and increasing frequency attenuation.

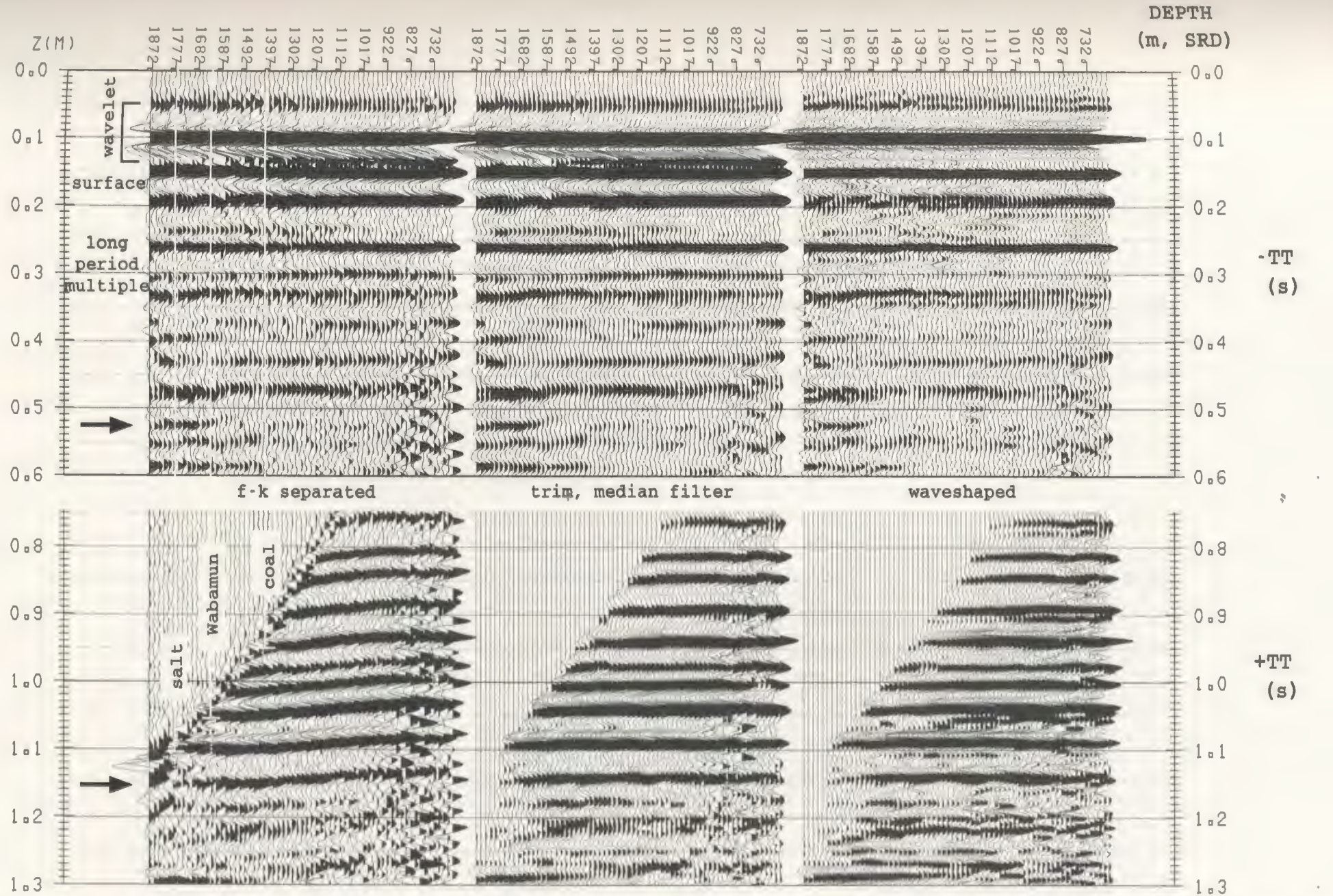

Figure 5.2.7b. Processing stages for the shelf VSP wavefields. Spectral division dephasing and whitening is performed tracewise using the wavelet contained within an 80ms window as indicated. The downgoing wavefield shows minor long-period amplitude anomalies at Wabamun depth (arrow), possibly two short period surface multiples, and a long period near-surface multiple. The upgoing wavefield shows an event (arrow) that is not expected to be a primary, but could be a surface ghost reflected by the salt or Wabamun.

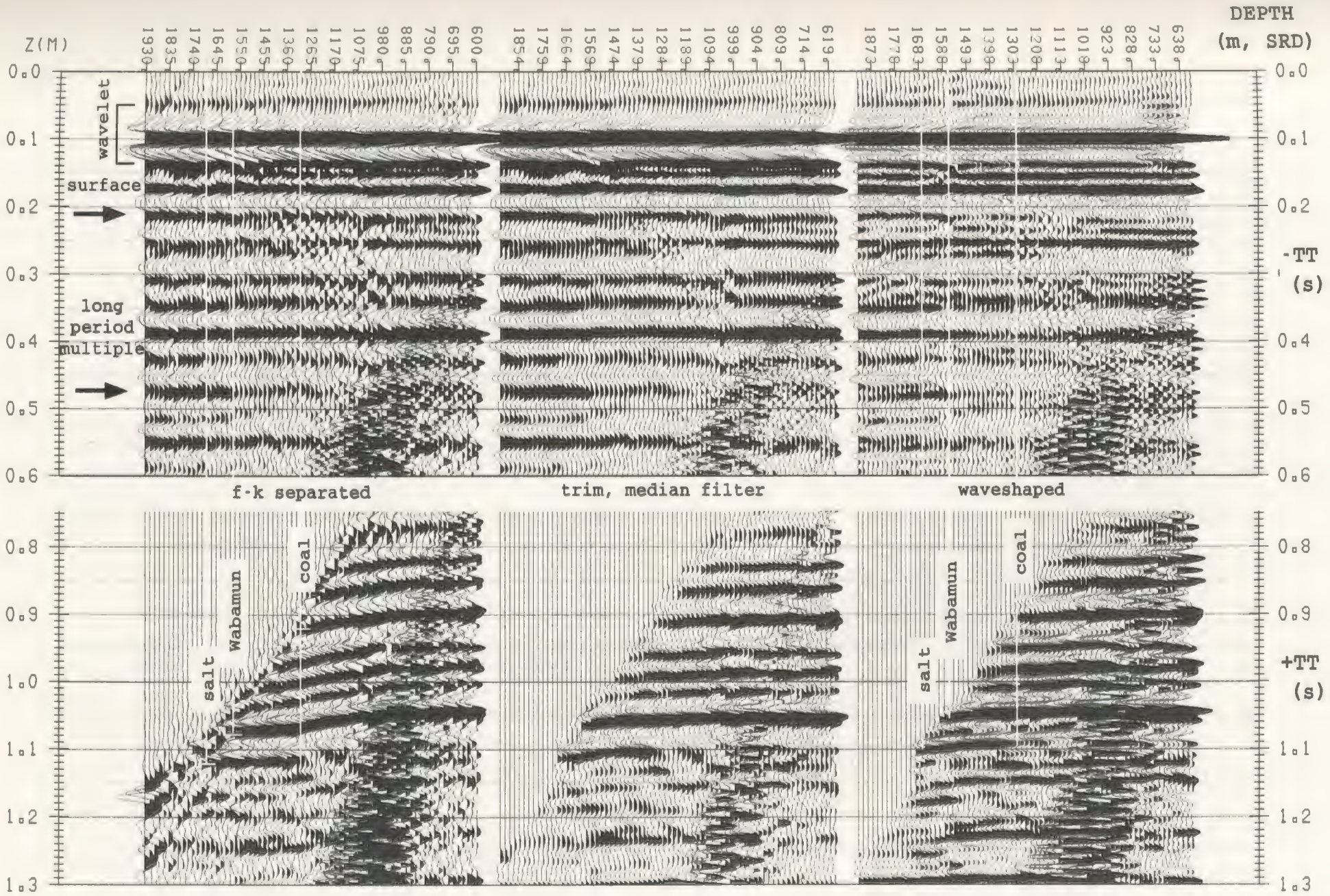

Figure 5.2.7c. Processing stages for the embayment VSP wavefields. Spectral division dephasing and whitening is performed tracewise using the wavelet contained within an 80ms window as indicated. The downgoing wavefield shows anomalies at Wabamun depth (arrows), a short period surface multiple, and a long period near-surface multiple. The upgoing wavefield shows discontinuous salt reflection at coal depth. Other subtle discontinuities in events exist at smaller magnitude.

The presence of energy trailing the initial wavelet on the shallowest trace in each VSP indicates that significant down-going multiple energy of long and short period is entering the sampled portion of the well from above. This confirms the presence of shallow multiple mechanisms. Instead of using this trace to enhance interbed multiples generated within the uniform portion of the VSP, the initial lags of the down-going compression are used to waveshape the VSP wavelet to a bandlimited spike. Corridor stacks are then more directly comparable to SSP data and become more effective in detecting multiples. The identified lags are used to identify interbed multiples which are maintained in relative amplitude. Multiple mechanism depths are unambiguous unless multiples enter the VSP interval from above. Since any multiple generating mechanism will create a down-going event that is delayed relative to the primary compression by the multiple period, the depth at which any VSP event discontinuities exist indicates the horizon depth. The separated down-going wavefields are interpreted for this activity (Figure 5.2.7a,b,c, top), and the Wabamun and salt events are expected to be involved.

At the reef location (Figure 5.2.7a), energy reflected back down at Wabamun depth (arrow) lags the initial compression by a delay of about 400ms which suggests the energy was reflected from deeper in the basin (near 1450ms on SSP). This suggests that all reflections below the Wabamun (eg. salt) will be redirected downward at this depth. Corridor stacks indicate a short period multiple (60 to 100ms delay) that suggests salt involvement. Energy with a peak-to-peak delay of 60ms in the downgoing wave directly indicates a multiple dominating these lags at all depths. This multiple originates in the near surface and correlates with the SSP static model delay between the base of weathering and the free surface. The third order reverberation of this multiple has a peak at 180ms delay. A

long period multiple with 260ms delay is also generated at an ambiguous depth in the near surface, interpreted as a peg-leg between the weathered layer and a subweathering reflector. To improve the evaluation of these multiples, the reef VSP was processed with checkshot traces included (dz=100m compared to the uniform sampling of dz=15m), and this validates a near surface mechanism. Each of the VSP's in Figure 5.2.7 have been processed to include checkshots which extend to near 300m depth at the shelf and reef, and to near 600m at the embayment. Each set of checkshots validates short period multiple contamination from the near surface.

A similar processing strategy was applied for separation of the up-going wavefield (Figure 5.2.7a,b,c, bottom). As expected for the undeviated reef well, the up-going wavefield exhibits little moveout effects compared to the deviated wells. A first order moveout correction was determined by temporal correlation (Figure 5.2.7, middle), and is considered sufficient in this case given the small source-receiver offsets relative to the target depth (although less than optimal for the embayment VSP). Residual down-going energy has been muted, and S/N has been boosted by a 3 point median filter. The same wavelet used to de-phase the down-going wavefield is used to shape the up-going wavefield (Figure 5.2.7, right). The autocorrelations and autoconvolutions of the down-going wavefield (Figure 5.2.8) both show the same multiple periodicity information as the wavefield itself. Dominant multiple energy is generated from above the recorded portion of the wells.

To interpret the up-going wavefield, the VSP data is correlated with the log impedance in depth and time (Figure 5.2.9a,b,c). All major impedance contrasts have associated up-going events with character intuitively matching the log. Reef response is relatively weak as expected, but a strong event interferes with the trough response of the

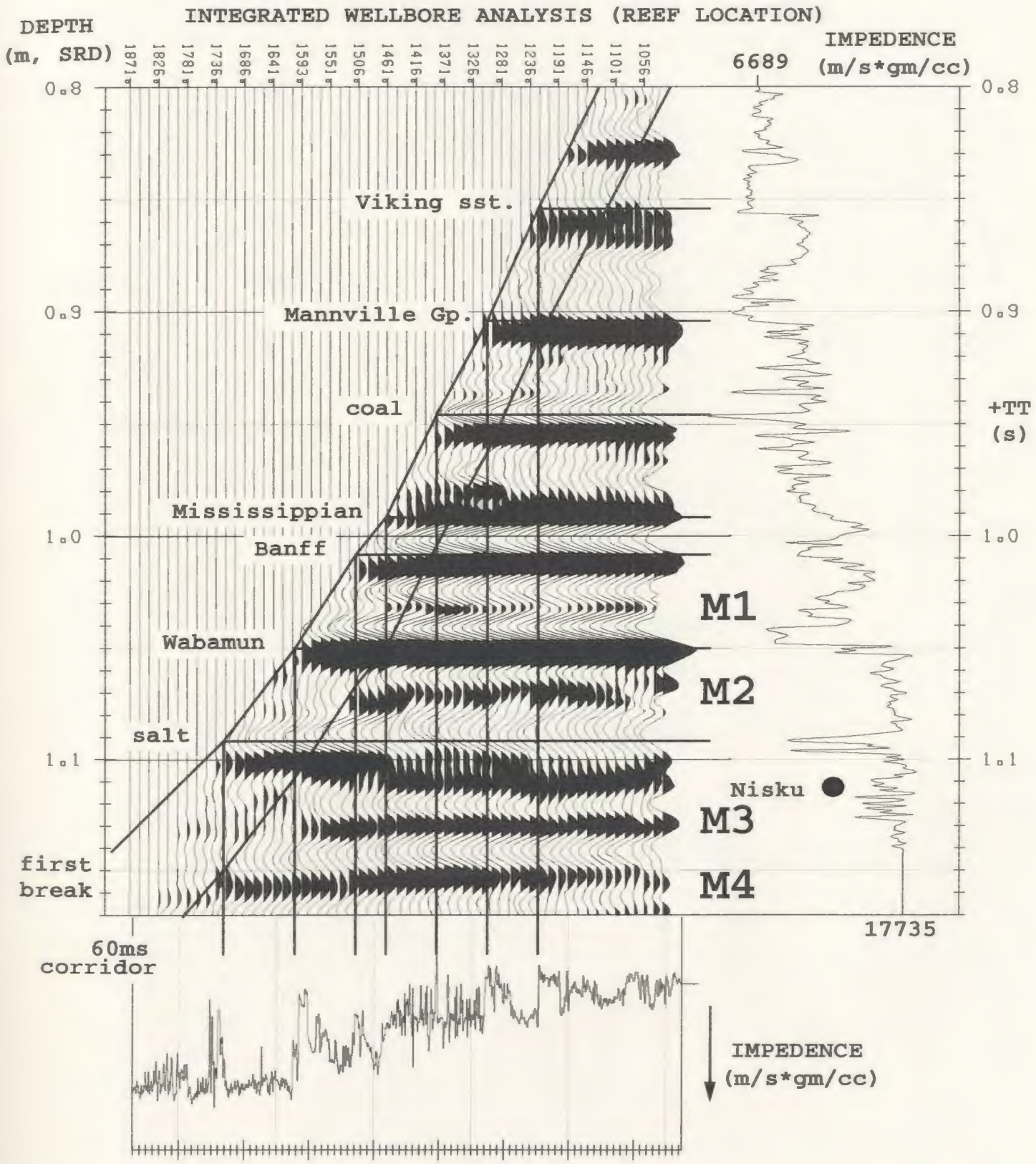

Figure 5.2.9a Integrated wellbore data from the reef location. The upgoing VSP wavefield in +TT time (equivalent to surface recorded TWT time) is compared to impedence logs in depth (TVD, SRD=900m) and in checkshot constrained time. The concept of an outside VSP corridor is illustrated by delaying the first break trajectory in time (60ms in thi example). At least four events (M) behave as interbed multiples.

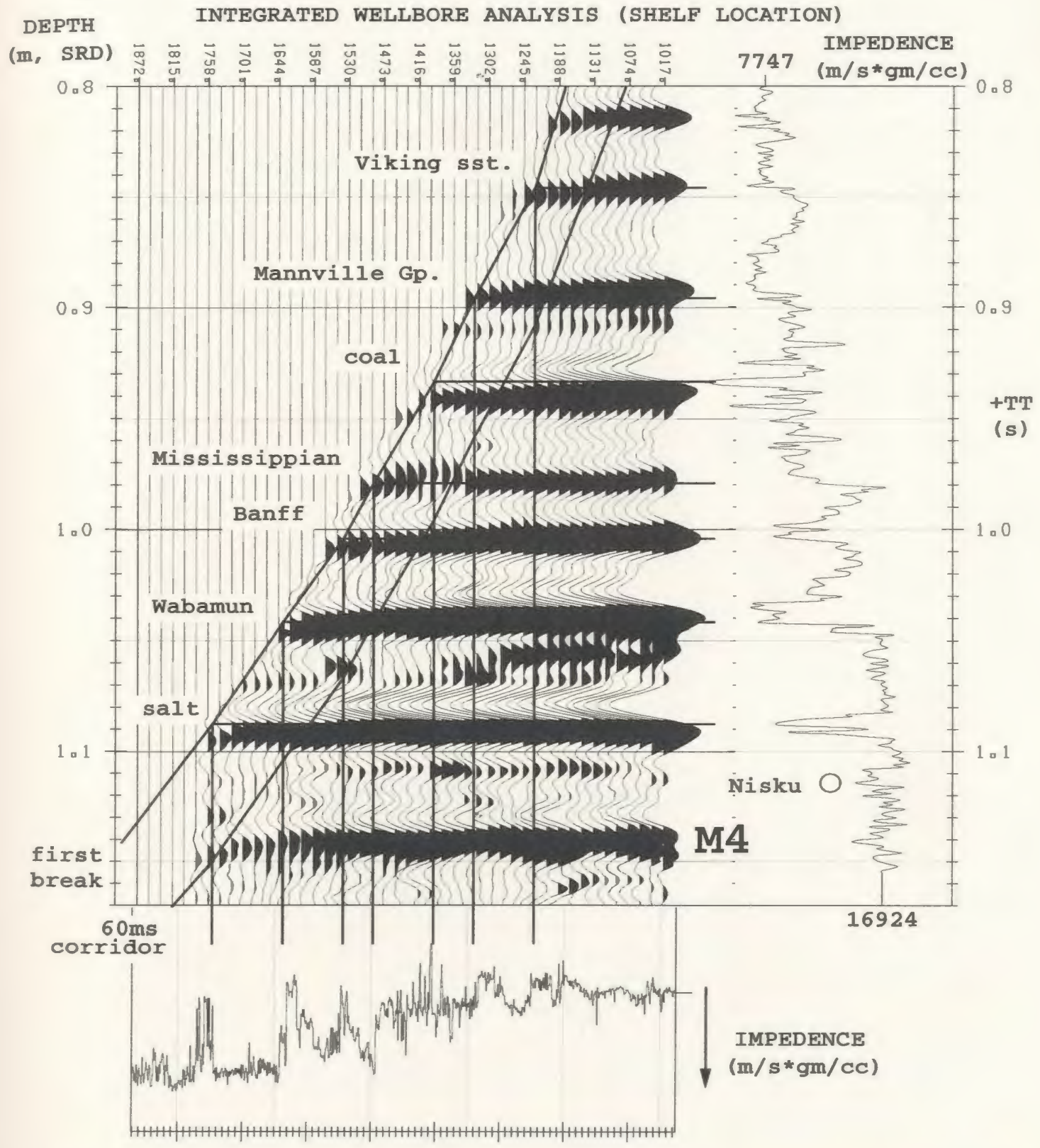

Figure 5.2.9b Integrated wellbore data from the shelf location. The upgoing VSP wavefield in +TT time (equivalent to surface recorded TWT time) is compared to impedence logs in depth (TVD, SRD=900m) and in checkshot constrained time. The concept of an outside VSP corridor is illustrated by delaying the first break trajectory in time (60ms in thi example). At least one event (M) behaves as an interbed multiple.

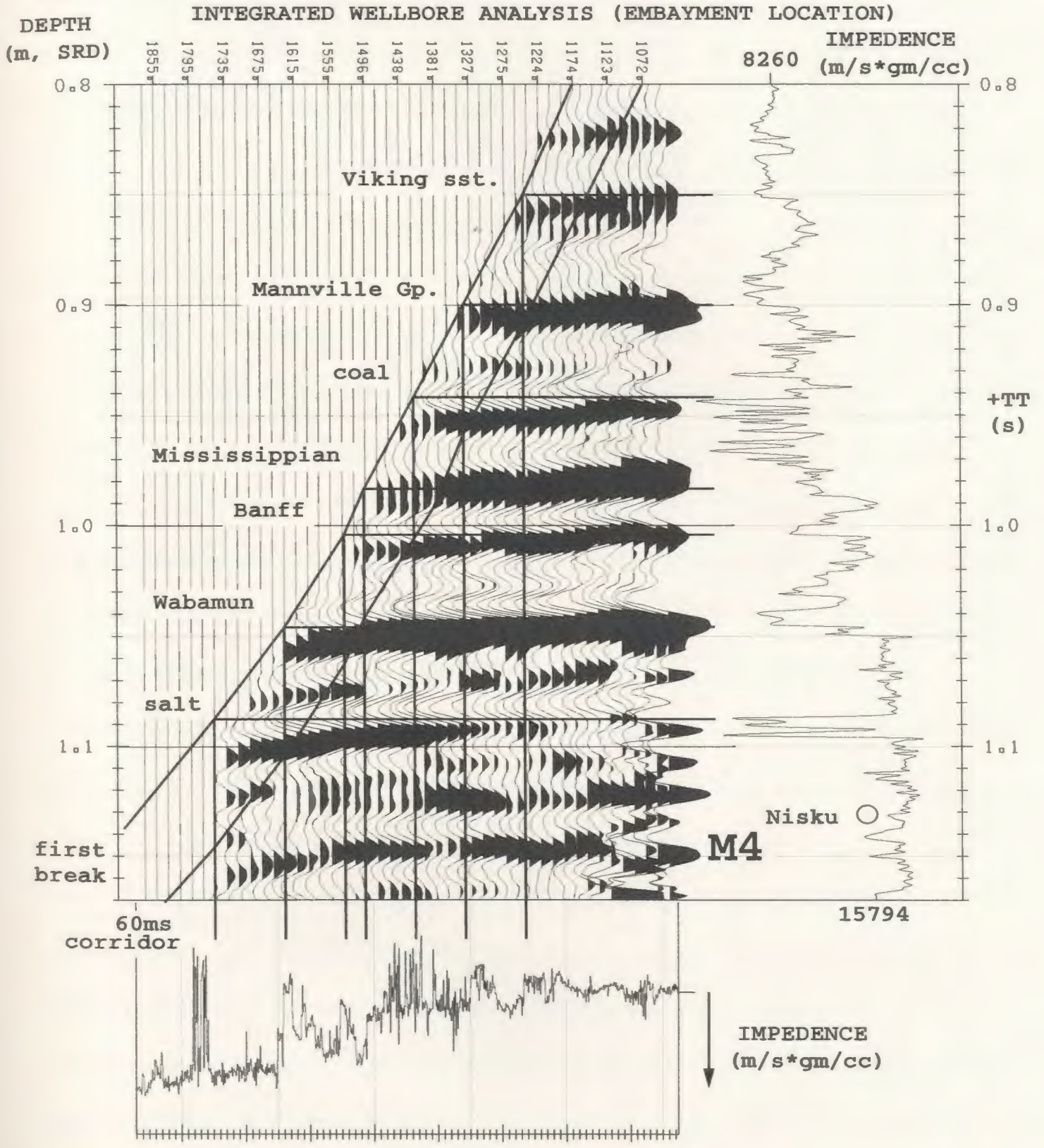

Figure 5.2.9c Integrated wellbore data from embayment location. The upgoing VSP wavefield in +TT time (equivalent to surface recorded TWT time) is compared to impedence logs in depth (TVD, SRD=900m) and in checkshot constrained time. The concept of an outside VSP corridor is illustrated by delaying the first break trajectory in time (60ms in thi example). At least one event (M) is suspect as an interbed multiple.

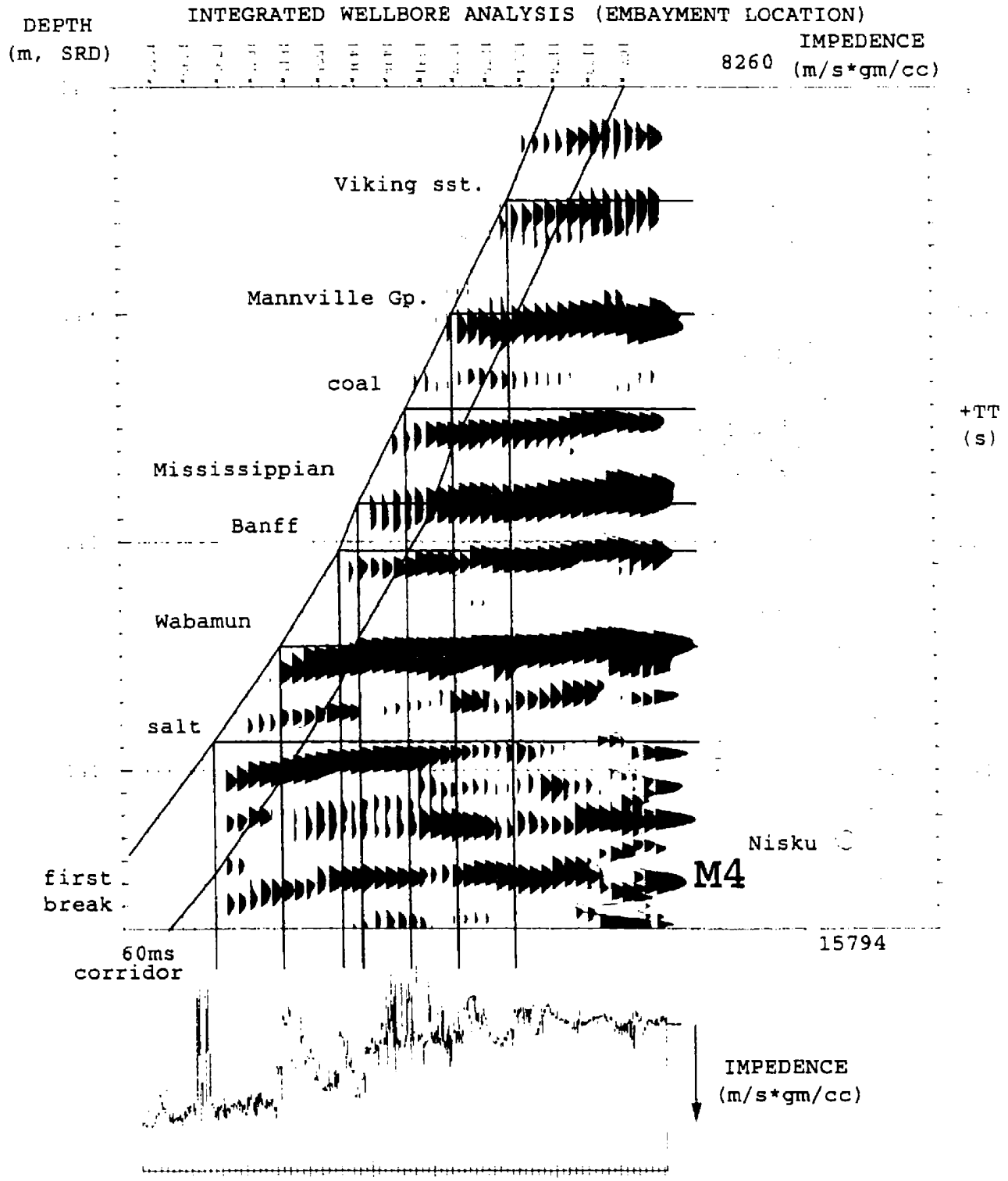

Figure 5.2.9c Integrated wellbore data from embayment location. The upgoing VSP wavefield in +TT time (equivalent to surface recorded TWT time) is compared to impedence logs in depth (TVD, SRD=900m) and in checkshot constrained time. The concept of an outside VSP corridor is illustrated by delaying the first break trajectory in time (60ms in this example). At least one event (M) is suspect as an interbed multiple.

porosity (near 1120ms). The VSP character of this energy resembles a reverse polarity zero phase wavelet centred at 1140ms. Both off-reef logs have penetrated the Ireton and Leduc Formations, but only the embayment well supports a strong primary event so this energy may or may not be a multiple at the reef location. At the reef, the first leg of this event does not intersect with the first break trajectory, but terminates at the Wabamun depth and lags the Wabamun primary by about 60ms (M3). In addition, the second leg of this event can be followed back to the depth of salt and lags the salt primary by about 60ms (M4). The Mississippian and Banff events also show a similar effect with comparable lags (events M1 and M2). The off-reef VSP's only indicate an up-going multiple below the salt.

During initial processing, an average wavelet was used for waveshaping and the M4 multiple event increased in strength at Wabamun depth, suggesting an interbed mechanism that correlated with the timing of the Wabamun and the Mannville coal. This would suggest that the interlying Mississippian and Banff reflectors do not play a significant role in Wabamun multiples. Because both the Wabamun and coal reflections have a dipolar nature of the same polarity, a first order multiple within these interfaces would have a dipolar up-going displacement response of opposite polarity, which does not agree with the event. In addition, the multiple event extended at lower amplitude below the Wabamun to depth of salt, suggesting that two multiples of different period may be interfering. Similarly, the expected multiple from this mechanism does not agree with the polarity of the event. Also, since there is no support for a down-going multiple from these depths on the reef VSP, the cause was interpreted to be a surface multiple effect not de-phased with the wavelet (simple surface multiple with period near 90ms). Following tracewise waveshaping, the event character has been better preserved across the Wabamun and the best explanation remains

that the dominant multiple contamination is due to a surface mechanism. However, other multiples may be contributing to the multiple energy at this level.

Since the waveshaping objective is to use the VSP to evaluate the multiple problem associated with the SSP data, and since the SSP data differs due to a buried source of different phase, standard VSP waveshaping and deconvolution methods are not readily applicable to the SSP problem when a surface multiple is suspect. To determine the timing relation of the surface multiple for the VSP surface source would give the surface peg-leg period that may be applicable to SSP multiple suppression. The waveshaping method applied in this case allows the periodicity of this multiple to be indicated by the corridor stacking method which allows direct correlation of VSP and SSP events. The periodicity could be validated by forward modelling using a Klauder wavelet, or optimised by inverse modelling to match the down-going wavefield. Application of prediction away from the well for the surface peg-leg still depends on surface definition by refraction statics.

In summary, VSP analysis has been useful in evaluation of Nisku multiples. The VSP waveshaping application has provided data for direct comparison to SSP data in terms of multiple contamination. The use of f-k zero wavenumber rejection has been useful by allowing checkshots to be included in the analysis to confirm to further constrain the depth of a near surface mechanism. The Wabamun has also been proven to contribute to multiple generation by the presence of a downgoing event from a reflection deeper in the section. The short period interbed multiples between the Wabamun and neighbouring reflectors do not appear to be significant in the presence of the surface peg-leg but may still contribute to multiple response. Reflectivity inversion can indicate this effect. First, VSP corridors, SSP stacks, and synthetics are integrated for robust multiple evaluation criteria.

5.3 Integrated Data and Modelling Analysis

In this section, VSP corridor stacks and autocorrelations are integrated into a display with range limited SSP stacks and well log synthetics to provide robust multiple identification criteria. The corridor stacks are of excellent quality and agree with the CMP data timing and character quite well at each location, except for unusually high amplitudes below the well bottom. The data have not been amplitude compensated for depth, but an unknown gain function has been applied by the industry contractor in pre-processing. The stacking process is not suspected since normalisation is applied based on unmuted samples. Unlike the surface data which in this case is not muted through the zone of interest, amplitudes on corridor stacks may be affected by the mute zone, hence their usage in multiple suppression may be limited to timing characteristics. To derive prediction operators using information from this integration, it is desirable to maintain absolute amplitude relationships between SSP multiples and primaries. If multiple timing can be determined by corridor stacks, then the most dominant multiple can be removed based on SSP design if appropriate. SSP autocorrelations may then indicate the next significant multiple mechanism. However, knowing the periodicity of the multiple is insufficient when R_p correlates with itself. The best approach in this case, if practical, is to support operator design from near offset SSP by amplitudes defined by inverted R_p, and two-way energy partitioning could be supported by one-way VSP predictions.

At the reef location (Figure 5.3.1a), the M4 multiple at 1140ms can be identified on a moveout basis by comparison of offset limited SSP stacks. Autocorrelations of these stacks are less revealing, largely due to lower frequency content with offset. The VSP corridor stacks suggest multiple contamination at the same level, and suggests a multiple period of

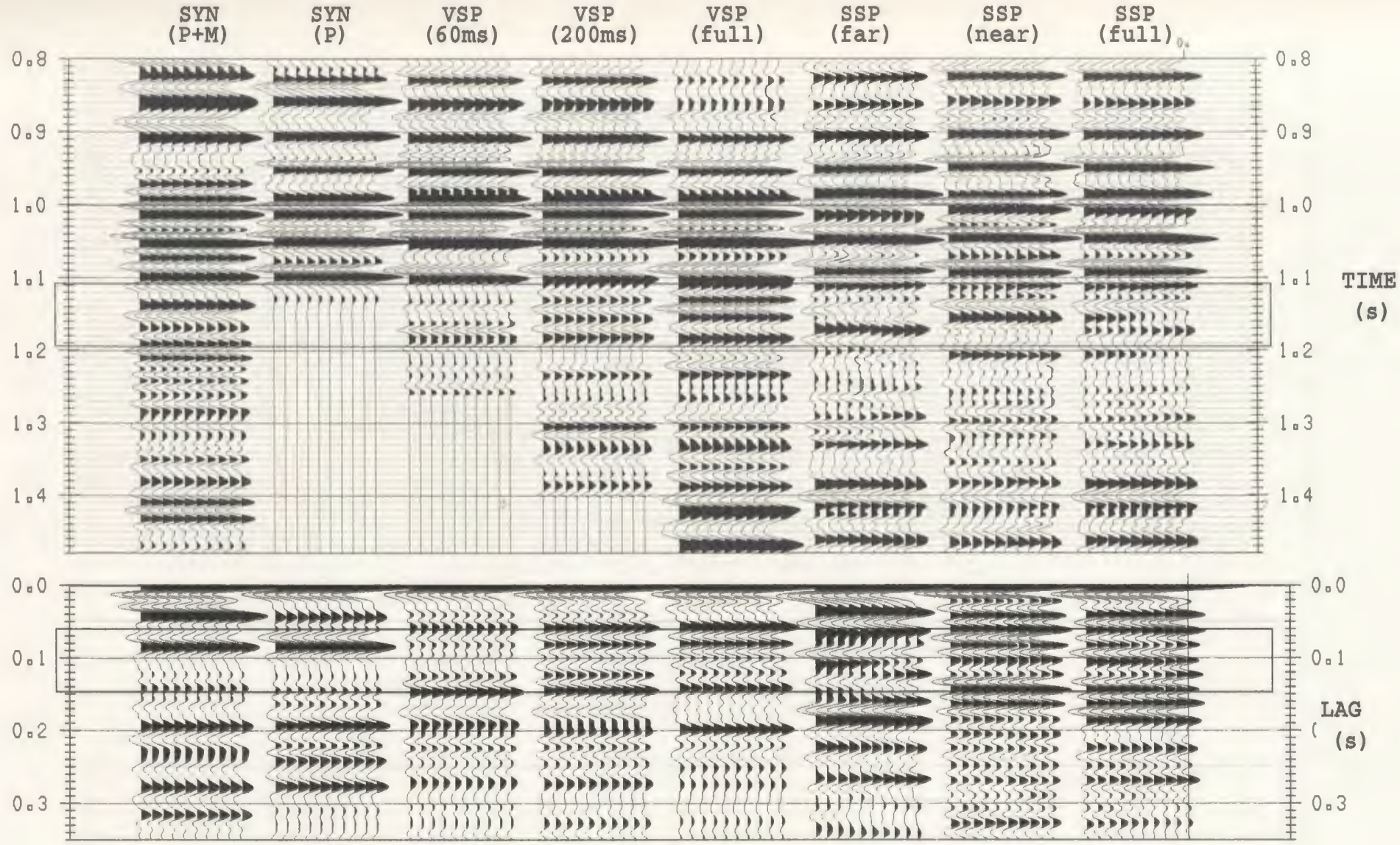

Figure 5.3.1a Integrated SSP, VSP, and syntehtic data (top) and ACORs (bottom)for the REEF location. From left to right is the primaries plus all interbed multiples synthetic (impulse response neglecting surface reflector), primary synthetic (35Hz Ricker), 60ms outside VSP corridor stack, 200ms outside VSP corridor, full VSP corridor stack, far CMP stack (1000-2000m), near CMP stack (200-1000m), and full CMP stack (200-2057m). The box overlay contains the data zone where significant multiple energy is suspected. The ACOR design window is 0.7-1.3s. PD can be subjectively chosen based on differences in ACOR lags of the VSP corridors.

more than 60ms but less than 200ms. Corridor stack autocorrelations suggest a period near 80ms. The primary synthetic does not go deep enough to show seismic response below the Nisku reservoir, but the impulse response predicts multiple energy at this level. The polarity of this multiple does not agree with the real data. This suggests that the mechanism might not be a local interbed generator. Synthetic autocorrelations are influenced to a small degree by interbed multiples at this location, and are not in good agreement with the real data. At the shelf and embayment locations (Figures 5.3.1b,c), data integration illustrates a similar situation of multiple contamination. The 60ms and 200ms short corridor stacks and corresponding autocorrelations show energy differences at lags corresponding to the weathering delay. This energy corresponds to multiple contamination identified by residual SSP moveout immediately below the Nisku level. Significant primary energy is also expected at this level, but this is supported only at the embayment location.

Overall, the SSP, VSP and primary synthetic data all share the same response at each well location except at salt and Nisku levels. The integration provides significant insight to multiple contamination. However, without defining the multiple mechanism, the prediction distance picked from the autocorrelations is subject to error. Since the mechanism cannot be defined by this method, it is dangerous to apply prediction based on these criteria alone. It may be beneficial to interpret the timing and polarity of autocorrelation events based on an understanding of the thin-bed reflectivity within this carbonate-clastic sequence. This may be difficult but may yield a more appropriate prediction operator. Alternatively, the inversion method seeks to derive a best fit primary sequence that can be used in prediction operator design, or in a spectral shaping procedure to remove this multiple.

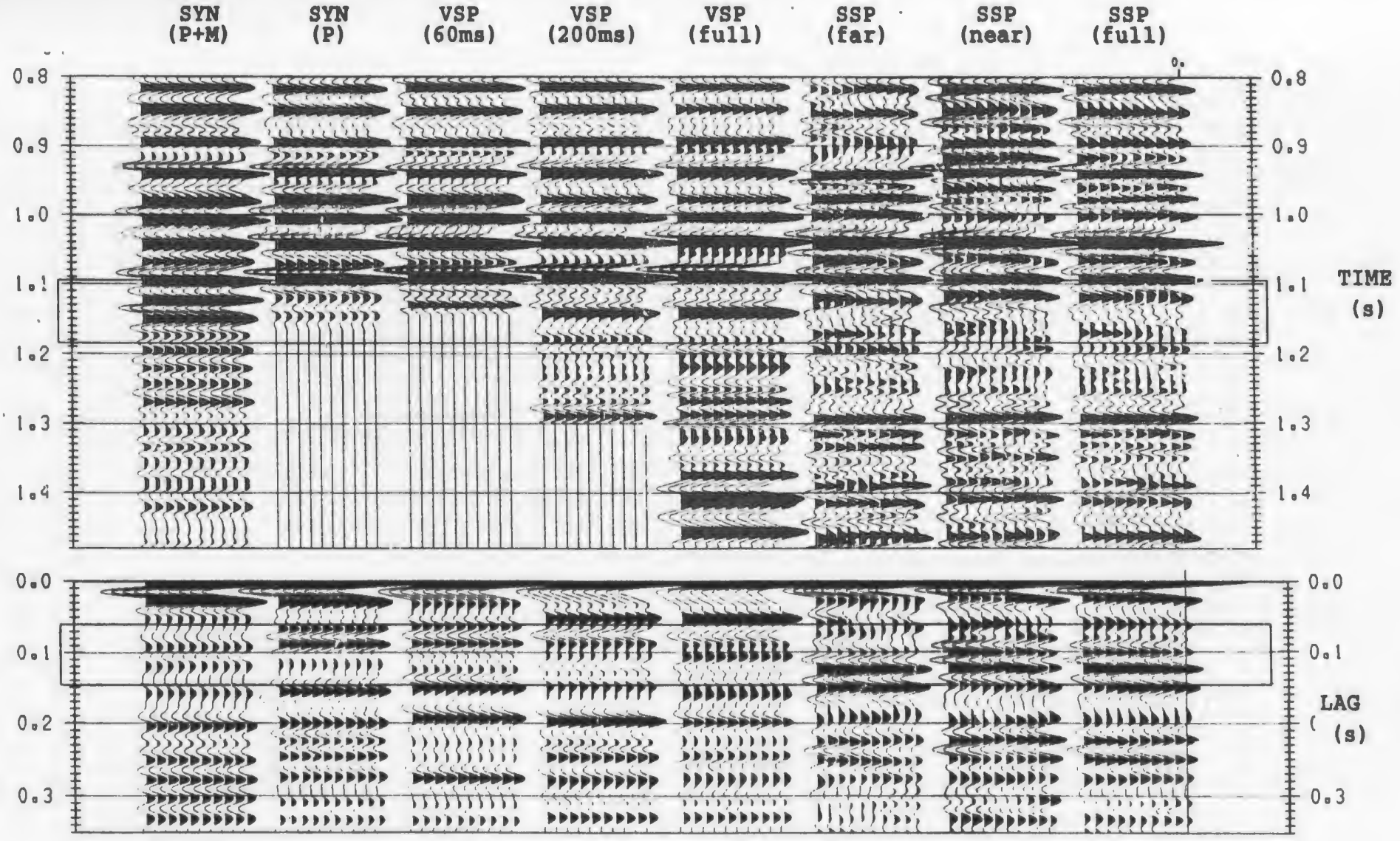

Figure 5.3.1b Integrated SSP, VSP, and syntehtic data (top) and ACORs (bottom)for the shelf location. ACOR design window is 0.7-1.3s.

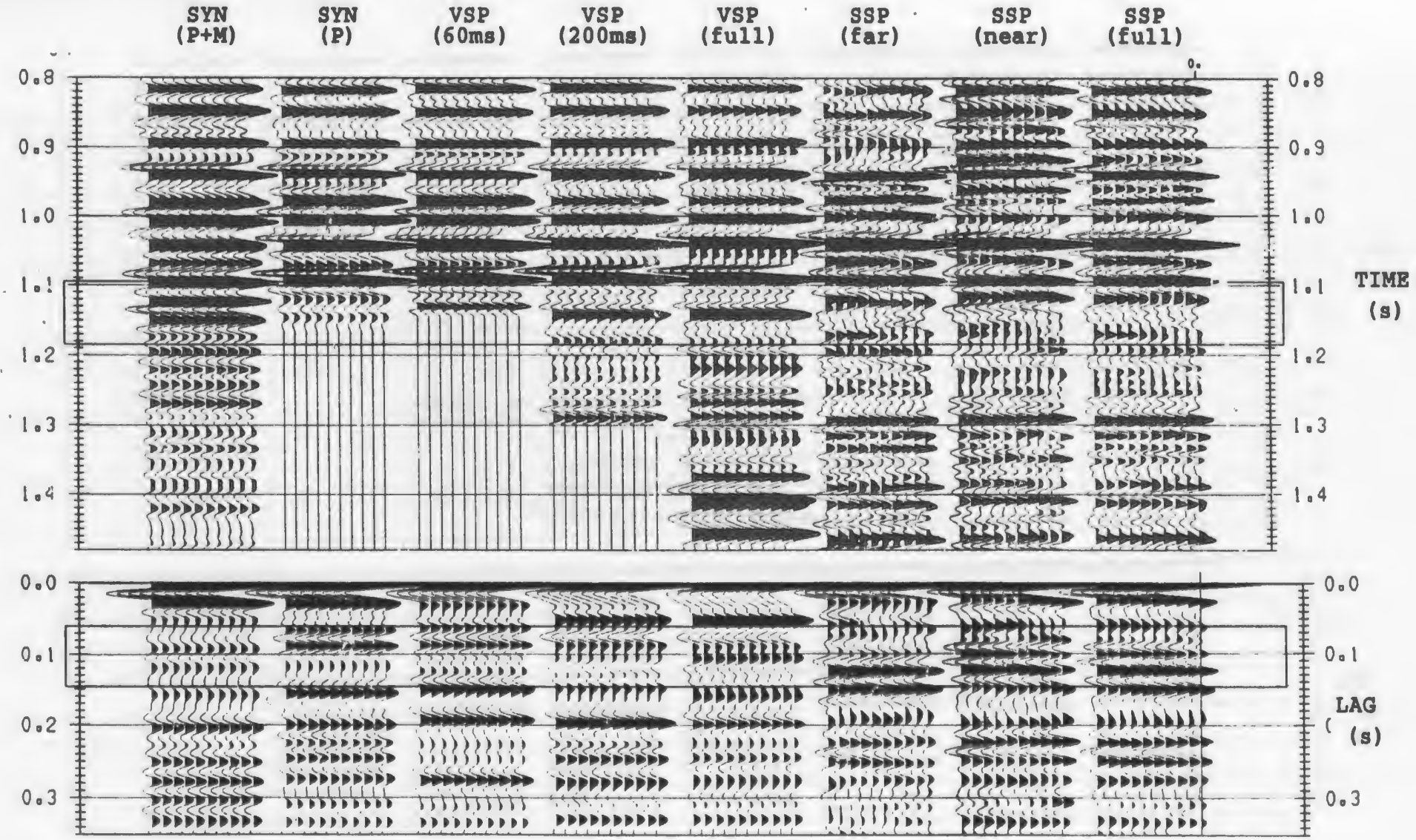

Figure 5.3.1b Integrated SSP, VSP, and syntehtic data (top) and ACORs (bottom)for the shelf location. ACOR design window is 0.7-1.3s.

5.4 Reflectivity Inversion Analysis

Preliminary investigation into the implementation of inversion for multiples was carried out successfully using synthetic seismograms (Lines, 1996). The method was then applied to the real SSP data from the reef location before and after post-stack predictive deconvolution for removal of near surface interference. The process was stabilized by a combinational choice of inversion parameters given a reasonable number of reflection coefficients within a reasonable time window. In initial inversion attempts, the wavelet approximation to Jacobian elements was employed. Convergence was slow over several iterations and unsatisfactory results were obtained. In the final inversion attempts, this approximation was adopted for the first iteration and typically produces minimal variation in parameters. The differencing method was adopted after the first iteration, and produced increased speed of convergence. However, the process does not only scale model reflectivity but also causes polarity reversals. The polarity of the dominant model reflectors is supported by wellbore data and it would be nice to maintain a geologically meaningful relationship. It could be argued that polarity should be allowed to change. Rapid change in polarity is controllable by winnowing, but convergence in general is limited and changes to dominant primary polarity occur because contamination includes surface multiples along with possible interbed multiples and the model is insufficient in matching the SSP multiple condition

The analysis was attempted using various windows of data. One window included all near-stack reflectors down to and including the Leduc, while other windows focused on shorter segments to improve the overall performance. When included for near surface multiples, the shallow section was modelled down to 800ms TWT using from 1 to 5 reflectors. Most efforts were applied to a window spanning from the Basal Fish Scales to

the Leduc, from 800 to 1200ms modelled using 15 to 26 primaries. The base level of 15 was derived based on manual log blocking against the up-going VSP wavefield for direct primary support subject to visual thresholding based on available resolution, and to geologic intuition regarding thin-bed dipoles. Nisku primary response at reef level was omitted initially in light of multiple contamination there. The inversion did not lead to a suitable solution under these conditions, prompting for the inclusion of lower magnitude impedance detail for a maximum of 26 reflectors within this window. In general, it was found that shorter windows excluding the shallower events in this zone ensured a faster more stable convergence as expected given the salt-Wabamun timing, but the resulting salt reflectivity typically was forced to change from the expected response of a reverse dipole.

Figure 5.4.1a shows inverted synthetics generated after each iteration using 26 reflectors derived from the blocky acoustic model at the reef location, and using 5 near-surface primaries parameterised based on the statics model and shallow stack events. The SSP near stack before predictive deconvolution for near surface multiples (fat left) is used to derive convergence criteria. Figure 5.4.1b compares the initial blocky reflectivity estimates against each iteration, and also shows the impulse response sequences. Note the dipole nature of the reflectivity that could only be described accurately in any detail by apriori well information. The main primary event is the Wabamun carbonate near 1050ms, which remains relatively stable throughout the inversion. The deeper group of events represents the Stettler salt on top of the Upper Nisku anhydrite that forms the seal for the Lower Nisku porous carbonate. Figures 5.4.2a and 5.4.2b are variations of this inversion where only the 26 reflectors from the target window are used to match the SSP following post-stack predictive deconvolution to suppress near surface multiples.

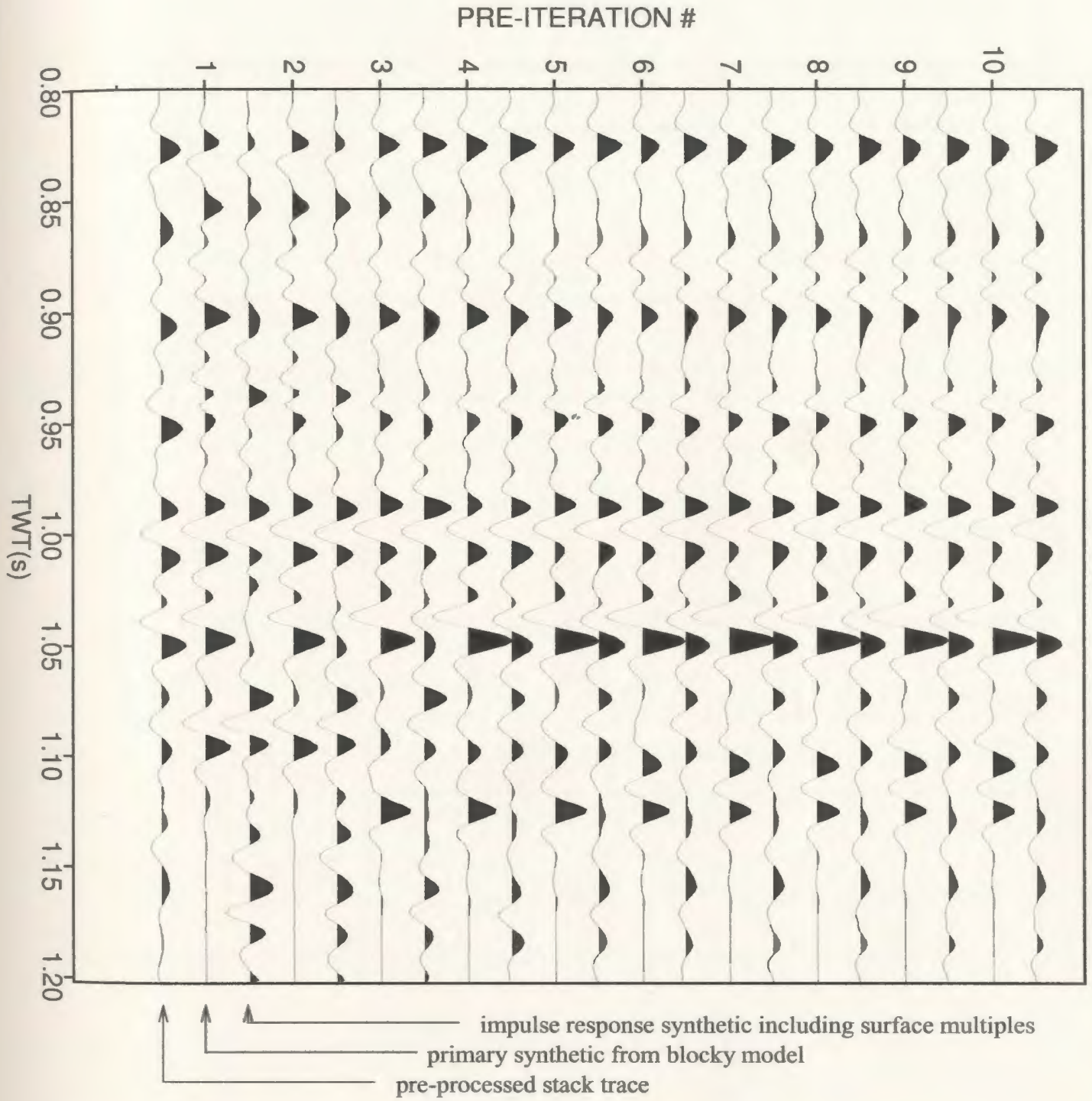

Figure 5.4.1a. Pairs of primary synthetics and corresponding impulse response synthetics derived from inversion for multiples at reef well. The near structural stack trace closest to the well is at far left. Multiples from 5 near surface reflectors are modelled in addition to all interbed multiples generated from 26 reflectors within the display window.

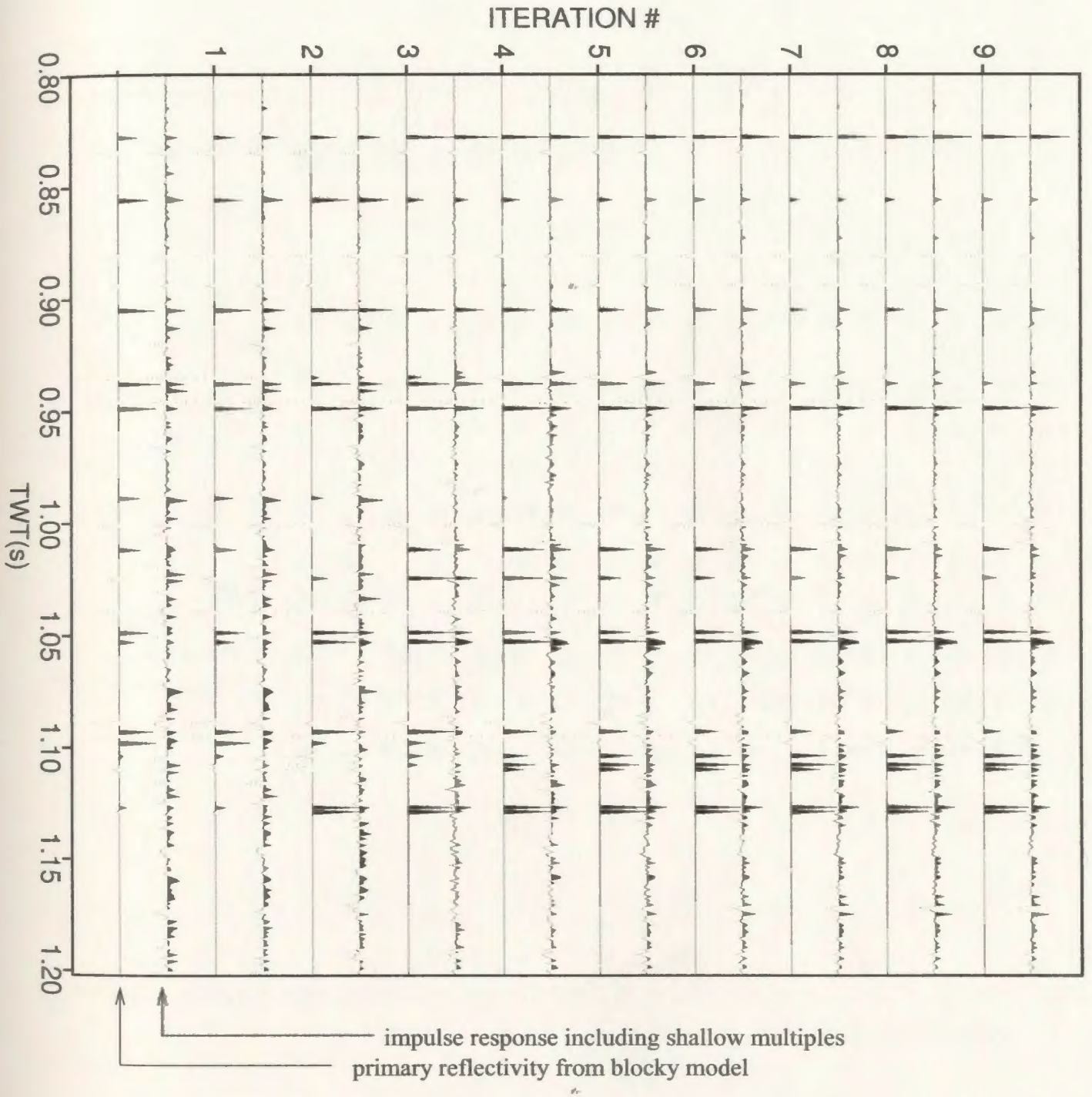

Figure 5.4.1b. Pairs of primary reflectivity and corresponding impulse response sequences derived from inversion for multiples at reef well. The original sequence generated by manual blocking of the well log impedence are shown at far left. Multiples from 5 near surface reflectors are modelled in addition to all interbeds generated from 26 reflectors within the display window.

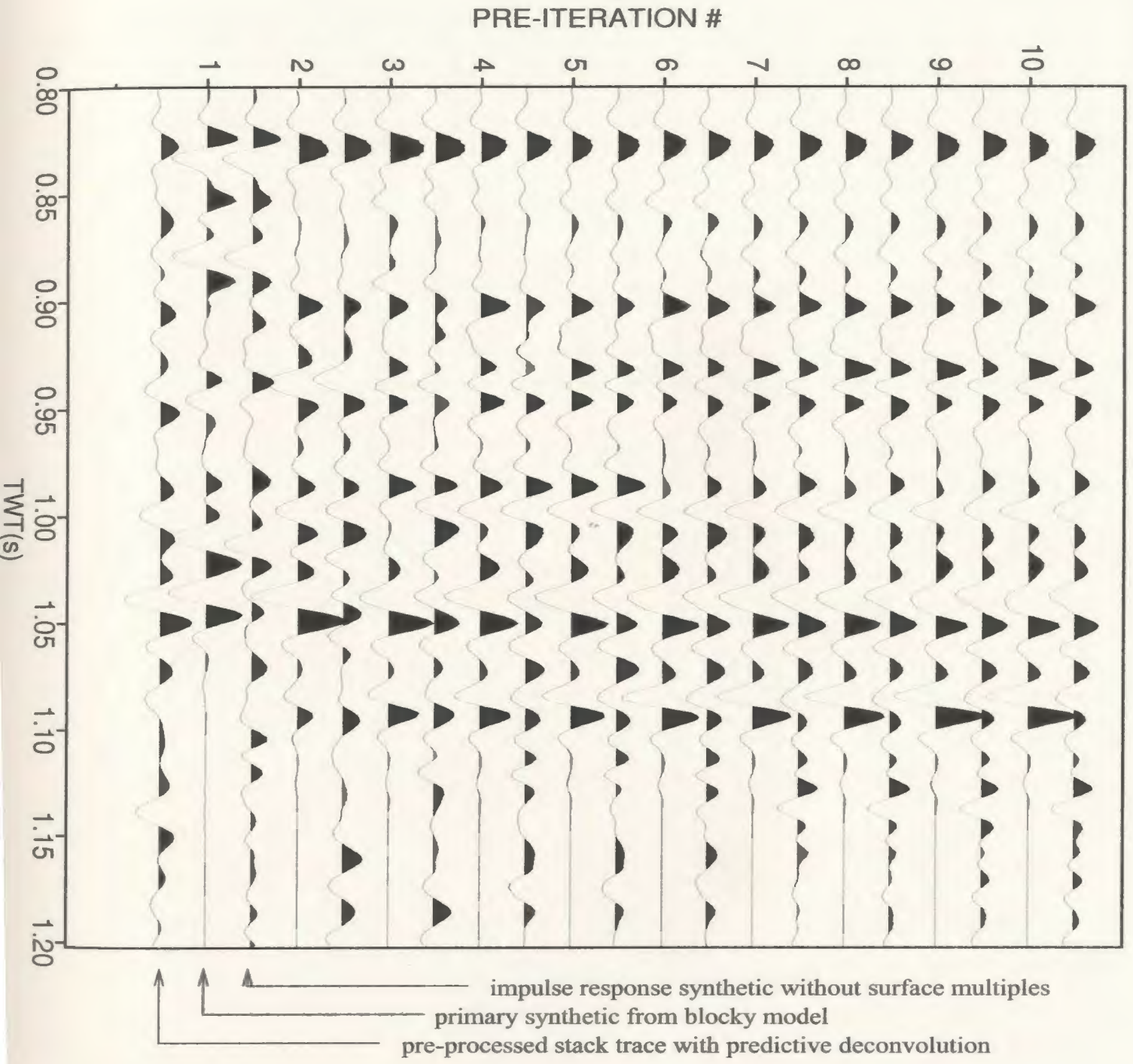

Figure 5.4.2a. Pairs of primary synthetics and corresponding impulse response synthetics derived from inversion for multiples at reef well. The near structural stack trace closest to the well following shallow prediction design to remove surface related multiples closest to the well is at far left. All interbed multiples generated from 26 reflectors within the display window are modelled.

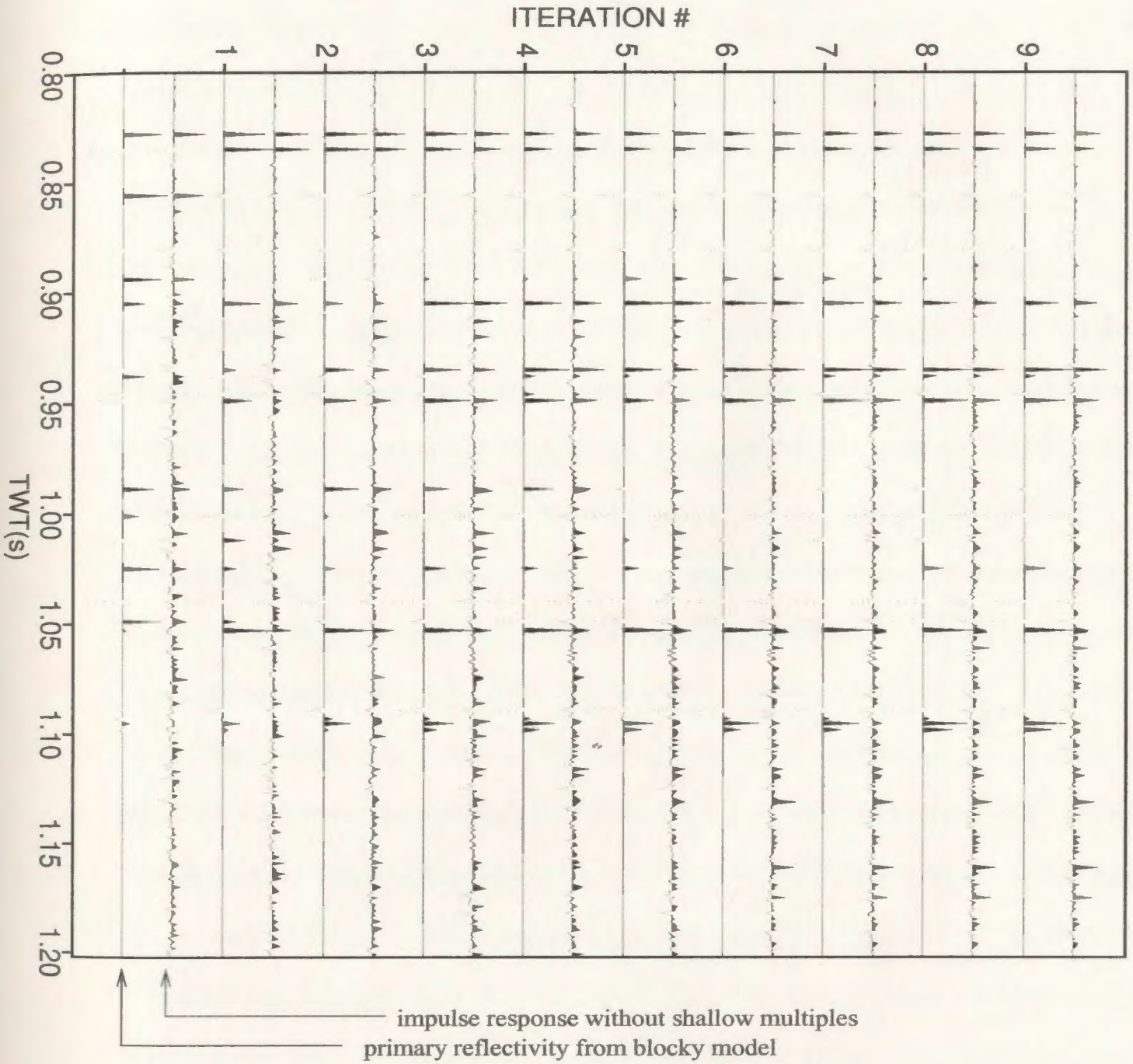

Figure 5.4.2b. Pairs of primary reflectivity and corresponding impulse response sequences derived from inversion for multiples at reef well. The original sequences generated by manual blocking of the well log impedence are shown at far left. All interbed multiples generated from 26 reflectors within the display window are modelled.

For 15 reflectors, inversion forced base of salt to change polarity with large amplitude while for 26 reflectors, the inversion produces a net positive sub-salt primary response to account for multiple energy. When the surface peg-leg mechanism is included, the same reflectors dominate the response and convergence is not improved. Near surface reflectivity plays a role in multiple generation but it is hard to define sufficient temporal distribution of blocky impedance in the shallow section. To invert the full section requires good quality TRA data in the shallow SSP section, and reliable log data would be useful. The inversion over the deeper section before prediction indicated that interbed multiples from the blocky impedance model cannot alone account for the multiple amplitudes in the SSP. After prediction, the interbed multiples still do not provide sufficient multiple contamination. It is not possible to derive a shaping filter that removes interbed multiples based on inversion unless surface multiples can first be removed to a better degree and or unless the model can be improved.

The inversion does indicate that interbed multiples can produce significant energy at Nisku level. The multiple energy at about 1140ms on the reef has a timing characteristic that corresponds to at least two possible first order interbed multiple generating mechanisms. A combination of these and other mechanisms could interfere with the reflection from reef porosity. First, the Mannville Group contains a low impedance layer separated from the Wabamun by about 100ms, the same lag as from the Wabamun to the multiple. Second, the Wabamun and top of salt are separated by about 40ms, the same lag as from the salt to the multiple. The interbed mechanisms appear to have periods conformable with predictive deconvolution, and the analysis could indicate the delay of the dominant multiple to be used as prediction distance. If the mechanism could be isolated in this way, prediction distance

could be extended laterally by horizon picks from the SSP provided operator design could avoid primary amplitudes.

In summary, results of this chapter do not provide the perfect solution to the Nisku imaging problem. Due to the nature of this SSP data, it has been illustrated that conventional multiple suppression methods are difficult to apply successfully. The goal of producing a wide frequency bandwidth primaries-only CMP stack has been partially reached, and the narrow band stack indicates anomalous Nisku reef reflectivity. The second goal of providing multiple distinction criteria has been successful at well locations. VSP wavefields were used to illustrate that significant VSP multiple contamination originates from above 300m depth. While this represents the major multiple interference, evidence also exists for interbed multiples and suggests that activity involves the Wabamun. The third goal, deriving a blocky primary reflectivity sequence that best describes the SSP near offset stack at well locations, has not been accomplished to a satisfactory degree. The match is not acceptable enough to warrant waveshaping of the impulse response to the primaries only synthetic. Overall, these methods have been illustrated to provide significant tools in multiple identification and evaluation of suppression performance.

CHAPTER 6. CONCLUSIONS AND DIRECTIONS

The goal of this thesis is to provide reliable Devonian reef hydrocarbon indicators from SSP data. The conventional approach to accomplishing this goal will normally involve processing of CMP gathers surface consistently for statics, TRA, wavelet deconvolution, and fine-tuned stacking velocity analysis. In many cases, an effort will be required to overcome limitations imposed on achieving this goal due to conditions of low temporal resolution, low S/N, and multiple interference. In this thesis, this effort involved the sacrifice of lateral resolution by trace binning to produce COF that provide improved sampling conditions and S/N ratio in the CMP domain. This also facilitates f-k suppression of seismic noise in the shallow section. The objective of this approach is to improve multiple indicators on the basis of NMO and autocorrelation. The objective of improving multiple indicators is to allow efficient evaluation of both pre-stack and post-stack multiple suppression applications and performance over the survey extents in an attempt to reach the thesis goal. Depending on the multiple problem, automated multiple attenuation methods based on differential dynamic moveout may be more effective and easier to implement when applied to COF gathers, while prediction design may be more reliable due to improved S/N in the autocorrelations. In this Nisku study, neither conventional method appears to provide adequate suppression using the available criteria.

SSP data for this Devonian reef prospect are limited in seismic resolution and are contaminated by multiple interference at the Nisku level. For each of the three wellbore analyses locations, multiple interference in the SSP occurs at or slightly below the target zone. SSP trace autocorrelation, partial stacks, and velocity analysis techniques assist in indicating the presence of this multiple energy so as to avoid this interpretation pitfall.

Coloured reflectivity over the deeper section made multiple characteristics difficult to identify by autocorrelation, but multiple and primary energy could be distinguished as having similar zero-offset lags over this window at the BOL location. The time response of partial stacks indicates multiples on the basis of moveout, but loss of frequency content with offset reduced post-stack autocorrelation effectiveness. The shallow data does not permit offset discrimination of multiples by virtue of limited offset. Assuming that the shallow section is not coloured, bandlimited autocorrelations indicated multiple energy with similar lag as the multiple identified at depth. This source of design criteria for multiple suppression by predictive deconvolution was more appropriate than Radon transforms given the condition of small but variable differential NMO over the line extents. Poor coherence over the available frequency band in the shallow section (due to low fold and low S/N) reduced the usefulness of the criteria in prediction. Pre-stack application is less effective than post-stack application but the stack process does provide attenuation of noise introduced by shallow operator design. Significant improvement to Nisku character does result from shallow prediction and anomalous reef response can be identified before and after significant sacrifice in bandwidth. In general, autocorrelations provided direct criteria for multiple identification, but windowing and frequency limitation are important considerations in this respect. This criteria did support the overall indicators of a surface peg-leg multiple, but data and stratigraphic conditions make mechanism identification difficult using SSP criteria.

With the objective of providing multiple identification and suppression criteria that agreed with SSP multiple indicators at the wells, I processed VSP data (that coincided with the SSP data) to employ the corridor stacking technique. Well model synthetics, SSP stacks,

and VSP corridor stacks were compared directly by data integration. Using a processing stream that purposely preserved surface related multiples in the wavefield, the inside and outside VSP corridor stacks confirmed multiple presence in agreement with multiples suspected in SSP range limited stacks. This implies generically that interbed multiples can also be detected by corridor stacks if processing can be applied appropriately to remove shallow multiples from the wavefield. This illustrates that VSP corridor stacking provides operator design criteria, and provides alternate criteria for SSP prediction operator design at well locations when R_p is coloured. Corridor stack autocorrelations can indicate multiple period, but amplitude relationships between VSP multiples and primaries will not agree with SSP data in general. Also, the technique does not distinguish which mechanism is responsible for the multiple interference. A surface multiple could be wrongly identified as an interbed multiple generated somewhere above the reef. When the periodicity of the multiple mechanism varies laterally, application of VSP multiple periodicity criteria away from the well relies on mechanism identification using both up-going and down-going VSP wavefields.

VSP wavefield separation and analysis provided the best indication of multiple mechanisms. At each well location, the downgoing wavefield suggests that dominant multiple generation occurs in the near surface. At the reef location, subtle indications suggest that each reflector in the stratigraphy that contributes to the up-going wavefield has associated trailing energy of similar delay. This condition is supported in the downgoing wavefield by the presence of energy that trails the initial down-going wavelet. Overall multiple interference at reef level could be attributed in part to interbed response, but no direct evidence exists for strong interbed multiples of similar periodicity. The indicators in

both wavefields support a surface peg-leg multiple mechanism in agreement with two-way SSP weathering delay. Since the thick weathering layer is suspected as being the mechanism, VSP checkshot traces are processed along with densely sampled VSP traces to show that the multiple originates at a depth above the first checkshot, somewhere in the near surface. As opposed to more traditional VSP processing strategies, this analysis required the use of f-k wavefield separation and the preservation of multiples during the waveshaping operation. The ability to select and control these processes are considered crucial to SSP multiple evaluation using VSP's.

The approach taken to suppress the surface peg-leg multiples is to design predictive deconvolution operators based on shallow data. This approach implemented design criteria in a manner that attacks a multiple mechanism that would not have been easily suspected without help from VSP indicators. The nature of the multiple mechanism suggested that prediction should work at near offsets where periodicity of peg-leg multiples should be constant under conditions of a sufficiently flat weathering layer. This approach is an adaptive application of an old method, and the procedure of deriving operators from shallow SSP data may offer a viable approach to the multiple problem in such cases. This is best accomplished using a processing strategy that preserves TRA normal-incidence impulse response in CMP gathers. Secondary interbed multiple mechanisms may require attenuation methods based on differential moveout relative to near-coincident primaries, or based on inverted reflectivity.

Absolute reflectivity inversion of VSP-constrained well log models from SSP normal incidence amplitudes requires weathering based near surface constraints in this Nisku case. Other shallow acoustic boundaries must also be included to preserve absolute reflectivity in

systems that are non-linear in reflectivity or appear non-linear due to superposition of multiple interference. VSP's should attempt to sample the wavefield at reflector interfaces, especially above the logged portion of a well. The depth and traveltime constraints in this zone should be complemented by density information. If the resulting blocky impedance model was reliable, the inversion scheme could include the total intrabed multiple effect on wavelet phase and amplitude using the unblocked impedance. The adjustment of the intrabed response at each iteration could adopt a blocking strategy for amplitude compensation. In general the interbed effect will be underestimated by too few reflectors.

To apply inversion before wavelet deconvolution, the synthetic model could include shot burial for ghosting effects by the addition of the impulse response to a version delayed by $2T_{uh}$ and scaled by surface reflectivity. $R_{p,surface}$ should also be included as a parameter since it is not expected to be unity. The main conclusion of the analysis is that when shallow multiples contribute to the SSP response, it is crucial to support the shallow impedance model with accurate SSP data from the shallow section. Considerations of this nature may lead to inversion success, thereby satisfying the objective of providing alternative multiple suppression criteria. This objective is set to satisfy the objective of successful multiple supression at well locations. If successful, this would evolve to the objective of extending the criteria away from the well. Successful flow through in these objectives would ultimately leads to satisfying the primary research goal of reliability in hydrocarbon indicators based on SSP data. The inverted reflectivity would provide alternate criteria to support the secondary research goal of porosity discrimination criteria based on SSP data by providing reliable extension to Nisku resolution.

Following SSP processing, seismic resolution at Nisku level remains insufficient to resolve reservoir facies. With field acquisition dynamic range at the current maximum of 24 bit data word size (I O system 1 in this Nisku study), it is reasonable to record using a 1ms sample rate as opposed to a 2ms sampling while maintaining 40 dB of field signal amplitude. This may allow the anti-alias field filter to be set higher (120 Hz in this Nisku study). It may be possible to extend the bandwidth by half an octave higher (12-125Hz) in SC-deconvolution without degrading the S/N ratio in a high-fold near-offset SSP stack. Non-linear vibrator sweeps could be tested to 125 Hz to match or exceed SSP bandwidth. Geophones of lower resonant frequency than 14hz will also help to extend the bandwidth for low octaves. These field considerations may seem rather nitty-gritty, but small extensions to bandwidth may produce big differences in Nisku resolution. In the case of multiple interference, it may be more appropriate to look for Nisku anomalies in the frequency limited normal incidence resposne, as illustrated for this SSP exploration.

Given large channel capacity of current acquisition systems, an auxiliary bank of channels should be employed for enhanced near surface definition in problem weathering areas. Specifically for this SSP survey, a thick low-velocity weathered layer acts as a peg-leg multiple generator, and other shallow reflectivity presents a source of reverberation. Shots could be skidded between every third station with live near-offset traces for direct arrival sampling to constrain V_w **by actual picks that complement uphole measurements.** This should also allow recording of reflection from base of weathering. Then, higher fold near-offset gathers could provide improved near-surface definition and hence shallow multiple information with higher S/N ratio in the normal incidence stack that relates to solving deeper multiple problems. Improvement in this area could lead to the

implementation of a more theoretical multiple attenuation approach based on ray-tracing for prediction-subtraction.

The goal of this thesis research was to provide reliable Nisku hydrocarbon indicators by successful multiple suppression applied to maximum bandwidth SSP data. These indicators would be derived through amplitude and timing character in the stack, through AVO techniques pre-stack, and by other conventional means. The conventional approach to this goal did not succeed. Two alternate approaches were focused upon so as to provide alternate suppression routines to allow conventional indicators to be derived. First, inversion attempted to derive a Nisku reflectivity sequence that satisfied multiple contaminated normal incidence data at well locations. Second, VSP data were processed to evaluate and confirm multiples and multiple mechanisms so as to support the conventional approaches and to assess the usefulness of VSP approaches to SSP multiple suppression. The inversion for reflectivity did not perform as desired due to limitations in the SSP data as mentioned. The VSP data did offer concrete criteria for identifying multiple presence and multiple mechanisms, but the nature of the problem did not allow VSP data to be used for reliable SSP multiple suppression at or away from the well. In the light of these limitations, failures, and shortcomings, the secondary goal of providing porosity distinction criteria by any of the conventional methods still requires a solution.

Overall, this thesis represents the results of considerable effort directed at attacking the difficult problem of identifying and removing multiple reflections in seismic data. The exercise of incorporating VSPs into SSP interpretation certainly illuminated the risk factor associated with Nisku exploration. The work thoroughly explores the problem and many small but important nuances are investigated that relate directly and indirectly to the

achievement of the thesis goals. The effort of completeness in discussion generates a wealth of technical and practical information, and reasonable success has been achieved in maintaining scientific soundness of these methods. I thank the reader for enduring the complexity of the written problem, and I hope this endurance pays off by allowing avoidance of the seismic multiple pitfall. I feel that this thesis research should provide an excellent insight into the processing and interpretation of any surface seismic experiment, and should also provide extensive subject matter for future seismic research.

BIBLIOGRAPHY

Anstey, N. A. and Newman, P., 1966, The sectional auto-correlogram and the sectional retro-correlogram, Geophysical Prospecting, **14**(4), 389-426.

Balch, A.H., and Lee, M.W., Eds., 1984, Vertical seismic profiling: technique, applications, and case histories, IHRDC, Boston.

Burton, A.J., and Lines, L.R., 1997, VSP detection of interbed multiples using inside-outside corridor stacking, Geophysics, **62**(2), 1628-1635.

Cased hole log interpretation: Principles Applications, 1989, Schlumberger Educational Services

Castagna, J.P., AVO analysis - tutorial and review, in Castagna, J.P., and Backus, M.M., Ed., 1993, Offset-dependent reflectivity -theory and practice of AVO analysis, SEG publication, p. 3-36

Chun, J.H., and Jacewitz, C.A., 1981, The weathering statics problem and first arrival time surfaces, 51st SEG Annual Internat. Mtg., Los Angeles, Reprints 81, Session S21.4. (also The first arrival time surface and estimation of statics, Extended Abstracts).

Claerbout, J.F., 1985, Imaging the earth's interior, Blackwell Scientific Publications, Inc. p. 325-326.

Fraser, D., and Jain, S., 1988, Exploration for porosity in carbonates: a synthetic based study, Journal of the CSEG, **24**(2), 141-153.

Gardner, G., Gardner, L., and Gregory, A., 1974, Formation velocity and density – the diagnostic basics for stratigraphic traps, Geophysics, **44**, 3-26.

Hampson, D., and Russell, B.H., 1984, First-break interpretation using generalised linear inversion, Journal of the CSEG, **20**(1), 40-54.

Hampson and Russell Software Services Ltd, Stratigraphic Analysis and Inversion (1993 STRATA^{TM}), reference manual.

Hampson and Russell Software Services Ltd, Amplitude Versus Offset (1993 AVO^{TM}), reference manual.

Hampson and Russell Software Services Ltd, 3D First Break Picking and Interpretation (1994 GLI3D^{TM}), reference manual.

Hampson, D., 1986, Inverse velocity stacking for multiple elimination, CSEG Journal, **22**(1), 44-45.

Hampson, D. and Mewhort, L., 1983, Using a vertical seismic profile to investigate a multiple problem in Western Canada, Journal of the Canadian Society of Exploration Geophysicists, **19**(1), 16-33.

Hardage, B., 1983, Vertical seismic profiling: Part A: Principles, 1st edition, Geophysical Press, Pergamon Press, London, UK (2nd edition 1985).

Hargreaves, N., Calvert, A.J., Hirsche, W.K., 1987, A fast inverse Q-filter, 57th SEG Annual International Meeting, Extended Abstracts, New Orleans, p. 252-254.

Hilterman, F., 1989, Is AVO the seismic signature of lithology?, The Leading Edge, **9**(6), 15-22.

Hinds, R.C., Kuzmiski, R.D., Botha, V.J., and Anderson, N.L., 1989, Vertical and lateral seismic, in Geophysical Atlas of Western Canadian Hydrocarbon Pools, a joint publication of the CSEG and CSPG.

Hunt, L., Cary, P., and Upham, W., 1996, The impact of an improved Radon transform on multiple attenuation, SEG Convention Extended Abstracts , Denver, p. 1535-1538.

Kallweit, R.S. and Wood, L.C., 1982, The limits of resolution of zero-phase wavelets,

Geophysics, 47(7), 1035-1046.

Kuhme, A.K., 1987, Seismic interpretation of reefs, The Leading Edge, **6**(8), 60-65

Landmark Graphics Corporation, 1994, Landmark Insight seismic processing software, reference manuals.

Lines, L.R., and Treitel, S., 1984, A review of least-squares inversion and its application to geophysical problems, Geophysical Prospecting, **32**, 159-186.

Lines, L.R., 1996, Suppression of short-period multiples - deconvolution or model inversion?, Canadian Journal of Exploration Geophysics, **32**(1), 63-72.

Lu, H.X., and Lines, L.R., 1995, AVO and Devonian reef exploration: difficulties and possibilities, The Leading Edge, **14**(8), 879-881.

Masuda, R.M., 1992, Just a bright spot?, Canadian Society of Exploration Geophysicists Recorder, March, p. 6-11

Mayne, H., 1962, Common reflection point horizontal data stacking techniques, Geophysics, **28**, 927-938.

McFadden, P.L., Drummond, B., and Kravis, S., 1986, The Nth-root stack: theory, application, and examples, Geophysics, **51**(10), 1879-1892.

Mitchell, A.R., and Kelamis, P.G., 1990, Efficient tau-p hyperbolic velocity filtering, Geophysics, **55**(5), 619-625.

Molyneux, J., Jones, M., and Schmitt, D., 1996, Identification of multiples contaminating surface seismic data using a VSP analysis Technique, SEG Convention, Extended Abstracts, Denver, p. 206-209.

Newman, P., 1973, Divergence effects in a layered earth, Geophysics, **38**(3), 481-488.

O'Doherty, R.F., and Anstey, N.A., 1971, Reflections on amplitudes, Geophysical

Prospecting, **19**, 430-458.

Ostrander, W.J., 1984, Plane-wave reflection coefficients for gas sands at nonnormal angles of incidence, Geophysics, **49**(10), 1637-1648.

Peacock, K., and Treitel, S., 1969, Predictive deconvolution: theory and practice, Geophysics, **34**(2), 155-169.

Potts, M., Schleicher, K., Wason, C. and Ellender, S., 1982, Prestack wavelet deconvolution, 52nd SEG Annual International Meeting., Expanded Abstracts.

Rennie, W., Leyland, W., and Skuce, A., 1989, Winterburn (Nisku) Reservoirs, in Geophysical Atlas of Western Canadian Hydrocarbon Pools, joint CSEG CSPG publication.

Ricker, N., 1953, Wavelet contraction, wavelet expansion and the control of seismic resolution, Geophysics, **18**(4), 769-792.

Robinson, E.A., 1967, Predictive deconvolution of time series with application to seismic exploration, Geophysics, **32**(3), 418-484.

Ronen, J., and Claerbout, J.F., 1985, Surface consistent residual statics estimation by stack-power maximization, Geophysics, **50**(12), 2759-2767.

Ryu, J., 1982, Decomposition (DECOM) approach applied to wavefield analysis with seismic reflection records, Geophysics, **47**(6), 869-883.

Sacchi, M.D., and Ulrych, T.J., 1995, High-resolution velocity gathers and offset space reconstruction, Geophysics, **60**(4), 1169-1177.

Schoenberger, M., 1996, Optimum weighted stack for multiple suppression, Geophysics, **61**(3), 891-901.

Schoenberger, M., and Levin, F.K., 1974, Apparent attenuation due to intrabed multiples,

Geophysics, 39(3), 278-291.

Schoenberger, M. and Levin, F. K., 1979, The effect of subsurface sampling on one-dimensional synthetic seismograms, Geophysics, **44**(11), 1813-1829.

Schoenberger, M., 1974, Resolution comparison of minimum-phase and zero-phase signals, Geophysics, **39**(6), 826-833.

Sheriff, 1981, Encyclopedic dictionary of geophysics, SEG publication, Tulsa

Sheriff, 1977, Limitations on resolution of seismic reflections and geologic detail derived from them, in Seismic stratigraphy - applications to hydrocarbon exploration, AAPG Memoir 26.

Shuey, R.T., 1985, A simplification of the Zoeppritz equations, Geophysics, **50**(4), 609-614.

Stewart, R., 1985, Median filtering: review and a new f/k analogue design, CSEG Journal, **21**(1), 54-63.

Stork, C., 1992, Singular value decomposition of the velocity-reflector depth tradeoff, part 2: High-resolution analysis of a generic model, Geophysics, **57**(7), 933-943.

Telford, W., Geldart, L., Sheriff, R., and Keys, D., 1976, Applied geophysics, Cambridge University Press.

Treitel, S., Gutowski, P.R. and Wagner, D.E., 1982, Plane-wave decomposition of seismograms, Geophysics, **47**(10), 1375-1401.

Vail P.R., Mitchum, R.M., Sangree, J.B., Todd, R.G., Widmier, J.M., and Bubb, J.M., and Hatlelid, W.G., 1977, Seismic stratigraphy and global changes of sea level, in Seismic stratigraphy - applications to hydrocarbon exploration, AAPG Memoir 26.

van Riel, P., and Berkhout, A.J., Resolution in seismic trace inversion by parameter estimation, Geophysics, **50**(9), 1440-1455.

Walden, A.T., and Hosken, J.W.J., 1988. Choosing the averaging interval when calculating primary reflection coefficients from well logs, Geophysical Prospecting, **36**, 799-824.

Widess, M.B., 1973. How thin is a thin bed, Geophysics, **38**(6), 1176-1180 (originally published in the Proceedings of the Geophysical Society of Tulsa in 1960).

Wiggins, R.A., 1966. Omega-k filter design, Geophysical Prospecting, **14**(4), 427-440.

Wiggins, R.A., Larner, K.L., and Wisecup, R.D., 1976, Residual statics analysis as a general linear inverse problem, Geophysics, **41**(5), 922-938.

Wuenschel, P.C., 1960, Seismogram synthesis including multiples and transmission coefficients, Geophysics, **25**, 106-129.

Yilmaz, O., 1987, Seismic data processing, SEG publication, Tulsa, 526 pp.

Zoeppritz, K., 1919, Erdbebenwellen VIIIB, On the reflection and propagation of seismic waves, Gottinger Nachrichten, I, p. 66-84